

**Applications of Amido-N-Heterocyclic Carbene Ligands in
Bifunctional Catalysis**

Thesis submitted for the degree of
Doctor of Philosophy
at the University of Leicester

by

Christopher G. Daly MChem
Department of Chemistry
University of Leicester

October 2012

Title: Applications of Amido-N-Heterocyclic Carbene Ligands in Bifunctional Catalysis

Author: Christopher G. Daly

Abstract

This thesis describes the synthesis of amino/amido-N-heterocyclic carbene (NHC) complexes of late transition metals, in order to investigate bifunctional catalysis involving a metal-amido bond.

Chapter one introduces bifunctional catalysis, with an emphasis on the mechanism of bifunctional bond-breaking during catalytic reactions. Mechanisms of C-H activation are described and the features of bifunctional C-H activation (AMLA) discussed. The ligand properties, and methods of synthesis, of NHC and amido ligands are described, and the choice of ligand to investigate bifunctional catalysis rationalised. Finally, the detailed aims and objectives of this research are stated.

Chapter two gives an overview of the synthesis of N-donor functionalised imidazolium salts, as precursors to functionalised NHC ligands. The synthesis of imidazolium salts that are precursors to tridentate (CNC) amido-*bis*NHC pincer ligands and bidentate (C,NR) amino/amido-NHC ligands are described.

Chapter three introduces the synthesis of pincer complexes containing NHC or amido donors. The syntheses of (CNC) amido-*bis*NHC complexes of palladium, platinum and nickel are described. Investigations into the stoichiometric bifunctional reactivity of a (CNC) Pd complex are also discussed.

Chapter four describes the synthesis of complexes containing an amino/amido-NHC (C,NR) ligand of palladium, platinum, ruthenium, rhodium and iridium. The stoichiometric reactivity of an iridium amido complex towards electrophiles is reported.

Chapter five reports the reactivity of amino/amido-NHC complexes in bifunctional catalysis. (C,NR) ruthenium, rhodium and iridium complexes are shown to be active precatalysts for the transfer hydrogenation (TH) of ketones. Evidence is presented that suggests that the metal-amido bond is participating in a bifunctional mechanism for TH. (C,NR) complexes of palladium are shown to be active precatalysts for the direct arylation (DA) of 2-*n*-butylfuran; however, DA of oxazole and thiazole proceeds only on addition of cocatalytic pivalic acid. Evidence suggests that a metal-amido species is not involved in a bifunctional mechanism; a palladium-pivalate species is implicated in the C-H activation step of DA.

Chapter six summarises the conclusions of the work reported in this thesis; potential future work is highlighted and discussed.

Acknowledgements

First, I would like to thank my supervisor, Dr. Warren Cross. His guidance and support has endured throughout this project, as well as his patience. I would also like to thank the numerous other members of the academic staff at the University of Leicester who have offered advice during the course of my research, including, but not limited to, Dr. Dai Davies, Dr. Gregory Solan, Dr. Sandeep Handa and Prof. Paul Cullis.

I must acknowledge the friendly and helpful support staff who have contributed to this work: Mr Kuldip Singh, for his fantastic crystallography skills and Dr. Gerry Griffith, for his help with NMR spectroscopy. I'd also like to thank Sai and Dave, for putting up with my annoyances. The teaching lab staff: Richard, Dawn, Katy and Carla, were fantastic company during the long hours of demonstrating.

I have had the pleasure of knowing many talented people at Leicester, and I would like to thank all of the postgrads and undergrads I've either worked with, or demonstrated to – I wish I had space to mention you all! However, I must thank Dr. Youcef Boutadla, who synthesised rhodium complexes, worked with me on the transfer hydrogenation work and spent many coffee breaks teaching me terrible French, and Luka Wright, who is the best chemistry lyricist I think I've ever met.

Of course, I couldn't have submitted this work if it hadn't have been for my family. They have always supported and encouraged me, even as I've been far away and out of contact. Mum, Dad, Sarah, Gran and Grandpa, Nanny and Grandad, all my aunties and uncles, you're all a part of this! Also, an apology to Kirstie, Jake and Rhiannon: I know I haven't been around as much as a brother should; hopefully I'll make up for it.

Finally, I want to thank Dr. Laura Wylie, my beautiful and talented fiancée. Over four years she's been supportive, kind and patient. In that time, we've covered thousands of miles to see each other, and now I finally have the pleasure of living with her. Thank you, my love.

Statement

This thesis is based on work conducted by the author in the Department of Chemistry at the University of Leicester, during the period between October 2008 and October 2012. All crystallography was performed by Mr K. Singh.

Thanks go to Rachel Ackerman, for preliminary work on the (C,NR) complexes, Sam Timson, for first synthesising compounds **4.30** and **4.31**, and to Dr. Youcef Boutadla, who first synthesised compounds **4.35** and **4.37** and worked in collaboration with the author on the transfer hydrogenation work reported in Chapter 5.

Some of the work in this thesis has been published; references to peer-reviewed papers including parts of this work are included in the Appendix.

All the work described in the thesis is original unless otherwise stated in the text or in the references. This work is not being presented for any other degree.

Signed: _____ Date: _____

Christopher G. Daly

Abbreviations

General and Physical

°C	Degrees Centigrade
Å	Angstroms
AMLA	Ambiphilic Metal Ligand Activation
Br s	Broad singlet
cal	Calories
<i>cf.</i>	Confer (compare)
CMD	Concerted Metallation-Deprotonation
COSY	Correlation Spectroscopy
d	Doublet
Da	Dalton
DA	Direct Arylation
dd	Doublet of doublets
DFT	Density Functional Theory
dt	Doublet of triplets
EA	Electrophilic Activation
eq.	Equivalents
ESI	Electrospray Ionisation
FAB	Fast Atom Bombardment
g	Gram
GC	Gas Chromatography
h	Hour
HMBC	Heteronuclear Multiple-bond Correlation Spectroscopy
HMQC	Heteronuclear Single-quantum Correlation Spectroscopy
HR	High Resolution
Hz	Hertz
<i>i.e.</i>	Id est (that is)
<i>in situ</i>	In the reaction mixture
<i>in vacuo</i>	Under vacuum (reduced pressure)
J	Joules

K	Kelvin
L	Litre
M	Molar (concentration)
m	Multiplet
mol	Moles
MS	Mass Spectrometry
NMR	Nuclear Magnetic Resonance
nOe	Nuclear Overhauser Effect
OA	Oxidative Addition
ppm	Parts per million
q	Quartet
RE	Reductive Elimination
RT	Room Temperature
s	Second
SBM	σ -Bond Metathesis
S _E Ar	Electrophilic Aromatic Substitution
sept	Septet
S _N 2	Bimolecular Nucleophilic Substitution
S _N Ar	Nucleophilic Aromatic Substitution
t	Triplet
TH	Transfer Hydrogenation
TLC	Thin Layer Chromatography
TOF	Turnover Frequency
TON	Turnover Number
TS	Transition State
<i>via</i>	By means of
<i>vide infra</i>	See below
δ	Delta, the NMR chemical shift
ΔG	Gibbs Free Energy Change
ΔH	Enthalpy Change
ΔS	Entropy Change

Chemical

acac	Acetylacetonate anion
B ₂ pin ₂	<i>Bis</i> (pinacolato)diboron
cod	Cyclooctadiene
Cp	Cyclopentadienyl anion
Cp*	Pentamethylcyclopentadienyl anion
cy	Cyclohexyl
dba	Dibenzylideneacetone
DBU	1,8-Diazabicyclo[5.4.0]undec-7-ene
DCM	Dichloromethane
DMA	Dimethyl acetamide
DMAD	Dimethylacetylenedicarboxylate
DME	Dimethoxyethane
DMF	Dimethyl formamide
dmpe	1,2- <i>bis</i> (dimethylphosphino)ethane
dppe	1,2- <i>bis</i> (diphenylphosphino)ethane
dppf	1,1'- <i>bis</i> (diphenylphosphino)ferrocene
Et	Ethyl
Fc	Ferrocene
IMe	1,3-Dimethyl imidazole-based NHC
IMes	1,3-Dimesityl imidazole-based NHC
<i>i</i> -Pr	<i>Isopropyl</i>
KHMDS	Potassium hexamethyldisilazide
Me	Methyl
nacnac	1,3-Diketiminato anion
NBA	3-Nitrobenzylalcohol
<i>n</i> -Bu	'Normal' butyl
NHC	N-Heterocyclic Carbene
OAc	Acetate anion
OPiv	Pivalate anion
OTf	Trifluoromethanesulfonate anion

Pd/C	Palladium on Carbon
Ph	Phenyl
Proton sponge	1,8-Bis(dimethylamino)naphthalene
<i>p</i> -tolCC	4-Ethynyltoluene
<i>t</i> -Bu	Tertiary butyl
TFA	Trifluoroacetate anion
THF	Tetrahydrofuran
TMS	Trimethylsilyl
Tp	Tris(pyrazolyl)borate
TscydN	<i>N-p</i> -Tosyl-1,2-cyclohexanediamine
TsDPEN	<i>N-p</i> -Tosyl-1,2-diphenylethylenediamine

List of Contents

1: Chapter 1 – General Introduction	1
1.1: Bifunctional Catalysis	3
1.2: C-H Activation	10
1.2.2: Mechanisms and Applications of C-H Activation	12
1.2.3: Control of the Regioselectivity of C-H Activation	23
1.3: N-Heterocyclic Carbenes	26
1.3.2: Synthesis of Transition Metal NHC Complexes	29
1.4: Late Transition Metal Amide Complexes	31
1.4.1: Bonding and Reactivity of Late Transition Metal Amides	31
1.5: Aims and Objectives	35
2: Chapter 2 – Synthesis of Amine-Functionalised Imidazolium Salts	38
2.1: Introduction	39
2.1.1: Synthetic Routes to Imidazolium Salts	39
2.1.1.1: Adding a C1 Unit to a Diimine	39
2.1.1.2: Condensation Onto a Pre-formed Aminal	40
2.1.1.3: From an N,N'-Disubstituted Formamidine	41
2.1.1.4: Heterocyclic Interconversion	43
2.1.1.5: Alkylation of N-Substituted Imidazoles	43
2.1.2: N-Donor Functionalised N-Heterocyclic Carbene Precursors	45
2.1.3: Aims and Objectives	49
2.2: Results and Discussion	52
2.2.1: Synthesis of Arylamino- <i>bis</i> -Imidazolium Salts	52
2.2.2: Synthesis of Arylamino Imidazolium Salts	55
2.3: Conclusions	60

2.4: Experimental	62
3: Chapter 3 – Synthesis and Reactivity of Complexes of Tridentate Amido-<i>bis</i>NHC Ligands	73
3.1: Introduction	74
3.1.1: Group 10 Metal Pincer Complexes	74
3.1.2: Group 10 Imidazolium NHC Pincer Complexes	76
3.1.3: Group 10 Amido Pincer Complexes	83
3.1.4: Aims and Objectives	89
3.2: Results and Discussion	90
3.2.1: Synthesis of CNC Group 10 Complexes	90
3.2.1.1: Synthesis of (CNC) Pd Complexes	90
3.2.1.2: Synthesis of (CNC) Pt Complexes	96
3.2.1.3: Attempted Synthesis of (CNC) Ni Complex	97
3.2.2: Reactivity of CNC Complexes	98
3.3: Conclusions	105
3.4: Experimental	107
4: Chapter 4 – Synthesis and Reactivity of Complexes of Bidentate Amino/Amido-NHC Ligands	116
4.1: Introduction	117
4.1.1: Amine/Amido-Functionalised (Bidentate) NHC Complexes	117
4.1.2: Aims and Objectives	122
4.2: Results and Discussion	124
4.2.1: Synthesis of (C,NR) complexes of Pd and Pt	124
4.2.2: Synthesis of Complexes of Unfunctionalised NHC Ligands	141
4.2.3: Synthesis of [C,NR] and [C,C] complexes of Ru, Rh and Ir	144
4.2.4: Reactivity of 4.36	157

4.3: Conclusions	165
4.4: Experimental	168
5: Chapter 5 – Bifunctional Catalysis by Amino/Amido-NHC Complexes	190
5.1: Introduction	191
5.1.1: Transfer Hydrogenation	191
5.1.2: Direct Arylation of Aromatic Heterocycles	194
5.1.3: Aims and Objectives	214
5.2: Results and Discussion	216
5.2.1: Transfer Hydrogenation of Acetophenone	216
5.2.2: Direct Arylation of Heterocycles	225
5.3: Conclusions	243
5.4: Experimental	245
6: Chapter 6 – Conclusions and Future Work	249
6.1: Conclusions	249
6.2: Future Work	257
7: Appendix	261
8: References	262

1: Chapter 1 – General Introduction

The synergistic effect of metal and ligand involved in bifunctional catalysis, where an electrophilic metal and nucleophilic ligand act in concert to activate the bonds of a substrate, allows low-energy pathways for catalytic reactions including transfer hydrogenation and hydroamination.¹⁻³ Bifunctional C-H activation⁴⁻⁷ is an emerging research area, which has been shown to allow efficient C-C coupling reactions;^{5,6,8,9} cross-couplings are of huge importance to organic synthesis, and are used routinely in the synthesis of pharmaceuticals and other fine chemicals.^{10,11} Catalytic C-H activation offers a low-energy, low-waste and low-cost alternative to traditional cross-coupling reactions, avoiding prefunctionalisation with a group that is wasted in the reaction.^{12,13}

N-heterocyclic carbenes (NHCs), as ligands, have had a huge impact on homogenous catalysis.¹⁴⁻¹⁶ Although NHC complexes have been well-studied, there are still few examples of bifunctional catalysis involving NHC complexes;¹⁷⁻²⁰ this lack of precedent is at least partly due to the fact that there are few functionalised-NHC complexes capable of participating in bifunctional catalysis.

The aim of this project was to synthesise complexes of the late transition metals with amino/amido-functionalised NHC ligands, containing a reactive metal-nitrogen bond suitable for bifunctional catalysis. We then investigated the ability of the amino/amido-NHC complexes to act as bifunctional catalysts in two reactions:

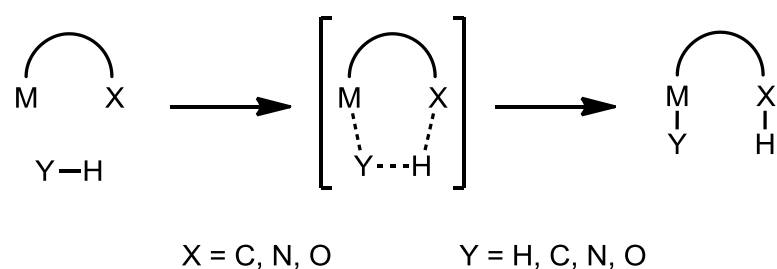
Chapter 1 – General Introduction

1. Transfer hydrogenation: a well-studied reaction that allowed us to compare the activity of the amino/amido-NHC complexes to known benchmarks.
2. Direct arylation of heteroarenes: the C-H activation step has significant challenges, including the control of regioselectivity and the need to develop milder reaction conditions.

This introduction will initially explain what bifunctional catalysis is, with a particular focus on how reactive M-X bonds can assist in bond cleavage during catalytic reactions. Secondly, C-H activation will be discussed, including a review of the mechanisms of C-H activation emphasising where these mechanisms have been implicated in catalysis. Thirdly, the properties of both metal N-heterocyclic carbene (NHC) and amido complexes will be described, including the properties of these ligands that make them suitable for bifunctional catalysis. Finally, the aims and objectives of this work will be stated in detail.

1.1: Bifunctional Catalysis

Metal-ligand bifunctional catalysis is where an electrophilic metal and nucleophilic ligand act synergistically to break and form chemical bonds, efficiently catalysing organic reactions.²¹ With a bifunctional catalyst, even unreactive H-H and C-H bonds can be activated (**Scheme 1.1**), allowing hydrogenation and C-C or C-X bond forming reactions, reactions that in some cases would be more difficult or impossible to achieve without the cooperation of metal and ligand.^{1,3,21,22}



Scheme 1.1: Metal-ligand bifunctional activation of Y-H bonds.

In order for bifunctional bond activation to take place, a complex must have both a relatively electrophilic metal centre that is able to form a new M-Y bond and a basic ligand that is able to pick up a proton. The ligand could have a monoanionic donor atom (alkoxide, carboxylate, amido ligands), a dianionic donor atom (imido, oxo, alkylidene), a trianionic ligand (nitrido, alkylidyne) or potentially a neutral donor atom with available lone pairs.

This work looked at metal-amido complexes, with a potentially reactive M-N motif. The metal center must be electrophilic and have a free d-orbital in order to receive electrons from the anionic Y group that is transferred from the metal. However, the electrophilicity of the metal must be balanced with the fact that the reactive lone pair

on the nitrogen donor can be made less nucleophilic by donation of the lone pair into empty d-orbitals on the metal;²³ therefore, we can conclude that d⁶ and d⁸ late transition metals in oxidation states of 2 or 3 could be the most capable of bifunctional reactivity. Further discussion into the bonding and reactivity of metal amides is included in Ch. 1.4.

The field most associated with bifunctional catalysis is that of hydrogen transfer reactions, such as the transfer hydrogenation of ketones and imines and the hydrogenation of unsaturated substrates with H₂. Several bifunctional catalysts for hydrogen transfer are known, **Figure 1.1**.

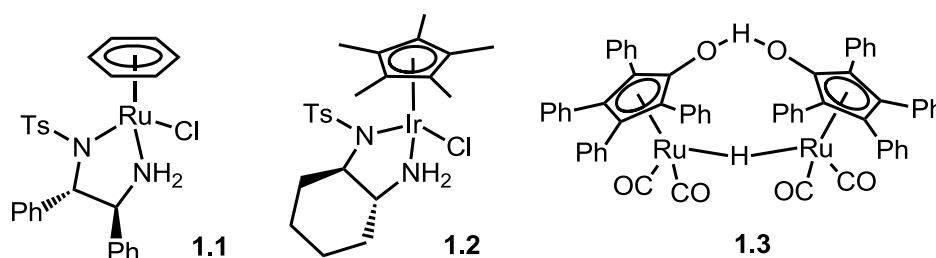
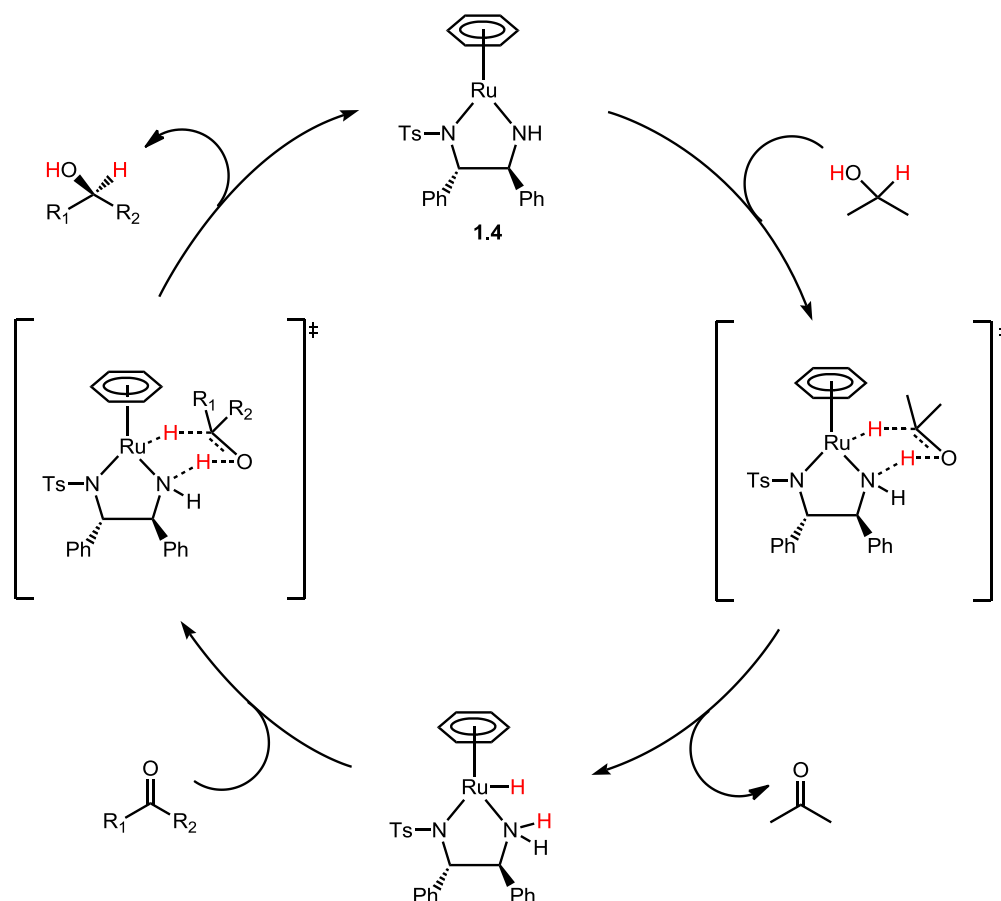


Figure 1.1: Examples of bifunctional hydrogen-transfer precatalysts.

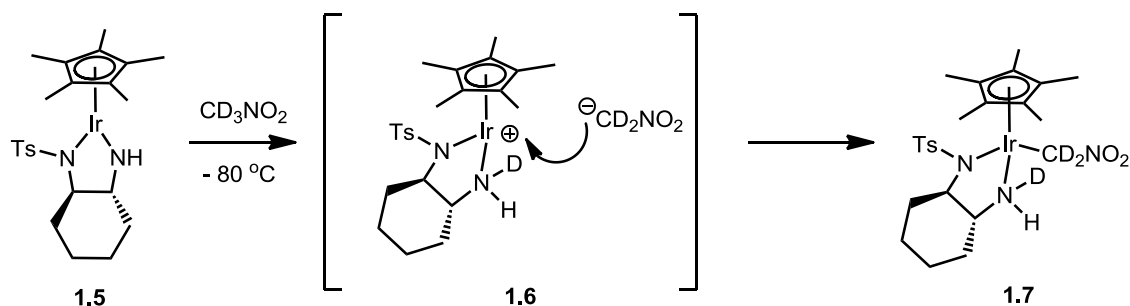
The ruthenium half-sandwich (diamine) complex **1.1** and similar iridium (**1.2**) and rhodium analogues are known to act as precatalysts for transfer hydrogenation of ketones and imines.^{24–26} It is important to note here that the species involved in the bond-cleavage event of transfer hydrogenation is a metal-amido complex (**1.4**), **Scheme 1.2**;²⁴ typically diamine or aminoalcohols are the ligands used. Transfer hydrogenation will be discussed in further detail in Ch. 5.1.1.



Scheme 1.2: Bifunctional mechanism of transfer hydrogenation of ketones by Ru(arene)(diamine)X precatalysts.

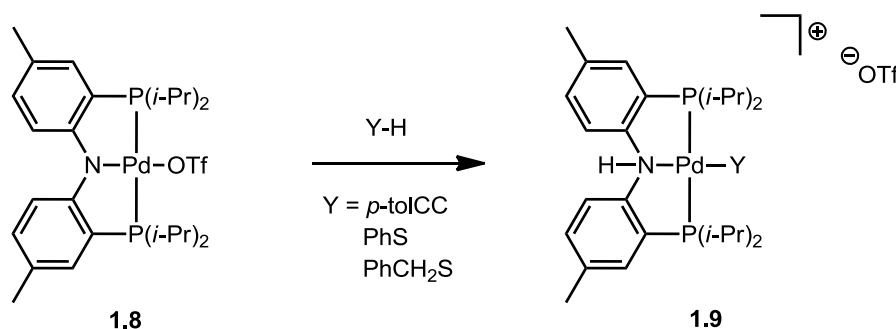
Ruthenium and iridium diamides formed from the amide-amine complexes **1.1** and **1.2** have also been shown to activate acidic C-H bonds, such as those of nitromethane, acetone, phenylacetylene and 1,3-dicarbonyl compounds.^{3,27} Few catalytic reactions involving this C-H activation pathway have been investigated, primarily asymmetric Michael additions of 1,3-dicarbonyl compounds to nitroalkenes or cyclic enones;^{28–30} in this regard, the bifunctional reactivity of metal amides with C-H bonds is yet to be fully explored. However, the reaction of iridium amide **1.5** with d₃-nitromethane, **Scheme 1.3**, appears to occur by deprotonation of the acidic substrate by the amido

ligand, forming an ion-pair (**1.6**); hence, the deprotonation and metallation steps may not be concerted in all cases.³



Scheme 1.3: Deprotonation of d_3 -nitromethane by an iridium amido complex.

1,2-Addition of Y-H (Y = H, C(sp), S) bonds to a palladium amide has been observed for PNP pincer palladium complex **1.8**, **Scheme 1.4**.³¹ The nitrogen-based lone pair acts to pick up the proton as the Y fragment coordinates to the cationic Pd centre. It was found that Y-H cleavage was disfavoured if Y is a strong base with at least two lone pairs available; the protonated nitrogen of **1.9** was easily deprotonated by weak bases, suggesting that the Pd-NHAr₂ fragment is relatively acidic.

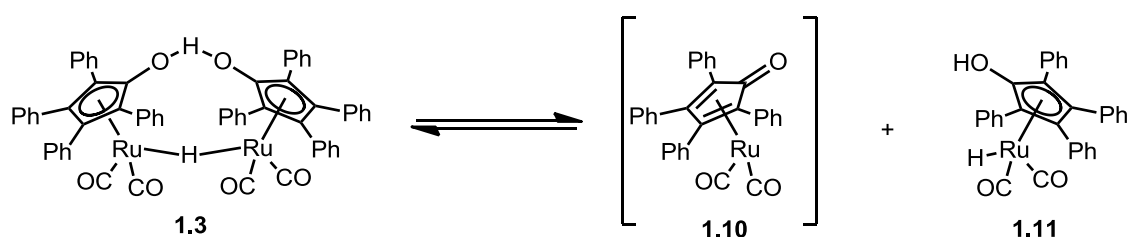


Scheme 1.4: 1,2-Addition of Y-H to (PNP)PdOTf **1.8**.

Shvo's complex, **1.3**, has been extensively studied as both a transfer hydrogenation and H₂-hydrogenation precatalyst; in this case, the basic site on the ligand involved in bond cleavage is remote and not directly bound to the metal.^{32,33} Complex **1.3** is a

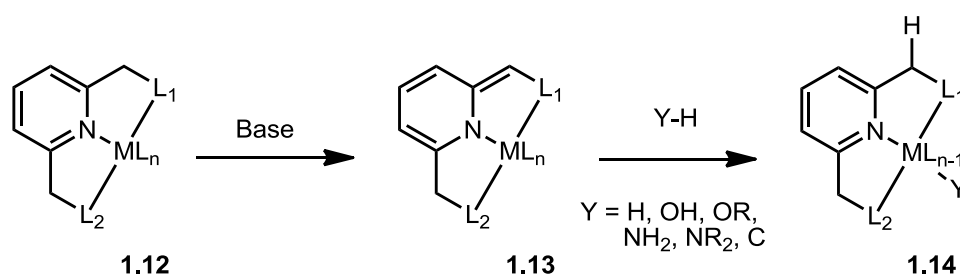
heterodimer of oxidising (**1.10**) and reducing (**1.11**) complexes, which form upon dissociation of **1.3** in solution (**Scheme 1.5**). Complexes **1.10** and **1.11** can be interconverted by transfer of H₂ to or from an acceptor or donor, respectively.

Mechanistic studies of the hydrogenation reactions of **1.3** suggest that the reactivity is bifunctional in nature, with the hydroxy hydride complex **1.11** transferring hydrogen to the unsaturated substrate.³³ Bifunctional catalysis allows for more selectivity than traditional heterogeneous hydrogenation catalysts such as Pd/C or Raney nickel.



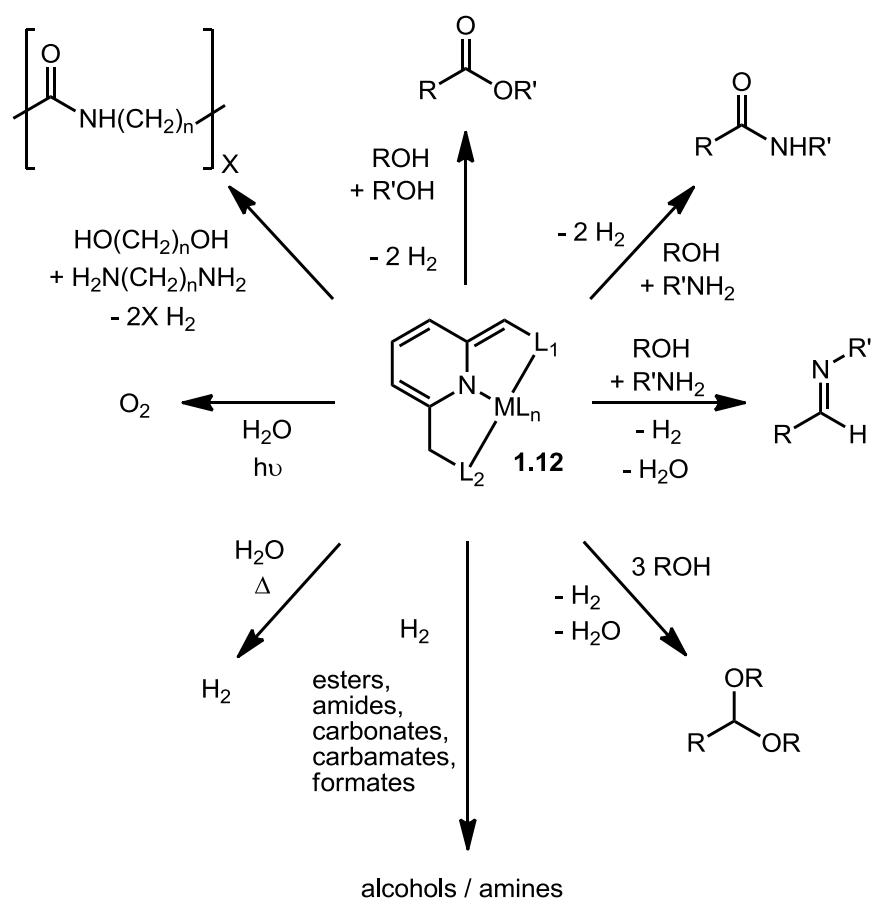
Scheme 1.5: Dissociation of Shvo's complex **1.3** in solution to give active oxidation/reduction catalysts.

Another form of bifunctional catalysis is based upon complexes containing a ligand which can activate substrates by aromatisation-dearomatisation; a Y-H bond is broken with the proton accepted by a remote C=C bond on the ligand, **Scheme 1.6**.³⁴ Pyridine-based pincer complexes **1.12**, where L₁ and L₂ are nitrogen or phosphorus donors, can deprotonate at the carbon adjacent to the pyridine ring, resulting in dearomatisation of the pyridine ring. The ligand and metal can now activate chemical bonds in a bifunctional fashion, resulting in protonation of the ligand and rearomatisation of the pyridine ring. This aromatisation acts as a driving force for the activation of the substrate.



Scheme 1.6: Activation of protic substrates by ligand aromatisation-dearomatisation.

The discoverer of this reactivity, Milstein, has since demonstrated the ability of complexes **1.13** to promote or catalyse several highly desirable reactions under mild conditions (**Scheme 1.7**), including the dehydrogenative coupling of alcohols and amines to esters,³⁵ amides,³⁶ imines³⁷ and acetals,³⁸ the thermal and photochemical activation of water to give H₂ and O₂ sequentially,³⁹ and the selective hydrogenation of difficult carbonyl substrates (including esters,⁴⁰ amides,⁴¹ carbonates, carbamates and formates⁴²) directly to alcohols and amines. The mild and environmentally benign conditions for these reactions are facilitated by the bifunctional mechanisms accessible to the dearomatised complexes **1.13**.³⁴ In order to participate in this form of bifunctional reactivity, a ligand must have a double bond adjacent to a dearomatised ring; however, L₁ and L₂ can be diverse, with amine, pyridine and phosphine donors used.



Scheme 1.7: Catalytic reactivity of complexes that operate by bifunctional ligand aromatisation-dearomatisation.^{35–43}

Although bifunctional catalysis has been a topic of research interest for over 15 years, there are currently few examples of NHC complexes involved in bifunctional catalysis.^{17–20}

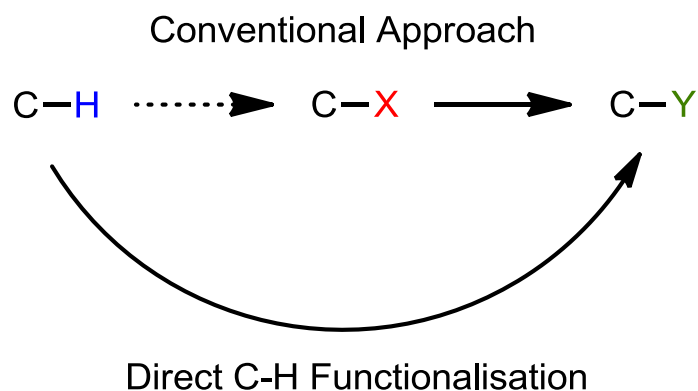
Bifunctional mechanisms are also implicated in the important field of C-H bond activation. C-H activation is an aspect of bifunctional catalysis that we were interested in exploring, and will be discussed further in the next section.

1.2: C-H Activation

The work in this thesis will include the study of aryl C-C cross-couplings where one partner is coupled through a C-H bond, this is termed direct arylation. An introduction to the direct arylation of heteroarenes is discussed in Ch. 5.1.2; however, a general overview of organometallic C-H activation and a discussion of the mechanisms through which C-H activation proceeds will be given here.

The ubiquitous C-H bond is found throughout organic chemistry, and is generally seen as inert due to the high strength (average C-H bond $\Delta H = 412 \text{ kJ mol}^{-1}$ at 298 K) and low polarity (Pauling values for electronegativity: C = 2.5; H = 2.1) of the bond.⁴⁴ C-H bonds are, therefore, rarely used as a site for synthetic chemistry, or replaced by a functional group to allow chemistry to take place. Traditional methods of direct C-H functionalisation include removal of H^+ by strong base, radical abstraction of H^\cdot with a radical reagent and electrophilic removal of H^- using a superacid.¹² These conventional approaches often require harsh conditions, are rarely functional group tolerant and can be unselective or have selectivity governed by the substrate.

Direct C-H bond functionalisation (**Scheme 1.8**) through activation of a C-H bond by a transition metal (organometallic C-H activation) is potentially a more desirable approach than the conventional methods, enabling catalytic functionalisation with less waste, improved functional group tolerance, milder conditions and high control of selectivity.

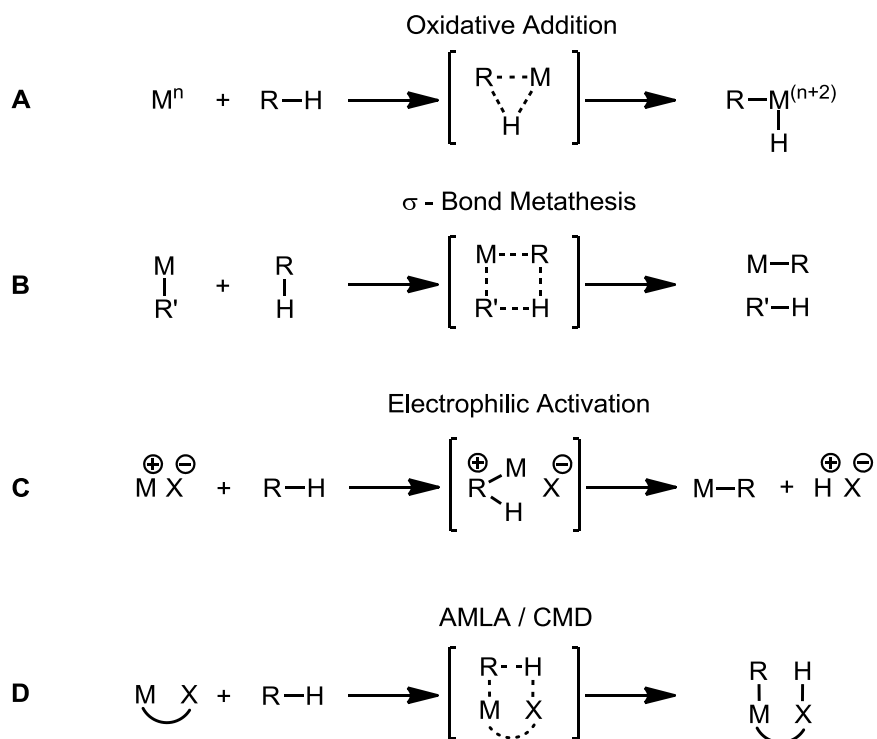


Scheme 1.8: Conventional and direct approaches to C-H functionalisation.

Conventional approaches to C-H functionalisation are indirect, using a substrate where the C-H bond has been converted to a more reactive C-X bond, for example where X = a halogen. The synthesis of drugs and other high-value chemicals requires the formation of carbon-carbon and carbon-heteroatom bonds which are often made using a conventional approach. Utilising C-H activation could considerably reduce industrial waste and costs and allow target molecules to be accessed rapidly in a step-economical manner. The pharmaceutical industry has recognised these advantages: aromatic C-H activation with a view to cross-coupling was identified as the top aspirational reaction for green synthetic chemistry in a survey of the six largest pharmaceutical companies.⁴⁵ In complex organic synthesis, selectivity of C-H functionalisation is potentially a major challenge, as most organic molecules have many C-H bonds; however, transition metal complexes can be tuned by modification of supporting ligands to potentially give highly selective reactions.⁴⁶

1.2.2: Mechanisms and Applications of C-H Activation

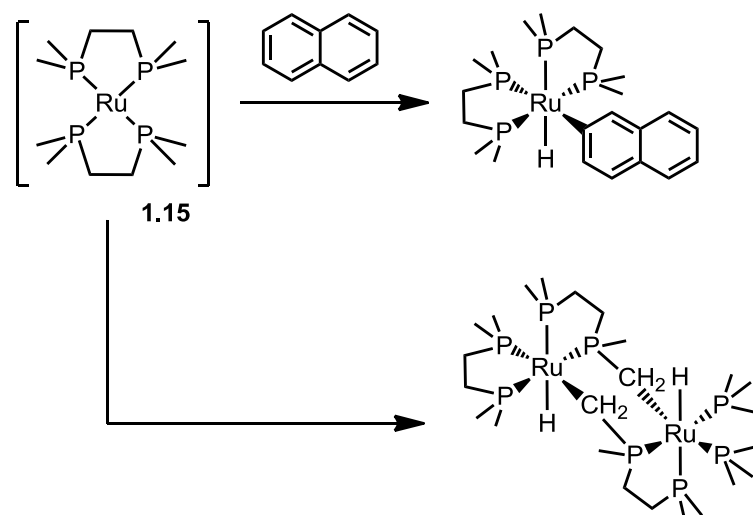
Several mechanisms for organometallic C-H activation have been identified, **Scheme 1.9**. Only two-electron C-H activation processes will be discussed in this introduction, not radical-type one-electron processes.



Scheme 1.9: Mechanisms of C-H activation.

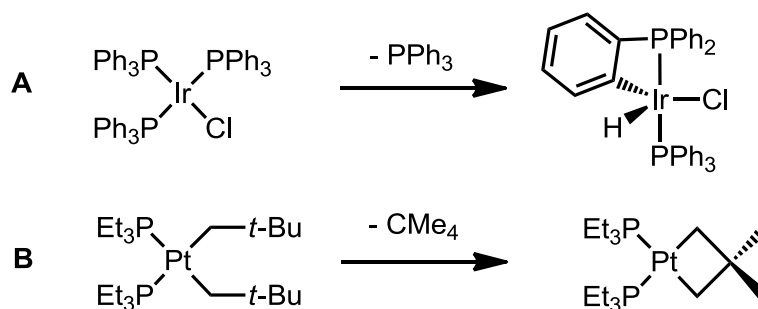
Oxidative addition (OA) of a C-H bond to a transition metal (**Scheme 1.9A**) can typically occur when the metal is electron-rich and coordinatively unsaturated. C-H activation subsequently increases the oxidation state and coordination number of the complex by two to yield a metal hydride with a metal-carbon bond.

The first report of oxidative addition of a C-H bond was by Chatt; he observed that the Ru^0 complex $Ru(dmpe)_2$ (**1.15**) could activate the sp^2 C-H bonds of naphthalene or the methyl sp^3 C-H of the dmpe ligand, **Scheme 1.10**.⁴⁷



Scheme 1.10: Oxidative addition of C-H bonds to $Ru(dmpe)_2$.⁴⁷

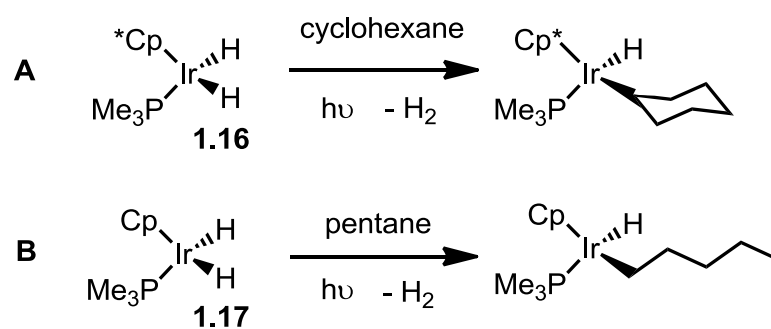
Other examples of intramolecular oxidative addition of a ligand C-H bond were later noted by Bennett⁴⁸ (aryl sp^2 C-H, **Scheme 1.11A**) and Whitesides⁴⁹ (aliphatic sp^3 C-H, **Scheme 1.11B**).



Scheme 1.11: Intramolecular oxidative addition of sp^2 (A) and sp^3 (B) C-H bonds.

Bergman⁵⁰ and Graham⁵¹ have both reported the intermolecular oxidative addition of alkane sp^3 C-H bonds by half-sandwich Ir complexes **1.16** and **1.17**, **Scheme 1.12**.

These complexes first undergo photodissociation of H_2 to form active Ir^I species which can insert into the C-H bond. Interestingly, these complexes show high selectivity for the activation of terminal C-H bonds, which are stronger than internal C-H bonds.



Scheme 1.12: Intramolecular oxidative addition of alkane C-H bonds.

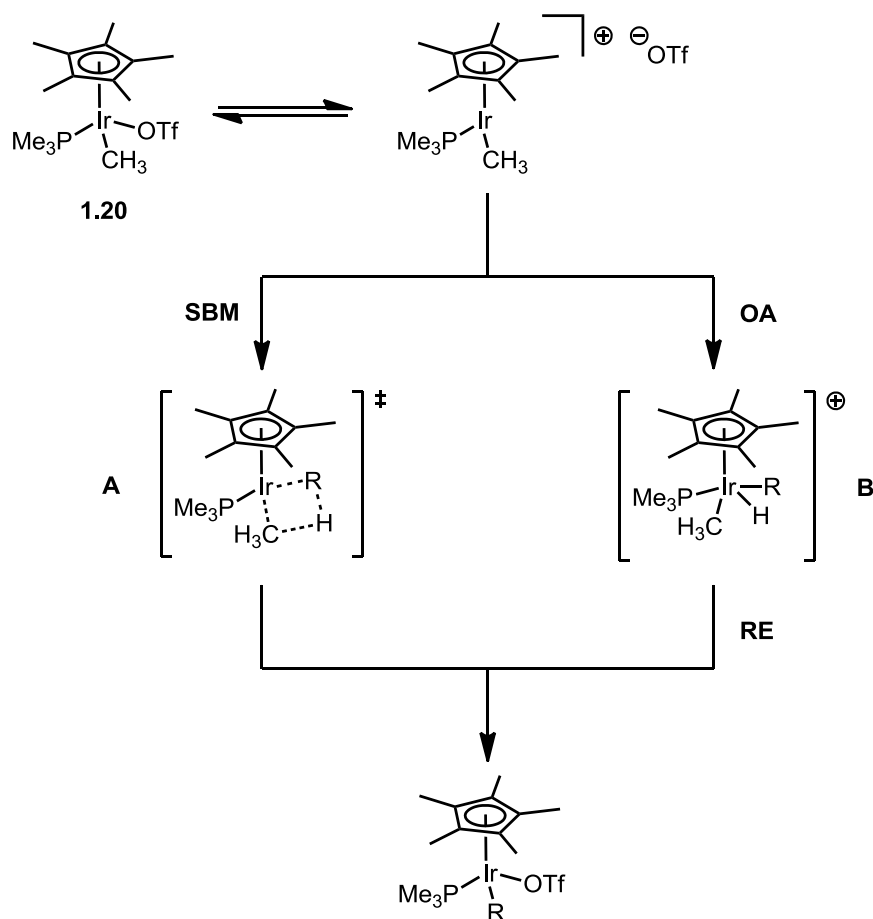
For a catalytic C-H functionalisation to occur by an oxidative addition / reductive elimination cycle, the complex in the low-oxidation state must favour oxidative addition of the C-H bond, while the complex in the high-oxidation state must favour reductive elimination of the oxidised product. Tuning the metal-ligand system to achieve this can be difficult, as facilitating oxidative addition can often make the corresponding reductive elimination more difficult. Also, C-H oxidative addition to already functionalised molecules can be problematic as weak C-halogen, C-heteroatom or even C-C bonds can preferentially add to the complex.

σ -Bond metathesis (SBM) C-H activation (**Scheme 1.9B**) is a mechanism observed in which two σ -bonds are broken and two new σ -bonds are created in a concerted fashion *via* a 4-membered transition state, with no change in metal oxidation state. This is most commonly observed in d^0 metal alkyl complexes which have no d electrons to participate in redox processes such as oxidative addition.

SBM of C-H bonds was first observed by Watson: exchange of the methyl ligand of Cp^*_2LuMe (**1.18**) with $^{13}\text{CH}_4$ in a cyclohexane solution, suggesting a mechanism with a 4-membered transition state.⁵² Bercaw *et al.* later reported a detailed study of Cp^*ScR ($\text{R} = -\text{CH}_3, -\text{C}_6\text{H}_5, -\text{C}_6\text{H}_4\text{CH}_3, -\text{CH}_2\text{C}_6\text{H}_5$) (**1.19**) with similar reactivity towards

several substrates including H₂, C-halogen and sp, sp² and sp³ C-H bonds, presenting evidence for a concerted SBM process.⁵³

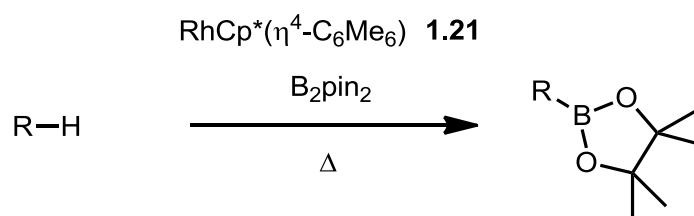
Distinguishing between oxidative addition and SBM can sometimes be only achieved by computational methods.⁴ Bergman has reported the C-H activation of alkanes by IrCp*(PMe₃)(Me)(OTf) **1.20**, which could proceed by a SBM mechanism (**Scheme 1.13A**) or an OA/RE process *via* an Ir^V species (**Scheme 1.13B**).^{54,55} Experimental data was insufficient to assign the mechanism; however, Hall *et al.* performed DFT calculations for the reaction of the [IrCp(PMe₃)(Me)]⁺ species with methane and found that an OA/RE mechanism was lower in energy, and no SBM transition state could be found.^{56,57} Further work by several groups^{58–61} has suggested that the SBM and OA/RE mechanisms are two extremes of a continuum (defined by Hall⁶²), with intermediate mechanisms that are dependant on the interaction between the metal and the substrate in the transition state.



Scheme 1.13: Possible mechanisms of C-H activation for $\text{IrCp}^*(\text{PMe}_3)(\text{Me})(\text{OTf})$ (**1.20**).

Catalytic C-H functionalisation by SBM is relatively unknown, as the mechanism usually results only in swapping of alkyl/aryl groups on the metal. Hartwig *et al.* have investigated a system for catalytic C-H borylation of alkanes by a dimeric boron pinacolate reagent, B_2pin_2 , catalysed by $\text{RhCp}^*(\eta^4\text{-C}_6\text{Me}_6)$ **1.21**, **Scheme 1.14**.^{63,58}

Calculations and some experimental evidence suggest an SBM mechanism for these reactions, assisted by the coordinated boron atom; however, an alternative higher energy pathway involving OA/RE is also possible.⁶⁴



Scheme 1.14: Catalytic alkane C-H borylation.^{63,58}

Electrophilic C-H activation (**Scheme 1.9C**) proceeds when a highly electrophilic metal centre attacks an electron rich carbon atom, forming a cationic intermediate which then loses a proton. Electrophilic C-H activation was first noted by Shilov in 1969, with methane H/D exchange observed in a D₂O solution of K₂PtCl₄.⁶⁵ Continuing research led to the mild catalytic methane oxidation system which is known as Shilov chemistry, **Scheme 1.15A**, which is a selective method for methanol synthesis.⁶⁶ A mild, selective catalytic method for methanol production from methane would be highly useful, as methanol is a useful liquid fuel and chemical feedstock, and methane is abundant in natural gas and oil fields but difficult to transport and use. Current technology for methanol production from methane involves the steam reforming of methane to syngas, followed by reaction of syngas over a Cu/ZnO/alumina catalyst to methanol, **Scheme 1.15B**; although catalytic both these processes require high temperature and pressure.⁶⁷ Unfortunately, although catalytic in Pt^{II}, Shilov's chemistry requires a stoichiometric Pt^{IV} oxidant, which is extremely expensive and limits the utility of this process.

an external or internal base, with a 4- or 6-membered transition state invoked in the C-H cleavage, rather than a Wheland-type cationic intermediate.^{4,72,73} This process, termed AMLA (Ambiphilic Metal-Ligand Activation) by Davies and Macgregor,⁴ or CMD (Concerted Metallation-Deprotonation) by Fagnou,⁶ is bifunctional in nature.

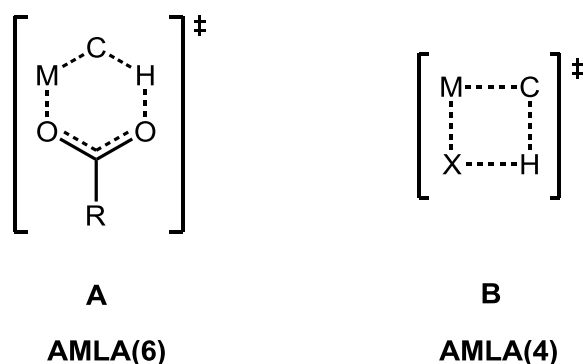


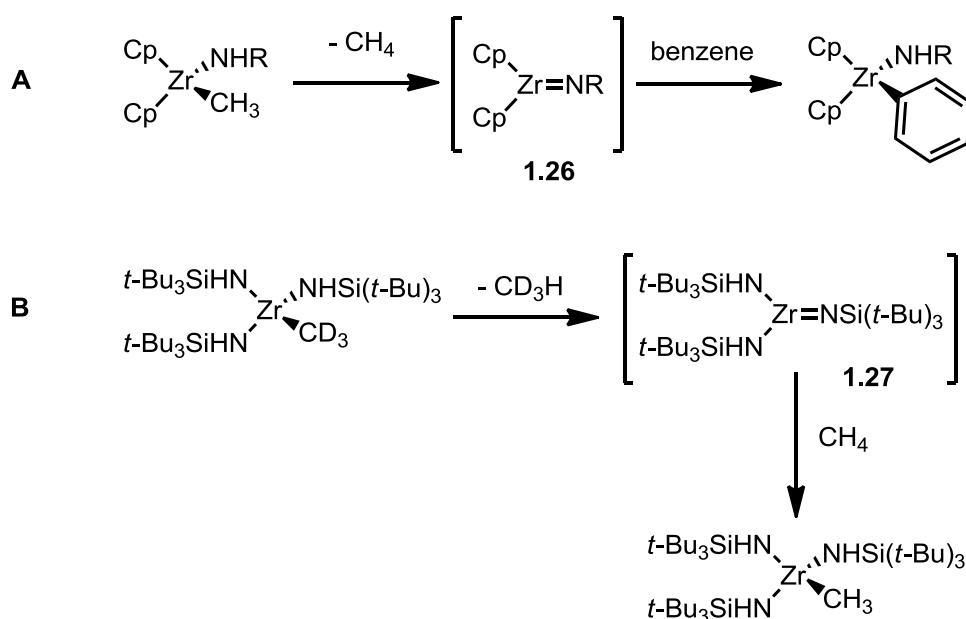
Figure 1.2: AMLA transition states for C-H activation.

AMLA proceeding *via* a 6-membered transition state (AMLA(6) or 1,4-addition, **Figure 1.2A**) generally involves the use of a metal complex along with a coordinated carboxylate base. Fagnou *et al.* have developed a catalyst system for direct arylation where C-H activation is carried out by a bifunctional Pd-pivalate intermediate that is derived from Pd(OAc)₂, pivalic acid and a carbonate base.^{5,8,74-76} Direct arylation will be further discussed in Ch. 5.1.2.

AMLA has also been demonstrated by the cyclometallation of 2-substituted pyridines by [IrCl₂Cp*]₂ (**1.23**), [RhCl₂Cp*]₂ (**1.24**) and [RuCl₂(*p*-cymene)]₂ (**1.25**) dimer complexes in the presence of acetate.⁷⁷ Indeed, sp³ C-H activation was noted in the reaction of acetyl pyridine with the Rh dimer (**1.24**). Computational and synthetic studies of the cyclometallation of dimethylbenzylamine with the Ir dimer (**1.23**) in the presence of several different carboxylate bases suggested that the rate determining step in this

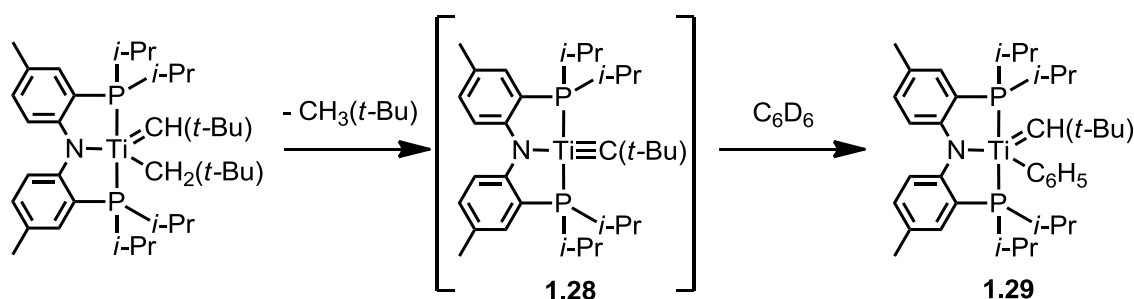
system is not the C-H activation, but rather the change in coordinated acetate from bidentate to monodentate on the iridium centre.⁷⁸ Moreover, DFT calculations suggested that even weak bases such as triflate could promote the C-H bond cleavage, indicating the ease in which an intramolecular base can assist C-H activation by an electrophilic metal centre.⁷⁸

Examples of AMLA where a 4-membered transition state is involved (AMLA(4), **Figure 1.2B**) are also known as 1,2-addition, as they result in the addition of a C-H bond across a metal-heteroatom bond. In 1988, Bergman⁷⁹ and Wolczanski⁸⁰ independently reported that transient Zr^{IV} imido complexes **1.26** and **1.27** could activate a C-H bond across the M=N bond, **Scheme 1.16**. A detailed computational study by Sakaki *et al.* suggests that an unoccupied metal d₂₂ orbital accepts electrons from the C-H bonding orbital, while the occupied d_π-p_π M-N bonding orbital (with significant lone-pair character on N) acts as a base to pick up the proton.⁸¹



Scheme 1.16: Activation of alkane C-H bonds by Zr imido complexes.^{79,80}

Similarly, metal alkylidyne complexes of early transition metals can activate C-H bonds; recent work by Mindiola *et al.* on the transient titanium alkylidyne complex **1.28** has shown that the metal-carbon triple bond can activate an aryl or SiMe₄ C-H bond by AMLA(4) to form a stable alkylidene **1.29**, **Scheme 1.17**.⁸²



Scheme 1.17: Activation of C-D of C₆D₆ by Ti alkylidyne **1.28**.⁸²

Late transition metal-heteroatom single bonds can also participate in AMLA(4) processes. Periana *et al.* showed that [Ir(acac)₂(OMe)(py)] (**1.30**) is capable of activating the C-H bond of benzene.⁸³ The mechanism was initially reported as an OA or SBM process, but further computational studies suggested that the lone-pair on the alkoxy ligand helped to remove the proton from benzene.^{72,73,84,85} Hence, an AMLA mechanism appears to be operating here.⁸⁴ Furthermore, the information gathered on this mechanism allowed the authors to suggest strategies for designing M-X type C-H activation catalysts, including focusing on d⁶ or higher d-electron count metal centres with filled d orbitals that repulse the M-X lone pair, along with reducing the electron density on the metal centre.⁸⁴ Obviously these two strategies are potentially at odds with each other, and therefore a balance of electron density on the metal is necessary.

Similarly, Gunnoe *et al.* reported evidence for the 1,2-addition of a C-D bond of d₆-benzene to an Ru-O bond in [TpRu(PMe₃)₂OH] (**1.31**).⁸⁶ The Ru-Ph intermediate could

Chapter 1 – General Introduction

not be isolated but catalytic H/D exchange was observed in D₂O at 100 °C.

Computational results agreed with the proposed AMLA mechanism.^{7,87}

It is clear from these examples that AMLA encompasses a broad mechanistic spectrum, being intermediate between two extremes of electrophilic activation (by the metal) and deprotonation (by the basic ligand).

The use of a bifunctional complex to allow mild, catalyst controlled aryl C-C coupling reactions *via* an AMLA(4) mechanism is an aim of the research in this report. There are, as noted above, currently very few known systems for C-H activation that involve an AMLA(4) mechanism; catalytic applications of AMLA(4) have not been fully explored. We hoped to explore whether an AMLA(4) mechanism can allow lower energy pathways for C-H activation than electrophilic/OA mechanisms, as has been observed with AMLA(6).^{4,78}

1.2.3: Control of the Regioselectivity of C-H Activation

The control of regioselectivity in C-H activation can often be a challenge; often in organic molecules several different C-H bonds are available to react. Several methods have been used to control regioselectivity in C-H activation, **Figure 1.3**.

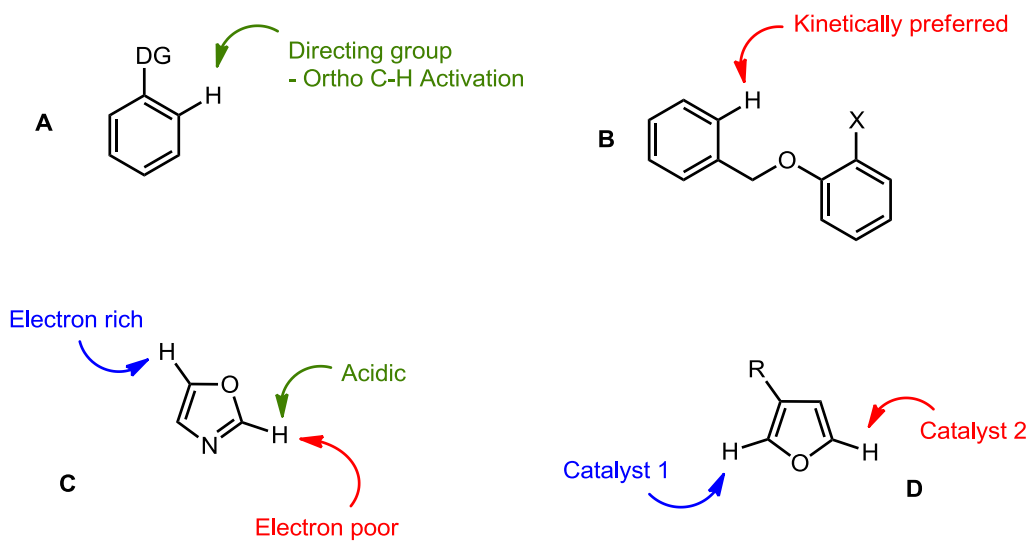


Figure 1.3: Influences on control of regioselectivity in C-H activation: Ortho-directing groups, **A**; intramolecular kinetic control, **B**; electronic factors of the substrate, **C**; catalyst control, **D**.

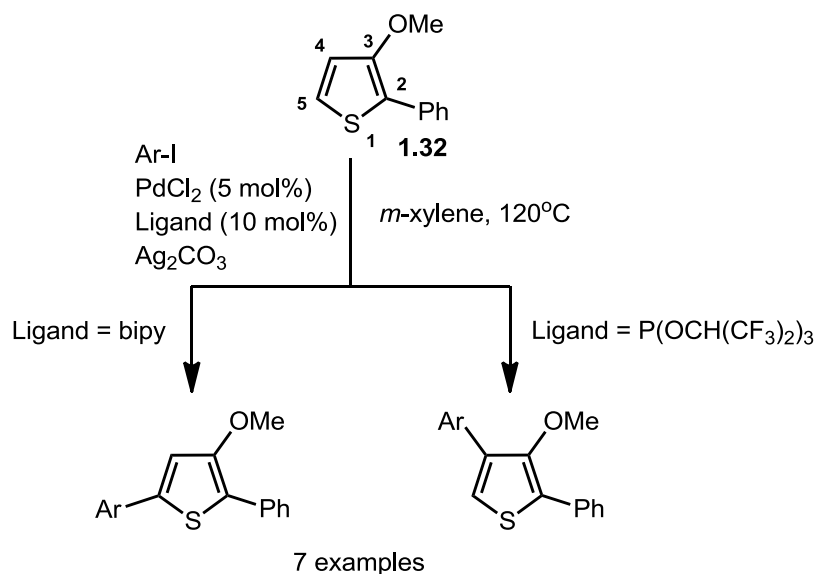
A common method of controlling C-H activation is to use a directing group (**Fig. 1.3A**), to which the metal complex coordinates, allowing metallation at the *ortho*- position on arenes, or the nearest available C-H site on non-aromatic substrates. A wide variety of directing groups have been investigated, including pyridine,^{88–91} oxazolines,⁹² other N-heterocycles,⁹³ ketones,⁹⁴ imines,^{95,96} carboxylic acids,⁹⁷ anilides,⁹⁸ ethers⁹⁹ and nitro groups.¹⁰⁰ Although the use of a directing group has proved to be a good general method to control the regioselectivity of C-H activation,

the selectivity is limited to the *ortho*- position on arenes; functional group tolerance in the reactions can also be an issue.

Intramolecular C-H activations (**Fig. 1.3B**) can be used to form biaryl molecules, with the C-H activation being directed to the most kinetically accessible site.^{8,101–103} In intramolecular C-H activation, the regioselectivity is typically very high; however, the reaction is limited to the most accessible carbon and the tethered aryl starting materials must first be synthesised.

Electronic factors (**Fig. 1.3C**) are a significant influence on the regioselectivity of C-H activation on heteroarenes. Electron-rich C-H bonds are susceptible to electrophilic-type C-H activations, while electron-poor C-H bonds are susceptible to deprotonations or nucleophilic C-H activations. Understanding the electronic factors controlling C-H activation of heteroarenes has allowed site-selective direct arylation reactions,^{104,105} which are reviewed in further detail in Ch. 5.1.2.

The least common method to affect the regioselectivity of C-H activation is through catalyst control (**Fig. 1.3D**), where an appropriate metal and ligand combination are used in order to selectively activate a C-H bond. An example of catalyst control is found in the direct arylation of thiophenes (**Scheme 1.18**), where changing the ligand used in concert with palladium dichloride can change the selectivity for arylation at C4 or C5, by affecting the mechanism of C-H activation.^{106,107}



Scheme 1.18: Ligand-controlled change of direct arylation regioselectivity on substituted thiophene **1.32**.

Catalyst control is a highly desirable method for control of regioselectivity, as it could ultimately be possible to simply choose a catalyst/ligand suitable for activating a particular C-H bond. Unfortunately, very few examples of catalyst control of C-H activation are known; we hoped to investigate if an AMLA(4) C-H activation mechanism can offer catalyst control by modification of ligands. An AMLA(4) mechanism can involve a ligand that is more basic than the carboxylates featured in the AMLA(6) mechanism, for example amides or alkoxides; it is possible that strongly basic ligands will alter the regioselectivity of C-H activation towards a site that favours deprotonation. These aspects of regioselectivity of AMLA(4) C-H activation have not been addressed, and may allow catalyst control of regioselectivity.

We therefore decided to investigate if amine-/amido-NHC complexes of late transition metals can facilitate an AMLA(4) mechanism of C-H activation and offer catalyst control of regioselectivity of C-H activation.

1.3: N-Heterocyclic Carbenes

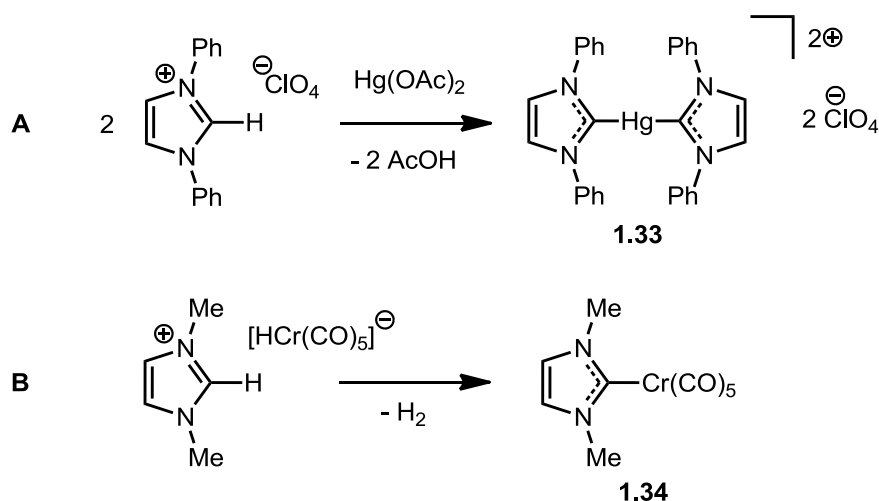
N-Heterocyclic carbenes (NHCs) are heterocycles in which at least one carbon in the ring has only 6 electrons, existing as a stable, singlet carbene, **Figure 1.4**. Due to the singlet nature of the carbene, NHCs have a single nucleophilic lone pair of electrons which allows them to act as 2-electron neutral ligands for metal centres.



Figure 1.4: An N-heterocyclic carbene.

NHCs have received much attention over the past 20 years as ligands for transition metal complexes. In terms of coordination chemistry, NHCs are comparable ligands to electron-rich alkyl phosphines, being strong σ -donors and weak π -backbonding acceptors.^{108,109}

The first metal-NHC complexes were synthesised as early as 1968, by the groups of Wanzlick¹¹⁰ (**1.33**, **Scheme 1.19A**) and Öfele¹¹¹ (**1.34**, **Scheme 1.19B**) by deprotonation of an imidazolium salt by the basic ligands of a metal complex.



Scheme 1.19: Synthesis of the first metal-NHC complexes.^{110,111}

However, it was not until the first isolated, stable N-heterocyclic carbene (**1.35**, **Figure 1.5**) was reported by Arduengo *et al.* in 1991 that NHC-metal complexes became a significant research topic.¹¹² NHC **1.35** was synthesised by deprotonation of an adamantyl-substituted imidazolium salt; initially it was believed that the steric bulk around the C2 carbon helped to stabilise the carbene and prevent dimerisation.¹¹² However, the Arduengo group later synthesised several other persistent carbenes, including the methyl-substituted carbene **1.36**, proving that imidazol-2-ylidenes are thermodynamically stable, not just kinetically stabilised by bulky substituents.¹¹³

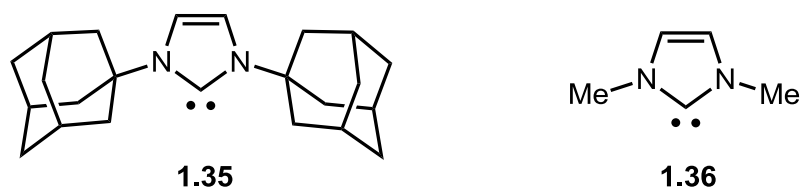


Figure 1.5: Arduengo's isolated stable NHCs.¹¹³

It is now generally accepted that the stability of imidazolyl N-heterocyclic carbenes results from a combination of electronic effects and the aromaticity of the carbene.¹¹⁴

Chapter 1 – General Introduction

The empty p-orbital on the carbene carbon is stabilised by electron density from the lone pairs of the adjacent nitrogen atoms. At the same time, the singlet carbene lone pair is stabilised by the inductive withdrawing effect of the nearby electronegative nitrogen atoms, as shown in **Figure 1.6**.

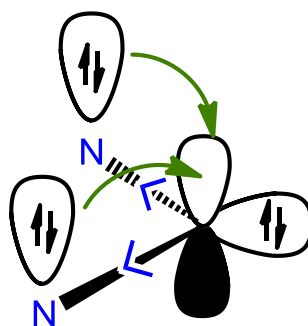


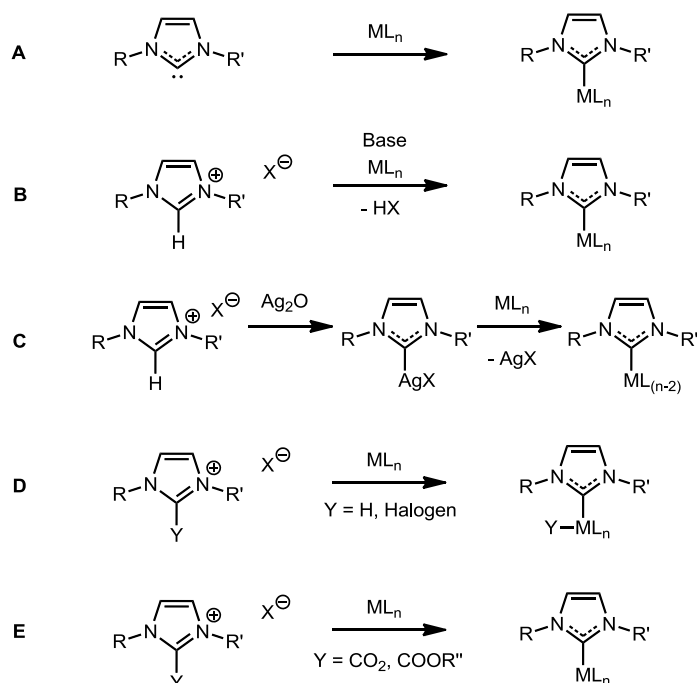
Figure 1.6: Stabilising effects on the carbene carbon in an NHC.

The first application of a metal-NHC complex in catalysis was by Herrmann *et al.*, who used [*cis*-(*IME*)₂PdI₂] (**1.37**) as a precatalyst for the Heck reaction. This initial report demonstrated the remarkable catalytic activity and long catalyst lifetime typical of metal-NHC complexes in catalytic reactions.¹¹⁵

Subsequently, transition metal-NHC complexes have been used as catalysts in a huge variety of reactions, showing considerable utility; this extensive topic has been reviewed recently by Nolan.^{14–16}

1.3.2: Synthesis of Transition Metal NHC Complexes

As metal-NHC complexes have become widespread, a variety of methods for their synthesis have been devised, **Scheme 1.20**.



Scheme 1.20: Methods of synthesis of metal-NHC complexes.

The most straightforward method for synthesis of NHC complexes is to react the free carbene with a metal complex containing either a displaceable ligand or having an unoccupied coordination site, **Scheme 1.20A**. Although this is used as a route to several complexes of NHCs, not all NHC ligands can be isolated as stable, free carbenes, and so this method is not generally applicable. The free carbenes are also very air and moisture sensitive, making their handling difficult. In order to circumvent these problems, the carbene is often generated *in situ*, by treatment of an azolium salt with a base in the presence of a metal salt, **Scheme 1.20B**. The choice of base often depends upon the azolium salt and metal salt used, and must generally be a strong,

non-nucleophilic base such as *t*-BuOK or KHMDS (pKa of imidazolium C2-H is 16-24);¹¹⁶ however, in certain cases basic ligands on the metal salt may deprotonate the azolium salt *via* a metal-assisted mechanism such as AMLA.¹¹⁷

Another widespread method for the synthesis of NHC complexes is transmetallation, most commonly from NHC-silver complexes, **Scheme 1.20C**.¹¹⁸ Ag₂O acts as a base to deprotonate the azolium salt and form a silver carbene; the NHC is then transferred to another metal with loss of AgX. The exclusion of the insoluble silver halide acts as a driving force for the transmetallation reaction. Although transmetallation from silver is by far the most common method, transmetallation from copper¹¹⁹ and nickel¹⁹ NHC complexes is known.

Oxidative addition of azolium C-H or C-X (X = halogen)¹²⁰⁻¹²² bonds to give an NHC-hydride or halide complex (**Scheme 1.20D**) is another complimentary strategy to synthesise NHC complexes; however, this method is not as generally applicable as those discussed above and requires a metal which is of low enough oxidation state to perform oxidative addition.

A more recent method for synthesising NHC complexes is to prepare an imidazolium-2-carboxylate, which upon addition to a metal salt produces an NHC complex with elimination of CO₂ or a carboxylic acid, **Scheme 1.20E**.^{123,124} Although applicable to many metals, this method has been shown to require two *cis*-vacant sites on the metal in order to allow C-C cleavage of the imidazolium-2-carboxylate.¹²³

We investigated several of these methods in subsequent chapters in order to synthesise the target amino-/amido-NHC complexes.

1.4: Late Transition Metal Amide Complexes

An amido ligand, in coordination chemistry, is one in which the donor atom is an anionic nitrogen, derived from either ammonia (parent amido) or a primary or secondary amine. Although alkali metal amides have been known since the late 19th century, and are used widely as strong bases in organic chemistry, very few transition metal amides were reported before 1980.¹²⁵ Since 1980, however, the field has rapidly expanded.^{23,125,126}

1.4.1: Bonding and Reactivity of Late Transition Metal Amides

The bonding picture for metal-amides is highly variable from complex to complex.^{23,125} σ -Bonding between the anionic amide and electrophilic metal is the primary interaction (**Figure 1.7A**); however, the lone pair on the amide can donate into an empty d-orbital on the metal to give some increased bond order. The degree of π -bonding can be assessed by the M-N bond length and the planarity of the nitrogen, with a more planar nitrogen suggesting increased donation of the N lone pair to the metal (**Figure 1.7B**). Amides can also act as a bridging ligand between two metal centres (**Figure 1.7C**), where the lone pair coordinates to another metal centre.

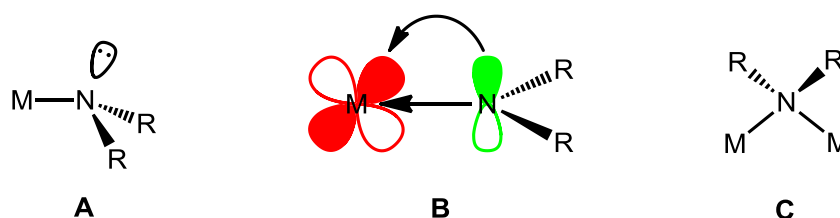
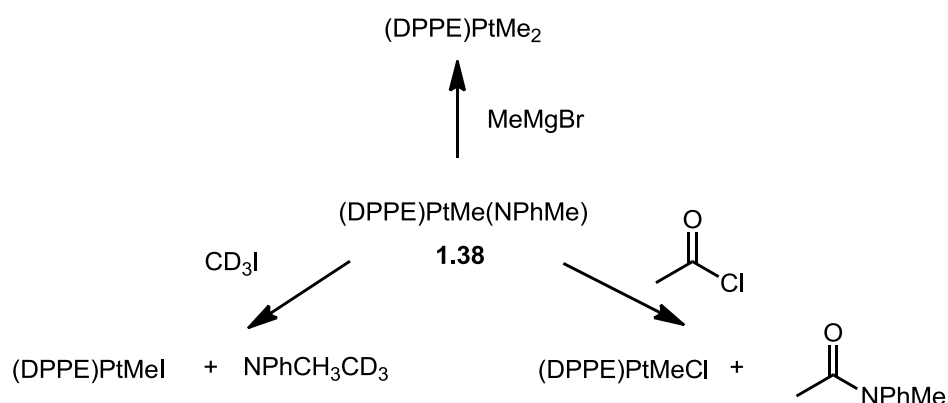


Figure 1.7: Bonding picture for metal amides: σ -bonding (sp^3) **A**; d_{π} - p_{π} interaction (sp^2) **B**; bridging of two metal centres **C**.²³

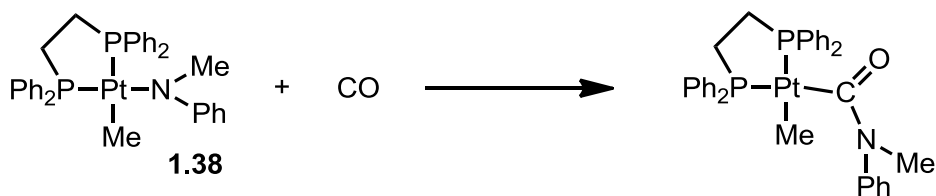
The amido ligand is generally considered to be a hard Lewis base, and could be considered a poor match for soft Lewis acid late transition metals. Indeed, most amide complexes are of the early transition metals, harder Lewis acids whose empty d-orbitals allow for multiple amide ligands with higher bond orders.¹²⁵ Filled d-orbitals on late transition metals tend to repulse the electrons in the N p-orbital, reducing the bond order and resulting in more lone pair character on nitrogen; however, examples of both planar and pyramidal nitrogen for late transition metal amides are known. Thermochemical data on M-N bond strengths is available for early transition metal amides (320-420 kJ mol⁻¹) but not for late transition metal amides.¹²⁵ Nevertheless, comparison of the relative bond energies of late transition metal amides (M-N) to the parent amine (N-H) allows estimation to show that these bonds are surprisingly strong when d_{π} - p_{π} repulsions are taken into account.¹²⁷ Also, 16-electron metal centres with available d-orbitals can be stabilised by donation from the amide filled p-orbital, as for early transition metals.¹²⁵ Stabilisation of the amide ligands by lone pair donation into a d-orbital can render the ligand inert to further reactivity. Availability of the nitrogen lone pair can make this ligand basic and nucleophilic; this can have implications on reactivity as discussed below.

Metal amides are basic in nature, and can be protonated.^{23,126} The metal-amide bond can also act as a nucleophile towards electrophiles and Lewis acids. Amido complex **1.38** will, for example, react with acetyl chloride, methyl iodide and Grignard reagents (**Scheme 1.21**).¹²⁸



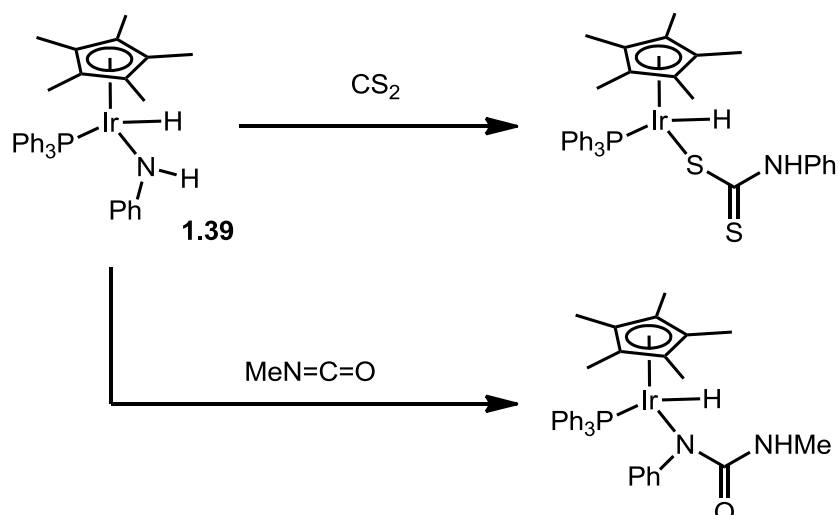
Scheme 1.21: Reactions of **1.38** with electrophiles.¹²⁸

Several small molecule ligands will undergo insertion into the metal amide bond. By far the most common is carbon monoxide, as shown in **Scheme 1.22** with the well-studied complex **1.38**, which interestingly shows preferential insertion into the M-N bond rather than the M-C bond to the methyl ligand.¹²⁸



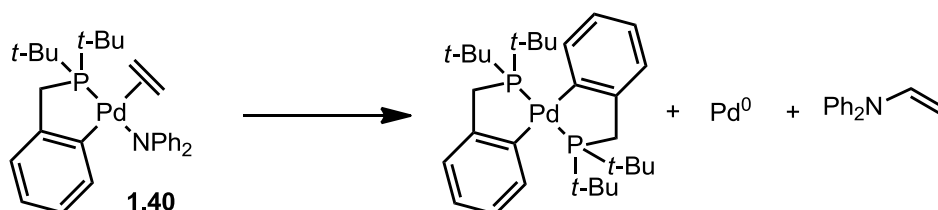
Scheme 1.22: Insertion of CO into the Pt-N bond of **1.38**.¹²⁸

Heterocumulenes (e.g. CO₂, CS₂, RNCO) have also been observed to react with metal amides, resulting in insertion of the heterocumulene into the C-N bond or N-H bond, for example with the iridium amide **1.39**, **Scheme 1.23**.¹²⁹



Scheme 1.23: Reaction of heterocumulenes with Ir amides.¹²⁹

Alkenes (usually electron-deficient) can also insert into a metal amide bond. Several examples of Pt complexes capable of this insertion have been described with acrylonitrile.¹³⁰ Pd amides can also undergo alkene insertion with electron-deficient dimethylacetylenedicarboxylate (DMAD),¹³¹ and more recently has been described with ethylene and octene, **Scheme 1.24**.¹³² Deuteration studies have shown that the insertion proceeds *via syn*-aminopalladation; electron-rich amide ligands react faster than electron-deficient amides.¹³² This step is an important part of the hydroamination catalytic cycle for some transition metal complexes.



Scheme 1.24: Insertion of ethylene into a Pd-N bond followed by β -H elimination to give an enamine.¹³²

1.5: Aims and Objectives

In this work, we aimed to synthesise complexes of amido-functionalised NHC ligands and investigate whether a bifunctional metal-nitrogen bond in an amido-NHC complex can facilitate bond cleavage steps in catalytic reactions. Specifically, we were interested in bifunctional C-H activation by an AMLA(4) mechanism, where the nitrogen donor would act synergistically with the metal to break a C-H bond. Although an AMLA(6) mechanism of C-H activation is known to occur both stoichiometrically and catalytically in several systems, catalytic AMLA(4) C-H activation is rare.⁴ Hence, catalytic C-H functionalisation systems based on AMLA(4) have not been well explored, and could potentially offer milder reaction conditions or catalyst control of regioselectivity.

The objectives of this project were to:

- 1.** Prepare amino/amido-NHC complexes of late transition metals with suitable M:L ratio and suitable supporting ligands
- 2.** Investigate the structure of appropriate complexes to attempt to gain insight into electronic properties of amide donor and metal
- 3.** Perform simple investigations into the reactivity of the amido-NHC complexes directed at catalytic applications
- 4.** Investigate the use of amino/amido-NHC complexes in bifunctional catalysis, specifically in transfer hydrogenation and direct arylation reactions
- 5.** Evaluate the performance of synthesised amino/amido-NHC complexes in catalysis in comparison to similar catalytic systems, in terms of activity and whether the regioselectivity of the reaction can be controlled.

The NHC donor ensured that the ligand remained bound to the metal in catalysis.

Electrophilic late transition metals (d^6 and d^8) were used, which, while having a free d-orbital to accept electrons, have mostly filled d-orbitals to prevent the reactive nitrogen lone pair being fully donated onto the metal centre. This choice of metal centre appears to be the best compromise to afford both an electrophilic metal and a basic amido ligand.

The NHC-tethered amino/amido ligands were introduced by deprotonation of amine-functionalised imidazolium salts, or by transmetallation from silver carbenes. The first aim was to synthesise the imidazolium salts (Chapter 2) by a route incorporating catalytic coupling reactions, aiming to make the synthesis both high-yielding and step, atom and cost efficient.

Once we synthesised the imidazolium salts, we prepared two types of complexes

(**Figure 1.8**): (i) Amido-*bis*NHC CNC pincer complexes of Pd, Pt and Ni: (CNC)ML (**Fig.**

1.8A) (Chapter 3); (ii) Amino-/amido-NHC complexes of Pd, Pt, Ru, Rh and Ir:

(C,NR)ML_n (**Fig. 1.8B**) (Chapter 4)

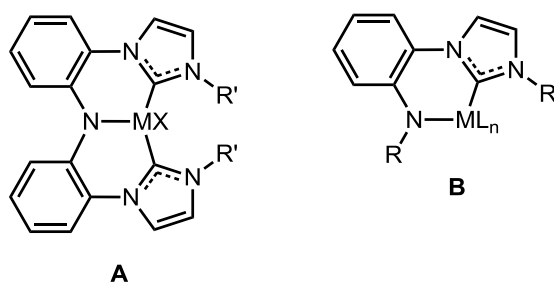


Figure 1.8: Target amino/amido-NHC complexes

Once both CNC and (C,NR) complexes were made (*Objective 1*), we investigated

whether the metal-nitrogen bond can allow the cleavage of C-H bonds. We tested a

Chapter 1 – General Introduction

(CNC)Pd complex for stoichiometric addition of C-H and H-H bonds; these reactions helped to determine if the metal-amido bond was capable of cleaving strong, non-polar bonds (*Objective 3*).

In Chapter 5, the catalytic reactivity of the amino/amido-NHC complexes is discussed. The complexes of Ru, Rh and Ir were investigated as catalysts/precatalysts for the transfer hydrogenation of ketones (*Objectives 4 and 5*). Transfer hydrogenation is known to occur by a bifunctional mechanism, and successful catalysis was an indicator for the involvement of the metal-nitrogen bond in bond breaking/forming reactions.

Several of the synthesised complexes were investigated as precatalysts for the direct arylation of heterocycles (*Objectives 4 and 5*); these reactions, when compared to reactions using suitable precatalysts that do not contain a reactive nitrogen donor ligand, allowed us to observe if C-H activation is occurring by an AMLA(4) mechanism. Also, we were able to observe if the ligands have any effect on regioselectivity of the C-H activation step, with a view to ligand control of selectivity in C-H functionalisation reactions; it was possible that the highly basic nature of an amido donor would allow AMLA reactions at C-H bonds that are more acidic.

2: Chapter 2 – Synthesis of Amine-Functionalised Imidazolium Salts

This chapter will describe the synthesis of amine-tethered imidazolium salts as ligand precursors for amino-/amido-NHC metal complexes; these complexes will be used to investigate if an M-N bond can participate in bond cleavage in catalytic reactions. The imidazolium salts have both an amine functionality and are unsymmetrical around the imidazole ring, which presents an interesting synthetic challenge; most NHCs used as ligands in catalysis are symmetrical and/or unfunctionalised.

The synthesis of amino-/amido-NHC complexes derived from the imidazolium salts described in this chapter will be discussed in Chapters 3 and 4 and catalytic applications of these complexes will be described in Chapter 5.

2.1: Introduction

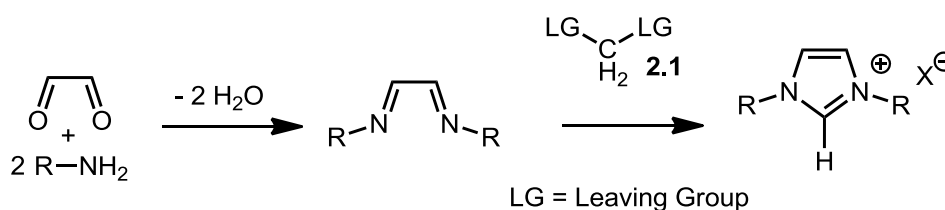
N-heterocyclic carbenes are, as previously discussed (Chapter 1.3), versatile ligands for transition metal complexes. This introduction will describe the synthesis of azolium salts as precursors to NHCs and a brief review of N-donor functionalised imidazolium salts and their applications.

2.1.1: Synthetic Routes to Imidazolium Salts

There are several types of N-heterocyclic carbene precursor,¹³³ this introduction will cover only the synthesis of precursors with an imidazolium core ring. Forming the imidazolium salt can be accomplished in several ways, these will be discussed here.

2.1.1.1: Adding a C1 Unit to a Diimine

Diimines are easily synthesised by double condensation of an alkyl/aryl amine with glyoxal, and can be used to synthesise imidazolium salts, **Scheme 2.1**. A 1,1-*bis*(electrophile) compound (**2.1**) reacts with the diimine to close the ring, affording the imidazolium salt.



Scheme 2.1: Formation of an imidazolium salt by adding a C1 unit to a diimine.

Several different 1,1-*bis*(electrophile) compounds have been used in this fashion to form imidazolium salts, including diiodomethane,¹³⁴ chloromethyl pivalate,¹³⁵

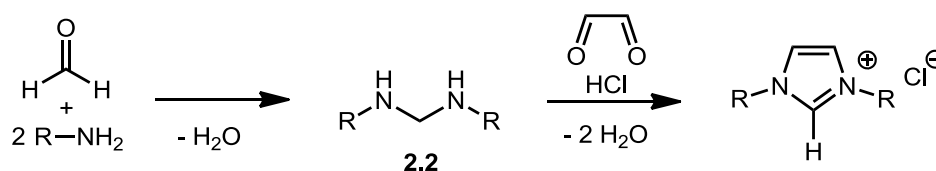
paraformaldehyde/acid,¹³⁶ and, most commonly, chloromethyl ethers.¹³⁷

Chloromethyl ethers have been extremely useful, giving high yields and good purity of resulting salts, even when the 'R' substituents have been very bulky aryl groups.

However, using a C1 unit can be a disadvantage when routes are needed to imidazolium salts with aryl substituents featuring an electron withdrawing group, as the diimines are difficult to synthesise due to the lack of nucleophilicity of the anilines used.¹³⁸ Also, unsymmetrical imidazolium salts such as the target compounds of this chapter can be difficult to synthesise by this route, as the initial condensation to form the diimines can be unselective and low-yielding.

2.1.1.2: Condensation Onto a Pre-formed Aminoal

The second ring-closing reaction to form imidazolium salts involves the condensation of a pre-formed aminoal moiety (**2.2**) with glyoxal; this method was patented by Arduengo in 1991.¹³⁹ Aminoals are formed initially by the condensation of two amines with formaldehyde, then the ring closed by double condensation with glyoxal in the presence of HCl, **Scheme 2.2**.

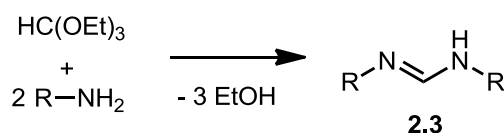


Scheme 2.2: Formation of imidazolium salts via a pre-formed aminoal.

Although this reaction is versatile, it suffers as many amines and anilines (especially if sterically congested) fail to condense in the first step, also yields and purity of the final product can be poor.¹³³

2.1.1.3: From an N,N'-Disubstituted Formamidine

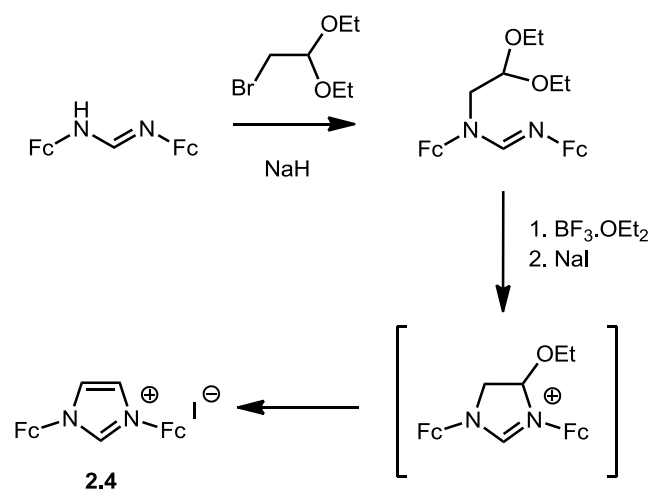
A more recent methodology for synthesis of imidazolium salts is via an N,N'-disubstituted formamidine, **2.3**. Although most often used to produce imidazolinium salts, in certain circumstances an imidazolium salt can be formed. Formamidines are synthesised from the reaction of two equivalents of an amine with triethylorthoformate, **Scheme 2.3**. This reaction has many advantages: it is usually easy to perform, high yielding and scalable, with a large scope of amines tolerated to give air and water stable products. It is also possible to react only one equivalent of amine first to afford a formimidate, then react with an equivalent of a different amine to form an unsymmetrically N,N'-disubstituted formamidine; however, these unsymmetrical formamidines are prone to disproportionation, giving symmetrical formamidines.¹⁴⁰



Scheme 2.3: Formation of N,N'-disubstituted formamidines.

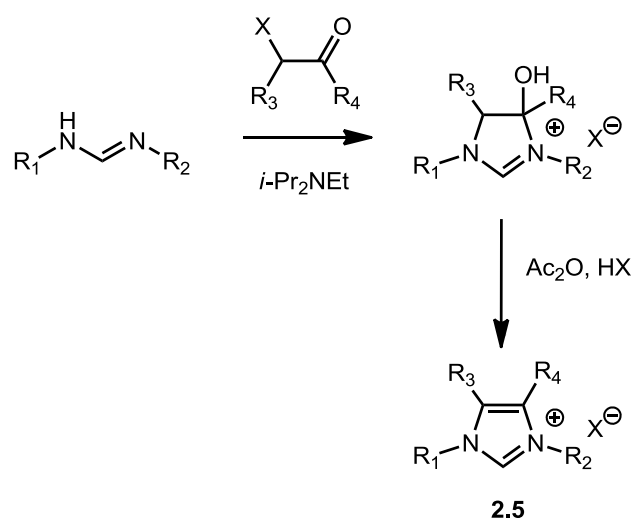
In order to form imidazolium salts, an alkylation/amination/elimination reaction sequence is needed. One example of this comes from Togni *et al.*, who reported the synthesis of planar chiral ferrocene-substituted imidazolium salts **2.4**, and their Pd complexes.¹⁴¹ Their route involved closing the ring with 1-bromo-2,2(diethoxy)ethane, **Scheme 2.4**.

Chapter 2 – Synthesis of Amine-Functionalised Imidazolium Salts



Scheme 2.4: Imidazolium salt synthesis from formamidines via alkylation / amination / elimination.¹⁴¹

Another variation of this methodology was used by Glorius *et al.* to synthesise a range of polysubstituted imidazolium salts (**2.5**) by closing the ring with readily available or easily prepared α -haloketones, **Scheme 2.5**.¹⁴²

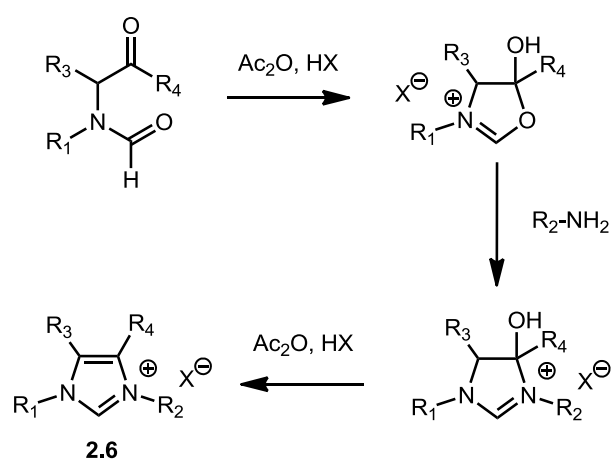


Scheme 2.5: Highly substituted imidazolium salts from formamidines.¹⁴²

In both these routes, a final elimination step results in aromatisation to an imidazolium, rather than imidazolinium salt, and this relatively new methodology has many potential applications.

2.1.1.4: Heterocyclic Interconversion

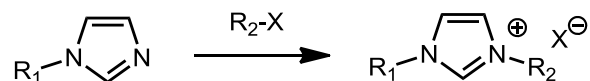
Converting another heterocycle into an imidazolium salt is an attractive route to unsymmetrical N-heterocyclic carbenes. Fürstner *et al.* described a route to substituted imidazolium salts **2.6** via conversion of an oxazolinium salt by condensation with an amine, followed by elimination to aromatised, **Scheme 2.6**.¹⁴³



Scheme 2.6: Heterocyclic interconversion route to highly substituted imidazolium salts.¹⁴³

2.1.1.5: Alkylation of N-Substituted Imidazoles

Another attractive route to unsymmetrical imidazolium salts is by alkylating an N-aryl or N-alkyl imidazole with an alkyl halide, **Scheme 2.7**.



Scheme 2.7: Alkylation of *N*-substituted imidazoles.

This alkylation methodology is well-studied, especially in the context of preparing imidazolium-based ionic liquids, such as the commercially available 1-butyl-3-methylimidazolium hexafluorophosphate, BMIM-PF₆, **Figure 2.1**.¹⁴⁴

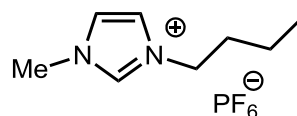
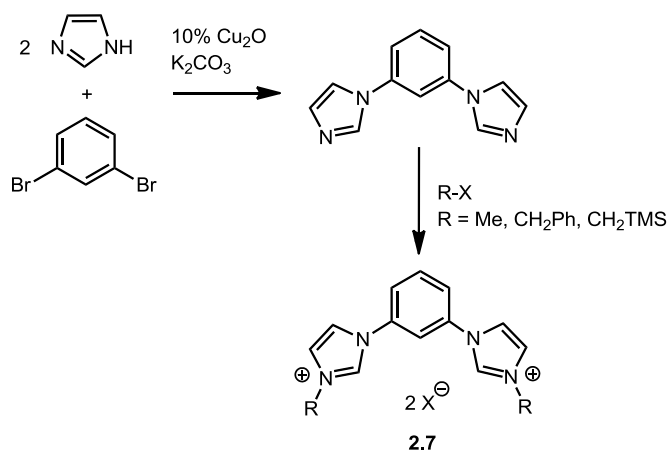


Figure 2.1: 1-Butyl-3-methylimidazolium hexafluorophosphate, BMIM-PF₆.

Many *N*-substituted imidazoles are commercially available, and others are easily accessed by various methods such as the condensation / ring-closing reactions mentioned above, or C-N bond-forming catalysis (Ullmann-type coupling). For example Hollis *et al.* synthesised a range of 1,3-*bis*(imidazolium)benzene salts **2.7** as precursors for bidentate carbenes for Pd, **Scheme 2.8**.¹⁴⁵ These imidazolium salts also proved useful for the formation of pincer-type CCC ligands for Zr,^{146,147} Hf¹⁴⁸ and Ti.¹⁴⁹



Scheme 2.8: Synthesis of 1,3-bis(imidazolium)benzene salts by Ullmann coupling and alkylation.¹⁴⁵

This route can allow access to many alkyl-alkyl and aryl-alkyl substituted imidazolium salts. However, aryl-aryl substituted products can only be accessed by a nucleophilic aromatic substitution, a potential limitation.

2.1.2: N-Donor Functionalised N-Heterocyclic Carbene Precursors

The addition of functional groups to azolium salts in order to produce functionalised NHCs is currently under active investigation, with examples of several functional groups of P, N, O and S donors known.¹⁵⁰ This section will briefly review the synthesis of amine-functionalised NHC precursors, including where the amine is part of a heterocycle.

In 2000, Cavell *et al.* first reported the synthesis of several N-donor functionalised imidazolium salts, including one with tertiary amine groups (**2.8**) and two with pyridyl

groups (**2.9**, **2.10**), **Figure 2.2**.¹⁵¹ These were all synthesised by alkylation of the appropriate N-substituted imidazole with alkyl or benzyl halides.

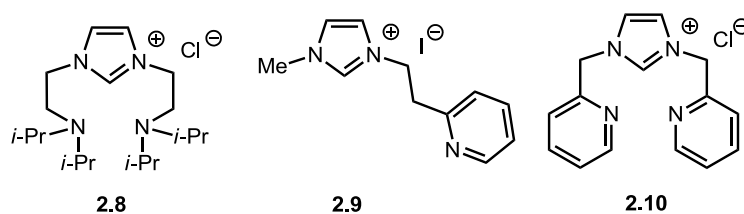


Figure 2.2: Cavell's N-donor functionalised imidazolium salts.¹⁵¹

Alkylation methodology has also been used to synthesise precursors to tridentate pincer NHC ligands with two imidazolium rings and a single pyridyl donor (**2.11** and **2.12**), **Figure 2.3**.^{152–155}

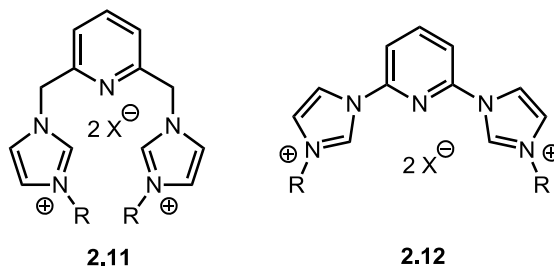
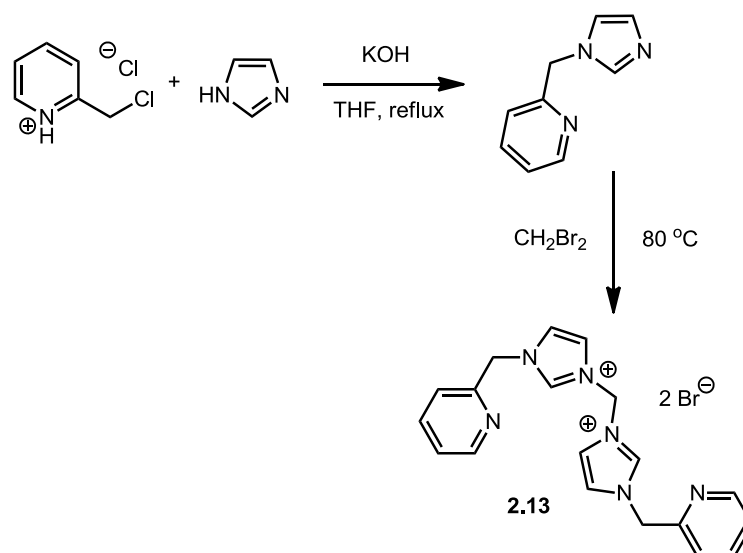


Figure 2.3: Pyridyl bis-imidazolium salts; precursors to [CNC] pincer ligands.^{152–155}

Tetradentate ligand precursors have also been synthesised by alkylation, such as **2.13**, which is synthesised by alkylation of 2-picolylchloride hydrochloride, followed by a symmetrical alkylation of the resultant imidazole with dibromomethane, **Scheme 2.9**.¹⁵⁶



Scheme 2.9: Synthesis of a bis-pyridyl bis-imidazolium salt.¹⁵⁶

Other heterocycles have also been used as N-donors, for example an imidazolium salt functionalised with a pyrazolyl group (**2.14**),¹⁵⁷ and an oxazolyl group (**2.15**),^{158–160}

Figure 2.4. **2.15** is synthesised by nucleophilic substitution of the 2-bromooxazoline by *N*-mesitylimidazole. In the case of **2.15**, the N-donor heterocycle can also be stereodirecting, adding additional functionality to the ligand.

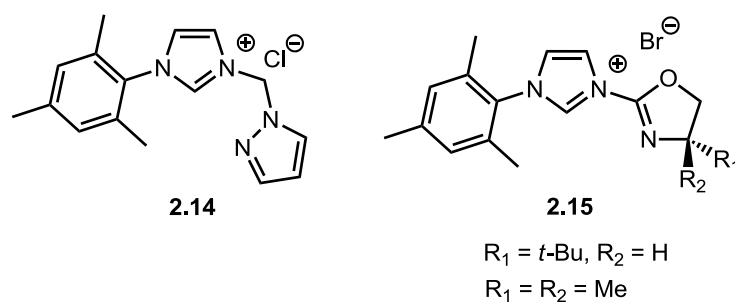


Figure 2.4: Heterocycle-functionalised imidazolium salts.^{157–160}

Arylamino-functionalised NHCs have been investigated by the group of Fryzuk,^{161–164} with bidentate (**2.16**) and tridentate (**2.17**) imidazolium salts synthesised by alkylation of imidazoles, **Figure 2.5**. Similar alkylamino-functionalised imidazolium salts (**2.18**)

have been synthesised and investigated as NHC precursors by Arnold *et al.*^{165,166} These functionalised, bidentate NHC precursor salts are closely related to the imidazolium salts that are synthesised and described in this thesis, *vide infra*.

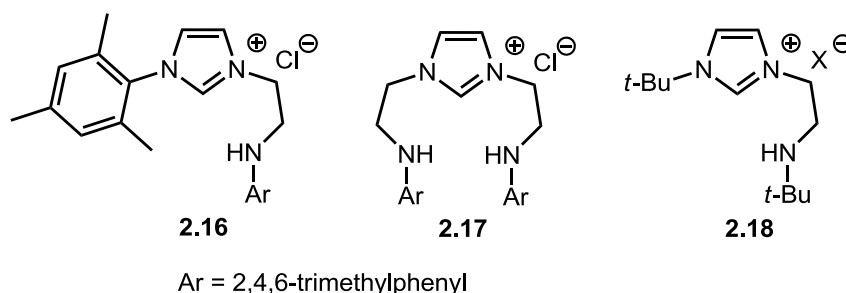
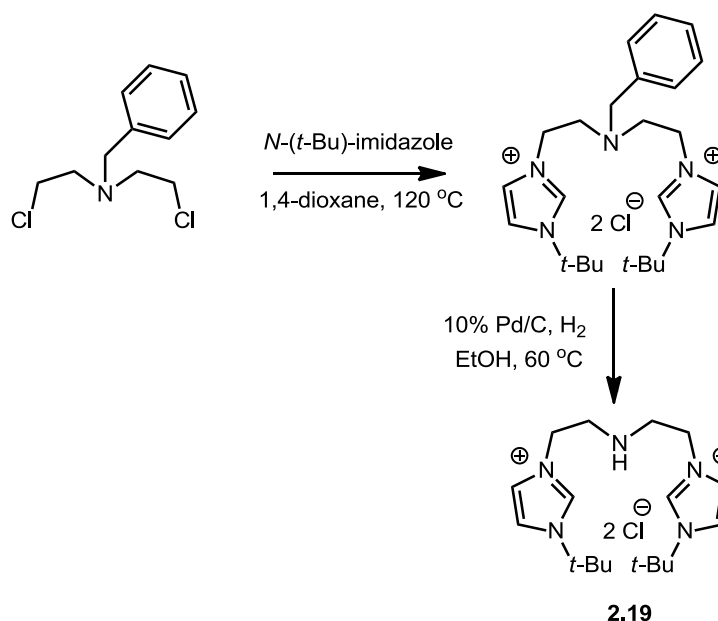


Figure 2.5: Arylamine and alkylamine functionalised imidazolium salts.^{161–166}

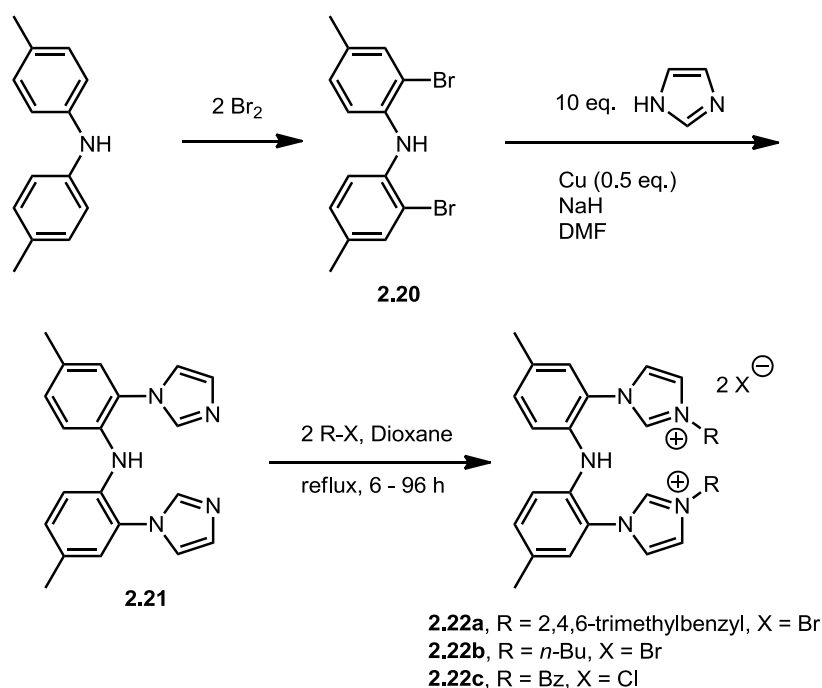
Amine functionalised bis-imidazolium salt **2.19** has been synthesised by Arnold^{167,168} and Douthwaite¹⁶⁹ by an alkylation route (**Scheme 2.10**). Protection of *bis*(2-chloroethyl)amine with a benzyl group was necessary before the alkylation step in order to prevent competitive oligomerisation.



Scheme 2.10: Douthwaite's route to amine-functionalised bisimidazolium salt **2.19**.¹⁶⁹

Most closely related to the imidazolium salts reported in Ch. 2.2.1, during the course of the reported research Luo *et al.* described the diarylamino *bis*(imidazolium) salts

2.22a-c, synthesised by a multi-step synthesis as shown in **Scheme 2.11**.¹⁷⁰



Scheme 2.11: Luo's route to diarylamino *bis*(imidazolium) salts, **2.20**.¹⁷⁰

2.1.3: Aims and Objectives

The aim of the work presented in this chapter was to synthesise and characterise a range of imidazolium salts as precursors to tridentate (CNC) and bidentate (C,NR) late transition metal amino-/amido-NHC complexes. The use of efficient catalytic methods to synthesise the imidazolium salts was desirable, avoiding waste and toxic reagents.

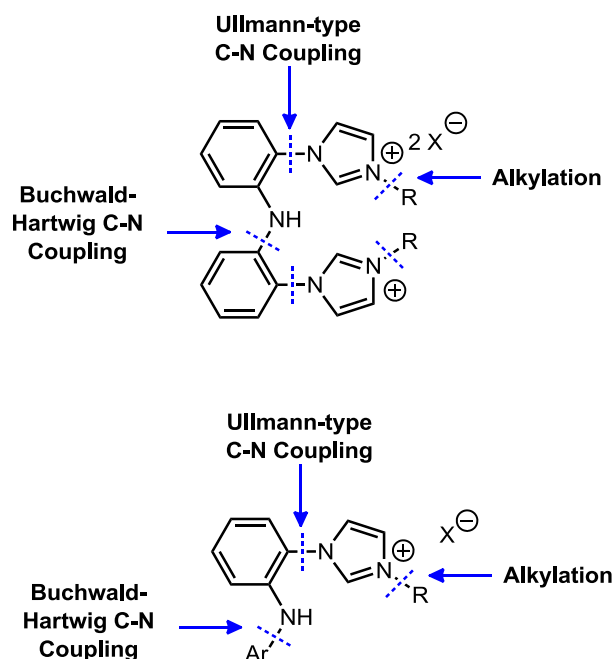


Figure 2.6: Bond disconnection of amine-functionalised imidazolium salts.

Both the imidazolium salts that are precursors to tridentate and bidentate ligands were related, and could be synthesised by the same methodology. A bond disconnection approach (**Fig. 2.6**) gave a route based on two successive metal-catalysed cross couplings: first, a Buchwald-Hartwig Pd-catalysed cross-coupling allowed the coupling of an aniline and a halogenated aryl ring; secondly an Ullmann-type Cu-catalysed cross-coupling allowed the coupling of the brominated aniline product to imidazole. Alkylation of the coupled imidazole with a haloalkane would then give the imidazolium salts. This strategy is similar to that used by Luo to make arylamine-*bis*imidazolium salts **2.22**;¹⁷⁰ however, the Buchwald-Hartwig coupling strategy can also be used to make unsymmetrical diaryl amines, allowing more structural diversity in imidazolium salts that are precursors to bidentate amino/amido-NHC ligands.

Chapter 2 – Synthesis of Amine-Functionalised Imidazolium Salts

Pincer ligands, as rigid tridentate ligands, would likely force the N-donor to coordinate, and give a stable scaffold for investigating the reactivity of the M-N bond.

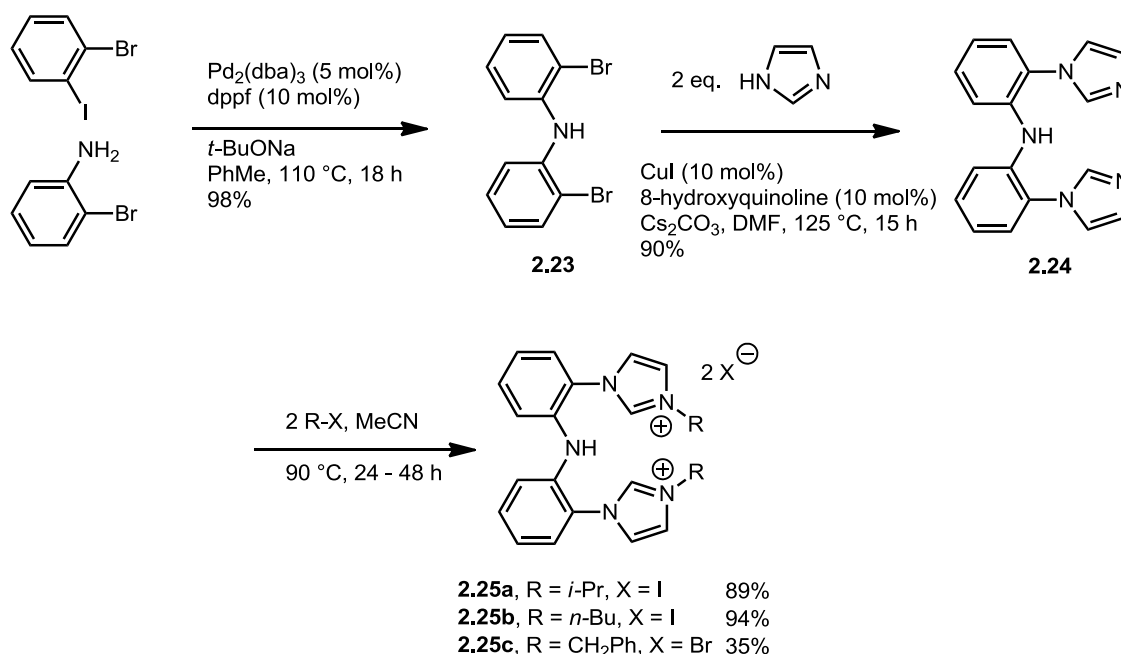
Bidentate ligands have the potential advantage of leaving more binding sites unoccupied on the metal than pincer ligands, which may be beneficial for catalytic activity in coupling reactions.

The imidazolium salts reported in this section are ligand precursors for complexes (described in Ch. 3 and 4) that were used to investigate if the amino-/amido-metal bond can facilitate breaking of H-H and C-H bonds in bifunctional catalysis by an AMLA mechanism.

2.2: Results and Discussion

2.2.1: Synthesis of Arylamino-*bis*-Imidazolium Salts

Imidazolium salts **2.25** were synthesised by an efficient 3-step procedure; salts **2.25a** and **2.25b** were used as precursors to (CNC) pincer complexes, discussed in Chapter 3.



Scheme 2.12: Synthesis of imidazolium salts **2.25**.

Bis(2-bromophenyl)amine (**2.23**), was synthesised according to a literature procedure:¹⁷¹ the palladium-catalysed reaction of 2-bromoiodobenzene with 2-bromoaniline afforded, after column chromatography, 98% yield of **2.23** as a pale yellow oil which crystallised on standing overnight. The ¹H and ¹³C NMR spectra of **2.23** were consistent with the reported values.

Bis(2-bromophenyl)amine, **2.23**, was reacted with imidazole in DMF at 125 °C for 15 h using a CuI / 8-hydroxyquinoline catalyst mixture and Cs₂CO₃ base to give *bis*(2-(1*H*-

imidazol-1-yl)phenyl)amine, **2.24**, in 90% yield after workup. **2.24** was isolated as a brown solid which unfortunately was not analytically pure; however, this did not hinder subsequent steps. This Ullmann coupling is more efficient than that used by Luo,¹⁷⁰ only 10% of CuI is needed, compared to 0.5 eq. Cu, and only 2 eq. of imidazole are needed, rather than the 10 eq. used by Luo. The ¹H NMR spectrum of **2.24** showed the expected signals, with two aromatic 2H triplets at δ 7.11 and 7.36 and a 4H multiplet of overlapping aromatic signals at δ 7.24-7.32. An NH singlet was observed at δ 5.12. The imidazole protons were observed only as a broad signal ca. 7.75 ppm. Similarly, in the ¹³C NMR spectrum several signals are not visible in the aromatic region, corresponding to imidazole carbons. The author speculates that this broadening is due to inter- and intramolecular H-bonding (**Fig. 2.7**), leading to a dynamic equilibrium between several different species which interconvert on the NMR timescale. This broadening or lack of signals in NMR spectroscopy for the imidazole ring was typical for N-aryl imidazoles prepared in this project. Interestingly, however, Luo's analogous compound **2.21** shows no line broadening for the imidazole protons.¹⁷⁰

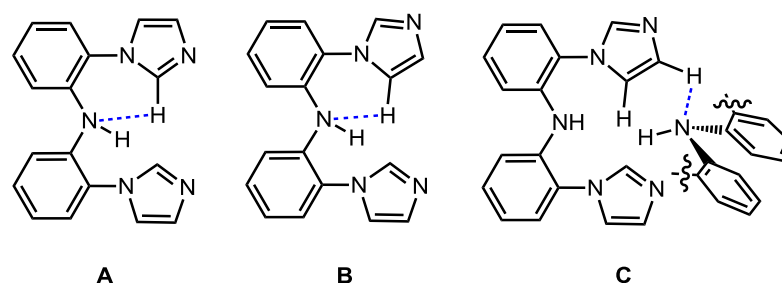


Figure 2.7: Possible intra- (**A, B**) and intermolecular (**C**) H-bonding in **2.26** that may account for broad NMR signals.

Finally, three imidazolium salts (**2.25a-c**) were synthesised by alkylation with the appropriate alkyl halide, **Scheme 2.12**.

The *isopropyl* imidazolium salt **2.25a**, and *n*-butyl imidazolium salt **2.25b** were prepared by heating an MeCN suspension of *bis*(2-(1*H*-imidazol-1-yl)phenyl)amine **2.24** with a slight excess of the appropriate alkyl iodide in a sealed vessel at 90 °C for 24 h. Filtration and removal of solvent gave analytically pure **2.25a** as an orange solid and **2.25b** as a brown solid in high yield (**2.25a**: 89%, **2.25b**: 94%). The ¹H NMR spectrum of **2.25a** showed characteristic signals of equivalent *isopropyl* groups, with a 12H doublet at δ 1.70, and a 2H septet at δ 4.97. The imidazolium ring showed characteristic CHCH peaks at δ 7.53 and 7.75 with very small ³J constants of 1.7 Hz, along with an easily identifiable NCHN peak at δ 9.56. Similarly, the ¹H NMR spectrum of **2.25b** contained characteristic signals for the NCHN (δ 9.72) and CHCH imidazolium (δ 7.56, 7.66) protons. Alkyl signals were observed at δ 0.95, 1.36, 1.92 and 4.40, with multiplicities consistent with two equivalent *n*-butyl groups. The ¹³C NMR spectrum of both **2.25a** and **2.25b** had the expected number of signals.

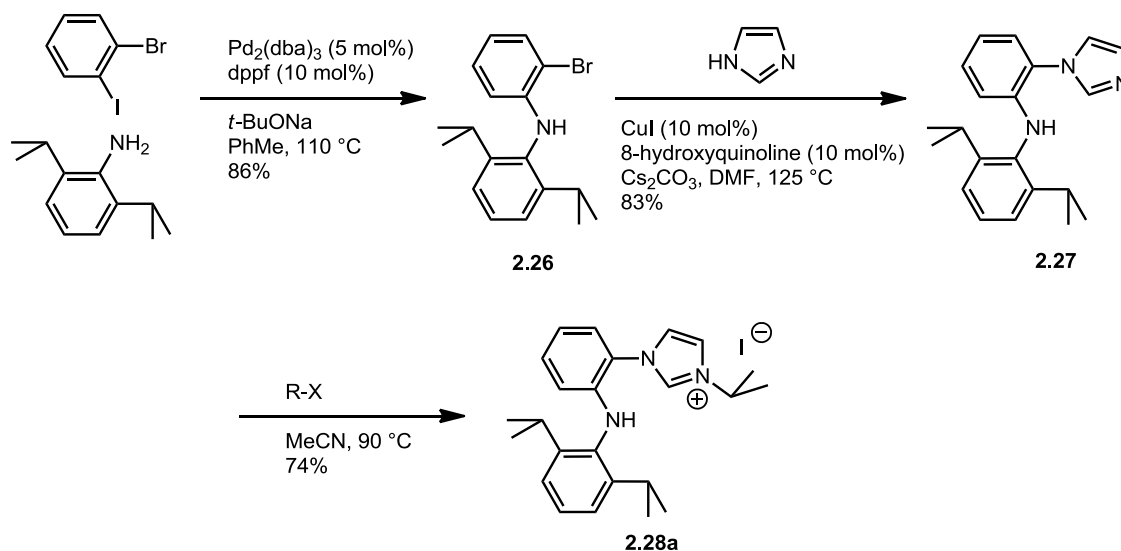
The benzyl imidazolium salt **2.25c** proved much more difficult to synthesise and purify than the alkyl imidazolium salts **2.25a** and **2.25b**. Reaction of *bis*(2-(1*H*-imidazol-1-yl)phenyl)amine **2.24** with 2.1 equivalents of benzyl bromide in MeCN at 90 °C took 10 days to go to completion, showing a much slower rate of alkylation than with alkyl iodides. The reason for this slow nucleophilic substitution could be that bromide is not as good a leaving group as iodide, resulting in a slower S_N2 reaction. Once the reaction was complete, several byproducts and starting benzyl bromide remained in the crude brown-grey product. Trituration with Et₂O removed most of the remaining

benzyl bromide, however other impurities remained. Precipitation of the product from DCM/Et₂O, in order to remove the remaining impurities, proved very difficult as the crude product tended to form a sticky purple oil unless vigorous stirring was applied as Et₂O was added. Only a poor (35%) yield of purple-white, analytically pure solid **2.25c** was isolated. The ¹H NMR spectrum of **2.25c** showed characteristic signals for the NCHN (δ 9.51) and imidazolium CHCH (δ 7.71, 7.75) protons, along with a 4H singlet at δ 5.50 for the benzyl CH₂. The spectrum proved impossible to fully assign, due to significant overlap of the aromatic signals arising from the benzyl and *N*-aryl groups. The ¹³C NMR spectrum of **2.25c** showed multiple aromatic signals as expected, along with a benzyl CH₂ peak at δ 54.5 and signals at δ 138.5 and 138.7, both attributable to the NCHN carbon. It is possible that the two signals originate from NCHN and NCDN species, as exchange of this proton has been observed by us in protic NMR solvents such as CD₃OD. Due to the difficulty in synthesis and purification of **2.25c**, along with the complicated NMR signals associated with it, it was decided not to investigate the coordination chemistry of this imidazolium salt.

2.2.2: Synthesis of Arylamino Imidazolium Salts

Imidazolium salt **2.28a** was synthesised by an efficient 3-step procedure similar to that used for imidazolium salts **2.25**. **2.28a** was used as a precursor to a (C,NR) amino/amido-NHC ligand on several complexes; these complexes are discussed in Chapter 4.

Chapter 2 – Synthesis of Amine-Functionalised Imidazolium Salts



Scheme 2.13: Synthesis of secondary arylamine imidazolium salt **2.28a**.

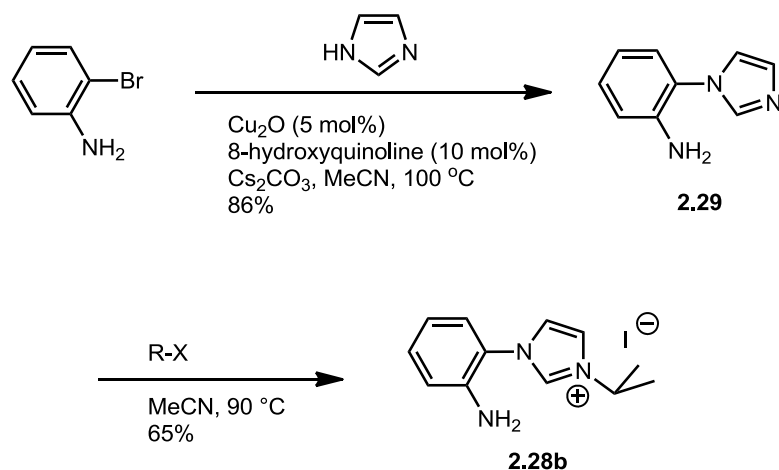
The synthesis of *N*-(2-bromophenyl)-2,6-diisopropylaniline **2.26** (Scheme 2.13) was accomplished *via* the same Buchwald-Hartwig coupling procedure as for *bis*(2-bromophenyl)amine, **2.23** (Ch. 2.2.1) but substituting 2-bromoaniline with 2,6-diisopropylaniline, giving the known compound **2.26** in 74% yield after column chromatography. The ^1H and ^{13}C NMR spectra for **2.26** displayed signals which matched closely with literature values.¹⁷²

N-(2-bromophenyl)-2,6-diisopropylaniline **2.26** was reacted with imidazole in DMF at 125°C for 72 h under Cu-catalysed Ullmann-type conditions to give *N*-(2-(1*H*-imidazol-1-yl)phenyl)-2,6-diisopropylaniline **2.27** in 83% yield (Scheme 2.13), in a similar fashion to *bis*(2-(1*H*-imidazol-1-yl)phenyl)amine, **2.24** (Ch. 2.2.1). The reaction to make **2.27** took longer to reach completion than for **2.24**, presumably because of the increased steric bulk of the aniline. The *isopropyl* groups gave clear signals in the ^1H NMR spectrum, with a doublet at δ 1.11 and a septet at δ 3.11. The NH signal could be observed at δ 5.83, and this proton was observed to exchange with deuterium over

time. Aryl signals were present but overlapping in some cases, and, as for the previous tridentate precursor **2.24**, the protons of the imidazole ring were observed only as a broad signal, implying hydrogen bonding (**Fig. 2.7**). Imidazole CH signals were absent in the ^{13}C NMR spectrum, for the same reason.

The secondary arylamine imidazolium salt *N*-(2-(3-*iso*-propyl-1*H*-imidazolium)phenyl)-2,6-diisopropylaniline iodide **2.28a** was synthesised by alkylation of **2.27** with *isopropyl* iodide in MeCN at 90 °C for 48 h. Filtration of the reaction mixture followed by precipitations from MeOH/Et₂O gave **2.28a** as an analytically pure white solid in good yield. Several key distinguishing features were observed in the ^1H NMR spectrum, including the imidazolium *isopropyl* signals at δ 1.75 (d) and 5.19 (sept), aryl *isopropyl* CH at δ 3.14 (sept) and aryl *isopropyl* CH₃ as two sets of distinct doublets at δ 1.11 and 1.21. Aryl and imidazolium CHCH were easily assigned, as was the NCHN peak at δ 9.36. The ^{13}C NMR spectrum was fully assigned by use of an HSQC experiment.

Imidazolium salt **2.28b** was synthesised by a 2 step procedure comprising an Ullmann-coupling and an alkylation. **2.28b** was used as a precursor to a (C,NR) amino/amido-NHC ligand on several complexes; these complexes are discussed in Chapter 4.



Scheme 2.14: Synthesis of primary arylamine imidazolium salt **2.28b**.

The Ullmann coupling method used for the synthesis of **2.24** and **2.26** proved to be unsuitable for the synthesis of the known compound 2-(1*H*-imidazol-1-yl)phenylamine **2.29**, as it gave low yields of impure product. It is possible that **2.29** was more water-soluble (and was removed during water washings) as it would be expected to be more polar than the secondary amine product **2.26**. To overcome this problem, using MeCN as a solvent greatly facilitated the isolation of product, as aqueous LiCl washes were no longer needed to remove residual DMF; however, the lower temperature necessary due to the lower boiling point of MeCN compared with DMF slowed the reaction considerably. Cu₂O, in combination with a bidentate ligand, is an extremely effective catalyst for the Ullmann coupling of imidazoles in several solvents;^{173,174} it was found that Cu₂O could be substituted for the CuI catalyst, increasing the rate of reaction so that completion was reached within 3 days at 100 °C, with isolation of **2.29** in 86% yield after workup. The ¹H and ¹³C NMR spectra of **2.29** were consistent with literature data.¹⁷⁵

The primary arylamine imidazolium salt 2-(3-*iso*-propyl-1*H*-imidazolium)phenylamine iodide **2.28b** was synthesised by alkylation of **2.29** with *isopropyl* iodide in MeCN at 90 °C for 72 h. Following recrystallisation from MeOH/Et₂O, **2.28b** was isolated as an analytically pure green product in 65% yield. The ¹H NMR spectrum of **2.28b** showed characteristic signals for the *isopropyl* group at δ 1.66 (d) and 4.79 (sept), with all aryl signals observed, including the NCHN signal at δ 9.27. The NH₂ protons were not observed; presumably exchanging with deuterium from the NMR solvent. The ¹³C NMR spectrum displayed all expected signals.

2.3: Conclusions

An efficient metal-catalysed cross-coupling strategy was used to prepare a series of imidazolium salts (**Fig. 2.8**) as precursors to N-donor functionalised N-heterocyclic carbene ligands.

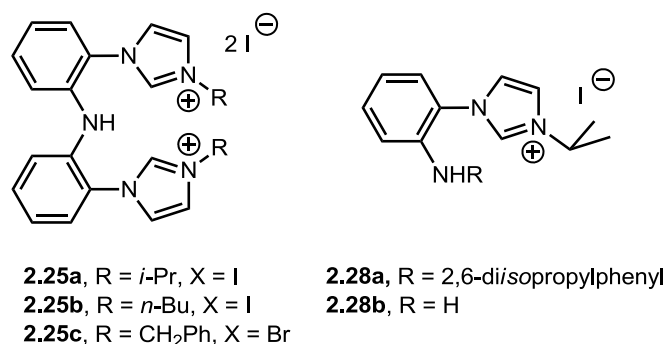


Figure 2.8: Synthesised imidazolium salts.

The amino-*bis*-imidazolium salts **2.25a-b** and **2.28a-b**, precursors to tridentate (CNC) amido-*bis*NHC ligands, were prepared in high purity and yield in three steps, involving a Pd-catalysed Buchwald-Hartwig coupling, Cu-catalysed Ullmann coupling and final alkylation. The benzyl substituted analogue **2.25c** was prepared and characterised, but difficulties in reaction and purification precluded further use. The secondary arylamino imidazolium salt **2.28a**, precursor to a bidentate (C,NR) diarylamino/amido-NHC ligand, was prepared by similar methodology in good yield and purity. The primary arylamino imidazolium salt **2.28b**, precursor to a bidentate (C,NR) amino/amido-NHC ligand, was synthesised by a two-step process. First, a modified Ullmann reaction protocol was developed to facilitate purification, followed by an alkylation step to afford **2.28b** in fair yield and high purity.

The synthetic methodology for compounds **2.25** and **2.28** utilised efficient metal-catalysed reactions, which reduced waste and were step and cost efficient.

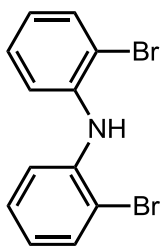
Chapter 2 – Synthesis of Amine-Functionalised Imidazolium Salts

In synthesising imidazolium salts **2.25** and **2.28**, part of *Objective 1* was fulfilled, as outlined in Ch. 1.5; **2.25** and **2.28** were used to synthesise amino-/amido-NHC complexes of the late transition metals (Ch. 3 and 4) in order to complete *Objective 1*. The complexes formed were used to investigate if the amino-/amido-metal bond can be used to facilitate bond cleavage during catalysis, by a bifunctional mechanism (Ch. 5).

2.4: Experimental

All reactions were performed under dry, oxygen free nitrogen using standard Schlenk techniques unless otherwise stated; however, all compounds were air stable once isolated. Anhydrous solvents were obtained either by distillation from an appropriate drying agent, from an Innovative Technology PureSolv MD 7 Solvent Purification System or purchased from Sigma Aldrich. All other reagents were obtained from Sigma-Aldrich, Johnson Matthey or Alfa Aesar and used as supplied. NMR spectra were recorded on a Bruker DPX300, DRX400 or AV500 spectrometer; chemical shifts have been referenced to the residual protonated solvent peak and are reported in ppm, *J* values are given in Hz. Electrospray mass spectra were recorded on a Micromass Quattro LC mass spectrometer with acetonitrile as solvent; FAB and HR mass spectra were recorded on a Kratos Concept mass spectrometer using NBA as a matrix.

Bis(2-bromophenyl)amine (2.23)



Synthesis adapted from Uchiyama *et al.*¹⁷¹

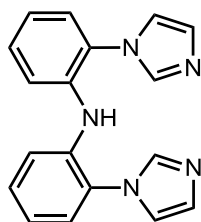
To a pre-dried Schlenk flask under N₂ was added 2-bromiodobenzene (9.770 g, 35.00 mmol, 4.500 mL), 2-bromoaniline (5.160 g, 30.00 mmol), sodium *tert*-butoxide (4.020 g, 42.00 mmol),

Pd₂(dba)₃ (1.370 g, 1.500 mmol), DPPF (1.660 g, 3.000 mmol) and toluene (50 mL).

The mixture was heated under reflux for 18 h and then allowed to cool to RT, whereupon the solvent was removed *in vacuo* to give a crude black oil. The oil was dissolved in DCM and filtered through a pad of Celite. Purification by column chromatography (1% Et₂O/petroleum ether (b.p. 40-60 °C)) gave **2.23** as a pale yellow oil which crystallized on standing (9.62 g, 98%, R_f = 0.68 (1% Et₂O/petroleum ether (b.p. 40-60 °C))).

δ_{H} (500 MHz, CDCl₃) 6.45 (1H, br s, NH), 6.85 (2H, td, *J* = 7.6, 1.5), 7.23 (2H, td, *J* = 7.6, 1.5), 7.30 (2H, dd, *J* = 8.0, 1.5), 7.59 (2H, dd, *J* = 8.0, 1.5); δ_{C} (125 MHz, CDCl₃) 114.2, 117.9, 122.5, 128.1, 133.2, 140.0.

Bis(2-(1H-imidazol-1-yl)phenyl)amine (2.24)

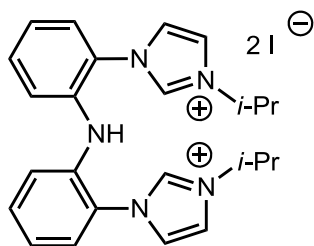


Compound **2.23** (2.970 g, 9.100 mmol), imidazole (1.240 g, 18.20 mmol), Cs_2CO_3 (11.86 g, 36.40 mmol), CuI (0.346 g, 1.820 mmol) and 8-hydroxyquinoline (0.264 g, 1.820 mmol) were suspended in DMF (5 mL) in a pre-dried sealable tube. The tube was sealed and heated at 125 °C for 15 h. The reaction mixture was then allowed to cool to room temperature and diluted with DCM (50 mL). The mixture was filtered through a pad of Celite and washed with a solution of 5% $\text{LiCl}_{(\text{aq.})}$ (5 x 100 mL) and brine (2 x 50 mL). The solution was then dried (MgSO_4) and the volatiles removed *in vacuo* to give **2.24** as a green solid (2.47 g, 90%) m.p. 80-82 °C.

δ_{H} (500 MHz, CD_2Cl_2) 5.12 (1H, s, NH), 7.11 (2H, app t, $J = 7.8$, Ar CH), 7.24–7.32 (4H, m, Ar CH), 7.36 (2H, app t, $J = 7.8$, Ar CH), 7.75 (br, imidazole CH); δ_{C} (75 MHz, CDCl_3) 119.3, 122.6, 127.6, 129.7, 137.7. $\nu_{\text{max}}/\text{cm}^{-1}$ (solid) 3116 w, 3096 w, 2914 w, 1593 m, 1510 s, 1500 s, 1482 s, 1459 m, 1312 s, 1278 m, 1236 w, 1108 m, 1088 w, 1059 s, 963 m, 907 m, 821 m, 772 s. m/z (ESI) 302 (100%, $\text{M}+\text{H}^+$), 324 (21% $\text{M}+\text{Na}^+$); HRMS $\text{C}_{18}\text{H}_{16}\text{N}_5$ calcd. 302.1400, found 302.1414.

Compound **2.24** could not be isolated in analytically pure form, but this did not hinder subsequent steps. Some signals are broad or not apparent in the NMR spectra; the author speculates that this is due to inter- and intramolecular H-bonding.

Bis(2-(3-*iso*-propyl-1*H*-imidazolium)phenyl)amine diiodide (2.25a)

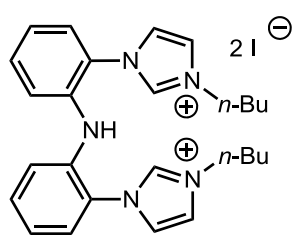


In a sealable tube under an atmosphere of air, *i*-propyl iodide (0.360 mL, 3.700 mmol) was added to a green suspension of **2.24** (0.500 g, 1.660 mmol) in MeCN (10 mL). The tube was sealed and heated at 90 °C for 24 h,

giving a red solution. The mixture was allowed to cool to RT and filtered. The volatiles were removed *in vacuo* to give **2.25a** as an orange solid (0.951 g, 89%) m.p. 81-84 °C.

δ_{H} (300 MHz, CDCl_3) 1.70 (12H, d, $J = 6.7$, $\text{CH}(\text{CH}_3)_2$), 4.97 (2H, sept, $J = 6.7$, $\text{CH}(\text{CH}_3)_2$), 7.14 (2H, dt, $^3J = 7.8$, $^4J = 1.2$, CH), 7.30 (2H, dd, $^3J = 7.9$, $^4J = 1.2$, CH), 7.36 (2H, dd, $^3J = 7.8$, $^4J = 1.5$, CH), 7.46 (2H, dt, $^3J = 7.9$, $^4J = 1.5$, CH), 7.53 (2H, app t, $J = 1.7$, NCHCHN), 7.75 (2H, app t, $J = 1.7$, NCHCHN), 9.56 (2H, app t, $J = 1.7$, NCHN); δ_{C} (75 MHz, CDCl_3) 22.9 ($\text{CH}(\text{CH}_3)_2$), 52.8 ($\text{CH}(\text{CH}_3)_2$), 121.5, 122.9, 123.8, 124.2, 126.1, 127.7, 132.0, 135.6, 137.7 (aromatic C). $\nu_{\text{max}}/\text{cm}^{-1}$ (solid) 3066 w, 2978 w, 1597 m, 1546 m, 1497 s, 1458 m, 1375 w, 1305 m, 1264 w, 1192 s, 1161 w, 958 w, 875 w, 827 w, 758 vs, 681 w, 650 s. m/z (ESI) 514 (18%, $[\text{M-I}]^+$), 386 (100% $[\text{M-I-HI}]^+$), 344 (36%, $[\text{M-I-HI-}^i\text{Pr}]^+$); HRMS $\text{C}_{24}\text{H}_{29}\text{I}_2\text{N}_5$ calcd. 514.1462, found 514.1465. Anal. Calcd. for $\text{C}_{24}\text{H}_{29}\text{I}_2\text{N}_5$: C, 44.95; H, 4.56; N, 10.92. Found C, 45.01; H, 4.27; N, 10.61%.

Bis(2-(3-butyl-1*H*-imidazolium)phenyl)amine diiodide (2.25b)

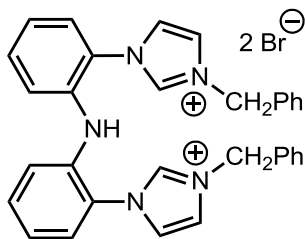


In a sealable tube under an atmosphere of air, *n*-butyl iodide (0.940 g, 5.110 mmol) was added to a green suspension of **2.24** (0.500 g, 1.660 mmol) in MeCN (10 mL). The tube was sealed and heated at 90 °C for 15 h, giving a red solution. The mixture was allowed to cool to RT and filtered. The volatiles were removed *in vacuo* to give **2.25b** as a light brown solid (1.450 g, 93%) m.p. 56-57 °C.

δ_{H} (400 MHz, CDCl_3) 0.95 (6H, t, $J = 7.5$, CH_3), 1.36 (4H, app sext, $J = 7.5$, CH_2), 1.92 (4H, app quint, $J = 7.5$, CH_2), 4.40 (4H, t, $J = 7.5$, CH_2), 7.10 (2H, t, $J = 7.6$, CH), 7.25 (2H, d, $J = 7.6$, CH), 7.39 (2H, d, $J = 8.2$, CH), 7.44 (2H, app t, $J = 8.2$, CH), 7.56 (2H, t, $J = 1.5$, NCHCHN), 7.66 (2H, app t, $J = 1.5$, NCHCHN), 9.72 (2H, s, NCHN); δ_{C} (100 MHz, CDCl_3) 13.6 CH_3 , 19.6 CH_2 , 31.6 CH_2 , 50.5 CH_2 , 122.8, 123.6, 123.8, 123.9, 126.1, 127.6, 132.1, 136.7, 137.7 (aromatic C). $\nu_{\text{max}}/\text{cm}^{-1}$ (solid) 3066 w, 2978 w, 1597 m, 1546 m, 1497 s, 1458 m, 1375 w, 1305 m, 1264 w, 1192 s, 1161 w, 958 w, 875 w, 827 w, 758 vs, 681 w, 650 s. m/z (ESI) 542 (34%, $[\text{M-I}]^+$), 414 (100% $[\text{M-I-HI}]^+$), 358 (30%, $[\text{M-I-HI-Bu}]^+$);

HRMS $\text{C}_{26}\text{H}_{33}\text{I}_2\text{N}_5$ calcd. 542.1781, found 542.1770. Anal. Calcd. for $\text{C}_{26}\text{H}_{33}\text{I}_2\text{N}_5$: C, 46.65; H, 4.97; N, 10.46. Found C, 46.25; H, 4.70; N, 10.13%.

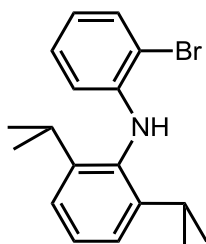
bis(2-(3-benzyl-1H-imidazol-3-ium)phenyl)amine bromide (2.25c)



In a sealable tube under an atmosphere of air, benzyl bromide (0.160 ml, 0.227 g, 1.330 mmol) was added to a green suspension of **2.24** (0.200 g, 0.664 mmol) in MeCN (10 mL). The reaction vessel was sealed and heated at 90 °C for 10 days with stirring. After cooling to RT, solvent was removed *in vacuo*. The resulting crude brown-grey solid was washed with diethyl ether (3 x 5 mL) and precipitated 4 times from DCM/Et₂O with vigorous stirring to give **2.25c** as a purple-white solid (0.149 g, 35 %) (m.p. 138-140 °C).

δ_{H} (500 MHz, CD₃OD) δ 5.50 (4H, s, CH₂), 7.06 (2H, d, J = 8.1, aryl CH), 7.19 (2H, app t, J = 7.8, aryl CH), 7.37-7.44 (12H, m, aryl CH), 7.49 (2H, d, J = 7.9, aryl CH), 7.71 (2H, d, J = 1.9, NCHCHN), 7.75 (2H, d, J = 1.9, NCHCHN), 9.51 (2H, s, NCHN); δ_{C} (125 MHz, CD₃OD) δ 54.5 (CH₂), 122.8, 124.2, 124.3, 125.1, 125.3, 125.4, 127.45, 127.5, 128.8, 130.0, 130.5, 133.2, 134.9 (aromatic C), 138.5, 138.7 (NCHN). FTIR (solid) 2962, 2926, 2870, 1587, 1487, 1449, 1403, 1334, 1266, 1216, 1132, 1077, 1039, 951, 882, 842, 743, 728, 682 cm⁻¹. m/z (ESI) 564 [M-Br]⁺, 483 [M-2Br+H]⁺, 393 [M-2Br-(CH₂Ph)+H]⁺ Anal. Calcd for C₃₂H₂₉N₅Br₂: C 59.73, H 4.54, N 10.88. Found: C 59.83, H 4.51, N 10.84.

N-(2-bromophenyl)-2,6-diisopropylaniline (2.26)

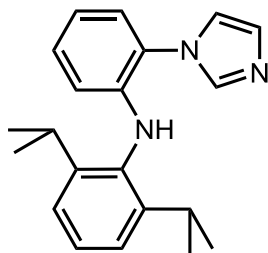


To a pre-dried Schlenk flask under N₂ was added 2-bromiodobenzene (9.770 g, 35.00 mmol, 4.500 mL), 2,6-diisopropylaniline (5.310 g, 30.00 mmol), sodium *tert*-butoxide (4.020 g, 42.00 mmol), Pd₂(dba)₃ (1.370 g, 1.500 mmol), DPPF (1.660 g, 3.000 mmol) and toluene (50 mL). The mixture was heated under reflux for 18 h and then allowed to cool to RT, whereupon the solvent was removed *in vacuo* to give a crude black oil. The oil was dissolved in DCM and filtered through a pad of Celite. Purification by column chromatography (1% Et₂O/petroleum ether (b.p. 40-60 °C)) gave **2.26** as a colourless oil which crystallized on standing (8.61 g, 86 %).

δ_{H} (400 MHz, CDCl₃): δ 1.11 (6H, d, $J = 6.9$), 1.18 (6H, d, $J = 6.9$), 3.09 (2H, sept, $J = 6.9$), 5.68 (1H, br s), 6.14 (1H, d, $J = 8.2$), 6.57 (1H, t, $J = 7.6$), 7.00 (1H, t, $J = 8.0$), 7.23 (2H, d, $J = 7.6$), 7.32 (1H, t, $J = 8.0$), 7.47 (1H, d, $J = 7.9$); δ_{C} (100 MHz, CDCl₃): 23.0, 24.7, 28.3, 108.9, 112.6, 118.3, 124.0, 127.8, 128.3, 132.4, 134.7, 144.9, 147.7.

Data matches that reported previously by Chianese *et al.*¹⁷²

***N*-(2-(1*H*-imidazol-1-yl)phenyl)-2,6-diisopropylaniline (2.27)**



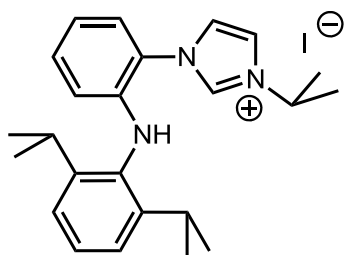
Compound **2.26** (2.000 g, 6.010 mmol), imidazole (0.409 g, 6.01 mmol), Cs₂CO₃ (3.916 g, 12.02 mmol), CuI (0.114 g, 0.601 mmol) and 8-hydroxyquinoline (0.087 g, 0.60 mmol) were suspended in DMF (10 mL) in a pre-dried sealable tube. The

tube was sealed and heated at 125 °C for 72 h. The reaction mixture was then allowed to cool to room temperature and diluted with DCM (75 mL). The mixture was filtered through a pad of Celite and washed with a solution of 5% LiCl_(aq.) (4 x 100 mL) and brine (100 mL). The solution was then dried (MgSO₄) and the volatiles removed *in vacuo* to give a green residue that was redissolved in DCM (30 mL). Hexane (70 mL) was then added and a solid precipitate removed by filtration. Volatiles were removed *in vacuo* to give **2.27** as a pale yellow powder (1.592 g, 83%) m.p. 142-144 °C.

δ_{H} (300 MHz, CD₃OD) 1.11 (12H, d, $J = 6.8$, CH(CH₃)₂), 3.11 (2H, sept, $J = 6.8$, CH(CH₃)₂), 5.83 (1H, br s, NH), 6.17 (1H, d, $J = 8.2$, ArH), 6.74 (1H, app t, $J = 7.2$, ArH), 7.10 – 7.32 (m, 6H, ArH), 7.50 – 8.40 (2H, br, ArH); δ_{C} (75 MHz, CDCl₃) 23.0 (CH(CH₃)₂), 24.4 (CH(CH₃)₂), 28.4 (CH(CH₃)₂), 112.7, 117.3, 124.0, 127.2, 127.9, 130.1, 133.6, 143.6, 147.4 (aromatic C); ν_{max} /cm⁻¹ (solid) 3205 w, 2961 w, 2868 w, 1603 m, 1586 w, 1511 s, 1493 m, 1465 m, 1453 m, 1310 m, 1057 m. m/z (ESI) 320 (100%, [M+H]⁺); HRMS (FAB) C₂₁H₂₅N₃ calcd. 320.21202, found 320.21208. Anal. Calcd. for C₂₁H₂₅N₃: C, 78.96; H, 7.89; N, 13.15. Found C, 79.03; H, 7.48; N, 13.04%.

Some signals are broad or not apparent in the NMR spectra; the author speculates that this is due to inter- and intramolecular H-bonding.

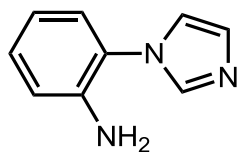
***N*-(2-(3-*iso*-propyl-1*H*-imidazolium)phenyl)-2,6-diisopropylaniline iodide (2.28a)**



In a sealable tube under an atmosphere of air, *i*-propyl iodide (0.350 mL, 3.40 mmol) was added to a green suspension of **2.27** (1.000 g, 3.140 mmol) in MeCN (10 mL). The tube was sealed and heated at 90 °C for 48 h, giving a red solution. The mixture was allowed to cool to RT and filtered through Celite. The volatiles were removed *in vacuo* to give a brown solid that was purified by two precipitations from MeOH (5 mL) upon addition of Et₂O (80 mL), giving **2.28a** (1.138 g, 74%) as a white solid m.p. 228-230 °C.

δ_{H} (300 MHz, CDCl₃) 1.11 (6H, d, $J = 6.8$, CH(CH₃)₂), 1.21 (6H, d, $J = 6.8$, CH(CH₃)₂), 1.75 (6H, d, $J = 6.7$, NCH(CH₃)₂), 3.14 (2H, sept, $J = 6.8$, CH(CH₃)₂), 5.19 (1H, sept, $J = 6.7$, NCH(CH₃)₂), 6.27 (1H, s, NH), 6.34 (1H, d, $J = 8.4$, ArH), 6.80 (1H, td, $^3J = 7.6$, $^4J = 1.1$, ArH), 7.20 (1H, t, $J = 8.4$, ArH), 7.21 (2H, d, $J = 7.0$, ArH), 7.28 – 7.34 (2H, m, ArH), 7.54 (1H, app t, $J = 1.7$, NCHCHN), 7.64 (1H, app t, $J = 1.7$, NCHCHN), 9.36 (1H, br s, NCHN); δ_{C} (75 MHz, CDCl₃) 22.7 (CH(CH₃)₂), 23.4 (CH(CH₃)₂), 24.9 (CH(CH₃)₂), 28.4 (CH(CH₃)₂), 54.0 (NCH(CH₃)₂), 115.3, 118.1, 120.0, 122.0, 123.4, 124.2, 127.4, 127.9, 131.8, 133.4, 135.3, 143.0, 147.3 (aromatic C). ν_{max} /cm⁻¹ (solid) 3215 w, 3070 w, 2962 m, 2867 w, 1608 m, 1563 w, 1549 w, 1505 s, 1463 m, 1432 w, 1303 m, 1199 w, 1120 w, 1048 w, 797 m, 743 vs. m/z (ESI) 362 (100 % [M-I]⁺); HRMS (FAB) C₂₄H₃₂N₃ calcd. 362.25882, found 362.25878. Anal. Calcd. for C₂₄H₃₂IN₃: C, 58.90; H, 6.59; N, 8.59. Found C, 59.07; H, 6.29; N, 8.69%.

2-(1H-imidazol-1-yl)phenylamine (2.29)



2-bromoaniline (1.000 g, 5.952 mmol), imidazole (0.607 g, 8.92 mmol), Cu₂O (0.043 g, 0.30 mmol), Cs₂CO₃ (3.881 g, 11.90 mmol) and 8-hydroxyquinoline (0.173 g, 1.19 mmol) were suspended in

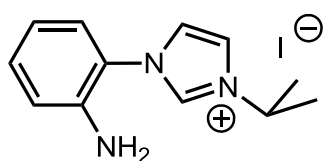
MeCN (10 mL) in a pre-dried sealable tube under an atmosphere of air. The tube was sealed and heated at 100 °C with stirring for 3 days. The volatiles were then removed *in vacuo* and the product extracted into CH₂Cl₂ (70 mL). The solution was washed with H₂O (3 x 150 mL) and brine (100 mL), dried (MgSO₄) and the solvent removed *in vacuo* to give **2.29** (0.791 g, 86%) as a brown solid m.p. 103-104 °C (lit. 103-106 °C).¹⁷⁵

δ_{H} (400 MHz, CDCl₃) δ 3.68 (2H, br s, NH), 6.81 (1H, t, $J = 7.9$), 6.84 (1H, d, $J = 7.9$), 7.12 (1H, d, $J = 7.6$), 7.23 (1H, t, $J = 7.6$).

Some signals are broad or not apparent in the NMR spectra; the author speculates that this is due to inter- and intramolecular H-bonding.

Data matches that reported previously by McNab *et al.*¹⁷⁵

2-(3-*iso*-propyl-1H-imidazolium)phenylamine iodide (2.28b)



In a sealable tube under an atmosphere of air, *i*-propyl iodide (0.770 mL, 7.60 mmol) was added to a suspension of **2.29** (1.070 g, 6.930 mmol) in MeCN (10 mL). The tube was sealed and heated at 90 °C for 3 days. The mixture was then allowed to cool to room temperature and the volatiles removed *in vacuo*. Recrystallisation from hot MeOH / Et₂O three times gave analytically pure **2.28b** (1.480 g, 65%) as pale green crystals m.p. 190-191 °C.

δ_{H} (400 MHz, *d*₄-MeOH) δ 1.66 (6H, d, *J* = 6.7, CHCH₃), 4.79 (1H, app sept, *J* = 6.7, CHCH₃), 6.79 (1H, app t, *J* = 7.7, ArH), 6.97 (1H, d, *J* = 8.2, ArH), 7.25 (1H, d, *J* = 7.7, ArH), 7.30 (1H, app t, *J* = 8.2, ArH), 7.71 (1H, s, NCHCHN), 7.92 (1H, s, NCHCHN), 9.27 (1H, s, NCHN); δ_{C} (100 MHz, *d*₄-MeOH) δ 23.0 (CHCH₃), 55.0 (CHCH₃), 118.4, 118.6 (ArCH), 121.9 (ArC), 122.4, 25.4 (NCHCHN), 128.1, 132.7 (ArCH), 137.2 (N₂CH), 144.8 (ArC); *m/z* (ESI) 202 (100%, [M-I]⁺); Anal. Calcd. for C₁₂H₁₆IN₃: C, 43.78; H, 4.90; N, 12.77. Found C, 43.69; H, 4.82; N, 12.60%.

3: Chapter 3 – Synthesis and Reactivity of Complexes of Tridentate Amido-*bis*NHC Ligands

Chapter 3 will discuss the synthesis and characterisation of amido *bis*-NHC complexes of the group 10 metals, from the imidazolium salts **2.25a-b** reported in Chapter 2.

Prepared pincer complexes containing a metal-amide bond could potentially allow C-H activation by a bifunctional AMLA(4) mechanism; this was further investigated in terms of direct arylation reactions in Chapter 5. Preliminary observations of a CNC Pd complex in C-H and H-H bond activation reactions, as an indicator of bifunctional reactivity, will also be discussed in this chapter.

3.1: Introduction

The use of tridentate pincer ligands to stabilise metal complexes has been an active topic of research for nearly 40 years, whilst bifunctional reactivity of complexes containing a pincer ligand has also been observed. This brief introduction will focus on the synthesis of group 10 metal pincer complexes only, and will specifically discuss pincer complexes including at least one NHC or amido donor.

3.1.1: Group 10 Metal Pincer Complexes

Pincer ligands are tridentate ligands coordinated in a meridional fashion, **Figure 3.1**.¹⁷⁶

Pincer ligands are usually abbreviated to a three-symbol shorthand designating the three donor atoms involved, for example NCN, PCP, CNC, SCS, CCC. Pincer complexes are often highly oxidatively and thermally stable, with metal dissociation from the ligand disfavoured due to the strong chelation effect.¹⁷⁷

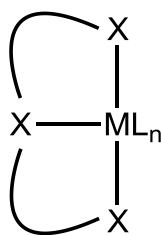


Figure 3.1: Metal complex with schematic pincer ligand.

The first examples of pincer complexes (**3.1**) were reported by Shaw in 1976, containing the PCP ligand 1,3-bis[(di-*t*-butylphosphino)methyl]benzene, **Figure 3.2**.¹⁷⁷ These complexes displayed excellent stability: the complex (PCP)NiCl was purified by sublimation at 240 °C under 1 atm of air, with no apparent decomposition.

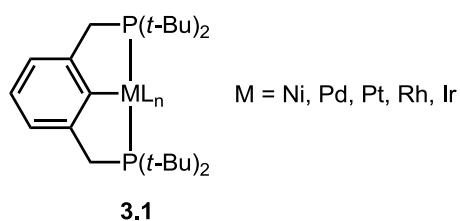


Figure 3.2: Shaw's first pincer complexes.

Since this first report, there have been a huge number of pincer complexes synthesized; a selection of catalytically active Pd and Ni complexes of differing architectures is shown in **Figure 3.3**. The complexes in **Figure 3.3** have shown catalytic activity in several reactions, including Kharasch additions (**3.2**),¹⁷⁸ Heck cross-couplings (**3.3, 3.4, 3.5, 3.7**),^{179–182} Suzuki cross-couplings (**3.3, 3.4**)^{183,184} and enantioselective aldol reactions (**3.6**)¹⁸⁵.

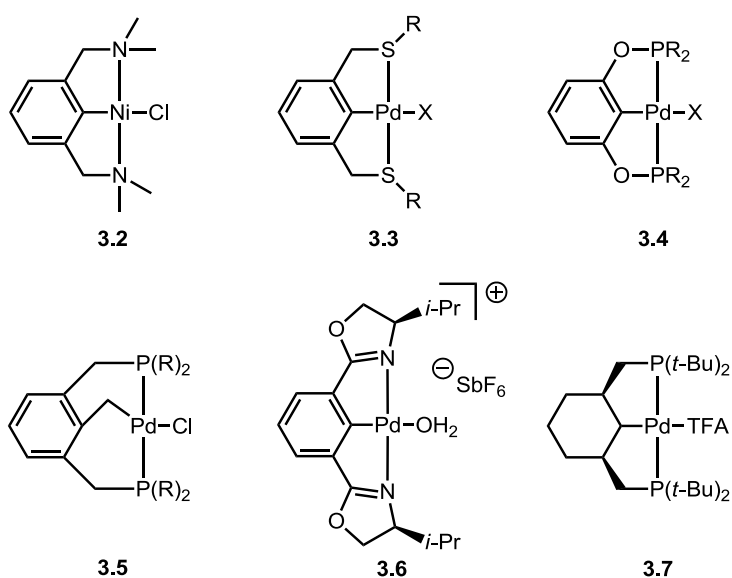
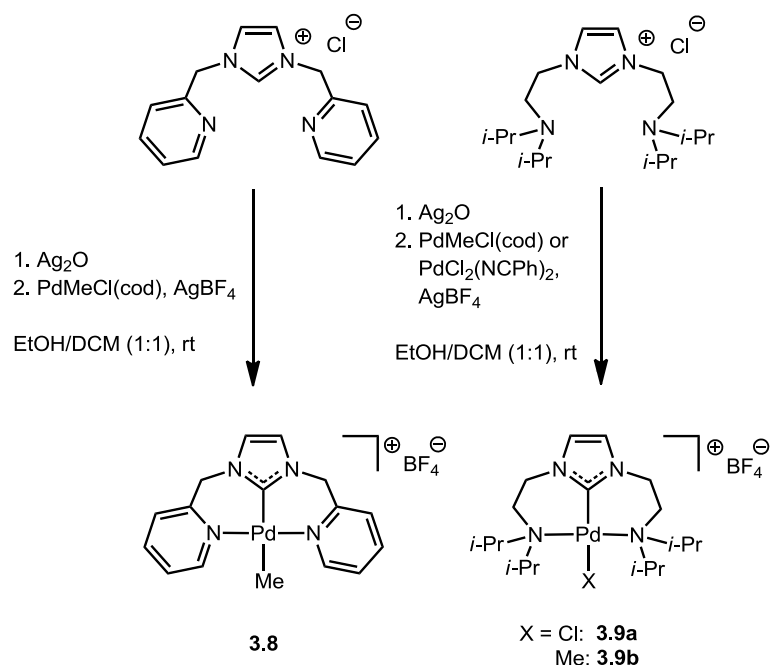


Figure 3.3: Selected pincer complexes of Pd, Ni.

3.1.2: Group 10 Imidazolium NHC Pincer Complexes

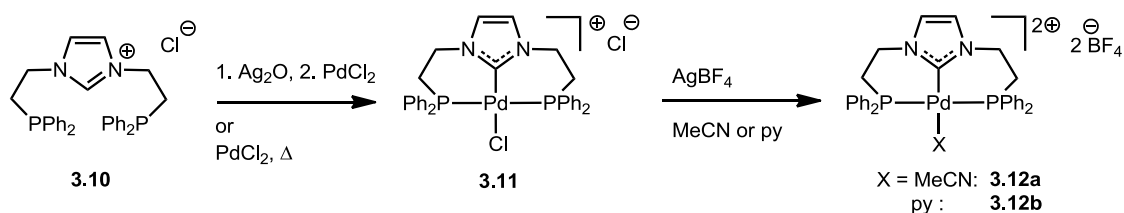
Recent research has been directed towards pincer ligands incorporating N-heterocyclic carbene donors, which have unique qualities compared with the pincer ligands described in Ch. 3.1.1. The metal-NHC bond is known to be highly stable and NHCs will not dissociate readily from the metal, imparting extra stability to the already highly resilient pincer complex. This section will discuss pincer ligands containing imidazolium-based NHCs.

The first NHC-pincer complexes were reported by Cavell *et al.*;¹⁵¹ Pd^{II} complexes of a *bis*-pyridyl NHC (**3.8**) and a *bis*-alkylamino NHC (**3.9a-b**) were synthesised by *in situ* transmetallation from silver carbene complexes, **Scheme 3.1**. Complexes **3.8** and **3.9a** were found to be very active catalysts for the Heck coupling of 4-bromoacetophenone with *n*-butyl acrylate, with very high TON of 230000 (72 h) for **3.8** and 660000 (120 h) for **3.9a**.



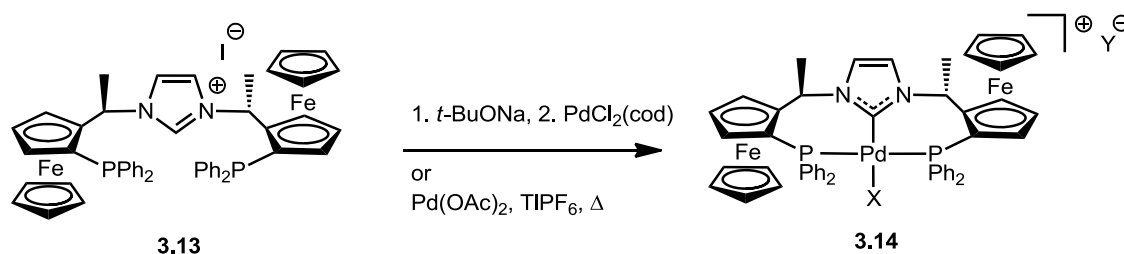
Scheme 3.1: Synthesis of (NCN) Pd complexes.¹⁵¹

NHC-*bis*-phosphine pincer complexes are also known. In 2004 Lee *et al.* reported the complexes **3.11** and **3.12a-b**, **Scheme 3.2**.¹⁸⁶ **3.11** was first formed by either Ag-carbene transmetalation or direct reaction of the imidazolium salt **3.10** with PdCl₂, with elimination of HCl. **3.12a-b** were then formed by halide extraction with AgBF₄ in the presence of the appropriate neutral ligand as solvent. Both **3.11** and **3.12a** showed catalytic activity in Heck couplings, with the dicationic **3.12a** displaying exceptional TONs of up to 5.6 × 10⁶ for the coupling of phenyliodide and styrene.



Scheme 3.2: Synthetic routes to (PCP) Pd complexes.¹⁸⁶

Togni reported similar Pd complexes of chiral PCP ligands, **3.14** ($X = \text{Cl}$, $Y = \text{PF}_6^-$; $X = \text{I}$, $Y = \text{OAc}^-$), synthesised by direct reaction of the imidazolium salt **3.13** with $\text{Pd}(\text{OAc})_2$ or by *in situ* deprotonation using *t*-BuONa in the presence of $\text{PdCl}_2(\text{cod})$, **Scheme 3.3**.^{187,188} **3.14** showed high activity in the asymmetric hydroamination of cyanoolefins, with product *ee* of up to 75%.



Scheme 3.3: Synthesis of chiral-PCP pincer complexes **3.14** ($X = \text{Cl}$, $Y = \text{PF}_6^-$; $X = \text{I}$, $Y = \text{OAc}^-$).^{187,188}

By far the most studied NHC-pincer metal complexes are those of *bis*-NHC-pyridine or -2,6-lutidine ligands, **Figure 3.4**, in which the carbenes are located on the ‘arms’ of the pincer ligand, rather than being the central donor.

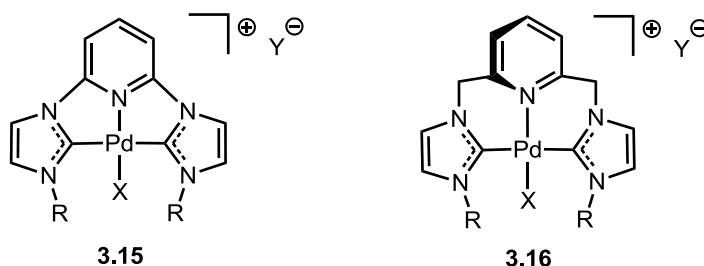


Figure 3.4: CNC pincer complexes: *bis*-NHC-pyridine (**3.15**) and -2,6-lutidine (**3.16**).

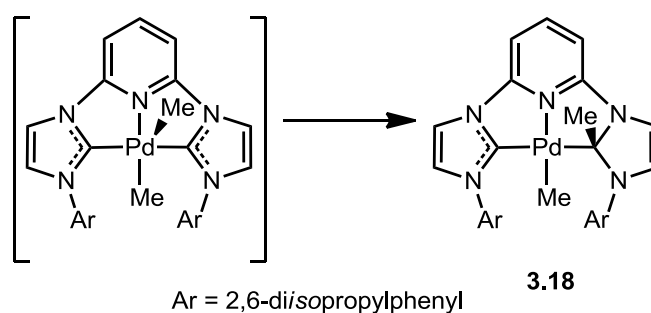
Complex **3.15a** ($R = \text{Me}$, X and $Y = \text{Br}$) has been shown by Peris and Crabtree to be a robust catalyst for Heck reactions, with activity maintained at 165 °C under aerobic

conditions; many other catalysts are either inactive or decompose under similar conditions.¹⁵⁴ **3.15a** (R = Me, X and Y = Br) was synthesised by heating imidazolium salt **3.17** directly with Pd(OAc)₂, eliminating acetic acid, **Scheme 3.4**.



Scheme 3.4: Synthesis of **3.15a** by direct reaction of imidazolium salt **3.17** with Pd(OAc)₂.¹⁵⁴

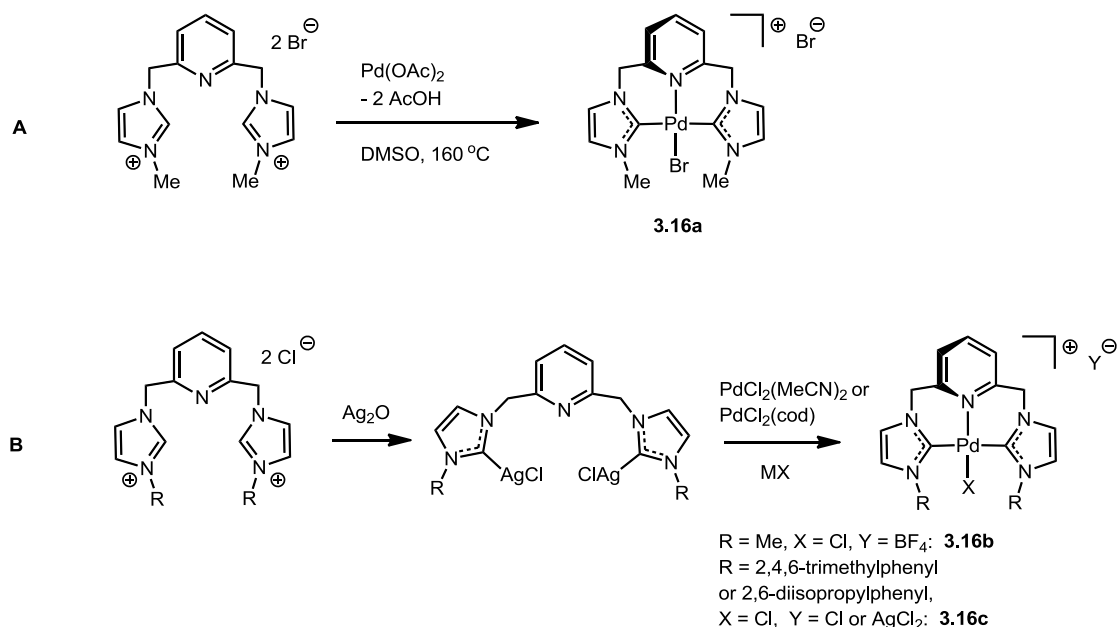
Experimental and computational studies with complexes **3.15c** (R = 2,6-diisopropylphenyl, X = Me) have shown that reductive elimination of a 2-methyl imidazolium salt is facile,¹⁸⁹ and migration of a methyl ligand onto a carbene are possible, with complex **3.18** fully characterised, **Scheme 3.5**.¹⁹⁰



Scheme 3.5: Migration of a methyl ligand onto a carbene donor in CNC Pd complexes.¹⁹⁰

Bis-NHC-2,6-lutidine Pd complexes **3.16** (**Figure 3.4**) have been synthesised independently by the groups of Crabtree (**3.16a**: R = Me, X and Y = Br),¹⁵³ Cavell

(**3.16b**: R = Me, X = Cl or Me, Y = BF₄)¹⁹¹ and Danopoulos (**3.16c**: R = 2,4,6-trimethylphenyl or 2,6-diisopropylphenyl, X = Cl, Y = Cl or AgCl₂).^{155,192} Crabtree's synthetic route to **3.16a** (Scheme 3.6A) employed the same direct reaction of an imidazolium salt and Pd(OAc)₂ previously used for complex **3.15a**, while Cavell and Danopoulos both used a silver transmetalation strategy to synthesise **3.16b-c** (Scheme 3.6B).



Scheme 3.6: Synthetic routes to bis-NHC-2,6-lutidine Pd complexes **3.16**.^{153,155,191,190}

Danopoulos has reported that complexes **3.16** adopt a helical conformation, exhibiting planar chirality, with two atropisomers formed, **Figure 3.5**.¹⁵⁵ Complexes **3.15** have not been observed to form atropisomers as the lack of a CH₂ group between the pyridine and NHC rings means that all three rings (pyridine and both NHCs) are coplanar. Crabtree, Clot and Eisenstein have shown that interconversion of the two atropisomers is possible, and this interconversion is dependant on solvent and counter-anion; VT-NMR and computational studies show it is possible for the lutidine

N to dissociate from the metal and allow coordination of nucleophilic counterions in a reversible process, resulting in interconversion of the atropisomers.¹⁹³

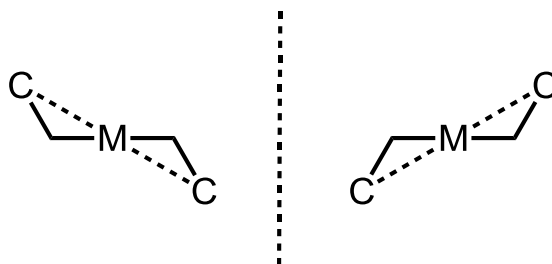
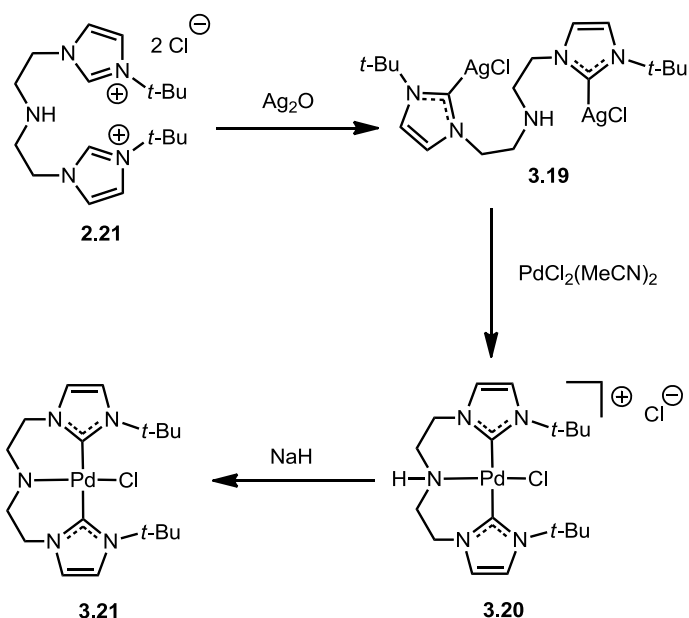


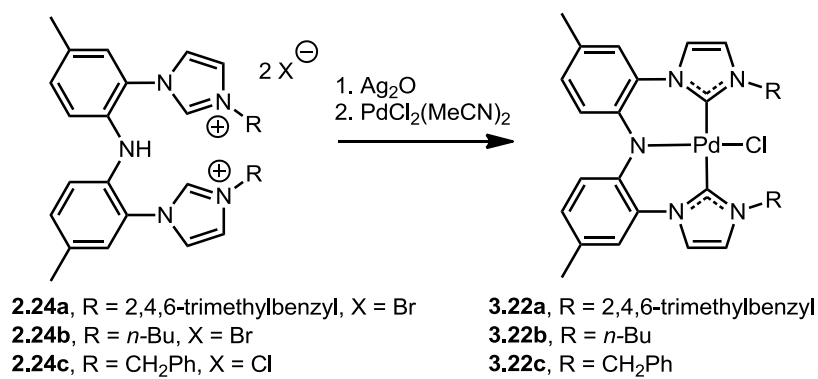
Figure 3.5: Representation of the two atropisomers in **3.16**; the view is down the X-M-N vector.

More closely related to the complexes reported in this chapter, Douthwaite synthesised the Pd amino-*bis*NHC complex **3.20** by transmetallation from the silver carbene **3.19** to PdCl₂(MeCN)₂, **Scheme 3.7**.¹⁶⁹ **3.20** could be deprotonated with NaH to give the amido-*bis*NHC complex **3.21**. As with **3.16** atropisomerism was observed, with **3.21** showing a single broad set of resonances in the ¹H NMR spectrum for the CH₂ protons which resolved into 8 individual peaks corresponding to the two atropisomers at -40 °C; similar atropisomerism was displayed by **3.20**.



Scheme 3.7: Synthesis of Douthwaite's amino- and amido-bisNHC pincer complexes.¹⁶⁹

During the course of this work, Luo *et al.* reported the Pd diarylamido-bisNHC pincer complexes **3.22a-c**, synthesised by *in situ* transmetalation of a silver carbene to $\text{PdCl}_2(\text{MeCN})_2$, **Scheme 3.8**.¹⁷⁰ In contrast to Douthwaite's report,¹⁶⁹ Luo's group were unable to isolate the silver carbene intermediate. Interestingly, in the complexation reaction the Pd amide was formed, rather than the amine complex. The authors suggested that, as Ag_2O is insufficiently basic to deprotonate a secondary aryl amine, HCl elimination occurs during the complexation. Complexes **3.22** existed as two atropisomers but high temperature NMR experiments showed no interconversion of isomers, suggesting that the ligand prevents isomerisation. Most likely the lack of isomerisation was due to the NHC and amide donors being strongly bound and preventing interconversion of the isomers by dissociation/reassociation of a pincer arm. **3.22** were found to be competent catalysts for the Suzuki-Miyaura coupling of a variety of aryl bromides and aryl boronic acids, unusually under aerobic conditions.

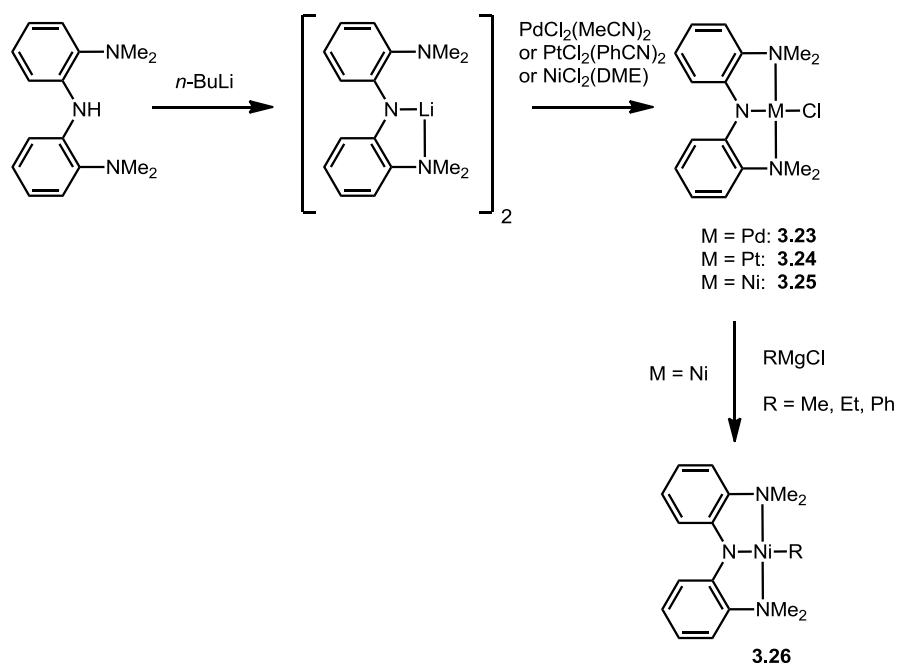


Scheme 3.8: Synthesis of Luo's amino- and amido-bisNHC pincer complexes.¹⁷⁰

3.1.3: Group 10 Amido Pincer Complexes

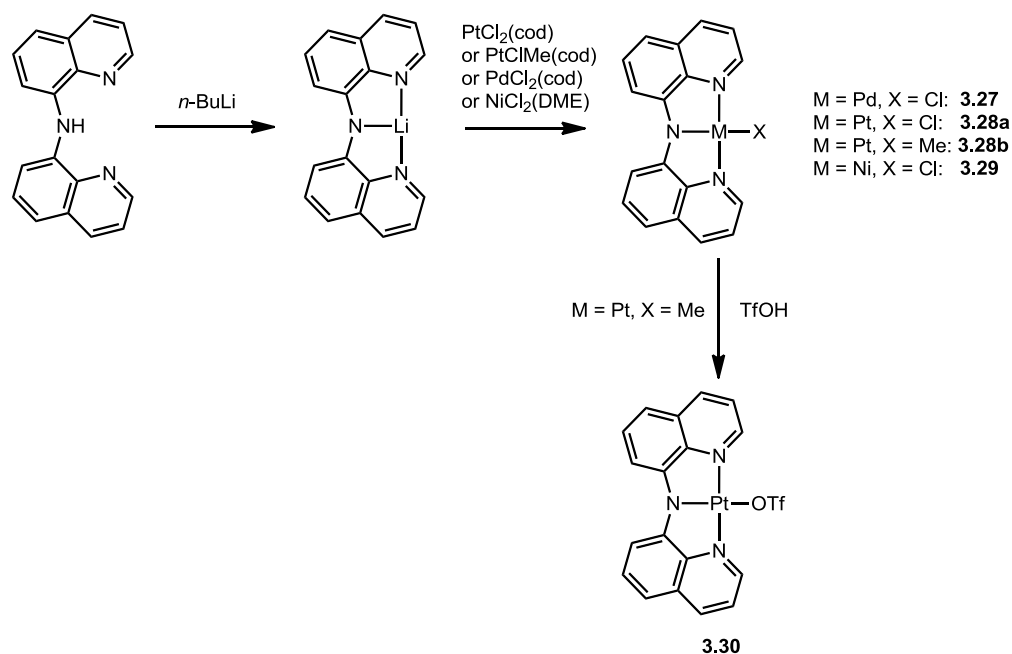
Several group 10 pincer complexes containing a metal-amido bond have been synthesised, and have shown interesting chemistry. The amido-*bis*NHC complexes (CNC)PdCl **3.21** and **3.22** have been discussed above (Ch. 3.1.2), and will not be discussed further in this section.

Diarylamino NNN complexes of Pd, Pt and Ni (**3.23**, **3.24**, **3.25**) have been synthesised by reacting metal salts with the lithiated ligand, **Scheme 3.9**.^{194,195} The Ni alkyl complexes **3.26** were synthesised by reaction of **3.25** with alkyl Grignard reagents. Ni complexes **3.26** have displayed good activity as catalysts in Kumada C-C coupling reactions.



Scheme 3.9: Synthesis of (NNN)MCl complexes.^{194,195}

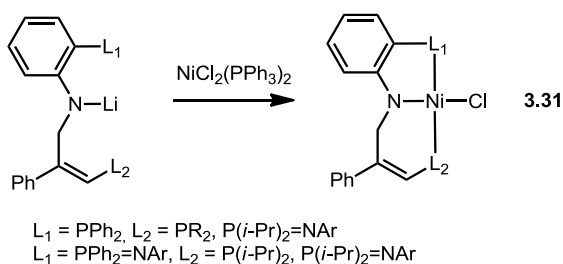
Reaction of a lithiated NNN ligand precursor with metal salts was also used by Peters *et al.* to make complexes **3.27**, **3.28a-b** and **3.29**, **Scheme 3.10**.^{196,197} Ligand exchange of **3.28b** with triflic acid gave **3.30**, which has displayed base-promoted C-H activation of benzene; the mechanism of this reaction has not been elucidated but an AMLA(4) mechanism involving the metal-amido bond is a possibility.¹⁹⁷



Scheme 3.10: Synthesis of (NNN)MX complexes.^{196,197}

The reaction of amido lithium complexes with $\text{NiCl}_2(\text{PPh}_3)_2$ was used by Wang to synthesise unsymmetrical PNP, PNN and NNN Ni complexes **3.31**, **Scheme 3.11**.¹⁹⁸

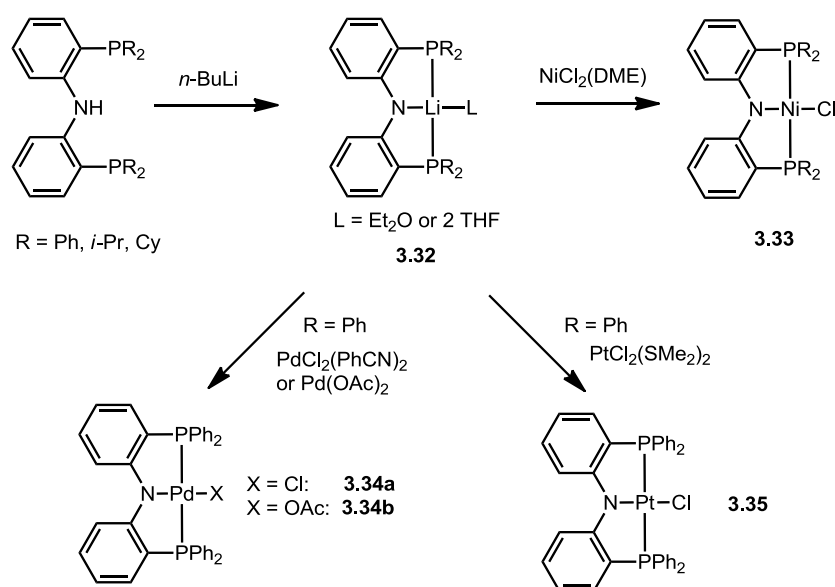
These complexes were all highly active in the Kumada coupling of aryl Grignard reagents and aryl halides; however, PNP complexes were less effective than their PNN and NNN analogues.



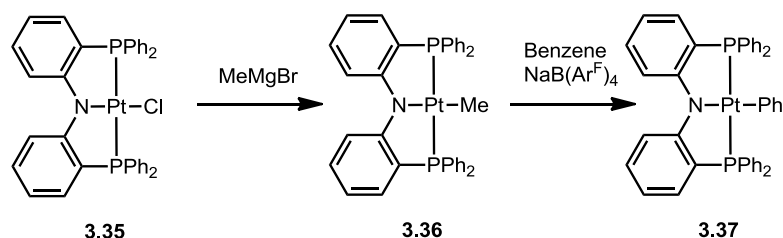
Scheme 3.11: Synthesis of unsymmetrical PNP, PNN and NNN Ni complexes.¹⁹⁸

The reaction of a lithiated ligand precursor has also been used as a strategy for synthesising diarylamido PNP complexes. Liang *et al.* isolated the amido lithium

complexes **3.32**; it was then possible to react **3.32** with $\text{NiCl}_2(\text{DME})$ to give $(\text{PNP})\text{NiCl}$ **3.33**, with $\text{PdCl}_2(\text{PhCN})_2$ or $\text{Pd}(\text{OAc})_2$ to give $(\text{PNP})\text{Pd}$ complexes **3.34**, or with $\text{PtCl}_2(\text{SMe}_2)_2$ to give $(\text{PNP})\text{PtCl}$ **3.35**.^{199–201} Reaction of **3.35** with MeMgBr gives $(\text{PNP})\text{PtMe}$ (**3.36**), which can activate a C-H bond of benzene to form $(\text{PNP})\text{PtPh}$ (**3.37**), **Scheme 3.13**; it is unclear whether the metal-amido bond participates in this C-H activation step.²⁰¹ Subsequently, similar stoichiometric C-H activation has been observed in the reaction of $(\text{PNP})\text{NiH}$ (**3.38**) with benzene.²⁰²



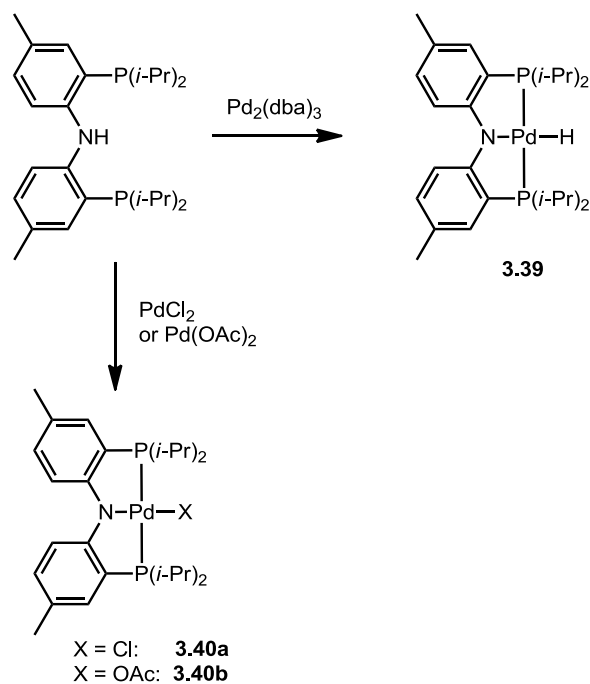
Scheme 3.12: Synthesis of PNP complexes.^{199–201}



Scheme 3.13: Stoichiometric C-H activation of benzene by **3.35**.²⁰¹

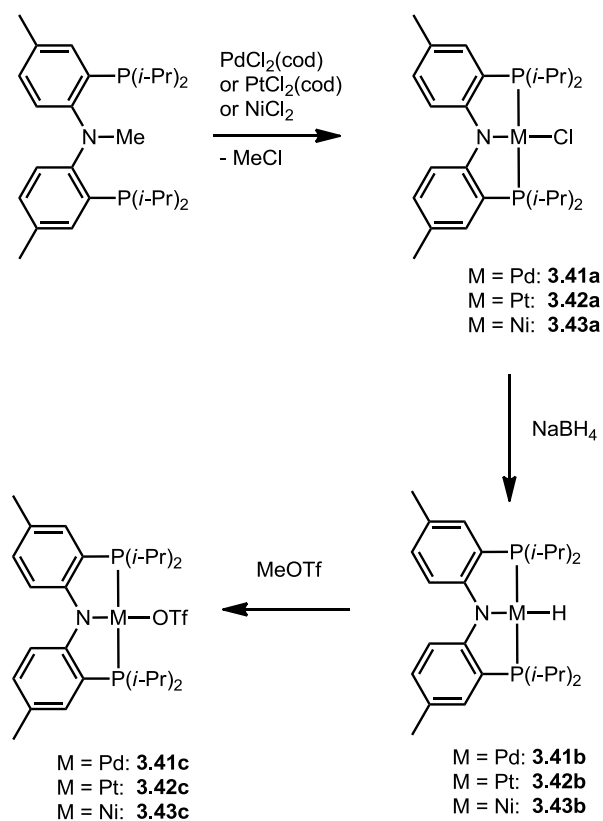
Another method for forming diarylamido PNP complexes is by direct reaction of PNHP with a metal precursor; this has been demonstrated by Ozerov *et al.*, **Scheme 3.14**.²⁰³

Oxidative addition of PNHP to Pd⁰ gives (PNP)PdH (**3.39**), while the anionic ligands on PdCl₂ and Pd(OAc)₂ act to deprotonate PNHP to give **3.40a-b**.



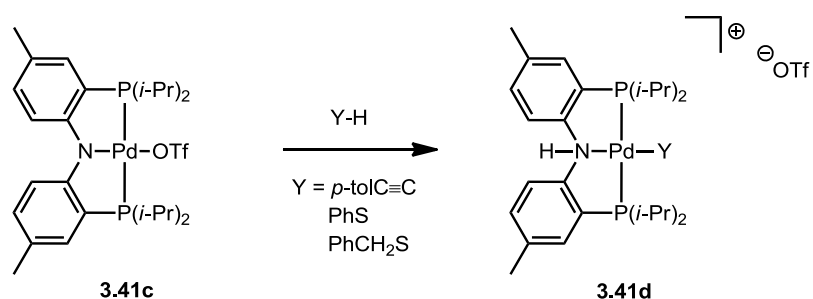
Scheme 3.14: Synthesis of (PNP)Pd complexes by direct reaction of PNHP with metal precursors.²⁰³

Unusually, the direct reaction of PN(Me)P with metal salts also results in formation of (PNP)M complexes, proceeding by N-C bond cleavage through oxidative addition and elimination of MeCl, **Scheme 3.15**.^{204,205}



Scheme 3.15: Synthesis of (PNP)M complexes by direct reaction of PN(Me)P with metal precursors.^{204,205}

(PNP)PdOTf (**3.41c**) has shown interesting bifunctional reactivity; the cleavage of C(sp)-H, S-H, and H-H bonds across the Pd-N bond has been observed,³¹ with B-H and B-B bond cleavage observed if a weakly-coordinating BAR_4^{F} anion is present.²⁰⁶



Scheme 3.16: Bifunctional Y-H bond splitting by (PNP)PdOTf **3.41c**.³¹

3.1.4: Aims and Objectives

The aim of the work presented in this chapter was to synthesise and characterise diarylamido *bis*-NHC CNC pincer complexes of the group 10 metals (**Fig. 3.1**), from the diarylamine-*bis*imidazolium salts **2.25a-b** reported in Chapter 2. The main objective was to find a synthetic route that give (CNC) pincer complexes in high purity for investigations into bifunctional catalysis.

Preliminary investigations into the reactivity of a (CNC) Pd complex with H-H and C-H bonds will also be described in this chapter, the activity of a (CNC) Pd complex in direct arylation reactions of heterocycles will be described in Ch. 5.

3.2: Results and Discussion

3.2.1: Synthesis of CNC Group 10 Complexes

3.2.1.1: Synthesis of (CNC) Pd Complexes

In order to prepare (CNC) complexes, the first strategy investigated was the transmetallation of a silver carbene to palladium, similar to the strategy used by Douthwaite¹⁶⁹ and Luo¹⁷⁰ to prepare amido-*bis*NHC (CNC) complexes. Unfortunately, the reactions of imidazolium salts **2.25a-b** with Ag₂O gave only an intractable mixture of products. Furthermore, the reaction of **2.25a** and Ag₂O when refluxed in DCE (84 °C) with powdered 4Å molecular sieves added still gave an intractable mixture; this procedure was adapted from a literature method²⁰⁷ for forming silver complexes with less reactive imidazolium salts. No reaction was observed when formation of the silver complex and transmetallation was attempted in the presence of the metal salts PdCl₂(cod), PtCl₂(cod), PdCl₂(MeCN)₂, PdCl₂ or Pd(OAc)₂; this is in contrast to Luo's reported synthesis method for similar CNC complexes **3.22 (Scheme 3.8)**.¹⁷⁰

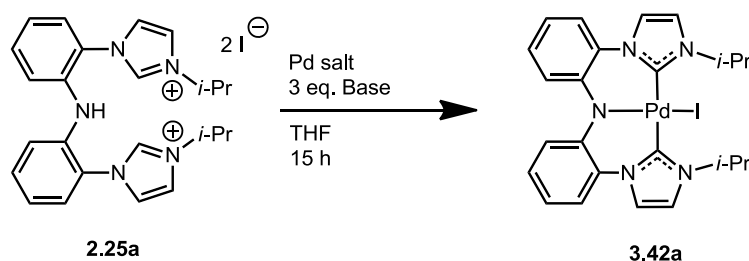
Attempts to isolate the free carbene from imidazolium salts **2.25** by deprotonation using several strong bases (NaH, *t*-BuONa, BuLi, KHMDS) also failed, leading only to intractable product mixtures.

Deprotonation of a ligand precursor with base in the presence of a metal salt is also a useful strategy for the synthesis of NHC and amido complexes.^{187,188} The reactions of **2.25a** with 3 equivalents of base in the presence of several palladium salts were attempted, **Scheme 3.17**. It was quickly found that KHMDS, a strong, non-nucleophilic

base, when stirred with a mixture of **2.25a** and PdCl₂(cod) in THF gave a crude ¹H NMR spectrum and MS peaks consistent with a mixture containing complex **3.42a**.

Crystallisation failed to isolate pure **3.42a**; however, it was found that **3.42a** was stable on silica, and so column chromatography was used to isolate pure **3.42a**, albeit in low (< 20%) yield.

FAB MS gave a peak assigned as [M]⁺ at 617 Da, confirming that iodide was bound in the fourth coordination site. The ¹H NMR spectrum of **3.42a** displayed an unusual downfield shift of the *i*-Pr CH resonance to δ 6.35. The ¹H NMR spectrum of **3.42a** lacked the imidazolium NCHN and NH resonances that were present in **2.25a**, confirming coordination of the CNC ligand. An interesting feature was the splitting of the *i*-Pr CH₃ resonances into two independent doublets, at δ 0.71 and 1.32, suggesting diastereotopic methyl groups. ¹³C NMR spectra showed the N₂C-Pd resonance at δ 165.3, this signal far downfield is typical of a highly electron-deficient carbene bound to Pd, and within the range reported for Luo's (CNC)PdCl complexes **3.22a-c** (164.8-165.7 ppm).¹⁷⁰



Scheme 3.17: Initial conditions for the synthesis of **3.42a**.

With a method to isolate pure **3.42a** now in hand, screening of conditions was conducted in order to improve the yield of the reaction. Several palladium salts were

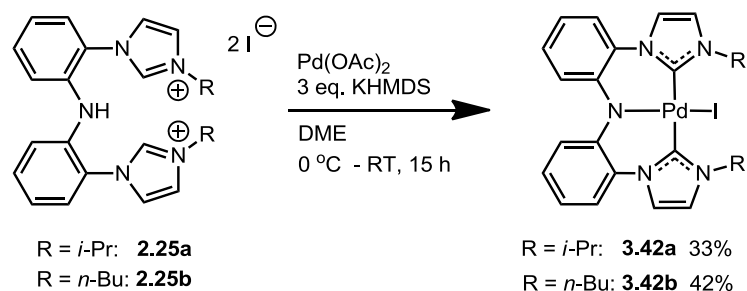
used (**Table 3.1**), with the best yield (31%) obtained with PdCl₂(cod) in THF. Other bases, including *n*-BuLi, LDA and *t*-BuONa failed to give better yields.

Table 3.1: Initial yields of **3.42a** from reaction of **2.25b** with KHMDS in THF.

Pd Salt	Isolated Yield of 3.42a (%)
PdCl ₂ (PhCN) ₂	6
PdCl ₂ (MeCN) ₂	0
PdCl ₂ (COD)	31
Pd(CF ₃ CO ₂) ₂	23
Pd(OAc) ₂	13

Conditions: imidazolium salt **2.25a** (1 eq.), metal precursor (1 eq.), KHMDS (3 eq., 1 M in PhMe), THF, -78 °C – RT, 15 h. Reported are isolated yields after column chromatography.

Poor solubility of the imidazolium salt in THF, along with the formation of several mixed byproducts in the reaction, accounted for the poor yields. Repeating column chromatography on an isolated sample of **3.42a** gave back a quantitative yield of analytically pure complex, showing no decomposition from the purification procedure. It was found that reactions could be carried out with better yield in DME solvent, giving an optimum yield of 33% using Pd(OAc)₂, with base addition at 0 °C. The reaction in DME proved highly reproducible.



Scheme 3.18: Synthesis of CNC Pd complexes.

Complex **3.42b** was synthesised in an identical procedure to **3.42a** from imidazolium salt **2.25b**, as an analytically pure red-brown solid in 42% yield. FAB MS gave a peak assigned as $[\text{M}]^+$ at 645 Da. The ^1H NMR spectrum of **3.42b**, as for **3.42a**, showed no NCHN or NH resonances, whilst the alkyl region is dominated by a 6H triplet at δ 0.72 (CH_3) and complex multiplets (δ 0.96-1.24 (4H), 1.25-1.43 (2H), 1.70-1.87 (2H), 4.12-4.24 (2H), 4.61-4.73 (2H)) resulting from two sets of diastereotopic *n*-butyl protons. Notably, the two closest methylene groups to the iodide ligand (NCH_2CH_2) both showed prominent downfield shifts in the ^1H NMR spectrum, like that observed for the *i*-Pr CH resonance of complex **3.42a**. The ^{13}C NMR spectrum of **3.42b** contained a $\text{N}_2\text{C-Pd}$ resonance at δ 167.0, similar to that of **3.42a** (165.3 ppm).

Crystals of **3.42a** and **3.42b** suitable for X-ray diffraction were formed by the slow evaporation of a C_6D_6 solution of **3.42a** or **3.42b**; an ORTEP figure for the structure of **3.42a** is shown in **Figure 3.6**, and **3.42b** in **Figure 3.7**; selected bond lengths and angles are shown in **Table 3.2**.

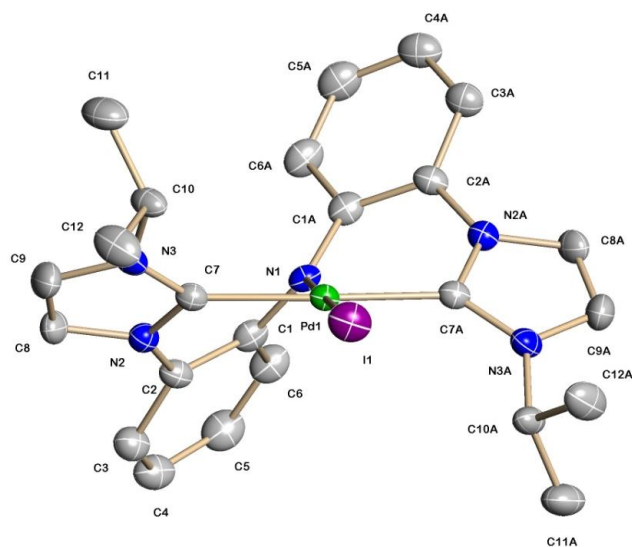


Figure 3.6: ORTEP view of **3.42a**. Figure shows 50% displacement ellipsoids, H-atoms are omitted for clarity.

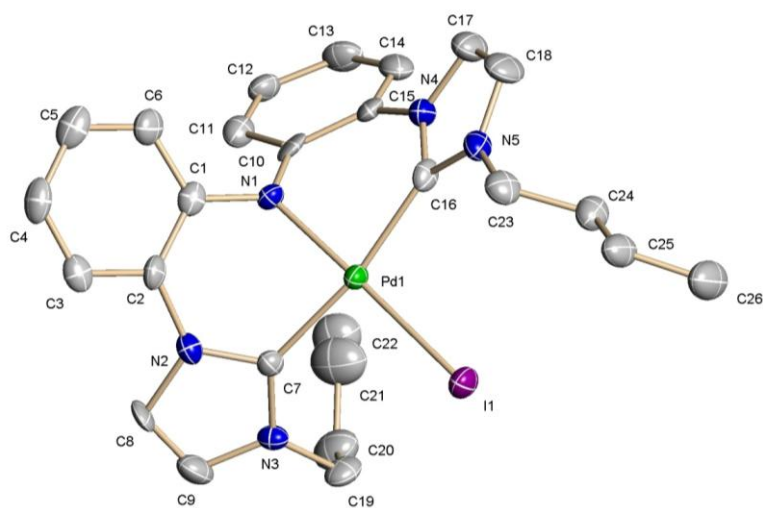


Figure 3.7: ORTEP view of **3.42b**. Figure shows 50% displacement ellipsoids, H-atoms and a single molecule of C₆D₆ are omitted for clarity.

Table 3.2: Selected bond lengths (Å) and angles (°) for **3.42a-b**

	3.42a	3.42b
M-N(amide)	2.023(3)	2.020(4)
M-C(NHC)	2.024(3)	2.020(6)
	2.024(3)	2.019(6)
M-I	2.5887(6)	2.6034(6)
C-Pd-C	170.61(17)	168.8(2)
N-Pd-I	180.0	178.65(17)

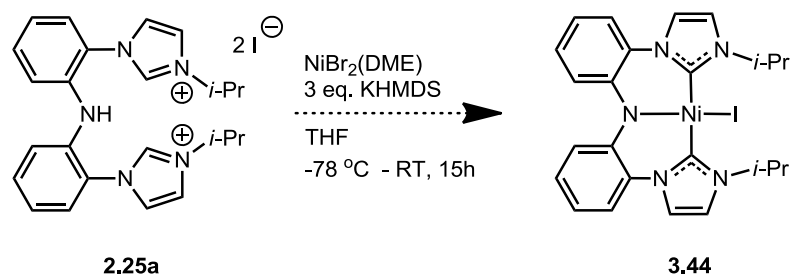
3.42a crystallised in the non-centrosymmetric chiral point group C222(1), with only one enantiomer present in the unit cell. The angle between the square plane around Pd and the trigonal plane of the amide nitrogen was 53.3°, showing the distortion from planarity and therefore atropisomerism of **3.42a**. VT-NMR up to 344 K showed no line broadening, consistent with no interconversion of the atropisomers; this is in contrast to the lutidine-bisNHC complexes **3.16**, which show solvent-dependant interconversion of atropisomers at elevated temperatures.^{155,193}

3.42b crystallised in the non-centrosymmetric achiral space group Aba2, and both enantiomers were observed in the unit cell. In this case, the angle between the square plane around Pd and the trigonal plane of the amide nitrogen was 57.4°.

Both **3.42a** and **3.42b** have several interesting features in their solid-state structures. The plane of the NHC rings in both complexes **3.42** lie at an angle of *ca.* 40° relative to the square plane around Pd (**3.42a**: 41.1°; **3.42b**: 38.7, 41.2°); this is indicative of a

replacing the imidazolium salt with **2.25b** gave **3.43b** as an analytically pure yellow solid in 12% yield. The poor yields were not improved by changing the solvent to DME, and like for Pd, complex mixtures were formed in all reactions. Both complexes **3.43a** and **3.43b** displayed an $[M-I]^+$ peak in ESI MS at m/z 579 and 607 respectively. The 1H NMR spectrum of **3.43a** showed the characteristic sets of *i*-Pr CH_3 doublets at δ 0.73 and 1.37, with the *i*-Pr CH septet located downfield at δ 6.38, again suggesting a close H-I contact with the iodide ligand. For the 1H NMR spectrum of **3.43b**, the *n*-butyl CH_2 appeared as multiplets at δ 1.27 (4H), 1.74 (2H), 1.98 (2H) and 4.52 (4H), suggesting the existence of two atropisomers as with the Pd analogue **3.42b**. In the ^{13}C NMR spectrum carbene resonances were observed at δ 162.5 (**3.43a**) and 164.0 (**3.43b**). Unfortunately, despite several attempts, no crystals of either **3.43a** or **3.43b** of quality sufficient for X-ray diffraction could be grown. However, the NMR data closely resemble those for the Pd analogues **3.43a** and **3.43b**, so the author is confident in the assignment of the structure of **3.43a-b**.

3.2.1.3: Attempted Synthesis of (CNC) Ni Complex



Scheme 3.20: Attempted synthesis of CNC Ni complex, **3.44**.

An attempt was also made to synthesise a CNC Ni complex **3.44**, **Scheme 3.20**.

Treatment of the imidazolium salt **2.25a** and $NiBr_2(DME)$ with KHMDS under the

conditions as described for the Pt complexes **3.43** gave, after filtration, a crude purple-brown solid. ^1H NMR spectroscopy of the crude solid showed a mixture containing one major product, which displayed characteristic signals of a CNC complex. Two 6H *i*-Pr CH_3 doublets were clearly visible at δ 0.74 and 1.12, with a corresponding *i*-Pr CH apparent septet at δ 6.13; however, aromatic signals were largely obscured by byproducts. ESI MS gave characteristic signals for $[\text{M-I}]^+$ and $[\text{M-I+MeCN}]^+$ at m/z 442 and 483 respectively. TLC of the crude mixture (33% EtOAc/pet. ether) showed a major purple spot, believed to correspond to the desired product, at $R_f = 0.02$. Unfortunately, during column chromatography the purple band was observed to degrade on silica, and no product was isolated. Crystallisation also failed to furnish pure **3.44**, and so the synthesis of complex **3.44** was abandoned.

3.2.2: Reactivity of CNC Complexes

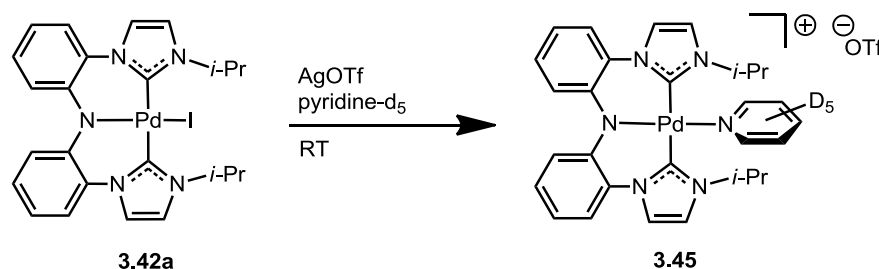
In line with the objective to investigate bifunctional reactivity of CNC pincer complexes, it was decided to look at the reaction of **3.42a** with C-H and H-H bonds. The author hoped to observe the metal-amide bond acting bifunctionally to break bonds, protonating the nitrogen donor and leading to an isolable complex which could be characterised further.

3.42a was chosen as a good candidate to test the reactivity of CNC Pd complexes, as the complex was relatively easily isolated on a larger scale (up to 0.5 g) and the *i*-propyl substituents gave easily recognisable resonances in ^1H NMR spectra.

First, the thermal stability of **3.42a** was tested by heating in various solvents to reflux, under aerobic conditions, without the exclusion of water. No decomposition of the complex was observed over 15 h in refluxing THF, benzene or toluene, with **3.42a** recovered as the only species present.

In order for a substrate to bind to the metal during a catalytic reaction, it is necessary to have a free coordination site. Hence, the lability of the iodide ligand of **3.42a** was investigated. **3.42a** was heated with excess LiCl in THF, and monitored by ^1H NMR spectroscopy and mass spectrometry. A slow exchange of the iodide ligand of **3.42a** with chloride was observed above a temperature of 60 °C, taking 5 days to approach 85% conversion. This suggests that the iodide ligand becomes labile to a significant extent only above 60 °C in poorly-coordinating solvents.

Dissolving **3.42a** in the coordinating NMR solvent pyridine- d_5 gave a mixture of two complexes. The first complex, identified by a downfield *i*-Pr CH apparent septet at δ 6.40, was most likely **3.42a**, although the identity of this complex could not be confirmed. The second complex was identified by an *i*-Pr CH apparent septet further upfield at δ 3.68, suggesting dissociation of the iodide ligand and coordination of pyridine; as there is no hydrogen-bonding interaction between the pyridine ligand and *i*-Pr CH, the CH resonance would be expected to be below 4 ppm.



Scheme 3.21: Synthesis of **3.45**.

Addition of 1.5 equiv. AgOTf to a pyridine- d_5 solution of **3.42a** gave quantitative conversion of **3.42a** to complex **3.45** (Scheme 3.21), which was characterized by NMR spectroscopy. Although bound pyridine- d_5 signals could obviously not be observed in the ^1H NMR spectrum, the aforementioned shift of the *i*-Pr CH apparent septet strongly suggested removal of the iodide ligand, as did the formation of insoluble silver halide in the reaction. Two 6H doublets were observed for the *i*-Pr CH_3 at δ 0.72 and 0.92, again demonstrating the atropisomerism common to these CNC complexes. All other expected resonances were observed in both ^1H and ^{13}C NMR spectra, including the Pd-C signal at δ 163.8 in the ^{13}C NMR spectrum. In the ^{19}F NMR spectrum of **3.45** a triflate CF_3 resonance was found at δ -77.2.

Incomplete removal of pyridine prevented isolation of analytically pure **3.45**, but crystals suitable for X-ray diffraction were grown by diffusion of pentane into a DCM/pyridine- d_5 solution of **3.45**. **3.45** crystallises in the centrosymmetric space group P-1, with two independent molecules in the unit cell; an ORTEP figure of **3.45** is shown in **Figure 3.8**, with significant bond lengths and angles in **Table 3.3**.

Unfortunately the crystal was weakly diffracting and hence the data is weak; however, the main structural features of the complex can be discussed. The geometry around Pd is square planar, with the CNC ligand and a molecule of pyridine bound to the

metal. The triflate anion is not coordinated to Pd, and also shows significant disorder in the crystal, requiring the splitting of one of the F atoms in one of the triflate ions.

Like for **3.42a** and **3.42b** there is significant twisting of the pincer ligand; in the two independent molecules of **3.45** present in the unit cell the angle between the square plane around the metal and the trigonal planar amide nitrogen is 49.9 and 49.4 ° and the torsion angle between the planes of the two *trans* NHC ligands is 72.8 and 70.5 °.

No significant difference is observed in the Pd-N or Pd-C bond lengths of **3.45** compared to **3.42a**.

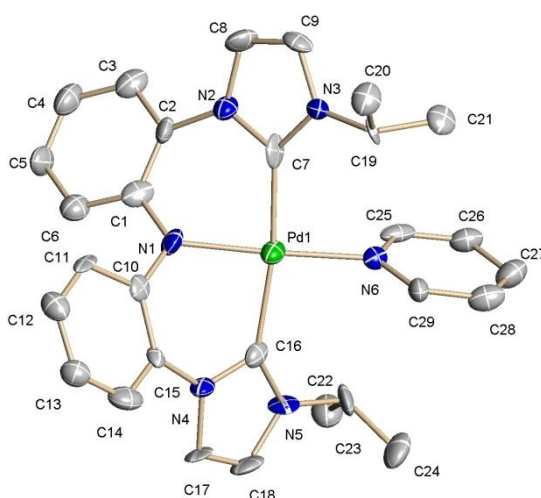


Figure 3.8: ORTEP view of **3.45**. Figures show 50% displacement ellipsoids. The CF_3SO_3 anions, disordered solvent molecules and H-atoms have been omitted from the diagrams.

Table 3.3: Selected bond lengths (Å) and angles (°) for 2 observed molecules of **3.45** in the unit cell.

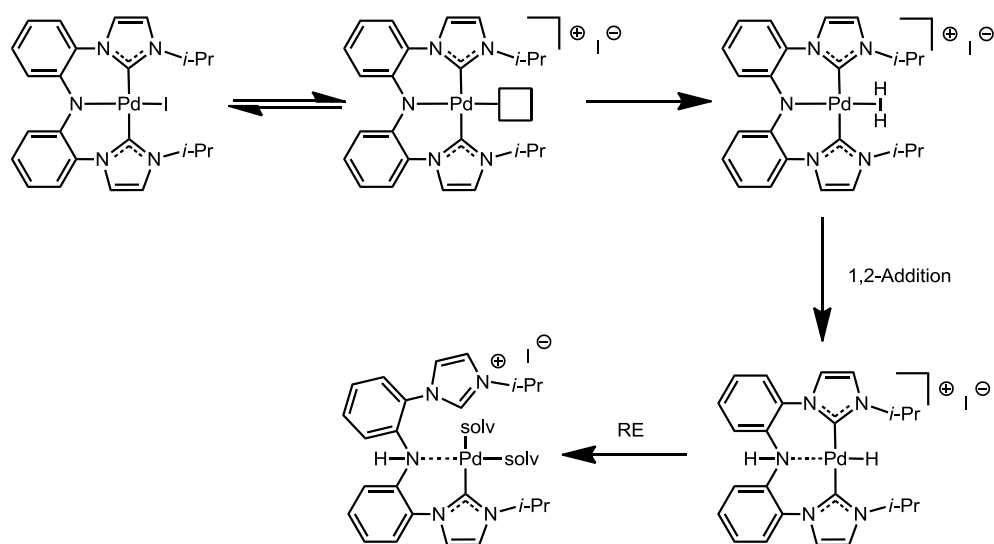
	3.45	
	molecule 1	molecule 2
M-N(amide)	2.022(8)	2.016(8)
M-C(NHC)	2.00(1)	2.027(11)
	2.036(9)	2.034(10)
M-N(py)	2.054(8)	2.072(11)
C-Pd-C	171.6(4)	171.6(4)
N-Pd-N	175.6(3)	179.1(3)

Stoichiometric C-H activation of benzene by **3.42a** was also investigated. Benzene has no directing groups, and has non-polar C-H bonds, making this intermolecular C-H activation a challenging reaction. It was hoped that the metal-amido bond of **3.42a** would act in a bifunctional manner to aid the C-H activation of benzene. Base-promoted C-H activation of benzene has previously been observed for amido pincer complexes of Pt, but the mechanism of this reaction is unclear.¹⁹⁷ Using a sealed NMR tube fitted with a Young's tap, **3.42a** was dissolved in dry C₆D₆ and degassed. Heating the NMR tube at 120 °C for 48 h gave a small amount of Pd black precipitate; however, the ¹H NMR spectrum showed mostly the original complex **3.42a**, with traces (< 5%) of other signals in the alkyl and aryl region, as determined by integration. NMR spectra after heating at up to 190 °C for several days showed no further change, and ESI MS showed no change from before heating. It is possible that any byproducts formed were also insoluble but NMR spectra in CD₂Cl₂ showed no difference to those in C₆D₆.

Similar data were obtained when **3.42a** was heated in non-deuterated benzene and the reaction sampled for ^1H NMR spectroscopy. These results gave no evidence for stoichiometric C-H activation of benzene by a bifunctional mechanism or otherwise.

As the dihydrogen H-H bond is the closest in terms of polarity and bond strength to a C-H bond,²⁰⁹ it was decided to investigate the reactivity of **3.42a** with H_2 . A sealable Young's tap NMR tube was charged with **3.42a** and dry CD_2Cl_2 , and then degassed and backfilled with 1 atm. H_2 . No reaction was observed over 72 h at RT, or on heating up to 50 °C. At 60 °C, Pd black was precipitated over 24-48 h, while the solution became a paler orange colour than it was before heating. ^1H NMR spectroscopy showed only traces of **3.42a** and the spectrum contained signals of a mixture of compounds. The major compound in the reaction mixture could not be completely identified; nevertheless, several resonances characteristic to an imidazolium salt were observed, primarily the NCHCHN peaks at δ 7.58, 7.72 and NCHN at δ 10.41, along with a 6H doublet (δ 1.55) and septet (δ 4.91) consistent with an *i*-propyl group. Performing the experiment in the absence of H_2 gave no reaction. The ^1H NMR spectral data, along with the observation that no reaction occurs in the absence of H_2 , suggests that activation of the H-H bond is occurring, followed by reductive elimination of an imidazolium salt from a Pd-NHC hydride species; a proposed mechanism is shown in **Scheme 3.22**, but the final steps to Pd^0 are unclear. The related reductive elimination of a 2-methyl imidazolium salt has been observed from an (NHC)PdMe complex; it has been suggested that a mono-NHC- Pd^0 complex may be a stable intermediate in catalyst decomposition.¹⁸⁹ The absence of any reaction below 60 °C is consistent with the observation that the iodide ligand of **3.42a** is only labile above this temperature,

as reported in Ch. 3.2.1. Hence, only upon heating to 60 °C is there a vacant site at the metal for H₂ to coordinate. The reaction of **3.42a** with H₂ demonstrated that the CNC complexes are capable of activating H-H bonds; it is possible that this activation occurred by a bifunctional mechanism involving the metal-amido bond (**Scheme 3.22**).



Scheme 3.22: Proposed mechanism for reaction of **3.42a** with H₂.

3.3: Conclusions

Amido *bis*-NHC pincer complexes of Pd (**3.42a**, 33%; **3.42b**, 42%) and Pt (**3.43a**, 9%; **3.43b**, 12%) have been prepared by reaction of the imidazolium salts **2.25a-b** with the non-nucleophilic base KHMDS in the presence of Pd(OAc)₂ or PtCl₂(cod). Complexes **3.42a-b** and **3.43a-b** display atropisomerism due to twisting of the CNC ligand around the N-M-I C2 axis, as evidenced by NMR spectroscopy and X-ray diffraction studies. Upon heating the complexes to 344 K in C₆D₆, there was no evidence for interconversion of the two atropisomers. Attempts to isolate a CNC Ni analogue **3.44** were unsuccessful, due to the sensitivity of the complex to column chromatography. Treatment of **3.42a** with AgOTf in pyridine-d₅ gave the cationic pincer complex **3.45**. Bifunctional reactivity of complex **3.42a** was investigated by attempted C-H activation of benzene and H-H activation of H₂ at elevated temperatures. **3.42a** showed no evidence for stoichiometric C-H activation of benzene up to 190 °C; however, some decomposition of **3.42a** to Pd metal was observed. **3.42a** decomposed above 60 °C in the presence of 1 atmos. H₂, to give Pd metal and imidazolium salt products. The reaction of **3.42a** with H₂ suggests that activation of non-polar, strong H-H bonds is possible with amido *bis*-NHC pincer Pd complexes. It is possible that the activation of H₂ proceeded *via* a bifunctional mechanism involving the metal-amide bond.

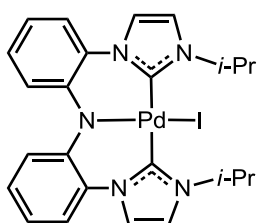
Chapter 4 will describe the synthesis of amino-/amido-NHC complexes derived from imidazolium salts **2.28a-b** of Pd, Pt, Ru, Rh and Ir. Some of the complexes reported in Chapters 3 and 4 were investigated as catalysts/precatalysts in reactions known to proceed by a bifunctional mechanism (transfer hydrogenation of ketones, direct arylation of heterocycles) in Chapter 5. As in this chapter, it was hoped that the

amino/amido-NHC complexes described in Chapter 4 would facilitate bifunctional reactivity involving the metal-amino or metal-amido bond.

3.4: Experimental

All reactions were performed under dry, oxygen free nitrogen using standard Schlenk techniques unless otherwise stated; however, all compounds were air stable once isolated. Anhydrous solvents were obtained either by distillation from an appropriate drying agent, from an Innovative Technology PureSolv MD 7 Solvent Purification System or purchased from Sigma Aldrich. Deuterated solvents (DCM-d₂, THF-d₈, pyridine-d₆, benzene-d₆) were purchased from Cambridge Isotope Laboratories. All other reagents were obtained from Sigma-Aldrich, Johnson Matthey or Alfa Aesar and used as supplied. NMR spectra were recorded on a Bruker DPX300, DRX400 or AV500 spectrometer; chemical shifts have been referenced to the residual protonated solvent peak and are reported in ppm, *J* values are given in Hz. Electrospray mass spectra were recorded on a Micromass Quattro LC mass spectrometer with acetonitrile as solvent; FAB and HR mass spectra were recorded on a Kratos Concept mass spectrometer using NBA as a matrix.

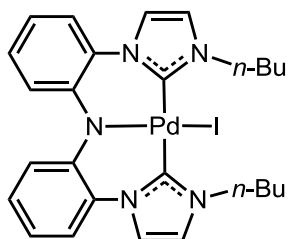
[CNC-*i*-Pr]PdI (**3.42a**)



A solution of Pd(OAc)₂ (0.026 g, 0.12 mmol) and the imidazolium salt **2.25a** (0.075 g, 0.12 mmol) in DME (15 mL) was cooled to 0 °C and a solution of 1 M KHMDS in toluene (0.36 mL, 0.36 mmol) added dropwise with stirring. The mixture was stirred for 6 h at 0 °C and then allowed to warm to RT overnight. The crude reaction mixture was filtered through Celite and the solvent removed *in vacuo* to give a red-brown solid. The solid was dissolved in DCM (*ca.* 20 mL) and the solution decanted to remove insoluble material. Purification by flash column chromatography (33% EtOAc/pet. ether) gave **3.42a** (0.024 g, 33%) as

an orange solid m.p. 272-275 °C, $R_f = 0.37$ (33% EtOAc/pet. ether). Crystals of **3.42a** suitable for structure determination by X-ray diffraction were obtained by slow evaporation of a solution of **3.42a** in C_6D_6 . δ_H (300MHz, C_6D_6) 0.71 (6H, d, $J = 6.7$, CH_3), 1.32 (6H, d, $J = 6.7$, CH_3), 6.23 (2H, d, $J = 1.8$, NCHCHN), 6.35 (2H, app sept, $J = 6.7$, $CH(CH_3)_2$), 6.60 (2H, app t, $J = 7.8$, CH), 6.71 (2H, d, $J = 1.8$, NCHCHN), 6.81 (2H, app t, $J = 7.8$, CH), 6.99 (2H, d, $J = 7.8$, CH), 7.09 (2H, d, $J = 7.8$, CH); δ_C (75MHz, C_6D_6) 23.2 ($CH(CH_3)_2$), 23.7 ($CH(CH_3)_2$), 53.5 ($CH(CH_3)_2$), 117.7, 118.9 (NCHCHN), 119.2 (NCHCHN), 121.3, 122.8, 127.4, 133.5, 144.7, 165.3 (N_2C-Pd); ν_{max}/cm^{-1} (solid) 2962w, 2926w, 2870w, 1587w, 1487s, 1449m, 1403m, 1334s, 1266m, 1216m, 1132m, 1077w, 1039w, 882w, 842w, 743s, 728s, 682s. m/z (ESI) 490 (65%, $[M-I]^+$), 531 (100%, $[M-I+MeCN]^+$); (FAB) 617 $[M]^+$; HRMS $C_{24}H_{26}N_5Pd$ ($[M-I]^+$) calcd. 490.1227, found 490.1239. Anal. Calcd for $C_{24}H_{26}IN_5Pd$: C, 46.66, H, 4.24, N, 11.34. Found: C, 46.70, H, 4.22, N, 11.37%.

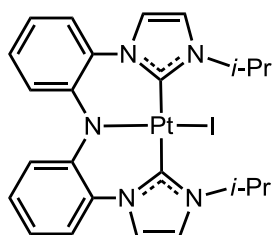
[CNC-*n*-Bu]PdI (**3.42b**)



A solution of $Pd(OAc)_2$ (0.067 g, 0.30 mmol) and the imidazolium salt **2.25b** (0.200 g, 0.299 mmol) in DME (15 mL) was cooled to 0 °C and a solution of 1 M KHMDS in toluene (1 M, 0.90 mL, 0.90 mmol) added dropwise with stirring. The mixture was stirred for 6 h at 0 °C and then allowed to warm to RT overnight. The crude reaction mixture was filtered through Celite and the solvent removed *in vacuo* to give a red-brown solid. The solid was dissolved in DCM (*ca.* 20 mL) and the solution decanted to remove insoluble material. Purification by flash column chromatography

(33% EtOAc/pet. ether) gave **3.42b** (0.082 g, 42%) as an orange solid m.p. 106-108 °C, $R_f = 0.37$ (33% EtOAc/pet. ether). Crystals of **3.42b** suitable for structure determination by X-ray diffraction were obtained by slow evaporation of a solution of **3.42b** in C_6D_6 . δ_H (300 MHz, C_6D_6) 0.72 (6H, app t, $J = 7.4$, CH_3), 0.96-1.24 (4H, m, $NCH_2CH_2CH_2CH_3$), 1.25-1.43 (2H, m, $NCH_2CH_2CH_2CH_3$), 1.70-1.87 (2H, m, $NCH_2CH_2CH_2CH_3$), 4.12-4.24 (2H, m, $NCH_2CH_2CH_2CH_3$), 4.61-4.73 (2H, m, $NCH_2CH_2CH_2CH_3$), 6.10 (2H, d, $J = 2.0$, NCH_2CH_2N), 6.61 (2H, app t, $J = 7.6$, CH), 6.64 (2H, d, $J = 2.0$, NCH_2CH_2N), 6.81 (2H, app t, $J = 7.6$, CH), 7.00 (2H, d, $J = 7.6$, CH), 7.03 (2H, d, $J = 7.6$, CH); δ_C (75MHz, C_6D_6) 14.2 (CH_3), 19.9 ($NCH_2CH_2CH_2CH_3$), 33.8 ($NCH_2CH_2CH_2CH_3$), 52.7 ($NCH_2CH_2CH_2CH_3$), 118.0 (NCH_2CH_2N), 119.2, 121.7, 123.0, 123.2, 127.9, 134.1, 145.2, 167.0 (N_2C-Pd); ν_{max}/cm^{-1} (solid) 2952 w, 2868 w, 1588 w, 1487 s, 1451 m, 1416 m, 1336 m, 1269 m, 1133 w, 1073 w, 1039 w, 952 w, 880 w, 745 s, 724 s, 696 s, 683 s. m/z (ESI) 518 (20%, $[M-I]^+$), 559 (100%, $[M-I+MeCN]^+$) (FAB) 645 $[M]^+$; HRMS $C_{26}H_{30}N_5Pd$ ($[M-I]^+$) calcd. 518.1557, found 518.1517; Anal. Calcd for $C_{26}H_{30}N_5Pd$: C, 48.35; H, 4.68; N, 10.84. Found C, 48.41; H, 4.68; N, 10.74%.

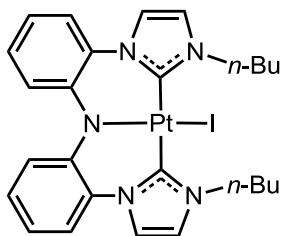
[CNC-*i*-Pr]PtI (**3.43a**)



A solution of $PtCl_2(cod)$ (0.292 g, 0.780 mmol) and **2.25a** (0.500 g, 0.780 mmol) in THF (15 mL) was cooled to $-78^\circ C$ and a solution of 0.55 M KHMDS in toluene (5.00 mL, 2.73 mmol) added dropwise with stirring. The mixture was stirred for 8 h at $-78^\circ C$ and then allowed to warm to RT overnight. The crude reaction mixture was filtered through Celite and the solvent removed under reduced pressure to give a

yellow-orange solid. The solid was dissolved in DCM (*ca.* 20 mL) and the solution decanted to remove insoluble salts. Purification by flash column chromatography (20% EtOAc/hexane) gave **3.43a** (0.043 g, 9%) as a yellow solid m.p. 287-289 °C, $R_f = 0.26$ (20% EtOAc/hexane). δ_H (300 MHz, C_6D_6) 0.73 (6H, d, $J = 6.9$, CH_3), 1.37 (6H, d, $J = 6.9$, CH_3), 6.19 (2H, d, $J = 2.2$, NCHCHN), 6.38 (2H, app sept, $J = 6.9$, $CH(CH_3)_2$), 6.60 (2H, app t, $J = 7.8$, CH), 6.68 (2H, d, $J = 2.2$, NCHCHN), 6.78 (2H, app t, $J = 7.8$, CH), 6.95 (2H, d, $J = 7.8$, CH), 7.09 (2H, d, $J = 7.8$, CH); δ_C (125MHz, CD_2Cl_2) 23.4 ($CH(CH_3)_2$), 24.1 ($CH(CH_3)_2$), 53.2 ($CH(CH_3)_2$), 118.5, 118.8 (NCHCHN), 119.4 (NCHCHN), 121.0, 122.2, 127.1, 133.1, 144.0, 162.5 (N_2C-Pt); ν_{max}/cm^{-1} (solid) 3061 w, 2971 w, 1563 w, 1489 s, 1451 m, 1401 m, 1340 s, 1268 m, 1214 m, 1131 w, 1079 w, 1037 w, 951 w, 889 w, 723 s, 690 s. m/z (ESI) 620 (25%, $[M-I+MeCN]^+$), 579 (100% $[M-I]^+$); m/z (FAB) 706 $[M]^+$; Anal. Calcd. for $C_{24}H_{26}IN_5Pt$: C, 40.80; H, 3.71; N, 9.91. Found C, 40.82; H, 3.75; N, 9.91%.

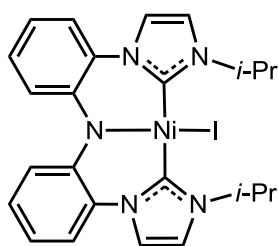
[CNC-*n*-Bu]PtI (**3.43b**)



A solution of $PtCl_2(cod)$ (0.280 g, 0.747 mmol) and **2.25b** (0.500 g, 0.747 mmol) in THF (15 mL) was cooled to $-78\text{ }^\circ\text{C}$ and a solution of 0.55 M KHMDS in toluene (2.24 mL, 2.24 mmol) added dropwise with stirring. The mixture was stirred for 8 h at $-78\text{ }^\circ\text{C}$ and then allowed to warm to RT overnight. The crude reaction mixture was filtered through Celite and the solvent removed under reduced pressure to give a yellow-orange solid. The solid was dissolved in DCM (*ca.* 20 mL) and the solution decanted to remove insoluble salts. Purification by flash column

chromatography (33% EtOAc/pet. ether) gave **3.43b** (0.057 g, 12%) as a yellow solid m.p. 169-171 °C, $R_f = 0.25$ (33% EtOAc/pet. ether). δ_H (500 MHz, CD_2Cl_2) 0.84 (6H, app t, $J = 7.4$, CH_3), 1.27 (4H, m, CH_2CH_3), 1.74 (2H, m, $CH_2CH_2CH_3$), 1.98 (2H, m, $CH_2CH_2CH_3$), 4.52 (4H, m, $CH_2CH_2CH_2CH_3$), 6.76 (2H, app t, $J = 7.3$, CH), 6.92 (4H, m, CH), 7.12 (2H, d, $J = 2.0$, NCHCHN), 7.37 (2H, d, $J = 8.0$, CH), 7.45 (2H, d, $J = 2.0$, NCHCHN); δ_C (125 MHz, CD_2Cl_2) 14.0 (CH_3), 19.9 (CH_2CH_3), 33.5 ($CH_2CH_2CH_3$), 52.5 ($CH_2CH_2CH_2CH_3$), 118.7, 118.8 (NCHCHN), 121.3, 122.4, 123.1 (NCHCHN), 127.4, 133.4, 144.2, 164.0 (N_2C-Pt); ν_{max}/cm^{-1} (solid) 2957 w, 2872 w, 1587 w, 1562 w, 1487 s, 1448 m, 1414 m, 1387 m, 1327 s, 1270 s, 1232 m, 1134 w, 1041 w, 951 m, 888 w, 717 s, 685 s. m/z (ESI) 735 (10%, $[M+H]^+$), 607 (100%, $[M-I]^+$); Anal. Calcd. for $C_{26}H_{30}IN_5Pt$: C, 42.51; H, 4.12; N, 9.53. Found C, 42.55; H, 4.17; N, 9.57%.

Attempted synthesis of $[CNC-i-Pr]NiI$ (**3.44**)

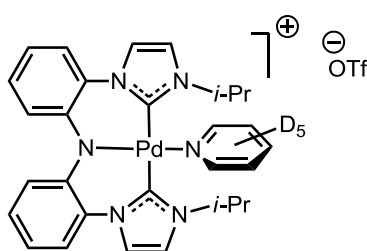


A solution of $NiBr_2(DME)$ (0.048 g, 0.156 mmol) and **2.25a** (0.100 g, 0.156 mmol) in THF (5 mL) was cooled to $-78^\circ C$ and a solution of 0.6 M $KHMDS$ in toluene (0.90 mL, 0.546 mmol) added dropwise with stirring. The mixture was stirred for 8 h at $-78^\circ C$ and then allowed to warm to RT overnight. The reaction mixture was filtered through Celite and the solvent removed under reduced pressure to give a crude purple/brown solid. TLC of the crude mixture showed a purple spot believed to be **3.44** at $R_f = 0.02$ (33% EtOAc/pet. ether); however, this complex was unstable to column chromatography and no pure material was isolated.

δ_{H} (400 MHz, C_6D_6) 0.74 (6H, d, $J = 6.8$, CHCH_3), 1.12 (6H, d, $J = 6.8$, CHCH_3), 6.13 (2H, app sept, $J = 6.8$, CHCH_3); aromatic signals were obscured by other products.

m/z (ESI) 442 (40%, $[\text{M-I}]^+$), 483 (100%, $[\text{M-I+MeCN}]^+$)

{[CNC-*i*-Pr]Pd-(d_5 -py)}OTf (3.45)



Iodide complex **3.42a** (0.012g, 0.019 mmol) was dissolved in d_5 -pyridine and AgOTf added (0.007g, 0.03 mmol). Crystals of **3.45** suitable for structure determination by X-ray diffraction were obtained by

diffusion of pentane into this solution. Attempts to isolate an analytically pure sample of **3.45** on a larger scale were unsuccessful as it was not possible to completely separate **3.45** from pyridine. δ_{H} (400 MHz, d_5 -pyridine) 0.72 (6H, d, $J = 6.7$, CH_3), 0.90 (6H, d, $J = 6.7$, CH_3), 3.68 (2H, app sept, $J = 6.7$, $\text{CH}(\text{CH}_3)_2$), 6.96 (2H, app t, $J = 7.9$, CH), 7.08 (2H, app t, $J = 7.9$, CH), 7.17 (2H, d, $J = 7.9$, CH), 7.64 (2H, d, $J = 2.1$, NCHCHN), 7.76 (2H, d, $J = 7.9$, CH), 8.14 (2H, d, $J = 2.1$, NCHCHN); δ_{C} (125 MHz, d_5 -pyridine) 21.9 (CH_3), 23.8 (CH_3), 51.7 ($\text{CH}(\text{CH}_3)_2$), 119.3, 120.2, 120.3, 121.8, 124.6, 128.1, 132.3, 143.8, 163.8 ($\text{N}_2\text{C-Pd}$); ^{19}F NMR (282 MHz, d_5 -pyridine) δ -77.2. m/z (ESI) 490 (65%, $[\text{M-OTf-py}]^+$), 531 (100%, $[\text{M-OTf-py+MeCN}]^+$).

Reactions of **3.42a** with benzene

3.42a (0.010 g, 0.016 mmol) was added to a dry, sealable NMR tube equipped with a Young's tap. Dry C₆D₆ (0.5 ml) was added and the tube was shaken until **3.42a** was fully dissolved. The NMR tube was degassed by the freeze-pump-thaw technique three times, then sealed under nitrogen and heated to the appropriate temperature. A ¹H NMR spectrum was recorded directly from the NMR tube after cooling to RT.

The ¹H NMR spectrum showed mostly the original complex **3.42a**, with traces (< 5%) of other signals in the alkyl and aryl region, as determined by integration.

Reactions of **3.1a** with H₂

3.42a (0.010 g, 0.016 mmol) was added to a dry, sealable NMR tube equipped with a Young's tap. Dry CD₂Cl₂ (0.5 ml) was added and the tube was shaken until **3.42a** was fully dissolved. The NMR tube was degassed by the freeze-pump-thaw technique three times, and then the solvent frozen in liquid nitrogen and vacuum applied. 1 atm. H₂ was introduced into the headspace of the NMR tube *via* the Young's tap, and then the NMR tube was sealed, allowed to warm to RT and shaken thoroughly. The NMR tube was then heated at 60-80 °C. Over 15 h, a black precipitate of Pd metal was observed; the orange solution also appeared much paler. A ¹H NMR spectrum was recorded directly from the NMR tube after cooling to RT.

Several resonances characteristic of an imidazolium salt were observed:

δ_{H} (400 MHz, CD_2Cl_2) 1.55 (6H, d, $J = 6.7$, CHCH_3), 4.91 (1H, sept, $J = 6.7$, CHCH_3), 7.58 (1H, br, NCHCHN), 7.72 (1H, br, NCHCHN), 10.41 (1H, s, NCHN).

X-ray Crystallographic Studies

All single crystal diffraction data were collected using graphite monochromated $\text{Mo-K}\alpha$ X-radiation ($\lambda = 0.71073 \text{ \AA}$) on a Bruker APEX 2000 CCD diffractometer at 150 K. The data were corrected for Lorentz and polarisation effects and empirical absorption corrections applied. Structures were solved by Patterson methods and structures refined by least-squares full-matrix refinement against F^2 employing SHELXTL version 6.10. Hydrogen atoms were included in calculated positions ($d(\text{C-H}) = 0.95$ to 0.99 \AA) riding on the bonded atom with isotropic displacement parameters set to $1.5 U_{\text{eq}}(\text{C})$ or methyl H atoms and $1.2 U_{\text{eq}}$ for all other C atoms. All non-H atoms were refined with anisotropic displacement parameters. Disordered solvent was removed using the SQUEEZE option of PLATON.²¹⁰

Crystal data for 3.42a·(2C₆H₆). $\text{C}_{36}\text{H}_{38}\text{IN}_5\text{Pd}$, $M_w = 774.01 \text{ gmol}^{-1}$, $T = 150(2) \text{ K}$, orthorhombic space group $\text{C}222(1)$, $a = 10.8012(19) \text{ \AA}$, $b = 19.746(4)$, $c = 15.230(3) \text{ \AA}$, $\alpha = \beta = \gamma = 90^\circ$, $V = 3248.2(10) \text{ \AA}^3$, $Z = 4$, $\rho_{\text{calcd}} = 1.583 \text{ Mgm}^{-3}$, $\mu = 1.555 \text{ mm}^{-1}$, $F(000) = 1552$, crystal size $0.33 \times 0.26 \times 0.21 \text{ mm}^3$, 13040 reflections collected, 3336 unique [$R(\text{int}) = 0.0341$] which were used in all calculations. Empirical absorption correction made, T_{min} and T_{max} 0.831 and 0.646 respectively. GOF = 1.064, final R indices [$I > 2\sigma$] $R_1 = 0.0260$, $wR_2 = 0.0661$, R indices (all data) $R_1 = 0.0277$, $wR_2 = 0.0667$. Largest diff. peak and hole 0.692 and $-0.554 \text{ e \AA}^{-3}$.

Crystal data for 3.42b·(C₆H₆). C₃₂H₃₆IN₅Pd, $M_w = 723.96 \text{ gmol}^{-1}$, $T = 150(2) \text{ K}$, orthorhombic space group Aba2, $a = 29.370(5) \text{ \AA}$, $b = 20.178(3) \text{ \AA}$, $c = 10.3042(17) \text{ \AA}$, $\alpha = \beta = \gamma = 90^\circ$, $V = 6106.4(18) \text{ \AA}^3$, $Z = 8$, $\rho_{\text{calcd}} = 1.575 \text{ Mgm}^{-3}$, $\mu = 1.648 \text{ mm}^{-1}$, $F(000) = 2896$, crystal size = $0.15 \times 0.14 \times 0.10 \text{ mm}^3$, 23246 reflections collected, 5940 unique [R(int) = 0.0843] which were used in all calculations. Empirical absorption correction made, T_{min} and T_{max} 0.802 and 0.628 respectively. GOF = 0.934, final R indices [$I > 2\sigma$] $R_1 = 0.0457$, $wR_2 = 0.0751$, R indices (all data) $R_1 = 0.0594$, $wR_2 = 0.0790$. Largest diff. peak and hole 0.894 and $-1.009 \text{ e \AA}^{-3}$.

Crystal data for 3.45·(0.75CH₂Cl₂). C_{30.75}H_{32.50}Cl_{1.50}F₃N₆O₃PdS, $M_w = 782.76 \text{ gmol}^{-1}$, $T = 150(2) \text{ K}$, triclinic space group P-1, $a = 10.372(4) \text{ \AA}$, $b = 11.933(5) \text{ \AA}$, $c = 26.284(11) \text{ \AA}$, $\alpha = 101.593(10)^\circ$, $\beta = 94.150(9)^\circ$, $\gamma = 95.257(10)^\circ$, $V = 3159(2) \text{ \AA}^3$, $Z = 4$, $\rho_{\text{calcd}} = 1.646 \text{ Mgm}^{-3}$, $\mu = 0.842 \text{ mm}^{-1}$, $F(000) = 1590$, crystal size $0.22 \times 0.13 \times 0.02 \text{ mm}^3$, 25010 reflections collected, 12296 unique [R(int) = 0.2109] (completeness to theta = 26.00° 98.9 %). Empirical absorption correction made, T_{min} and T_{max} = 0.802 and 0.338 respectively. GOF = 0.795, final R indices [$I > 2\sigma$] $R_1 = 0.0910$, $wR_2 = 0.1639$, R indices (all data) $R_1 = 0.1872$, $wR_2 = 0.1958$. Largest diff. peak and hole 1.347 and $-2.118 \text{ e \AA}^{-3}$.

4: Chapter 4 – Synthesis and Reactivity of Complexes of Bidentate Amino/Amido-NHC Ligands

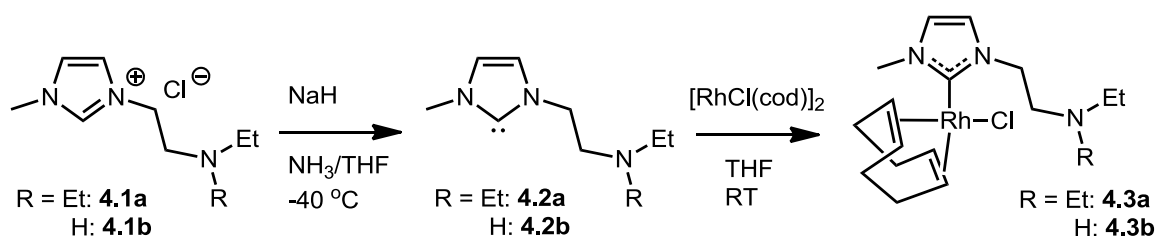
As stated in Chapter 1, the author was interested in the applications of complexes with metal-nitrogen bonds as bifunctional catalysts, especially in their potential ability to activate C-H bonds. Complexes with bidentate amino and amido ligands have been strongly-associated with bifunctional catalysis,²¹¹⁻²¹⁴; the second donor of the chelating ligand helps to prevent undesirable M-N bond cleavage and dissociation from the metal centre.²¹⁵ Many chelating groups can be used to tether a reactive nitrogen to the metal; for example hydrogenation catalysts have been synthesised with a variety of second chelating donors such as aryl carbon,²¹⁶ phosphines,²¹⁷⁻²¹⁹ thiol/thioether,²²⁰ and the well-studied sulfonamide¹ donor. However, there are relatively few examples of late-transition metal amine/amino-functionalised NHC complexes; their synthesis and reactivity will be discussed in this introduction. Subsequently, the synthesis and characterisation of amino/amido-NHC complexes of several late transition metals derived from the amine-functionalised imidazolium salts **2.28a** and **2.28b** reported in Chapter 2, will be discussed.

4.1: Introduction

4.1.1: Amine/Amido-Functionalised (Bidentate) NHC Complexes

Secondary and tertiary alkylamine-functionalised NHC complexes of Rh^I were initially synthesised by Herrmann *et al.* by the reaction of the free carbene with [RhCl(cod)]₂,

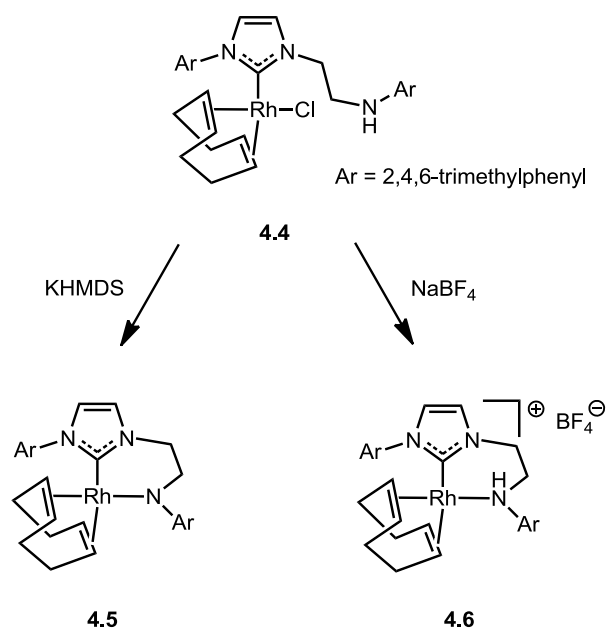
Scheme 4.1.²²¹ Deprotonation of the amine functionalised imidazolium salts **4.1** with NaH in a THF/NH₃ solution gave the amine-NHCs **4.2**; subsequent reaction of **4.2** with [RhCl(cod)]₂ gave complexes **4.3**, in which the amine-NHC ligand is coordinated only through the NHC.



Scheme 4.1: Synthesis of alkylamine-functionalised NHC complexes of Rh^I.²²¹

Fryzuk subsequently synthesised a similar secondary arylamine complex **4.4**, **Scheme**

4.2.¹⁶³ Reaction of **4.4** with KHMDS led to deprotonation of the arylamine and coordination of the nitrogen atom to give an arylamide complex, **4.5**. In addition, reaction of **4.4** with NaBF₄ allowed the amine tether to coordinate in the cationic complex **4.6**. In hydrogenation reactions, complexes **4.4-4.6** were not significantly more reactive than colloidal rhodium and showed no activity in transfer hydrogenation of ketones.

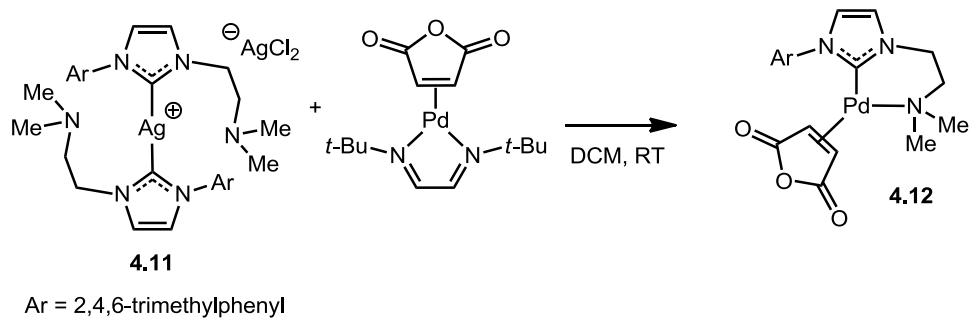


Scheme 4.2: Synthesis of bidentate arylamine (**4.6**) and arylamide (**4.5**) NHC complexes from a monodentate amine-functionalized NHC complex (**4.4**).¹⁶³

Fryzuk has also investigated his secondary arylamine-functionalised NHC as a ligand for ruthenium alkylidene complexes **4.7-4.9**,²²² as analogues of the widely studied second generation Grubbs' catalyst for alkene metathesis, **Scheme 4.3**.²²³ It was found that the arylamine donor was not permanently bound to Ru, with an equilibrium set up that favoured coordination of the amine in complexes with less bulky PMe₃ and py ligands, and non-coordination with the bulky phosphine PCy₃. Complexes **4.7-4.9** underperformed in both ring-closing metathesis and ring-opening metathesis polymerisation compared to known benchmarks, suggesting that the arylamine had a deleterious effect on the reactions.

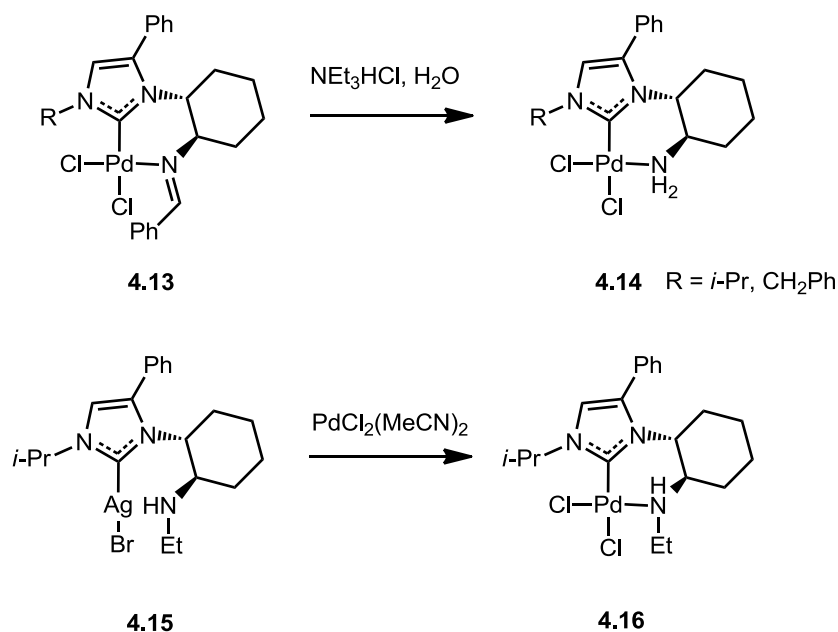
Chapter 4 – Synthesis and Reactivity of Complexes of Bidentate Amino/Amido-NHC Ligands

Elsevier later synthesised analogous tertiary alkylamine-functionalised NHC complexes of Pd⁰ by transmetallation from silver *biscarbene* **4.11** and found complex **4.12** (**Scheme 4.5**) to be a competent catalyst for the transfer hydrogenation of 1-phenyl-1-propyne, with a moderate TOF of 14.7 and high Z-selectivity for the resultant alkene.^{225,226}



Scheme 4.5: Synthesis of the tertiary alkylamine-functionalised NHC complex **4.12**, active in transfer hydrogenation of alkynes.^{225,226}

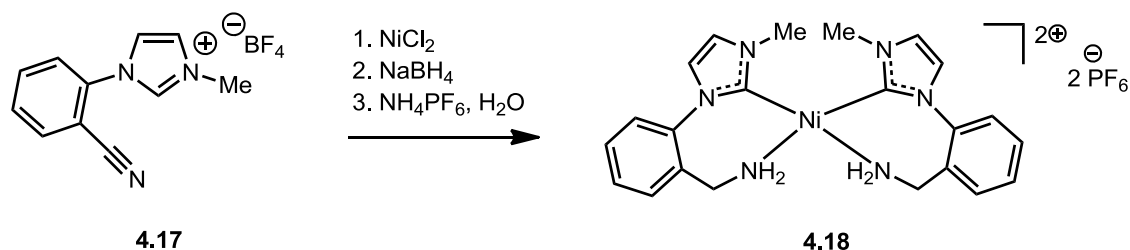
Chiral primary amine and secondary alkylamine NHC complexes of Pd (**4.14** and **4.16** respectively) have been reported by Douthwaite *et al.*, **Scheme 4.6**.²²⁷ Complex **4.14** was synthesised by the slow (14 day) hydrolysis of the imine-functionalised NHC complex **4.13**. Complex **4.16** was formed by transmetalation of the pre-formed Ag carbene **4.15** onto PdCl₂(MeCN)₂; this methodology failed for **4.14**, giving only an insoluble precipitate.



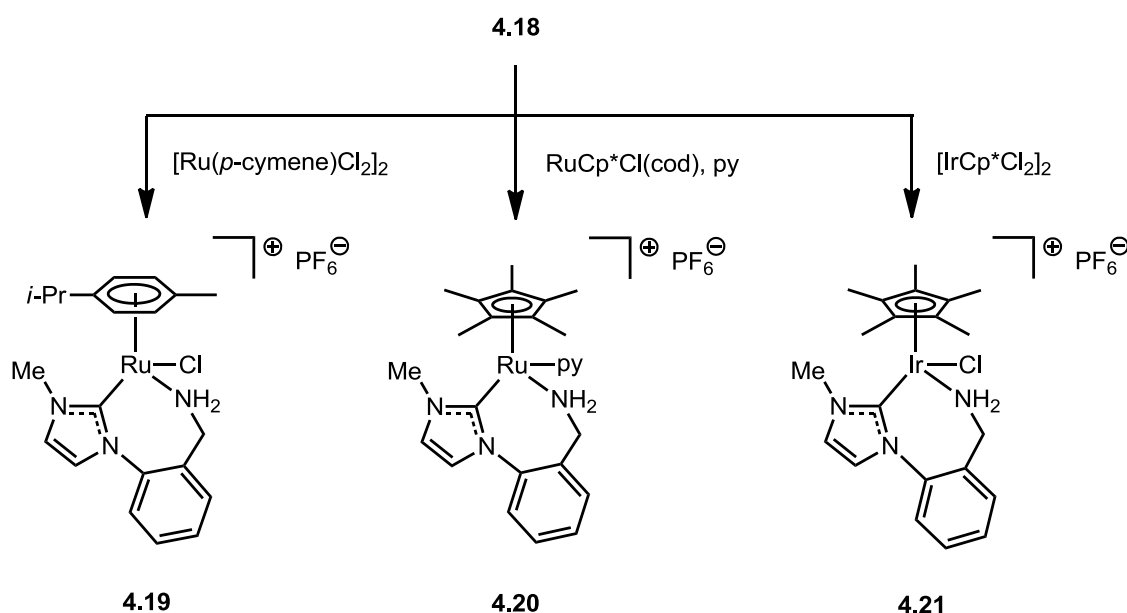
Scheme 4.6: Synthesis of chiral primary amine (**4.14**) and secondary alkylamine (**4.16**) functionalized NHC complexes of Pd.²²⁷

Closely related to the work in this chapter, Morris *et al.* have reported the benzylic amine-functionalised NHC Ni complex **4.18**, synthesised by *in-situ* coordination and reduction of a benzonitrile-substituted NHC ligand, **4.17** (Scheme 4.7).¹⁹ This complexation is low yielding (30%); however, the Ni complex **4.18** is an excellent transmetallation reagent, capable of transferring the NHC to Ru^{II} and Ir^{III} to afford half-sandwich complexes **4.19**, **4.20** and **4.21**, Scheme 4.28.^{19,18,228–230} These complexes have been well-studied in terms of their application as hydrogenation and transfer hydrogenation catalysts; this reactivity will be discussed in more detail in Chapter 5, as it is relevant to the transfer hydrogenation reactivity of amino/amido-NHC complexes we report later in this chapter.

Chapter 4 – Synthesis and Reactivity of Complexes of Bidentate Amino/Amido-NHC Ligands



Scheme 4.7: Synthesis of **4.18** by in situ reduction of a benzonitrile-functionalised NHC.¹⁹



Scheme 4.8: Transmetalation reactions of **4.18**, to form half-sandwich complexes **4.19**, **4.20** and **4.21**.^{19,18,228–230}

4.1.2: Aims and Objectives

The aim of this work was to prepare late transition metal complexes of amine-/amido-functionalised NHC ligands, in order to investigate them as bifunctional catalysts for organic reactions.

Chapter 4 – Synthesis and Reactivity of Complexes of Bidentate Amino/Amido-NHC Ligands

d^6 and d^8 late transition metals were chosen as targets, as these metal centres have mostly filled d-orbitals to repulse the amido nitrogen lone pair, improving the nucleophilicity of the amido ligand compared to earlier transition metal centres. Also, d^6 and d^8 metal centres can be electrophilic and have at least one free d-orbital to accept electrons in a bond cleavage step during bifunctional catalysis. Labile supporting ligands (halides, pyridine, PPh_3), along with a 1:1 ratio of amino/amido-NHC ligand to metal, will ensure that empty coordination sites are available at the metal centre during catalysis.

Several methods of coordinating NHCs based on the imidazolium salts **2.28** were investigated, and the resultant complexes of Pd, Pt, Ru, Ir and Rh isolated and characterised. The preparation of Pd and Pt (C,NR) complexes will be reported first, followed by the preparation of Ru, Rh and Ir (C,NR) half-sandwich complexes. Finally, investigations into the reactivity of an iridium amide complex will be discussed.

4.2: Results and Discussion

4.2.1: Synthesis of (C,NR) complexes of Pd and Pt

The aim in this section of work was to isolate and characterise a variety of square planar Pd^{II} and Pt^{II} amino/amido complexes of bidentate amine-functionalised NHC ligands, of the general form shown in **Figure 4.1**.



Figure 4.1: General schematic of target Pd and Pt amino/amido complexes. L = neutral ligand, X = anionic ligand, C = N-heterocyclic carbene donor.

In the case of amino-NHC complexes, the metal-amido bond could be expected to form *in situ* by deprotonation of the amine donor by a base during a catalytic reaction with elimination of HX; in this respect, it is not necessarily a requirement to have a metal-amido complex as precatalyst as long as an amine donor and base/basic ligand are available. Therefore, the coordination of the non-labile NHC donor of the (C,NR) ligands was the primary objective. The variation of R group on the amine could allow control of both the sterics and electronics of the amido donor, including the acidity of the amine proton; this could allow for tuning of the bifunctional reactivity of the complexes.

Chapter 4 – Synthesis and Reactivity of Complexes of Bidentate Amino/Amido-NHC Ligands

The Pd^{II} complexes were expected to act as precatalysts for direct arylation reactions, which would most likely proceed *via* a Pd⁰ active catalyst generated from the Pd^{II} species *in situ*.

First, the reactions of imidazolium salts **2.28a** and **2.28b** with the strong, non-nucleophilic base KHMDS were investigated, in order to isolate a free carbene.

Isolation of the free carbene had been unsuccessful with the tridentate (CNC) ligands reported in Chapter 3, and again this proved to be the case with **2.28a** and **2.28b**; only complex mixtures of unidentified products were obtained.

Subsequently, attempts were made to synthesise the target complexes directly from the imidazolium salts **2.28** by treatment with a base in the presence of metal salts, as was successful with the [CNC] complexes **3.42a-b** and **3.43a-b**. A variety of bases of differing basicities were used, including KHMDS, NaH, *t*-BuONa, Cs₂CO₃ and K₂CO₃, to deprotonate the imidazolium salt at the C2 and amine positions before or during coordination. The metal salts used were Pd(OAc)₂, Pd(TFA)₂, PdCl₂(cod), PdCl₂(MeCN)₂ and PtCl₂(cod), with the aim of synthesising complexes of the form shown in **Figure 4.2**. In all cases, the reactions gave intractable mixtures of products, with NMR spectra showing multiple overlapping peaks, and ESIMS giving signals containing the Pd/Pt isotope pattern but not corresponding to any identifiable or expected complex.

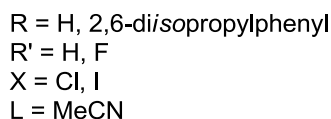
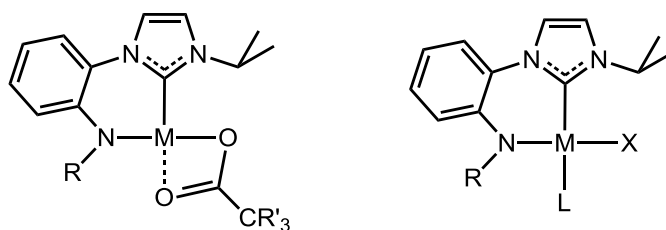


Figure 4.2: Initial target (C,NR) Pd/Pt complexes.

A well-studied type of precatalyst used in cross-coupling reactions are the PEPPSI complexes (pyridine-enhanced precatalyst preparation, stabilization and initiation) as shown in **Figure 4.3**.²³¹ These complexes are known for their air and moisture stability and their ease of synthesis. They display excellent activity as precatalysts due to their ability to dissociate the pyridine ligand and generate a reactive NHC-Pd⁰ complex by reduction.²³² The synthesis of these complexes is straightforward; reaction of an imidazolium salt with PdCl₂ and K₂CO₃ in the appropriate pyridine under air at 80 °C affords the product in high yield.

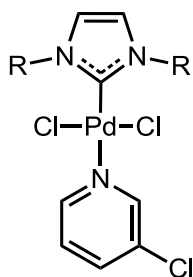
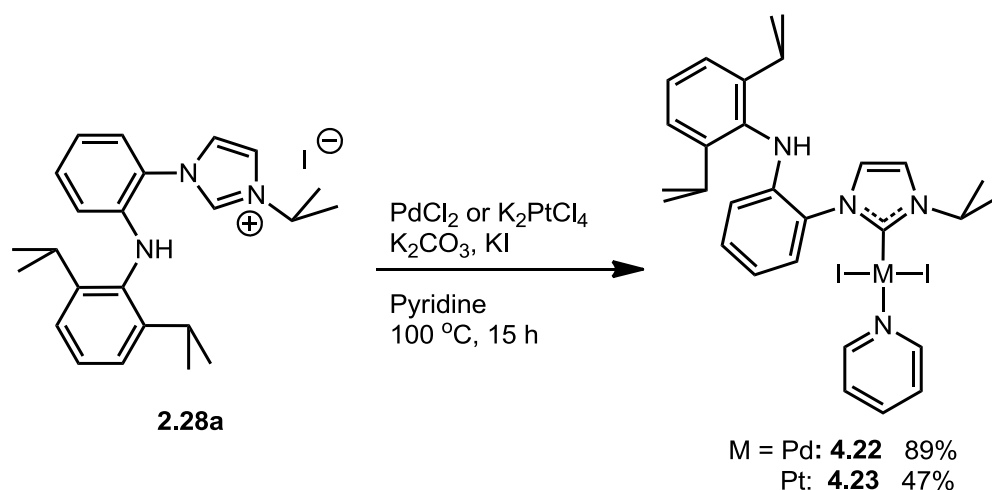


Figure 4.3: PEPPSI-type complexes for cross-coupling catalysis.



Scheme 4.9: Synthesis of **4.22** and **4.23**.

Applying this methodology to the reaction of PdCl₂ and K₂CO₃ with imidazolium salt **2.28a** in pyridine at 80 °C gave a mixture containing complex **4.22**, **Scheme 4.9**.

Increasing the reaction temperature to 100 °C gave complete conversion over 15 h, whilst addition of KI suppressed the formation of any chloride complex. **4.22** proved to be especially stable, and could be isolated in high purity and yield (89%) from the crude mixture by column chromatography on silica gel. Repeating this reaction with K₂PtCl₄ as the metal salt gave the Pt analogue **4.23** in 47% yield after column chromatography, **Scheme 4.9**.

The NMR spectra of **4.22** and **4.23** had several similar characteristic features. Broad signals were seen for the 2,6-diisopropyl substituent on the NHC ligand in both the ¹H spectrum and ¹³C spectrum, possibly due to restricted rotation around the N-Aryl bond. A downfield shift for the NHC *isopropyl* CH resonance was observed for both the Pd and Pt complexes (δ 5.79 (**4.22**), 5.99 (**4.23**)); these chemical shifts are similar to that observed for the [CNC] Pd complex **3.42a** (δ 6.35), and they suggest an interaction of the *i*-Pr CH with the iodide ligands. The carbene resonances for **4.22** and

4.23 were difficult to conclusively assign in the ^{13}C NMR spectra. For **4.22** the sharp signal at δ 147.3 was most likely the carbene resonance, two nearby quaternary carbon signals at δ 146.6 and 148.0 are broad as observed for those assigned to the 2,6-diisopropyl substituent on the amine. The carbene resonance for **4.23** was similarly assigned to the sharp signal at δ 143.6 rather than broad signals at δ 147.2 and 148.2; unfortunately no ^{195}Pt satellites were observed to confirm this assignment. These carbene resonances fall within the range of those previously reported for other *trans*- $\text{NHC}M\text{X}_2\text{py}$ (M = Pd, Pt) complexes.^{233–235}

Crystals suitable for X-ray diffraction of both **4.22** and **4.23** were produced, these are presented as ORTEP diagrams **Figures 4.4** and **4.5** respectively, with selected bond lengths in **Table 4.1**. Solid-state structures show reasonably close contacts between the *i*-Pr CH and I in both complexes (range across the two independent molecules in the unit cell: 3.263–4.133 Å for **4.22**, 3.340–4.149 Å for **4.23**); the [CNC] Pd complex **3.42a** has a closer contact (2.859 Å) and hence a further downfield shift for the *i*-Pr CH resonance in the ^1H NMR spectrum. In **4.22**, the bond lengths and angles around the square planar Pd center were very similar in both independent molecules in the unit cell, with only a slight difference in the angle between the mean plane of the NHC and mean square plane around the Pd centre (78.4°, 87.2°); however, the angles between the mean plane of the NHC and the pyridine ring were more radically different between the two molecules (14.9° and 40.2°). The Pd-C bond lengths (1.957(7) and 1.981(7) Å) were shorter in **4.22** than for the [CNC] Pd complexes **3.42** (**3.42a**: 2.024(3) Å; **3.42b**: 2.020(6) Å), this reflects the weaker *trans* influence of the pyridine ligand compared to a second NHC.

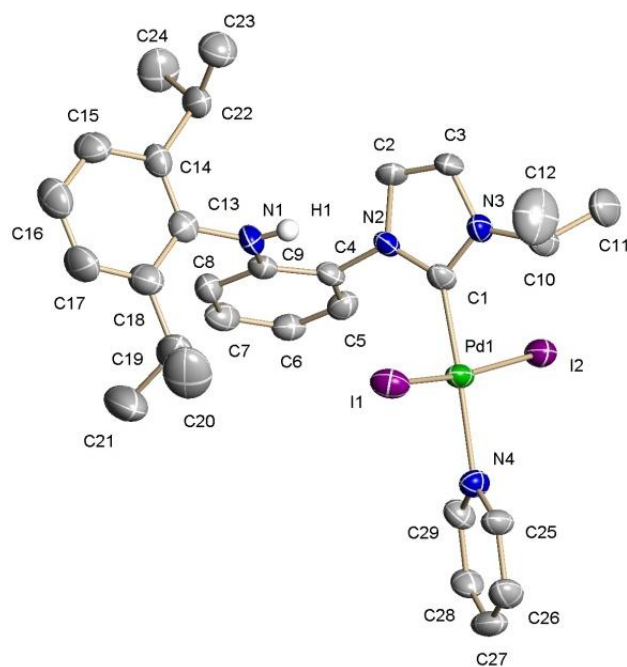


Figure 4.4: ORTEP view of **4.22**. Figures show 50% displacement ellipsoids.

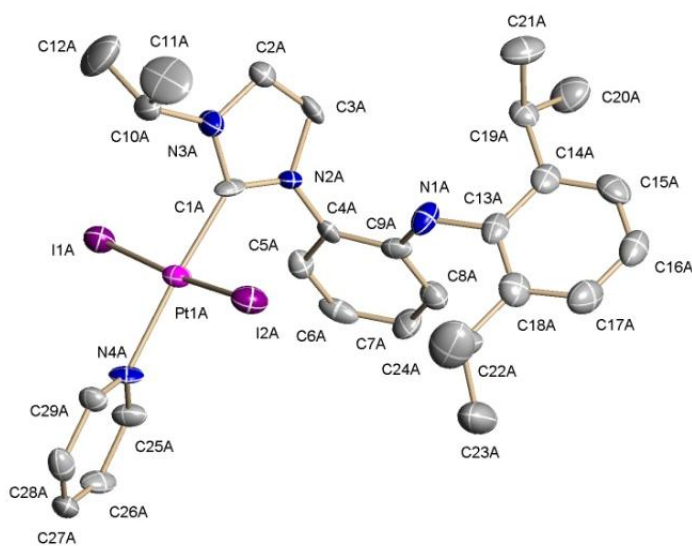


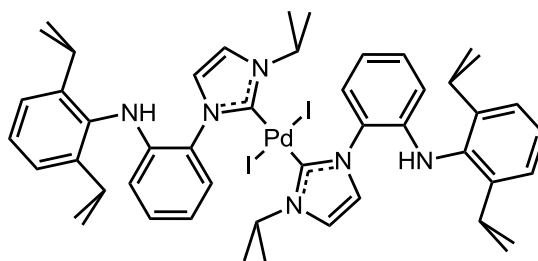
Figure 4.5: ORTEP view of **4.23**. Figures show 50% displacement ellipsoids.

Table 4.1: Selected bond lengths (Å) and angles (°) for complexes **4.22-4.24**.

	4.22 molecule 1	molecule 2	4.23 molecule 1	molecule 2	4.24
M-C(NHC)	1.957(7)	1.981(7)	1.965(13)	1.968(11)	2.016(6)
M-N(py)	2.121(6)	2.086(6)	2.094(10)	2.102(8)	-
M-I	2.5902(18)	2.5889(16)	2.5901(10)	2.5969(11)	2.5971(10)
	2.6063(17)	2.6054(15)	2.6024(10)	2.6060(10)	
C-M-N	176.5(3)	177.2(3)	176.3(5)	175.2(4)	-
I-M-I	170.99(3)	172.43(3)	173.79(4)	173.58(3)	180.00(2)

The main byproducts removed by chromatography from the reaction to form **4.22** were the known complexes *trans*-PdCl₂py₂²³⁶ and *trans*-PdI₂py₂²³⁷ which were identified by NMR, MS and X-ray diffraction data reported in literature. However, a single crystal of quality sufficient for X-ray diffraction of the *trans*-bisNHC complex **4.24** was also isolated from a mixed fraction.

An ORTEP view of **4.24** is shown in **Figure 4.6**, with selected bond lengths in **Table 4.1**. **4.24** features two *trans*-NHC ligands which are co-planar with respect to each other, but are at 79.7° to the square plane around Pd; this near-right angle is consistent with known *trans*-NHC complexes of Pd.^{233,234,238–240} The Pd-C bond length in **4.24** (2.016(6) Å) is longer than those of **4.22** (1.957(7) and 1.981(7) Å) and closer to that observed in the [CNC] pincer Pd complexes **3.42** (**3.42a**: 2.024(3) Å; **3.42b**: 2.020(6) Å) as expected due to the stronger *trans* influence of an NHC versus a pyridine ligand.



4.24

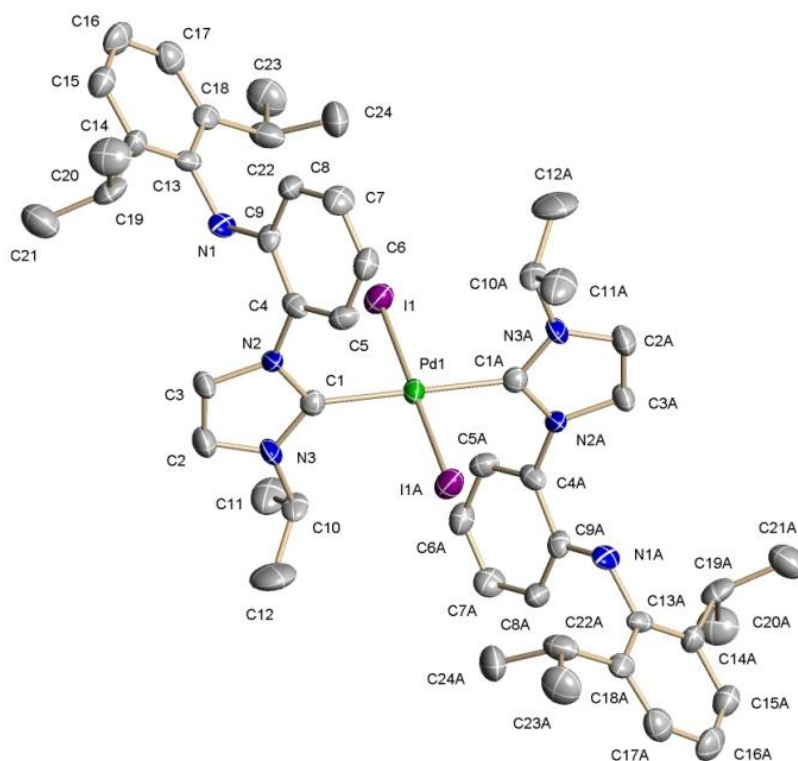
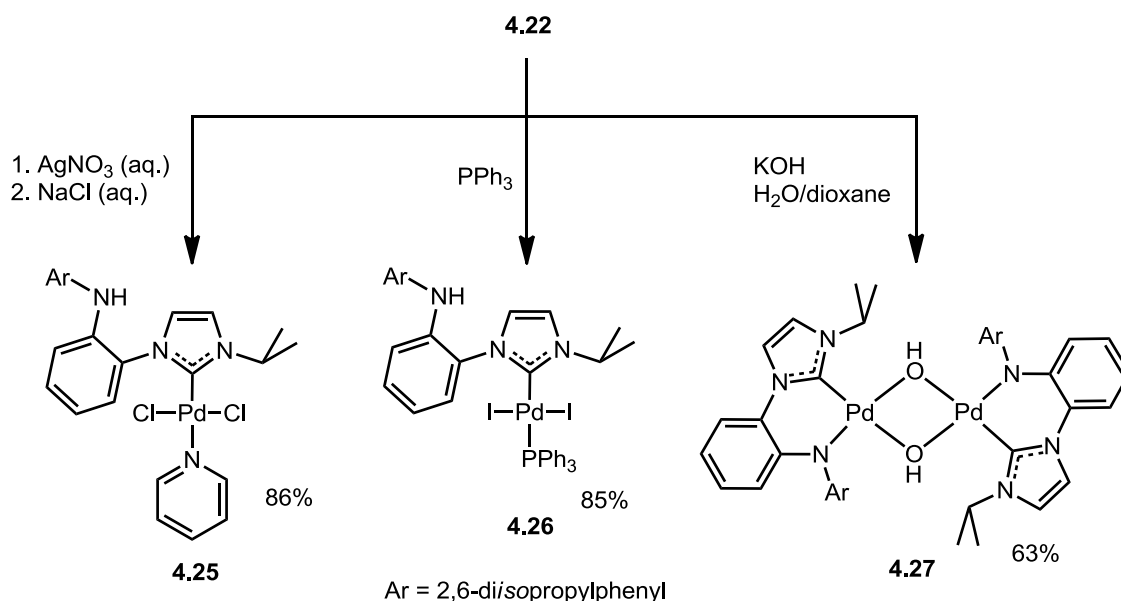


Figure 4.6: Isolated *trans*-NHC complex **4.24** including ORTEP view. Figure shows 50% displacement ellipsoids.

Complex **4.22** proved useful as a precursor to other NHC Pd complexes, **Scheme 4.10**.



Scheme 4.10: Reactions of **4.22** to form complexes **4.25-4.27**.

In order to later investigate whether the halide ligands of the precatalysts have an effect on catalysis, **4.25** was prepared. Adding NaCl under the reaction conditions that afforded **4.22** did not yield the expected chloride complex **4.25**; however, **4.25** could be synthesised by a two-step reaction of a DCM solution of **4.22** with aqueous AgNO₃ to remove the iodide ligands, then a wash with aqueous NaCl to give **4.25** in 86% yield after separation. The intermediate cationic species displayed very broad signals in the ¹H NMR spectrum, and ESIMS could only establish that it was possible to have a mix of water/nitrate or the N-Aryl substituent as ligands coordinated to the metal, with the remaining nitrate(s) acting as non-coordinated anions giving complexes of the general formula NHCPdpy(H₂O)_x(NO₃)₂. **4.25** was identified by NMR spectroscopy, showing similar resonances to **4.22**. In the ¹H NMR spectrum, the *i*-Pr CH signal comes at δ 6.01, suggesting a stronger interaction between the proton and Cl ligand in **4.25** than the proton to I ligand contact in **4.22** (δ 5.79). As Cl is more electronegative than I,

stronger H-bonding would be expected; however, crystals of **4.25** of quality sufficient for X-ray diffraction studies could not be grown to inspect this. The carbene resonance in the ^{13}C NMR spectrum is again tentatively assigned as δ 150.8, not as the broad quaternary carbons at δ 144.0 or 135.0; this signal for the carbene resonance is close to that observed for **4.22** (δ 147.3). ESIMS gave signals assigned to $[\text{M-Cl-py}]^+$, $[\text{M-Cl-py+MeCN}]^+$, $[\text{M-Cl}]^+$ and $[\text{M-Cl+MeCN}]^+$; these species containing only Cl, and not I, along with a satisfactory elemental analysis confirmed that chloride was the halide ligand present.

As the pyridine ligand is expected to be labile during catalysis, the author wanted to ensure that the pyridine ligand could be easily substituted for another neutral ligand. The lability of the pyridine ligand in **4.22** was demonstrated by stirring a DCM solution of **4.22** with 1.5 eq. of PPh_3 at RT, which resulted in complete exchange of the pyridine for the phosphine after 2 h, **Scheme 4.10**. The resulting complex **4.26** was isolated as orange crystals in 85% yield after recrystallisation from Et_2O /pentane at 3 °C. The ^1H and ^{13}C NMR spectra for **4.26** showed similar resonances as those recorded for **4.22** and **4.25**, with broad signals in both ^1H and ^{13}C spectra for the 2,6-diisopropylphenyl group. The *i*-Pr CH resonance comes at δ 5.39, suggesting a similar level of interaction with the iodide ligand as for **4.22**, and the solid state structure has similar H-I distances of 4.010 and 3.365 Å. The aryl protons proved difficult to assign; the presence of 3 additional phenyl groups on the phosphine led to significant overlap, displaying several multiplets in the ^1H NMR spectrum. Similar problems were encountered in the ^{13}C NMR spectrum, and an HSQC experiment could not help with differentiation of peaks; however, the carbene resonance was assigned at δ 156.8,

which is within the range of previously reported *trans*-NHCPdX₂PR₃ carbene signals.^{241–243} The crystalline **4.26** proved suitable for X-ray diffraction; an ORTEP view of **4.26** is presented in **Figure 4.7**, with selected bond lengths in **Table 4.2**. The solid state structure of **4.26** shows significant distortion of the square plane around Pd, with the I-Pd-I angle at 167.5° and the C-Pd-P angle at 173.4°, this has been previously observed with an unsymmetrical arylalkyl-NHC trans to a PPh₃ ligand on Pd.²⁴² Distortion around the square plane is perhaps unsurprising given the steric bulk of PPh₃. The C-Pd bond length, at 2.025(9) Å, is longer than for **4.22** (1.957(7), 1.981(7) Å), and very similar to that of **4.24** (2.016(6) Å) and the [CNC] pincer complexes **3.42** (**3.42a**: 2.024(3) Å; **3.42b**: 2.020(6) Å), reflecting the similar σ -donating properties of phosphines and carbenes. The C-Pd and P-Pd bond lengths are virtually identical to those reported for other *trans*-NHCPdX₂PPh₃ complexes.^{241–243}

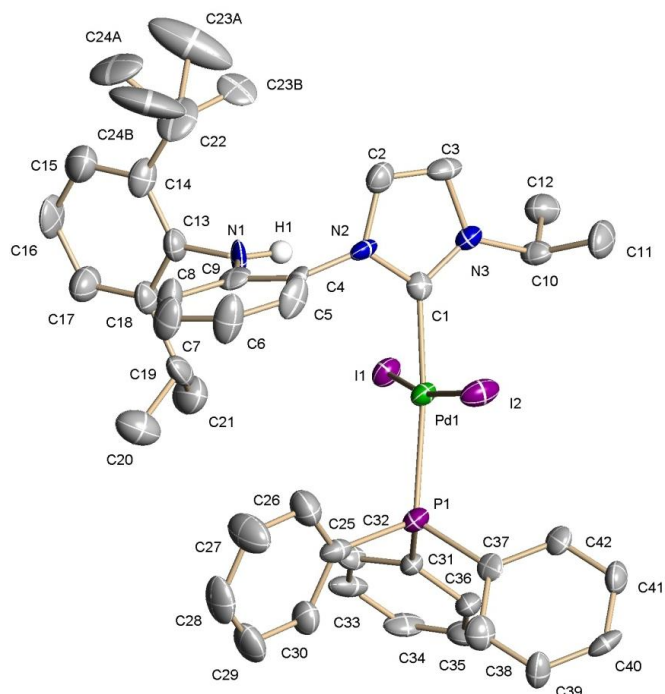


Figure 4.7: ORTEP view of **4.26**. Figures show 50% displacement ellipsoids. Atoms C(23) and C(24) of one of the isopropyl groups are disordered and have been split. H-atoms (except NH) have been omitted for clarity.

Table 4.2: Selected bond lengths (Å) and angles (°) for complex **4.26**.

4.26	
M-C(NHC)	2.025(9)
M-I	2.6000(19)
	2.622(2)
M-P	2.355(3)
I-M-I	167.52(4)
C-M-P	173.4(3)

All of the complexes reported so far in this section have the functionalised-NHC coordinated only in a monodentate fashion, not as a bidentate amino/amido-NHC ligand, as targeted in **Figure 4.2**. This is most likely due to the bulky N-aryl donor being too sterically hindered to easily coordinate in place of a halide ligand or K_2CO_3 being insufficiently basic to deprotonate the amine donor. Although a bidentate complex was originally targeted, it is possible for the amine functionality to deprotonate and coordinate as an amido ligand under catalytic reaction conditions. The author wanted to investigate if this coordination could happen stoichiometrically, forming an isolable amido-NHC complex. In order to obtain a bidentate complex, it was first attempted to remove the halide from **4.22** with silver salts, freeing a coordination site for the N-donor substituent; this strategy was used by Fryzuk in order to coordinate the amine donor of the amine-NHC ligand of **4.6**.¹⁶³ The addition of silver salts to **4.22** led only to complex mixtures, from which no single complex could be isolated. The second strategy was to react **4.22** with a base to deprotonate the amine, eliminate HX and consequently form a Pd-amido complex. Several bases were attempted, including NaOAc, NaOMe, *t*-BuONa, *n*-BuLi, LiHMDS and LDA. All these bases produced a complex mixture of products; however, using KHMDS produced one major product which was identified as the dimeric mixed hydroxide/amide $\{[C,NAr]Pd(\mu-OH)\}_2$ **4.27**.

The 1H NMR spectrum was insufficient to fully identify **4.27** but displayed a characteristic signal for the bridging hydroxide at δ -3.97; this is slightly upfield of the typical range of *ca.* -0.25 to -3.5 ppm for cationic and neutral $Pd(\mu-OH)_2$ moieties.²⁴⁴⁻

²⁴⁸ An amido ligand in the complex was implied by the lack of visible amine N-H resonances in the 1H NMR spectrum. In the ^{13}C NMR spectrum for **4.27**, the carbene

signal could not be clearly identified as there are four signals for ^4C atoms between δ 144-148.

Crystals of **4.27** suitable for X-ray diffraction were grown, which aided in the identification of **4.27**; an ORTEP view is presented in **Figure 4.8**, with selected bond lengths in **Table 4.3**.

Two crystallographically equivalent monomer units make up the dimer in **4.27**, with a near planar Pd_2O_2 ring (Pd-O-Pd-O torsion angle of 4.7°). The Pd-Pd distance of $3.2348(6)$ Å suggests no bonding interaction between the two metal centres. The Pd-O bond *trans* to the NHC ($2.086(2)$ Å) is longer than the Pd-O bond *trans* to the amido ligand ($2.052(2)$ Å) due to the stronger *trans* influence of the carbene; both Pd-O bond lengths in **4.27** are similar to those reported for complexes with a phosphine *trans* to the $\mu\text{-OH}$ ligand.^{244,249,250} The Pd-C ($1.945(3)$ Å) and Pd-amide ($1.998(3)$ Å) bond lengths of **4.27** are the shortest of all the Pd complexes reported in this thesis. The 2,6-diisopropylphenyl group in **4.27** appears to shield the bridging hydroxide, which sits *ca.* 2.54 Å above the aromatic ring in the solid state; this explains the upfield shift of the hydroxide proton resonances in the ^1H NMR spectrum of **4.27**. In the previously reported β -diiminato complex $\{[\text{Ph}_2\text{nacnac}]\text{Pd}(\mu\text{-OH})\}_2$ the hydroxide protons were observed at -5.24 ppm in the ^1H NMR spectrum, even further upfield than those of **4.27** ($\delta -3.97$), most likely as a consequence of the shielding effect of the two nearby phenyl groups of the Ph_2nacnac ligands.²⁴⁸

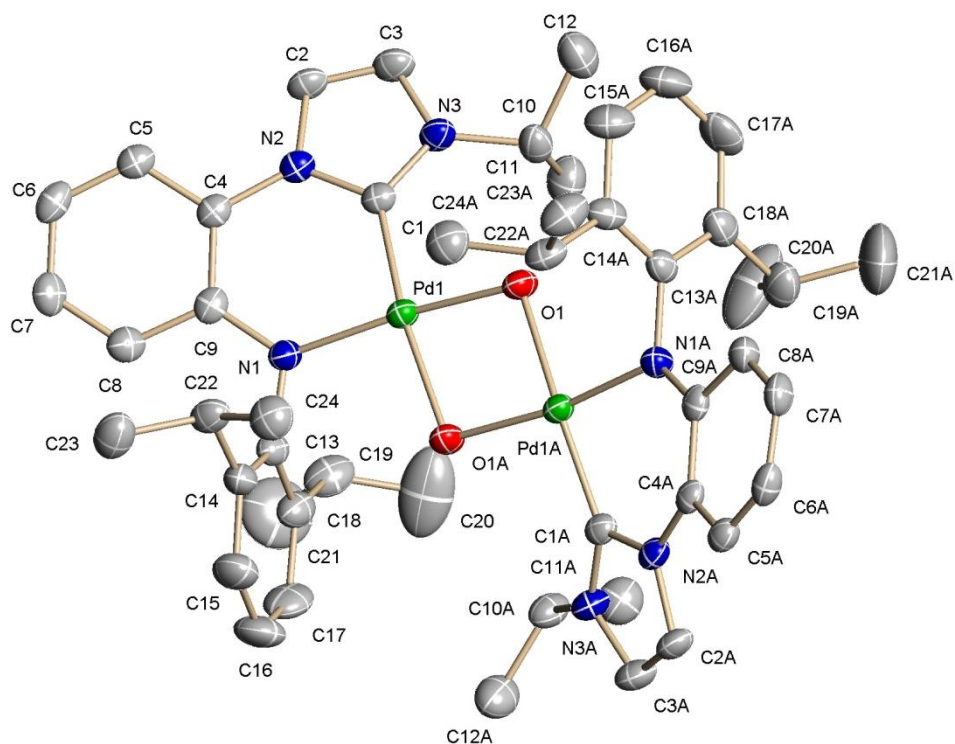


Figure 4.8: ORTEP view of **4.27**. Figures show 50% displacement ellipsoids. The 'A' atoms are generated by symmetry, symmetry operation $-x+1, -y+1/2, z$. Disordered pentane and H-atoms have been omitted for clarity.

Table 4.3: Selected bond lengths (Å) and angles (°) for complex **4.27**.

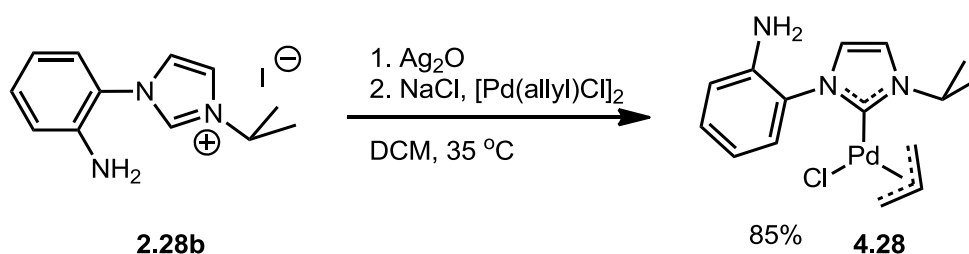
4.27	
M-C(NHC)	1.945(3)
M-N(amide)	1.998(3)
M-O	2.052(2)
	2.086(2)
O-Pd-C	169.70(10)
Pd-O-Pd	102.82

Chapter 4 – Synthesis and Reactivity of Complexes of Bidentate Amino/Amido-NHC Ligands

The hydroxide ligands of **4.27** were presumably produced from adventitious moisture, and this reaction showed poor reproducibility. Attempts to produce a more consistent reaction by using other sources of KHMDS, performing the reaction under moist air or adding water to a rigorously dry reaction mixture all failed to improve the reproducibility and purity of the reaction. However, a reproducible synthesis was accomplished by stirring a solution of **4.22** in 1,4-dioxane with aqueous KOH, giving **4.27** in 63% yield, **Scheme 4.10**.

Attempts to prepare the Pt analogue of **4.27** by reaction of Pt amino-NHC **4.23** under the same conditions failed; there was no reaction at 40 °C and increasing the temperature to 60 °C gave an intractable mixture of products. Ligand substitution reactions are generally slower for Pt than Pd; the lack of reactivity of **4.23** compared to **4.22** is consistent with a mechanism where hydroxide reacts at the metal first, substituting a halide ligand.^{251–253}

Attempts to form PEPPSI-type complexes from the primary amine-functionalised imidazolium salt **2.28b** by reaction of PdCl₂ or K₂PtCl₄ with K₂CO₃ in pyridine resulted in intractable mixtures of products, inseparable even by column chromatography. A different methodology to coordinate a primary amine-functionalised NHC ligand to palladium was therefore needed. A silver to palladium transmetallation strategy failed for most metal salts attempted; however, reaction of imidazolium salt **2.28b** with Ag₂O followed by addition of [Pd(allyl)Cl]₂ gave complex **4.28** in 85% yield, **Scheme 4.11**. Complexes of the type (NHC)Pd(allyl)Cl have excellent activity as precatalysts in dehalogenation and C-C and C-N coupling reactions.^{254–256}



Scheme 4.11: Synthesis of **4.28**.

4.28 was isolated as a yellow-white solid which is air-stable up to 98 °C; however, the complex proved unstable in solution over several hours, with palladium black precipitating from the solution. The ¹H NMR spectrum of **4.28** displayed a 2H singlet at δ 4.36 for the NH₂ protons, suggesting that the amine donor was most likely non-coordinated. Five inequivalent proton signals were observed for the allyl ligand, as would be expected for an η³-allyl ligand in an unsymmetrical complex. The carbene resonance in the ¹³C NMR spectrum is at δ 180.5, similar to the carbene resonances reported for other (NHC)Pd(allyl)Cl complexes.²⁵⁵

Despite the instability of **4.28**, crystals of **4.28** suitable for X-ray crystallography were grown and the solid state structure is shown in **Figure 4.9**. Crystallography confirmed that the amine functionality was not coordinated, showing that the NHC was coordinated in a monodentate fashion, with the pseudo-square plane around the metal completed by an η³-allyl and a chloride ligand. The chloride ligand sits at 90.4° from the carbene, with the mean plane of the carbene sitting at 70.4° to the square plane defined by C(1)-Pd-Cl; the allyl ligand sits mostly in this square plane with some minor distortion. The NHC-Pd and Pd-Cl distances (2.030(3) and 2.3836(10) Å respectively) are consistent with previously reported (NHC)Pd(allyl)Cl complexes.²⁵⁵

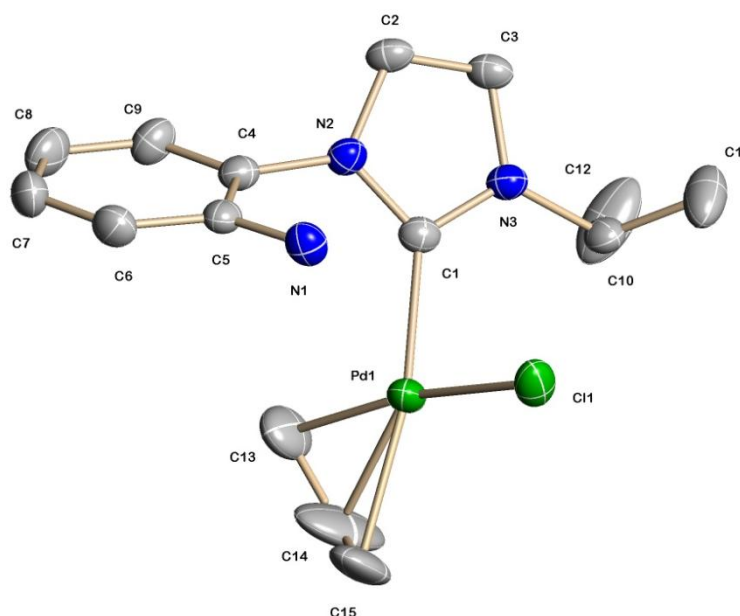
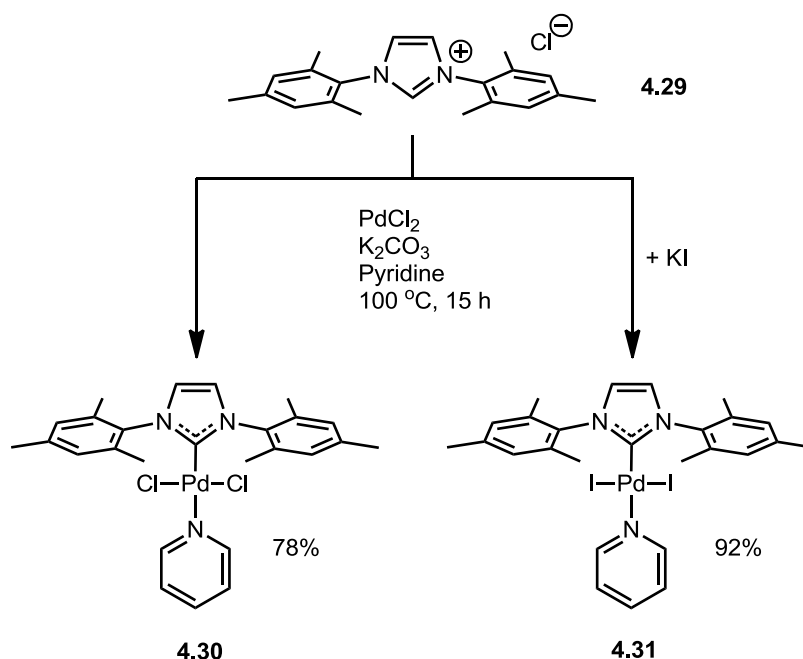


Figure 4.9: ORTEP view of **4.28**. Figures show 50% displacement ellipsoids. H-atoms have been omitted for clarity. Selected bond lengths (Å) and angles (°): Pd-C(NHC): 2.030(3); Pd-Cl: 2.3836(10); C(1)-Pd-Cl: 90.35(8).

4.2.2: Synthesis of Complexes of Unfunctionalised NHC Ligands

Complexes of a normal unfunctionalised NHC were prepared, to use as controls in catalytic reactions, as a comparison for the catalytic activity of (C,NR) complexes **4.22**-**4.28**. PEPPSI-type complexes of the NHC IMes were produced by the methodology used for precatalyst **4.22**, using the known imidazolium salt **4.29**, which was synthesised by the method of Arduengo.¹³⁹ Heating **4.29** with PdCl₂ and K₂CO₃ in pyridine gave the complex IMesPdCl₂py **4.30**, whilst addition of excess KI into the reaction mixture gave IMesPdI₂py **4.31**, both in good yield after crystallisation (**4.30**: 78%, **4.31**: 92%), **Scheme 4.12**. Having complexes of both halides accessible allowed us to evaluate the role of the halide ligands in any catalysis.



Scheme 4.12: Synthesis of IMes PEPPSI-type complexes **4.30** and **4.31**.

In the ^{13}C NMR spectra of **4.30** and **4.31** carbene resonances are visible at δ 153.0 (**4.30**) and 151.8 (**4.31**); these are close to the assigned values for **4.22** (δ 147.3) and **4.25** (δ 150.8) and within the reported range for *trans*-NHCPdX₂py complexes.^{233–235}

Crystals of both complexes suitable for X-ray diffraction were grown, ORTEP views of **4.30** and **4.31** are shown in **Figure 4.10** and **Figure 4.11**, respectively, with selected bond lengths in **Table 4.4**. Both complexes feature a square plane about the metal, with a significant torsion angle between the square plane and the mean plane of the NHC (77.4° for **4.30**, 67.7° for **4.31**). As observed for complexes **4.22** and **4.25**, the mean plane of the pyridine ligand sits at an angle compared with the mean plane of the NHC (52.9° for **4.30**, 47.3° for **4.31**). The carbene-Pd bond lengths ($1.967(2)$ Å for **4.30**, $1.984(3)$ Å for **4.31**) are similar to **4.22** ($1.957(7)$, $1.981(7)$ Å), and as expected are shorter than *trans*-NHC Pd complex **4.24** ($2.016(6)$ Å).

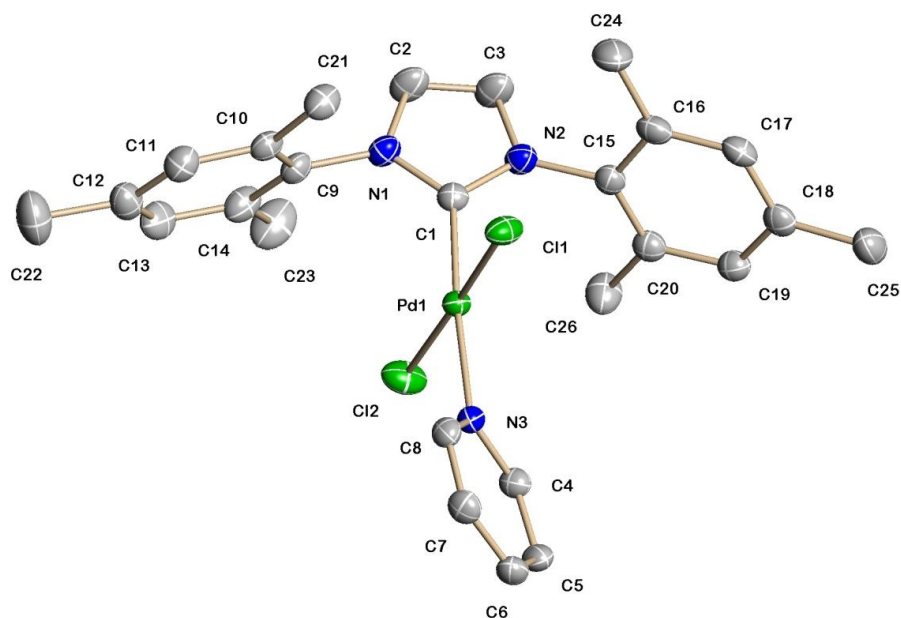


Figure 4.10: ORTEP view of **4.30**. Figures show 50% displacement ellipsoids. H-atoms have been omitted for clarity.

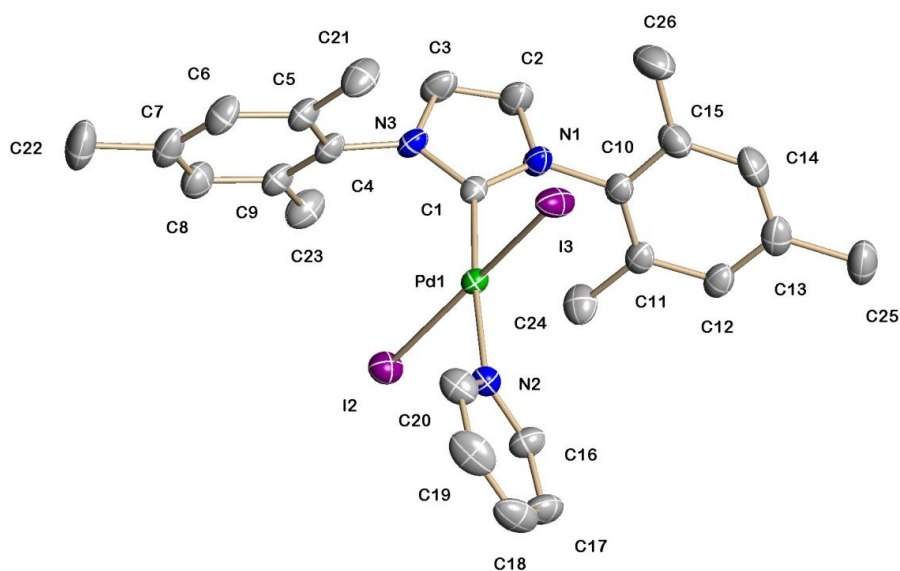


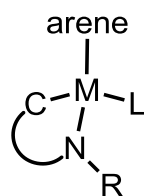
Figure 4.11: ORTEP view of **4.31**. Figures show 50% displacement ellipsoids. A molecule of DCM and the H-atoms have been omitted for clarity.

Table 4.4: Selected bond lengths (Å) and angles (°) for complexes **4.30** and **4.31**.

	4.30	4.31
M-C(NHC)	1.984(3)	1.967(2)
M-N(py)	2.088(3)	2.0867(16)
M-X	2.5994(5)	2.2970(7)
	2.6043(5)	2.2979(7)
C-Pd-N	174.60(7)	174.29(12)
X-Pd-X	177.66(2)	173.127(12)

4.2.3: Synthesis of [C,NR] and [C,C] complexes of Ru, Rh and Ir

Following on from the successful isolation of Pd and Pt complexes in **Ch. 4.2.1**, it was decided to synthesise half-sandwich complexes of bidentate amine-functionalised NHC ligands, of the general form shown in **Figure 4.12**. As for the (C,NR) Pd and Pt complexes reported in **Ch. 4.2.1**, variation of R group on the amine could allow control of both the sterics and electronics of the amido donor, allowing tuning of the bifunctional reactivity of the complexes. The piano-stool scaffold of the complexes was chosen as half-sandwich amido complexes are used as catalysts in several bifunctional reactions, including Ru, Rh and Ir catalysed hydrogenation^{1,24,26} and Ir catalysed hydroamination.²⁵⁷



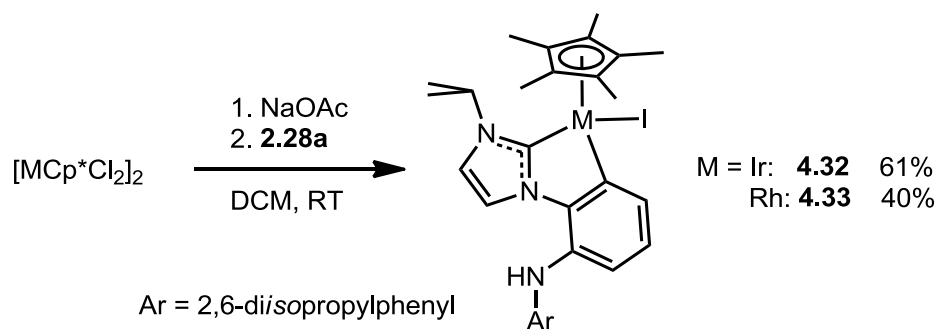
R = H, 2,6-diisopropylphenyl
arene = *p*-cymene, Cp*

Figure 4.12: General schematic of target Ru, Rh and Ir amino/amido complexes. L = anionic or neutral ligand, C = N-heterocyclic carbene donor.

The author attempted to synthesise the target complexes based on the reactions of imidazolium salt **2.28a** and the metal half sandwich dimers [Ru(*p*-cymene)Cl₂]₂, [IrCp*Cl₂]₂ and [RhCp*Cl₂]₂, using several bases to deprotonate the imidazolium salt. Ag₂O^{258–260} and NaOAc^{261–264} have been used to prepare half-sandwich NHC complexes previously; *t*-BuONa, as a strong, non-nucleophilic base, could allow deprotonation of the imidazolium salt to form both the carbene and amido donors, and was also used.

The reaction of **2.28a** and [Ru(*p*-cymene)Cl₂]₂ with either Ag₂O, NaOAc or *t*-BuONa in DCM gave intractable mixtures of products.

In contrast, the reaction of the imidazolium salt and NaOAc with either [IrCp*Cl₂]₂ or [RhCp*Cl₂]₂ gave the unexpected cyclometallated complexes **4.32** and **4.33** in moderate yields (**4.32**: 61%; **4.33**: 40%) after purification by column chromatography, **Scheme 4.13**. The cyclometallation proceeded much faster for Ir than Rh, this is consistent with literature observations for acetate-assisted cyclometallation with Cp*Rh complexes and Cp*Ir complexes.^{265,266}



Scheme 4.13: Synthesis of cyclometallated complexes **4.32** and **4.33** by reaction of $[MCp^*Cl_2]_2$ and NaOAc with imidazolium salt **2.28a**.

In the same way, reacting **2.28a** and $[IrCp^*Cl_2]_2$ or $[RhCp^*Cl_2]_2$ with Ag_2O did not give an amino/amido complex as product: no reaction occurred in the case of Rh, and with $[IrCp^*Cl_2]_2$ a slow reaction occurred to form the cyclometallated complex **4.32**.

Reacting **2.28a** and $[RhCp^*Cl_2]_2$ with *t*-BuONa gave low conversion to the cyclometallated complex **4.33**; however, the reaction of $[IrCp^*Cl_2]_2$ with *t*-BuONa gave an intractable mixture of products, with no sign of formation of **4.32**.

4.32 and **4.33** were easily identified as the cyclometallated (C,C) complexes rather than having a (C,N) bidentate ligand. 1H NMR spectroscopy revealed an nOe between the protons of the NHC ring and the NH signal in both complexes (NH resonances: **4.32**: 4.85 ppm; **4.33**: 4.78 ppm), confirming the amine was not bound to the metal. Only three signals were seen for the protons on the aryl ring linking the NHC and the amine in both complexes, suggesting cyclometallation; this could be further confirmed with **4.33** as in the ^{13}C spectrum the resonance for the aryl carbon bound to rhodium was observed as a doublet (δ 158.3, $J_{Rh-C} = 40$ Hz) due to the spin-active nature of the ^{103}Rh nucleus.

Crystals of both **4.32** and **4.33** suitable for X-ray diffraction were grown; ORTEP views of **4.32** and **4.33** are shown in **Figure 4.13** with selected bond lengths and angles in **Table 4.5**. **4.32** and **4.33** were both racemates with a stereogenic metal centre. **4.32** and **4.33** both crystallise in the centrosymmetric space group $P2_1/C$ with both enantiomers in the unit cell; the unit cell dimensions were almost identical for **4.32** and **4.33**. The complexes have very similar structures, both adopting a piano-stool geometry. The metal-NHC (**4.32**: 1.978(8) Å, **4.33**: 1.993(6) Å) and metal-aryl (**4.32**: 2.048(7) Å, **4.33**: 2.048(6) Å) bond lengths were near identical between the two complexes; this is indicative of the similar ionic radii of Rh^{III} and Ir^{III} .²⁶⁷ The Ir-NHC bond length was similar to other reported Cp^*Ir cyclometallated species.^{261–263,268–271} The C,C ligands featured a twist of *ca.* 11.5° between the mean planes of the NHC and cyclometallated aryl ring, apparently due to the *ortho*-amine substituent. The 2,6-diisopropylphenyl rings sit virtually perpendicular to the cyclometallated aryl rings as a consequence of the steric bulk of the *isopropyl* substituents. In both **4.32** and **4.33** there is a tilt in the Cp^* ring relative to the metal centre: in each complex the two M-C(Cp^*) bonds opposite the iodide ligand are the shortest (2.161(6) to 2.198(7) Å), whilst the three M-C(Cp^*) bonds opposite to the NHC and aryl ligands are longer (2.231(6) to 2.280(7) Å). This difference in bond lengths reflects the relative *trans* influence of the other three ligands. At *ca.* 78°, the ligand bite angles were consistent with 5-membered rings comprising a cyclometallated NHC ligand around Cp^*Ir ;^{268–270} **4.33** is the only reported $Rh(C,C)$ cyclometallated NHC complex known to the author.

Chapter 4 – Synthesis and Reactivity of Complexes of Bidentate Amino/Amido-NHC Ligands

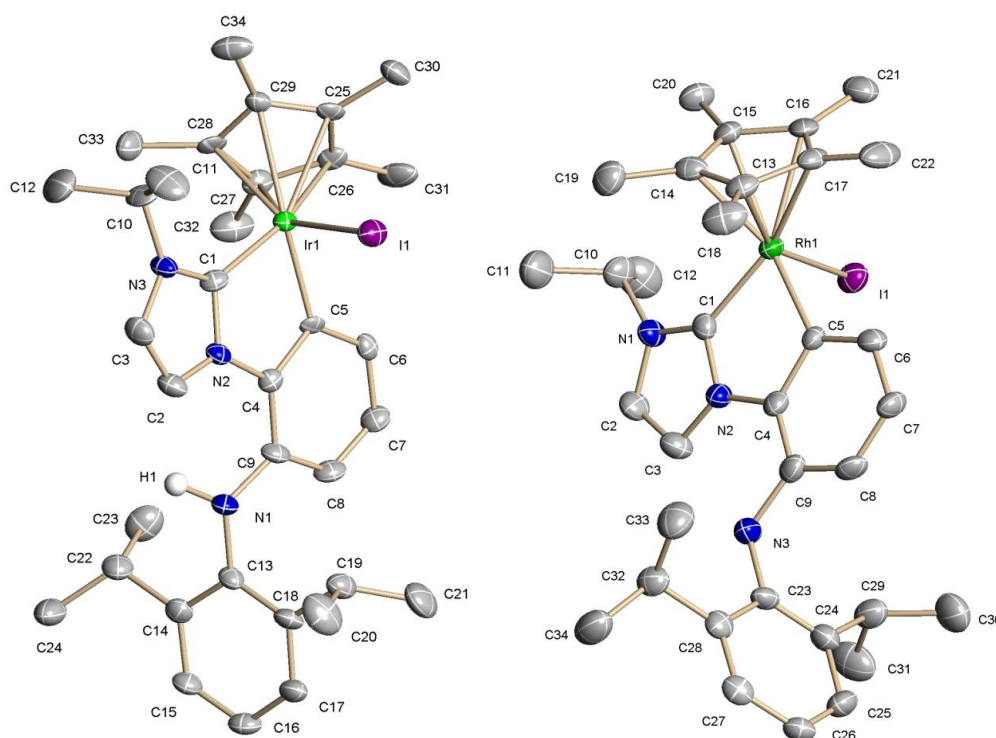


Figure 4.13: ORTEP views of **4.32** and **4.33**. Figure shows 50% displacement ellipsoids.

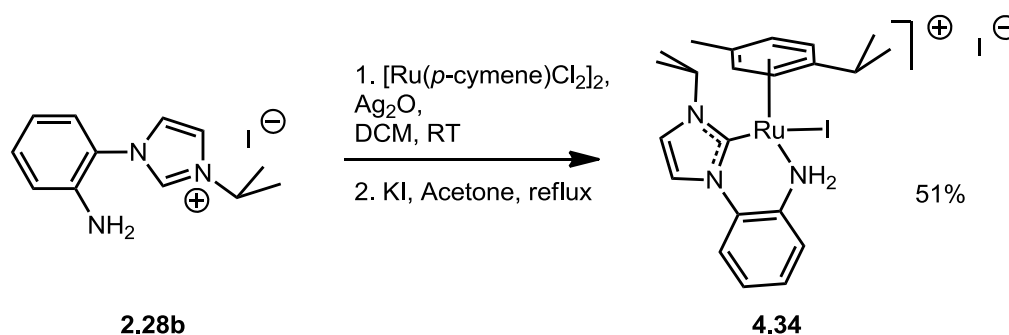
Table 4.5: Selected bond lengths (Å) and angles (°) for complexes **4.32** and **4.33**.

	4.32	4.33
M-C(1) (NHC)	1.993(6)	1.978(8)
M-C(5) (aryl)	2.048(6)	2.048(7)
M-I	2.6756(9)	2.6693(8)
M-C(Cp*)	2.161(6)	2.169(7)
	2.188(6)	2.198(7)
	2.231(6)	2.253(8)
	2.271(6)	2.264(7)
	2.276(5)	2.280(7)
C(1)-M(1)-C(5)	78.2(2)	78.1(3)

It appears that the bulky diisopropylphenyl substituent prevents coordination of the NH to the metal centre. As the nitrogen donor is not-coordinated and unable to interact closely with the metal centre, and the aryl carbon donor is strongly bound to

the metal, **4.32** and **4.33** are obviously not suitable for bifunctional catalysis involving a metal-nitrogen bond, as originally proposed. However, cyclometallated NHC Cp*Ir(C,C)X complexes are known as effective pre-catalysts for H/D exchange,²⁶² diboration of alkenes,²⁶³ and water oxidation.^{269,271}

To investigate if the bulky diisopropylphenyl substituent prevented coordination of the arylamine donor, next the primary amine functionalised imidazolium salt **2.28b** was reacted with $[M(\text{arene})X_2]_2$ and base in order to isolate the target $[(\text{arene})M(\text{C},\text{NH})X]$ complexes.



Scheme 4.14: Synthesis of **4.34** by in-situ transmetalation of a silver carbene to $[Ru(p\text{-cymene})Cl_2]_2$.

The reaction of $[Ru(p\text{-cymene})Cl_2]_2$ and **2.28b** with Ag_2O , followed by treatment with KI, gave the (C,N) complex **4.34** in 51% yield after column chromatography, **Scheme 4.14**. **4.34** showed several characteristic signals in the 1H NMR spectrum. Two mutually coupling NH doublets (δ 4.17 and 8.52 ppm, $J = 10.8$ Hz) indicated the amine was coordinated to ruthenium. The *p*-cymene aryl protons are displayed as four signals, two overlapping doublets (δ 5.21) and two separate doublets (δ 5.76, 6.22), further evidence for the coordination of the bidentate (C,N) ligand and a halide. The

Chapter 4 – Synthesis and Reactivity of Complexes of Bidentate Amino/Amido-NHC Ligands

carbene ^{13}C resonance was determined to be 175.9 ppm, which is similar to the reported value (δ 175.1) for the carbene of the structurally similar complex **4.19**.¹⁹

Crystals of **4.34** suitable for X-ray diffraction were obtained; an ORTEP view of **4.34** is presented in **Figure 4.14**, with selected bond lengths and angles in **Table 4.6**. **4.34** crystallises in the centrosymmetric P-1 space group with two unique molecules in the unit cell. The Ru–C distance (2.054(11), 2.082(13) Å) and Ru–N distance (2.154(8), 2.114(9) Å) in **4.34** are similar to those reported for the related complex **4.19** (Ru–C = 2.092(5); Ru–N = 2.146(4) Å).¹⁹ The (C,N) ligand bite angle is much smaller in the 6-membered chelate ring of **4.34** (*ca.* 80°) than in the 7-membered chelate ring of **4.19** (91.98(17)°).¹⁹ In forming this 6-membered chelate, the mean planes of the aryl and NHC rings take on a twist, with a torsion angle about C(4)–N(2) of 38.8° and 31.7° in the two independent molecules of **4.34**. Intermolecular hydrogen bonding is also observed between one of the amine NH_2 protons and the non-coordinated iodide counterion.

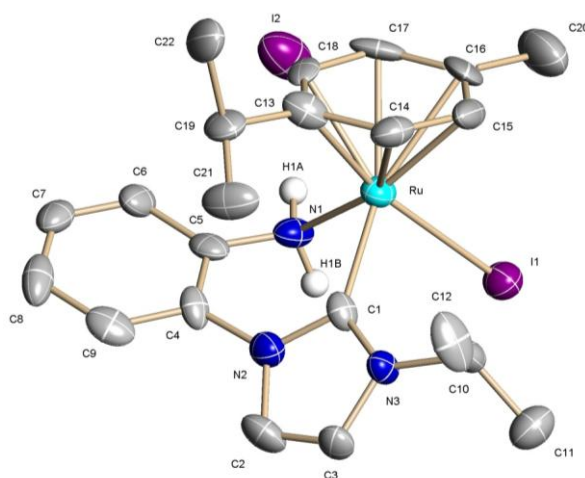
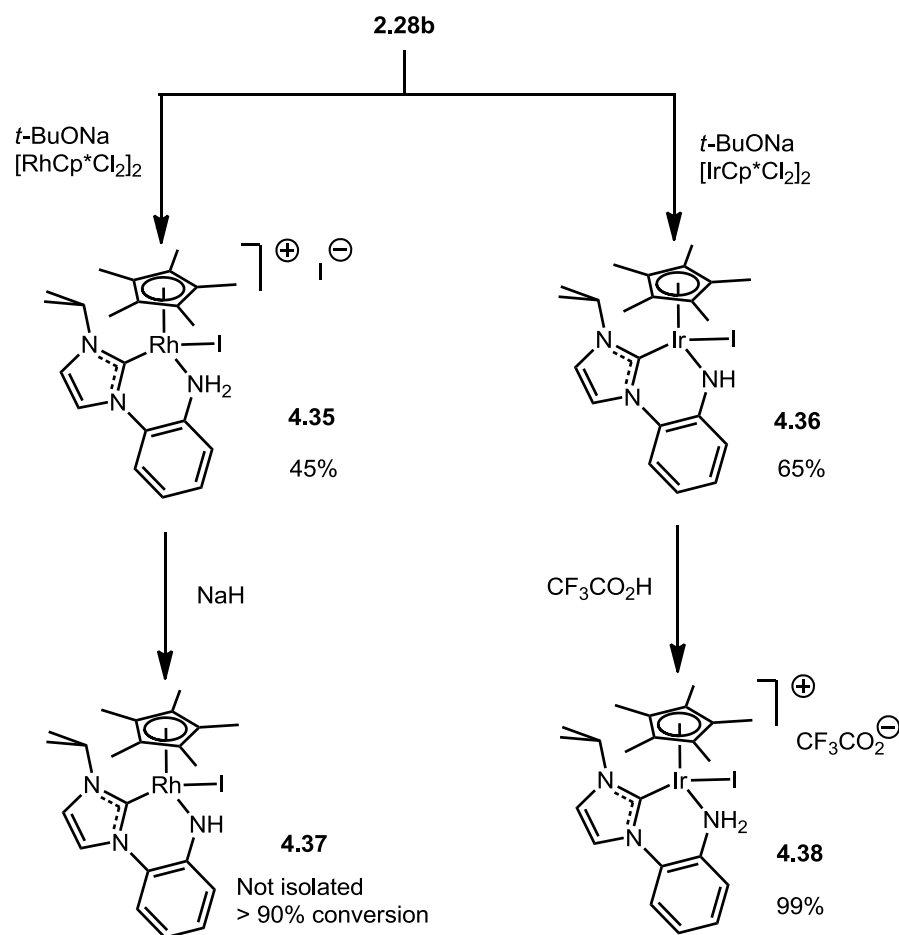


Figure 4.14: ORTEP view of **4.34**. Figure shows 50% displacement ellipsoids.

Chapter 4 – Synthesis and Reactivity of Complexes of Bidentate Amino/Amido-NHC Ligands

Attempting the reaction of $[\text{Ru}(p\text{-cymene})\text{Cl}_2]_2$ and **2.28b** with either NaOAc or *t*-BuONa as the base also gave **4.34** as product but in much lower conversion than with Ag_2O . Replacing $[\text{Ru}(p\text{-cymene})\text{Cl}_2]_2$ with $[\text{Ru}(p\text{-cymene})\text{I}_2]_2$ in the reaction of metal dimer and **2.28b** with Ag_2O in order to prevent the need for halide exchange after the reaction was attempted. It was found that reaction of $[\text{Ru}(p\text{-cymene})\text{I}_2]_2$ and **2.28b** with Ag_2O under similar conditions does not proceed; dimer cleavage of $[\text{Ru}(\text{arene})\text{I}_2]_2$ has been noted to be more difficult than for $[\text{Ru}(\text{arene})\text{Cl}_2]_2$ and it has been stated that the driving force for dimer formation (*i.e.* the reverse of the required reaction) in this case is the insolubility of the iodo dimer compound.²⁷²

Reaction of $[\text{IrCp}^*\text{Cl}_2]_2$ or $[\text{RhCp}^*\text{Cl}_2]_2$ with **2.28b** using NaOAc or Ag_2O as base gave intractable mixtures of products, from which no pure complex could be isolated. However, it was found that the reaction $[\text{RhCp}^*\text{Cl}_2]_2$ with **2.28b** using *t*-BuONa as the base led to the formation of Rh amino complex **4.35**, **Scheme 4.15**. The formation of **4.35** when imidazolium salt **2.28b** was used is in contrast with the reaction of $[\text{RhCp}^*\text{Cl}_2]_2$ with **2.28a** and *t*-BuONa, which resulted in low conversions to the cyclometallated complex **4.33**; the lack of amine coordination is presumably due to the steric bulk around the diarylamine of **2.28a**. **4.35** was identified initially by its ^1H NMR spectrum, which displayed two broad doublet resonances for the NH_2 protons (δ 4.76 and 7.32), similar to those observed for **4.34**. In addition, four (C,N) ligand aryl protons were clearly observed, proving that no cyclometallation had occurred on this ring. The carbene resonance was assigned as a doublet at 169.5 ppm in the ^{13}C NMR spectrum, with a $J_{\text{Rh-C}}$ of 54 Hz. Confirmation of the identity of **4.35** was provided by satisfactory elemental analysis and X-ray crystallography, *vide infra*.



Scheme 4.15: Synthesis of Rh and Ir amino/amido-NHC complexes.

The reaction of $[\text{IrCp}^*\text{Cl}_2]_2$ with **2.28b** using $t\text{-BuONa}$ as the base led to the formation of Ir amide complex **4.36**, **Scheme 4.15**. The ^1H NMR spectrum of **4.36** displayed four signals for the (C,N) ligand aryl protons, thus discounting cyclometallation of the aryl ring. An NH resonance was assigned to a broad 1H singlet at δ 2.39-2.59. The carbene resonance was assigned at 154.6 ppm in the ^{13}C NMR spectrum. Confirmation of the identity of **4.36** was provided by satisfactory elemental analysis and X-ray crystallography, *vide infra*.

Chapter 4 – Synthesis and Reactivity of Complexes of Bidentate Amino/Amido-NHC Ligands

The different products of the reactions of imidazolium salt **2.28b** and *t*-BuONa with Ir and Rh suggest the involvement of the metal in the deprotonation step at the amine: Ir^{III} is more electropositive than Rh^{III} and so an amine coordinated to Ir will be more acidic than one coordinated to a Rh centre.²⁷³

As access to both amido and amino Rh and Ir complexes could be advantageous for investigations into bifunctional catalysis, complexes **4.35** and **4.36** were reacted with base/acid as appropriate. The amino-NHC Rh complex **4.35** showed no signs of deprotonation with *t*-BuONa, but stirring **4.35** at RT with 1.5 equivalents of NaH in dry THF gave complete conversion of **4.35** to a mixture containing *ca.* 90+% **4.37**, according to ¹H NMR spectroscopy. The ¹H NMR spectrum obtained was notably similar to that of the Ir amido-NHC complex **4.36**, with a single broad 1H NH resonance at δ 5.29, and all aryl and NHC ring protons accounted for. The amido nitrogen of **4.37** appeared, however, to be much more basic than that of **4.36**: any attempts to purify **4.37** by precipitation or crystallisation resulted in conversion back to starting amino-NHC complex **4.35**, probably due to adventitious water. As a result, complex **4.37** is not fully isolated or characterized in this thesis.

It was found that the amido nitrogen of Ir amido-NHC complex **4.36** was easily protonated with trifluoroacetic acid, to quantitatively afford **4.38**, **Scheme 4.15**. The ¹H NMR spectrum of **4.38** featured the expected two NH₂ doublet resonances at δ 5.87 and 6.78. The aryl CH signals for **4.38** (δ 7.33-7.48) are further downfield than those of **4.36** (δ 6.38-7.05), reflecting a significant delocalisation of charge from the amido nitrogen of **4.36** into the aryl ring. The carbene resonance was observed at δ 156.4 in the ¹³C NMR spectrum, very similar to the carbene in **4.36** (δ 154.6). The

Chapter 4 – Synthesis and Reactivity of Complexes of Bidentate Amino/Amido-NHC Ligands

counterion CF_3CO_2^- was also observable by ^{13}C NMR spectroscopy, with the CF_3 and CO_2 signals displaying as quartets due to C-F coupling (CF_3 : 115.5 ppm, $J = 287.4$ Hz; CO_2 : 160.1 ppm, $J = 39.9$ Hz).

Crystals suitable for X-ray diffraction of **4.35**, **4.36** and **4.38** were grown; ORTEP views are presented in **Figure 4.15-4.17** respectively, with selected bond lengths and angles in **Table 4.6**.

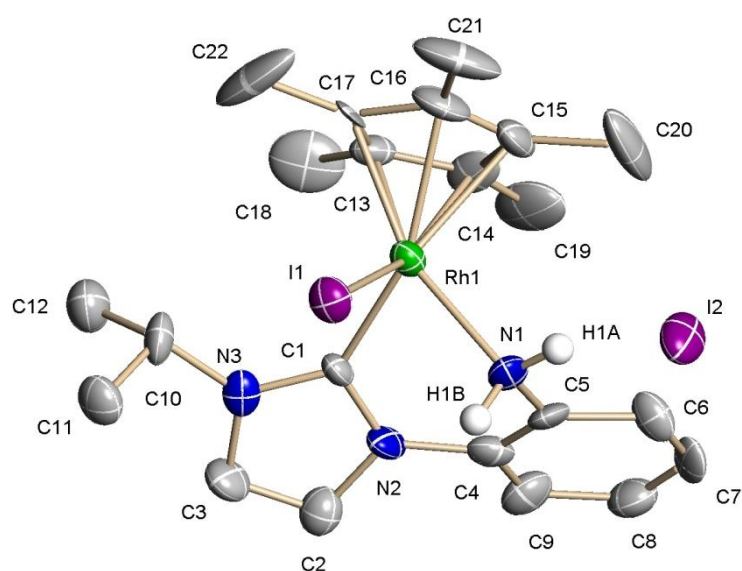


Figure 4.15: ORTEP view of **4.35**. Figure shows 50% displacement ellipsoids.

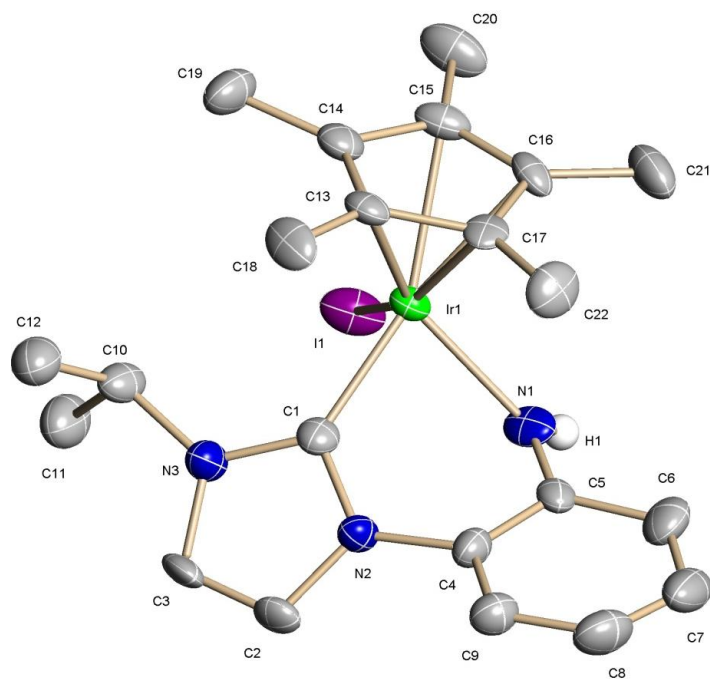


Figure 4.16: ORTEP view of 4.36. Figure shows 50% displacement ellipsoids.

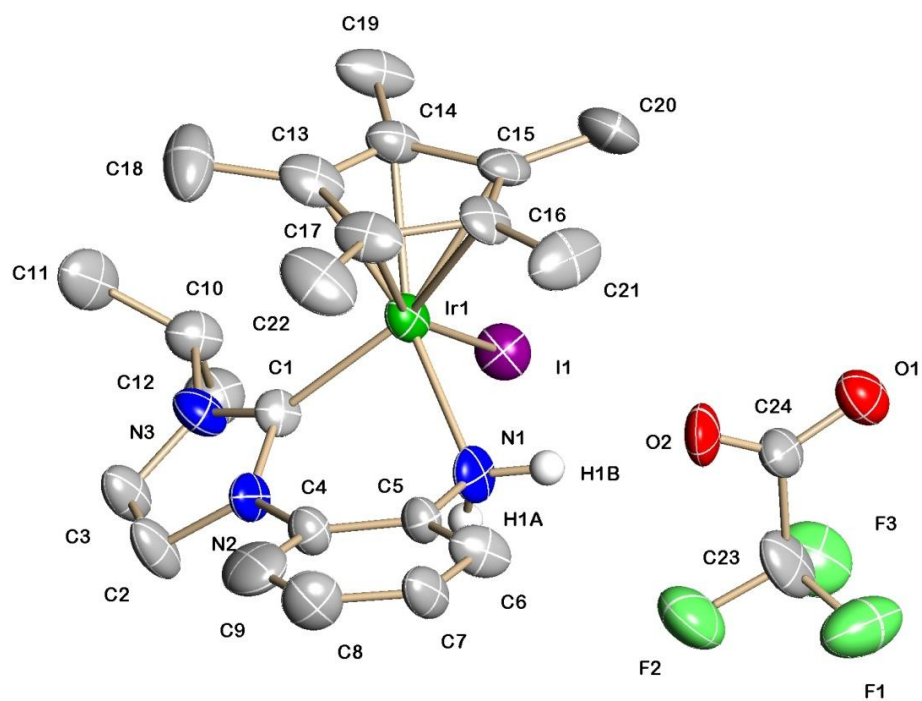


Figure 4.17: ORTEP view of 4.38. Figure shows 50% displacement ellipsoids.

Table 4.6: Selected bond lengths (Å) and angles (°) for complexes **4.34**, **4.35**, **4.36** and **4.38**.

	4.34		4.35		4.36	4.38
	molecule 1	molecule 2	molecule 1	molecule 2		
M-C(1)	2.054(11)	2.082(13)	2.041(12)	2.060(11)	1.978(9)	2.026(9)
M-N(1)	2.154(8)	2.114(9)	2.121(9)	2.118(10)	2.101(7)	2.153(7)
M-I(1)	2.7116(16)	2.7177(17)	2.6985(16)	2.7034(16)	2.6843(11)	2.7082(9)
M-C(arene)	2.163(12)	2.175(13)	2.143(12)	2.136(13)	2.129(8)	2.172(10)
	- 2.275(11)	- 2.342(19)	- 2.231(13)	- 2.227(12)	- 2.228(9)	- 2.256(9)
C(1)-M(1)-N(1)	80.4(4)	79.9(4)	80.4(5)	80.7(4)	81.1(3)	80.0(3)

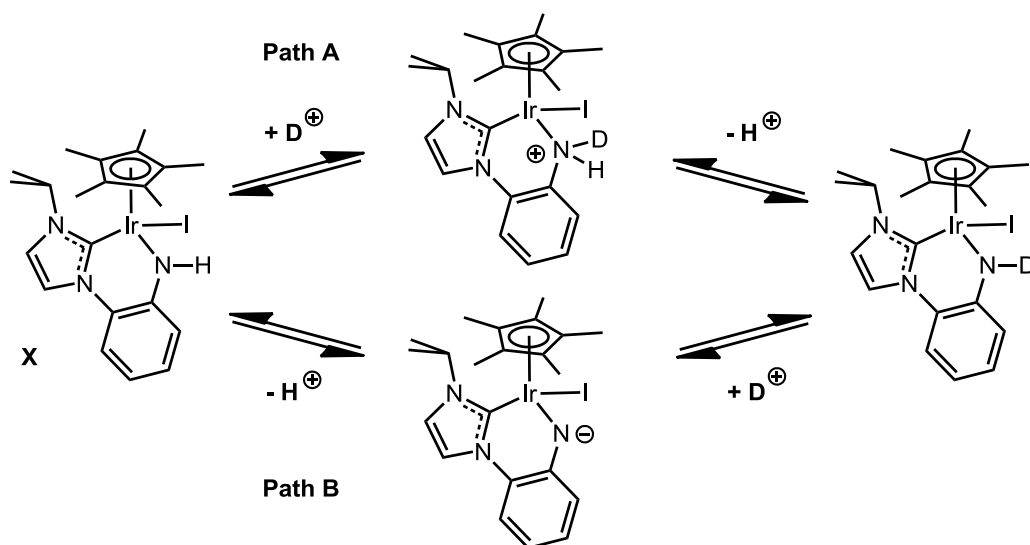
The solid state structures of amino complexes **4.35** and **4.38** have many similar features. Both the M-C (**4.35**: 2.041(12), 2.060(11) Å; **4.38**: 2.026(9) Å) and M-N (**4.35**: 2.121(9), 2.118(10) Å; **4.38**: 2.153(7) Å) bond lengths are similar, and intermolecular hydrogen bonding from one amino NH to the non-coordinated anion is present. The M-C and M-N bond lengths are also close to those of the previously discussed Ru amino complex **4.34** (M-C: 2.054(11), 2.082(13) Å; M-N: 2.154(8), 2.114(8) Å). The Ir amido complex **4.36** displays a slightly shorter M-N (2.101(7) Å) bond length than the Ir amino complex **4.38** (2.153(7) Å) as would be expected due to the anionic character of the amido nitrogen. The C(5)-N(1) bond length of **4.36** (1.328(11) Å) is shorter than that of **4.38** (1.431(11) Å), suggesting significant double bond character, most likely resulting from delocalisation of the nitrogen lone pair into the aryl ring. All the amino/amido-NHC half-sandwich complexes studied by X-ray diffraction in this chapter have similar (C,N) ligand bite angles of *ca.* 80° to form 6-membered chelate rings; this is in contrast to the much larger bite angle of 7-membered chelate ring of **4.19** (91.98(17)°).¹⁹ **4.35**, **4.36** and **4.38** have pronounced twists between the NHC and

aryl rings of the (C,N) ligand (torsion angles around C(4)-N(2): **4.35**: 31.7, 32.4°; **4.36**: 35.9°; **4.38**: 36.7°). The M-N(1)-C(5) angles of **4.36** (116.7°) and **4.38** (110.5°) reflect the nature of the nitrogen donor: the anionic amido nitrogen of **4.36** has an angle closer to the ideal trigonal planar value (120°) while the neutral amino nitrogen of **4.38** has an angle closer to the ideal tetrahedral value (109.5°).

4.2.4: Reactivity of **4.36**

As **4.36** was, to the best of the author's knowledge, the first primary amido-NHC complex of Ir, it was decided to examine the reactivity of the complex beyond simple protonation, in order to gain insight into the nucleophilicity of the amido ligand. Shaking a CDCl₃ solution of **4.36** with D₂O at RT resulted in complete deuteration of the amido NH within minutes, as judged by the disappearance of the NH resonance in the ¹H NMR spectrum. Deuteration could conceivably occur by reversible deprotonation of D₂O by the amido ligand of **4.36** followed by loss of a proton (**Path A**), or initial deprotonation of the amido ligand followed by deuteration by D₂O (**Path B**), **Scheme 4.16**. The basicity of late transition metal amides has not been well-studied but the ruthenium parent amido complex Ru(DMPE)₂(NH₂)H has been shown to be capable of deprotonating several weak acids with liberation of NH₃.²⁷⁴ Evidence suggests liberation of NH₃ occurs *via* an initial ion pair resulting from the amide ligand deprotonating the weak acid substrate, as with **Path A**, **Scheme 4.16**. The fact that no base (except the amido ligand of **4.36**) is necessary for this deuteration to occur

suggests that **Path B** is unlikely to be operative; dianionic imido donors in half-sandwich iridium complexes are also quite rare.²⁷⁵



Scheme 4.16: Pathways to the deuteration of amido NH of **4.36**.

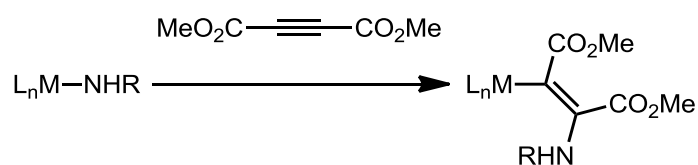
In order for **Path A** to proceed, the nitrogen lone pair must be available to pick up the proton and not be too strongly locked in a d_{π} - p_{π} interaction with the metal or, in this case, not too delocalized into the aryl ring of the ligand. The H/D exchange reaction suggested that the amido nitrogen of **4.36** may act as a nucleophile towards electrophilic species.

The reactions of **4.36** with the electrophiles trimethylsilylchloride, acetyl chloride and tosyl chloride at RT all resulted in mixtures containing amine donor complexes resulting from protonation of the amido donor, as evidenced by the appearance of NH_2 doublet signals in the 1H NMR spectrum previously observed with **4.38**. This presumably occurred due to the generation of HCl in the reaction from the electrophilic reagent, possibly with adventitious water. Rigorously dry conditions and/or the addition of NEt_3 to quench any HCl had no effect on the reaction, and pure

Chapter 4 – Synthesis and Reactivity of Complexes of Bidentate Amino/Amido-NHC Ligands

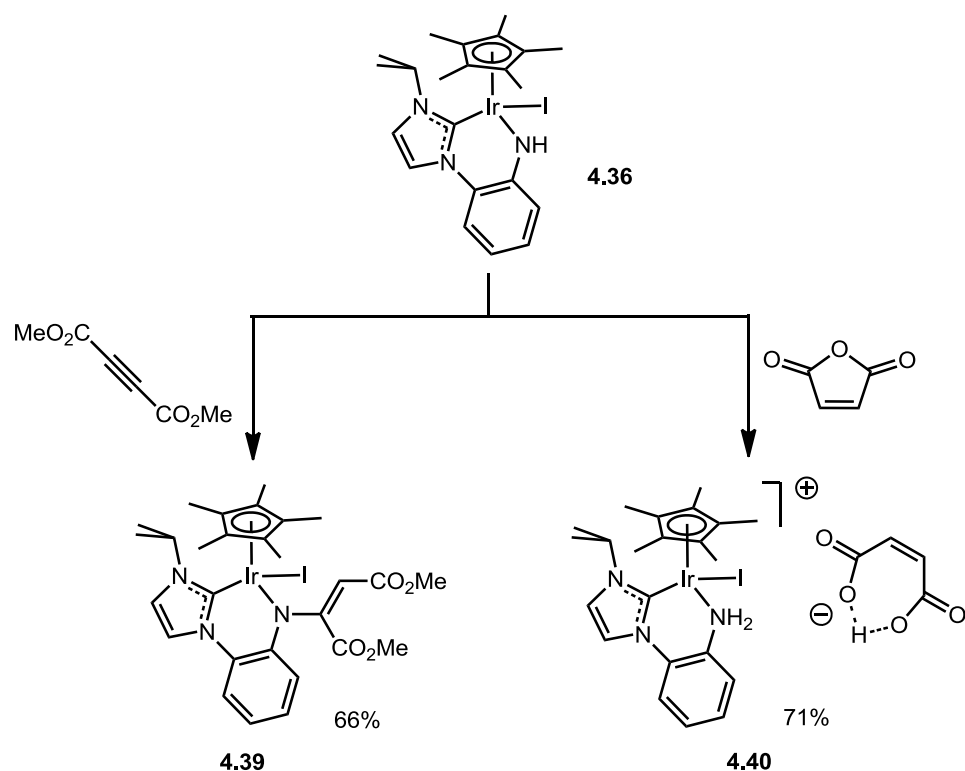
complexes were not isolated. Methyl iodide was also observed to react slowly with **4.36** at RT by ^1H NMR spectroscopy but gave an intractable mixture of products.

Electron deficient alkynes such as dimethylacetylenedicarboxylate (DMAD) are known to insert into late transition metal-amide bonds to give coordinated metal enamines, **Scheme 4.17**, with examples known for Ni,²⁷⁶ Pd,²⁷⁷ Pt,²⁷⁸ Rh,²⁷⁹ and Ru.²⁸⁰ This reaction results in formation of a C-N bond and is of interest as a step in catalytic hydroamination reactions of alkynes.²⁸¹



Scheme 4.17: Insertion of DMAD into metal-amide bonds.

The author was interested to see if iridium amido complex **4.36** would react in a similar manner with DMAD. Addition of 1 equivalent of DMAD to a solution of **4.36** in DCM at RT gave complete conversion to the unexpected product **4.39** over 1 h, **Scheme 4.18**. The analytically pure complex was isolated in 66% yield after precipitation.



Scheme 4.18: Reactions of iridium amido-NHC complex **4.36**.

ESIMS confirmed that a single molecule of DMAD had been incorporated into the product, while the ^1H NMR spectrum of **4.39** contained two prominent singlet resonances for the CO_2CH_3 protons at δ 3.61 and 3.64. A singlet resonance at δ 5.14 was initially difficult to assign, as it could belong to an NH or C=CH proton, but a HMQC spectrum gave a correlation to a ^{13}C resonance at δ 107.8, identifying it as an alkene proton. These spectral data suggested that DMAD had not inserted into the Ir-N bond of **4.36**, but had instead formally inserted into the N-H bond of the amido ligand; X-ray crystallography confirmed this (ORTEP view of **4.39** is displayed in **Figure 4.18**, selected bond lengths and angles in **Table 4.9**). The carbene resonance for **4.39** was observed at δ 156.5 in the ^{13}C NMR spectrum, similar to that for **4.36** (δ 154.6) and **4.38** (δ 156.4). The Ir-C bond length of **4.39** (2.024(5) Å) is slightly closer to that of amino complex **4.38** (2.026(9) Å) than amido complex **4.36** (1.978(9) Å), while the Ir-N

bond of **4.39** (2.118(4) Å) is slightly closer in length to that of amido complex **4.36** (2.101(7) Å) than amino complex **4.38** (2.153(7) Å). Partial double bond character is suggested by the short C-N bond lengths of both C(5)-N(1) (1.392(6) Å) and C(23)-N(1) (1.369(6) Å) of **4.39**; although these are longer than the C(5)-N(1) bond of **4.36** (1.328(11) Å), delocalisation of the nitrogen lone pair would be expected to occur into both the aryl ring and the α,β -unsaturated π -system. The sum of the angles around the secondary amido nitrogen of **4.39** (N(1)) is 356.9°, near to the 360° expected for a perfect trigonal plane as would be expected for an anionic amido ligand. The (C,N) ligand bite angle of **4.39** is the largest of the iridium complexes at 84.1°. The C(23)-C(24) bond length, at 1.337(7) Å, is consistent with that of a C=C bond (*ca.* 1.34 Å).⁴⁴ The formal insertion of methylisocyanate into the N-H bond of an iridium amido complex has been observed before;¹²⁹ also formal insertion of CO₂ and *t*-butylisocyanate into an iridium 2-azametallacyclobutane N-H bond is known.²⁸² This heterocumulene insertion has been explained as a nucleophilic attack of the amido nitrogen onto the electrophilic reagent, with migration of the NH proton onto the resultant negatively charged atom (*i.e.* conjugate addition);¹²⁹ this is consistent with the observed reaction to form **4.39**. The lack of insertion of DMAD into the Ir-N bond suggests that the alkyne does not displace the iodide ligand of **4.39**, resulting in an outer-sphere reaction; migratory insertion cannot proceed without coordination of the alkyne to the metal.

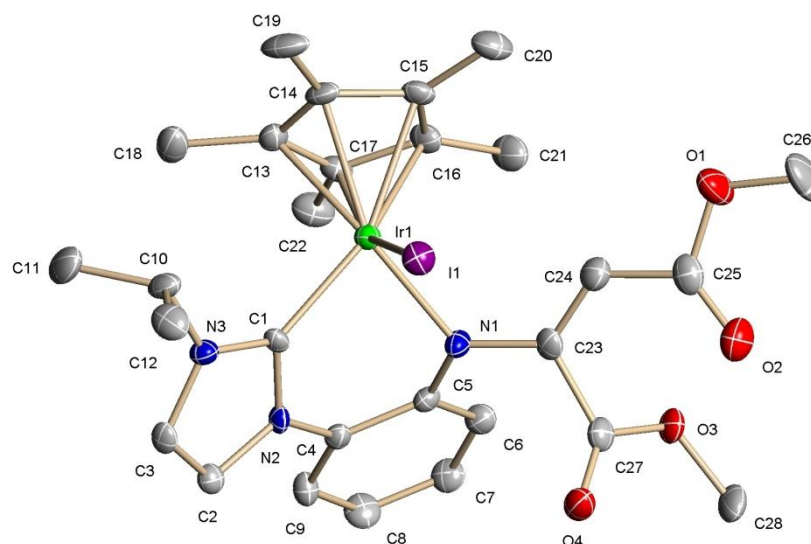


Figure 4.18: ORTEP view of **4.39**. Figure shows 50% displacement ellipsoids.

Table 4.7: Selected bond lengths (Å) and angles (°) for complexes **4.39** and **4.40**.

	4.39	4.40
Ir-C(NHC)	2.024(5)	2.016(7)
Ir-N(amide)	2.118(4)	2.137(6)
Ir-I	2.7169(6)	2.7001(7)
Ir-C(Cp*)	2.142(5)-	2.165(8)-
	2.239(5)	2.254(7)
N(1)-C(23)	1.369(6)	-
C(23)-C(24)	1.337(7)	-
C(1)-Ir-N(1)	84.11(17)	80.3
Ir-N(1)-C(5)	115.1(3)	112.0
Ir-N(1)-C(23)	123.7(3)	-
C(5)-N(1)-C(23)	118.1(4)	-

Chapter 4 – Synthesis and Reactivity of Complexes of Bidentate Amino/Amido-NHC Ligands

The reactions of some other, non-electron-deficient alkynes with **4.36** were also investigated. *Bis*-trimethylsilylacetylene showed no reactivity with **4.36** at RT or elevated temperatures, this is consistent with the electron-rich nature of this alkyne. *p*-Tolyl acetylene reacted at RT with **4.36** with > 90% conversion as judged by ^1H NMR spectroscopy. ESIMS showed a molecular ion consistent with the reaction of a single molecule of *p*-tolyl acetylene with **4.36** but both the ^1H and ^{13}C NMR spectra, with 2-dimensional NMR techniques, were unable to unambiguously identify the product of this reaction. Unfortunately no crystals suitable for X-ray crystallography for this product could be grown, and so it is not identified or characterised in this thesis.

As the amide nitrogen of **4.36** acted as a nucleophile towards DMAD, an excellent Michael acceptor, it was decided to test the reactivity of **4.36** with other Michael acceptors. No reaction was observed between **4.36** and methyl acrylate, dimethyl fumarate or dimethyl maleate at RT or elevated temperatures. **4.36** was observed to react with maleic anhydride at RT in DCM to give **4.40** with quantitative conversion, **Scheme 4.18**. **4.40** displayed two broad singlets in the ^1H NMR spectrum (δ 5.51, 8.70) which suggested an amino-coordinated complex; ESIMS showed no evidence of insertion of maleic anhydride into the NH or Ir-N bonds in the observed molecular ion peaks. X-ray crystallography confirmed the identity of **4.40**: an ORTEP view of **4.40** is displayed in **Figure 4.19**, selected bond lengths and angles in **Table 4.7**. The maleic anhydride was hydrolysed by a single molecule of water, forming a non-coordinated monoanion of maleic acid which is the counterion to the $[\text{Cp}^*\text{Ir}(\text{C},\text{NH}_2)]^+$ cation. Like **4.38**, **4.40** showed intermolecular hydrogen bonding from the NH_2 protons to the counterion. NMR spectral data of **4.40** is comparable to that of **4.38**, with the inclusion

Chapter 4 – Synthesis and Reactivity of Complexes of Bidentate Amino/Amido-NHC Ligands

of a 2H singlet at δ 6.27 in the ^1H NMR spectrum for the counterion $(\text{CO}_2)\text{CH}$ protons. The solid state structure of the cation of **4.40** is virtually identical to that of the cation of **4.38**; Ir-C (**4.40**: 2.016(7); **4.38**: 2.026(9) Å), Ir-N (**4.40**: 2.137(6); **4.38**: 2.153(6) Å) and Ir-I (**4.40**: 2.7001(7); **4.38**: 2.7082(9) Å) bond lengths and the (C,N) ligand bite angle (**4.40**: 80.3°; **4.38**: 80.0°) are similar. As adventitious water appeared to be the source of **4.40**, the reaction was repeated under rigorously dry conditions; no reaction was observed until the mixture was exposed to moist air, whereupon the reaction proceeded immediately to **4.40**. The source of maleic anhydride was found to be pure, with no observed traces (by ^1H NMR spectroscopy) of maleic acid which could catalyse hydrolysis. Stirring maleic anhydride in wet DCM showed no significant hydrolysis over 24 h, suggesting that **4.36** acts to promote the hydrolysis of maleic anhydride. It appears most likely that the amido nitrogen of **4.36** acts as a base to generate reactive hydroxide from water.

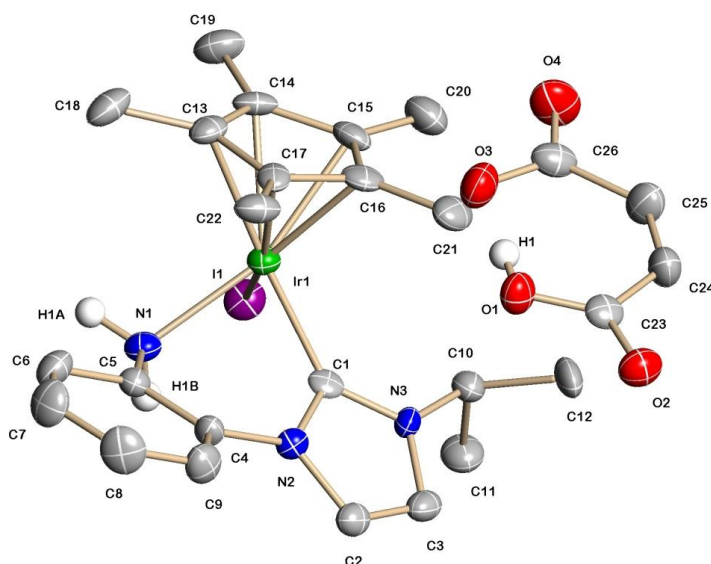


Figure 4.19: ORTEP view of **4.40**. Figure shows 50% displacement ellipsoids.

4.3: Conclusions

In this chapter, the coordination chemistry of amine-functionalised NHC ligands, generated from precursor imidazolium salts **2.28a** and **2.28b** was investigated, with a variety of transition metal salts using several different strategies.

PEPPSI-type (C,NHAr) complexes of Pd (**4.22**) and Pt (**4.23**), where the (C,N) ligand coordinates in a monodentate fashion through the NHC donor, were synthesised by a facile procedure from imidazolium salt **2.28a**, K₂CO₃ and PdCl₂ or PtCl₂(cod) in a refluxing pyridine suspension. **4.22** and **4.23** proved highly stable to air/moisture and were isolated by chromatography in good to moderate yields (**4.22**: 89%, **4.23** 47%). **4.22** could be converted to the chloro analogue **4.25** in 86% yield by treatment with AgNO₃ followed by brine; the pyridine ligand of **4.22** proved labile in the presence of PPh₃, affording **4.26** in 85% yield. Treatment of **4.22** with aqueous KOH in 1,4-dioxane afforded the amido-NHC dimer complex **4.27**, featuring bridging hydroxide ligands, in 63% yield. The analogous reaction between **4.23** and KOH under the same conditions did not proceed to give the corresponding dimeric Pt amido complex. Attempts to make a PEPPSI-type complex of the (C,NH₂) ligand led to intractable mixtures. Nevertheless, the complex **4.28** was synthesised from imidazolium salt **2.28b** and [Pd(allyl)Cl₂]₂ using Ag₂O in 85% yield, *via* transmetallation from an intermediate silver carbene.

Two PEPPSI-type complexes of the unfunctionalised carbene IMes (**4.30**, **4.31**) were also synthesised as standard precatalysts for studies into direct arylation, which will be discussed in Chapter 5.

Chapter 4 – Synthesis and Reactivity of Complexes of Bidentate Amino/Amido-NHC Ligands

Half-sandwich complexes of (C,NR) ligands were also synthesised, for potential applications in bifunctional catalysis. It was found that reacting imidazolium salt **2.28a** and a base in the presence of $[\text{Ru}(p\text{-cymene})\text{Cl}_2]_2$ gave intractable mixtures of products; the analogous reactions with $[\text{IrCp}^*\text{Cl}_2]_2$ and $[\text{RhCp}^*\text{Cl}_2]_2$ gave the cyclometallated (C,C) complexes **4.32** and **4.33** in 40% and 61% yields respectively, when NaOAc was used as the base. Reactions of $[\text{M}(\text{arene})\text{Cl}_2]_2$ and base with imidazolium salt **2.28b** were also investigated. $[\text{Ru}(p\text{-cymene})\text{Cl}_2]_2$ reacted to form **4.34** in 51% yield using Ag_2O as a base in a transmetallation strategy; NaOAc or *t*-BuONa gave the same product but in lower conversions. Reaction of $[\text{RhCp}^*\text{Cl}_2]_2$ with **2.28b** and *t*-BuONa gave the amino complex **4.35** in 45% yield, while the analogous reaction between $[\text{IrCp}^*\text{Cl}_2]_2$, **2.28b** and *t*-BuONa gave the amido complex **4.36** in 65% yield, reflecting the difference in basicity of the coordinated amino group on Rh and Ir. Attempts to form the amido complex **4.37** from deprotonation of **4.35** with NaH were successful, but the resulting **4.37** was extremely sensitive to hydrolysis and is not fully characterized. The iridium amino-NHC complex **4.38** was accessible by protonation of **4.36** with TFA.

The amido ligand of **4.36** proved reactive as both a base and a nucleophile. **4.36** was protonated by trace HCl from TMSCl, TosCl and AcCl, seemingly in preference to any nucleophilic reactivity. No reaction was observed between **4.36** and the electrophiles *bis*-trimethylsilylacetylene, methyl acrylate, dimethyl fumarate or dimethyl maleate; **4.36** and methyl iodide reacted to form intractable mixtures of products. **4.36** did show nucleophilic reactivity towards DMAD, resulting in complete conversion to **4.39**, with a formal insertion of a single alkyne into the amido N-H bond. The analogous

Chapter 4 – Synthesis and Reactivity of Complexes of Bidentate Amino/Amido-NHC Ligands

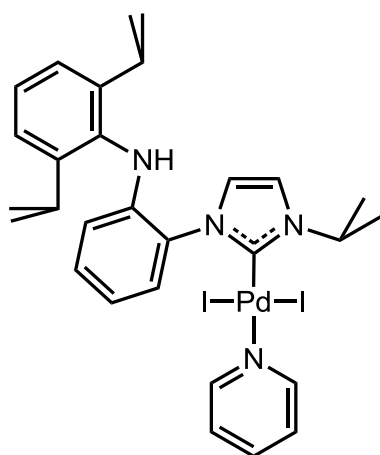
reaction with *p*-tolyl acetylene led to a single major product that proved impossible to fully characterise. Finally, **4.36** appeared to promote the hydrolysis of maleic anhydride, resulting in the isolation of **4.40**.

The next chapter will discuss investigations into bifunctional catalysis, using the complexes described in this chapter as catalysts/precatalysts in transfer hydrogenation and direct arylation of heterocycles.

4.4: Experimental

All reactions were performed under dry, oxygen free nitrogen using standard Schlenk techniques unless otherwise stated; however, all compounds were air stable once isolated. Anhydrous solvents were obtained either by distillation from an appropriate drying agent, from an Innovative Technology PureSolv MD 7 Solvent Purification System or purchased from Sigma Aldrich. Deuterated solvents (DCM-d₂, THF-d₈, pyridine-d₆, benzene-d₆) were purchased from Cambridge Isotope Laboratories. All other reagents were obtained from Sigma-Aldrich, Johnson Matthey or Alfa Aesar and used as supplied. NMR spectra were recorded on a Bruker DPX300, DRX400 or AV500 spectrometer; chemical shifts have been referenced to the residual protonated solvent peak and are reported in ppm, *J* values are given in Hz. Electrospray mass spectra were recorded on a Micromass Quattro LC mass spectrometer with acetonitrile as solvent; FAB and HR mass spectra were recorded on a Kratos Concept mass spectrometer using NBA as a matrix.

[C,NHR]PdI₂py (4.22)



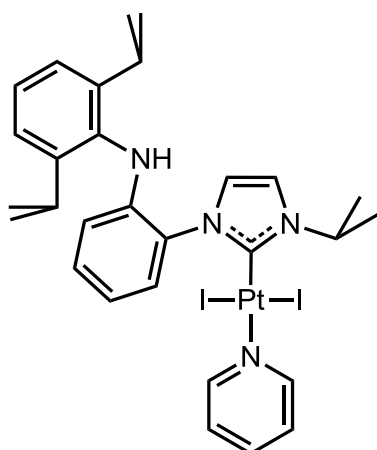
Imidazolium salt **2.28a** (0.150 g, 0.307 mmol), PdCl₂ (0.050 g, 0.28 mmol), K₂CO₃ (0.193 g, 1.40 mmol) and KI (0.232 g, 1.40 mmol) were suspended in pyridine (10 mL) and heated at 100 °C for 18 h. After cooling to RT, the reaction mixture was diluted with DCM (30 mL), filtered through Celite and the volatiles removed *in vacuo*. Purification by flash column chromatography

(17% EtOAc/pet. ether) gave **4.22** as a yellow-orange solid (0.199 g, 89%) m.p. 122-123

Chapter 4 – Synthesis and Reactivity of Complexes of Bidentate Amino/Amido-NHC Ligands

$^{\circ}\text{C}$, $R_f = 0.18$ (17% EtOAc/pet. ether). Crystals suitable for structure determination by X-ray diffraction were obtained by diffusion of hexane into a saturated DCM solution of **4.22**. δ_{H} (300 MHz, CD_2Cl_2) 1.11 (12H, br d, $J = 6.8$, $\text{CH}(\text{CH}_3)_2$), 1.62 (6H, d, $J = 6.8$, $\text{NCH}(\text{CH}_3)_2$), 3.15 (1H, br, $\text{CH}(\text{CH}_3)_2$), 3.48 (1H, br, $\text{CH}(\text{CH}_3)_2$), 5.27 (1H, s, NH), 5.79 (1H, sept, $J = 6.8$, $\text{NCH}(\text{CH}_3)_2$), 6.32 (1H, d, $J = 8.2$, ArH), 6.94 (1H, app t, $J = 7.6$, ArH), 7.17-7.35 (8H, m), 7.74 (1H, t, $J = 7.6$, pyH), 7.16 (1H, d, $J = 7.9$, ArH), 8.88 (2H, br d, $J = 4.9$, pyH); δ_{C} (125.8 MHz, C_6D_6) 21.9 ($\text{NCH}(\text{CH}_3)_2$), 22.3 ($\text{CH}(\text{CH}_3)_2$), 22.7 ($\text{CH}(\text{CH}_3)_2$), 25.0 ($\text{CH}(\text{CH}_3)_2$), 25.5 ($\text{CH}(\text{CH}_3)_2$), 28.5 ($\text{CH}(\text{CH}_3)_2$), 28.7 ($\text{CH}(\text{CH}_3)_2$), 53.9 ($\text{NCH}(\text{CH}_3)_2$), 116.1, 117.7, 118.8, 123.8, 124.2, 124.9, 125.1, 127.0, 127.6, 130.4, 131.5, 135.4, 136.8, 144.0, 146.6 (Ar/py C), 147.3 (N_2CPd), 148.0 (Ar C), 154.1 (py CH). $\nu_{\text{max}}/\text{cm}^{-1}$ (solid) 3386 w (NH), 2965 m, 2865 w, 1603 m, 1506 m, 1444 m, 1430 m, 1362 w, 1326 m, 1300 m, 1240 w, 1210 m, 1111 w, 1070 w, 1045 w, 1020 w, 957 w, 937 w, 880 w, 803 m, 754 s, 726 m, 685 s. m/z (ESI) 466 (100 % $[\text{M-I-HI-py}]^+$); 507 (70 % $[\text{M-I-HI-py+MeCN}]^+$). Anal. Calcd. for $\text{C}_{29}\text{H}_{36}\text{I}_2\text{N}_4\text{Pd}$: C, 43.49; H, 4.53; N, 7.00. Found C, 43.51; H, 4.45; N, 7.12%.

[C,NHR]PtI₂py (4.23)

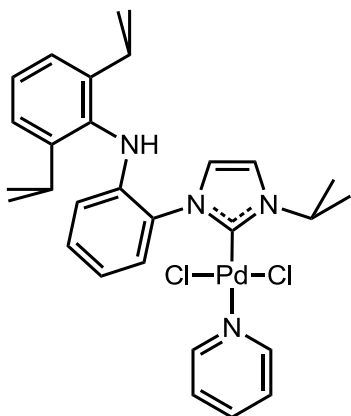


Imidazolium salt **2.28a** (0.400 g, 0.818 mmol), K_2PtCl_4 (0.309 g, 0.744 mmol), K_2CO_3 (0.513 g, 3.72 mmol) and KI (0.617 g, 3.72 mmol) were suspended in pyridine (15 mL) and heated at $100\text{ }^{\circ}\text{C}$ for 48 h. After cooling to RT, the reaction mixture was diluted with DCM (30

Chapter 4 – Synthesis and Reactivity of Complexes of Bidentate Amino/Amido-NHC Ligands

mL), filtered through Celite and the volatiles removed *in vacuo*. Purification by flash column chromatography (13% EtOAc/pet. ether) followed by crystallisation from Et₂O/pentane gave **4.23** (0.313 g, 47%) as yellow crystals m.p. 206-208 °C (dec.), R_f = 0.3 (13% EtOAc/pet. ether). Crystals suitable for structure determination by X-ray diffraction were obtained by slow evaporation of a saturated DCM solution of **4.23**. δ_{H} (300 MHz, CD₂Cl₂) 1.11 (12H, d, *J* = 6.5, CH(CH₃)₂), 1.60 (6H, d, *J* = 6.7, NCH(CH₃)₂), 3.10 (1H, br, CH(CH₃)₂), 3.53 (1H, br, CH(CH₃)₂), 5.99 (1H, sept, *J* = 6.7, NCH(CH₃)₂), 6.30 (1H, d, *J* = 8.2, ArH), 6.90 (1H, app t, *J* = 7.6, ArH), 7.14-7.33 (8H, m, CH), 6.73 (1H, app t, *J* = 7.6, pyH), 8.01 (1H, d, *J* = 7.9, ArH), 8.90 (2H, d, *J* = 5.3, pyH); δ_{C} (125.8 MHz, CD₂Cl₂) 22.4 (NCH(CH₃)₂), 22.8 (CH(CH₃)₂), 24.4 (CH(CH₃)₂), 25.0 (CH(CH₃)₂), 25.5 (CH(CH₃)₂), 28.2 (CH(CH₃)₂), 28.8 (CH(CH₃)₂), 53.1 (NCH(CH₃)₂), 115.1, 117.3, 117.9, 124.2, 124.6, 125.2, 126.7, 127.6, 129.9, 131.2, 135.1, 136.7, 137.9 (Ar/py C), 143.6 (N₂Cpt), 147.2, 148.2 (Ar C), 154.1 (py C). ν_{max} /cm⁻¹ (solid) 3389 w (NH), 2966 m, 2866 w, 1605 m, 1445 m, 1416 m, 1370 w, 1328 m, 1300 m, 1240, 1210 m, 1117 w, 1071 w, 1043 w, 1022 w, 958 w, 938 w, 883 w, 800 m, 758 s, 730 m, 693 s. *m/z* (ESI) 555 (100 % [M-I-HI-py]⁺); 634 (10 % [M-I-HI-py+MeCN]⁺). Anal. Calcd. for C₂₉H₃₆I₂N₄Pt: C, 39.16; H, 4.08; N, 6.30. Found C, 39.27; H, 4.17; N, 6.18%.

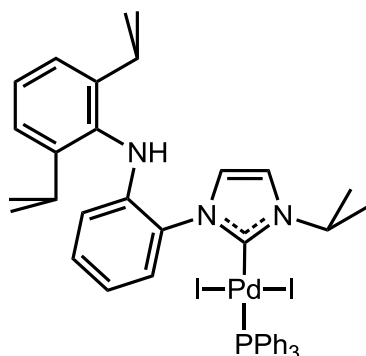
[C,NHR]PdCl₂py (4.25)



A solution of **4.22** (0.100 g, 0.125 mmol) in 15 mL DCM was added to a solution of AgNO₃ (12 mL, 0.25 M) and stirred vigorously for 30 min at RT. The resulting purple-brown emulsion was allowed to separate and the organic layer collected. The organic layer was then added to saturated brine (15 mL) and stirred vigorously for 24 h.

The brown aqueous layer was separated and dried (MgSO₄), and solvent removed in vacuo to give **4.25** as a red brown solid (0.066 g, 86%), m.p. 210 °C (dec.). δ_{H} (400 MHz, CDCl₃) 1.09 (12H, br d, $J = 6.4$, CH(CH₃)₂), 1.67 (6H, d, $J = 6.8$, NCH(CH₃)₂), 3.09 (1H, br, CH(CH₃)₂), 3.46 (1H, br, CH(CH₃)₂), 5.51 (1H, s, NH), 6.01 (1H, sept, $J = 6.8$, NCH(CH₃)₂), 6.36 (1H, d, $J = 8.2$, ArH), 6.90 (1H, app t, $J = 7.6$, ArH), 7.18 (5H, m), 7.23 (1H, d, $J = 7.6$, ArH), 7.28 (2H, m, pyH), 7.71 (2H, m, pyH, NCHCHN), 8.88 (2H, m, pyH); δ_{C} (125 MHz, CDCl₃) 22.5 (NCH(CH₃)₂), 23.4 (CH(CH₃)₂), 24.8 (CH(CH₃)₂), 53.4 (NCH(CH₃)₂), 115.2, 117.8, 118.4 (Ar CH), 123.9-124.3 (br, Ar CH), 124.4, 124.8 (Ar CH), 126.1 (Ar C), 127.1, 130.2, 130.4 (Ar CH), 135.0 (Ar C), 138.0 (Ar CH), 144.0 (Ar C), 150.8 (NCN), 151.4, (Ar CH). m/z (ESI) 502 (100 % [M-Cl-py]⁺); 543 (30 % [M-Cl-py+MeCN]⁺); 581 (15 % [M-Cl]⁺); 622 (35 % [M-Cl+MeCN]⁺). Anal Calcd. for: C₂₉H₃₆Cl₂N₄Pd: C, 56.37; H, 5.87; N, 9.07; Found C, 56.46; H, 5.91; N, 9.02%.

[C,NHR]PdI₂PPh₃ (4.26)

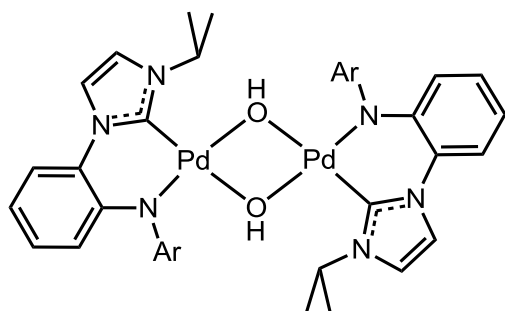


4.22 (0.100 g, 0.125 mmol) and PPh₃ (0.049 g, 0.19 mmol) were stirred in DCM (7 mL) at RT. The reaction was monitored by TLC (50% EtOAc/pet. ether.), and judged to be complete after 2 h. Solid residues were removed by filtration, and solvent removed *in vacuo* to

give a crude golden orange solid which was placed under high-vacuum to remove residual pyridine. The crude product was then recrystallised from Et₂O/pentane (1:2) at 3 °C to give **4.26** as orange crystals (0.105 g, 85%) m.p. 222-223 °C, R_f = 0.78 (50% EtOAc/pet. ether). These crystals were suitable for structure determination by X-ray diffraction.

δ_{H} (400 MHz, CD₂Cl₂) 1.05 (12H, br s, CH(CH₃)₂), 1.59 (6H, d, *J* = 6.7, NCH(CH₃)₂), 3.26 (2H, br s, CH(CH₃)₂), 5.24 (1H, s, NH), 5.39 (1H, sept, *J* = 6.7, NCH(CH₃)₂), 6.35 (1H, d, *J* = 8.2, ArH), 6.92 (1H, app t, *J* = 7.5, ArH), 7.18-7.42 (15H, m, ArH), 7.50-7.58 (6H, m, ArH), 8.12 (1H, d, *J* = 8.2, ArH); δ_{C} (125 MHz, CD₂Cl₂) 22.6 (NCH(CH₃)₂), 25.1 (CH(CH₃)₂), 28.5 (CH(CH₃)₂), 53.8 (NCH(CH₃)₂), 115.7, 118.2, 118.3, 118.4, 124.3, 125.1, 126.5, 127.5, 128.0, 128.1, 130.1, 130.4, 131.2, 133.0, 133.5, 135.2, 135.7, 135.8, 143.8 (Ar C), 156.8 (NCN); *m/z* (ESI) 856 (100%, [M-I]⁺), 897 (50%, [M-I+MeCN]⁺) Anal Calcd. for: C₄₂H₄₆I₂N₃PPd: C, 51.26; H, 4.71; N, 4.27; Found C, 51.19; H, 4.83; N, 4.22%.

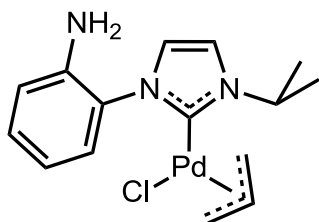
{[C,NR]Pd(μ -OH)}₂ (4.27)



Ar = 2,6-diisopropylphenyl

A solution of complex **4.22** (0.100 g, 0.125 mmol) in 1,4-dioxane (18 mL) was stirred vigorously with a solution of KOH (0.350g, 6.25 mmol) in H₂O (3 mL) at 40 °C for 24 h. After cooling to RT, the volatiles were removed *in vacuo*. The crude solid was re-dissolved in DCM (15 mL), dried (MgSO₄) and filtered through Celite. Removing the solvent under reduced pressure gave **4.27** (0.076 g, 63%) as an orange/red powder m.p. 190 °C (dec.). Crystals suitable for structure determination by X-ray diffraction were obtained by slow evaporation of an Et₂O/pentane solution of **4.27**. δ_{H} (300 MHz, CD₂Cl₂) -3.97 (2H, s, OH), 0.96 (12H, d, J = 6.9, CH(CH₃)₂), 1.11 (12H, d, J = 6.7, NCH(CH₃)₂), 1.46 (12H, d, J = 6.9, CH(CH₃)₂), 3.49 (4H, sept, J = 6.9, CH(CH₃)₂), 5.17 (2H, sept, J = 6.7, NCH(CH₃)₂), 5.80 (2H, d, J = 8.1, CH), 6.23 (2H, app t, J = 7.7, CH), 6.63 (2H, app t, J = 8.1, CH), 7.02 (2H, d, J = 2.2, NCHCHN), 7.08 (6H, br s, 2,6-ⁱPr₂C₆H₃), 7.22 (2H, d, J = 7.7, CH), 7.50 (2H, d, J = 2.2, NCHCHN); δ_{C} (75 MHz, C₆D₆) 23.8 (CH(CH₃)₂), 24.7 (CH(CH₃)₂), 25.5 (CH(CH₃)₂), 28.1 (CH(CH₃)₂), 50.1 (NCH(CH₃)₂), 110.8, 117.4, 117.7, 117.8, 118.9 (ArCH), 122.9 (ArC), 124.7, 125.2, 126.7 (ArCH), 144.7, 145.7, 147.4, 147.5 (4°C). ν_{max} /cm⁻¹ (solid) 3601 w (OH), 2961 m, 2863 w, 1598 m, 1493 s, 1455 m, 1426 m, 1410 m, 1356 s, 1337 s, 1284 m, 1221 m, 1161 w, 1124 w, 1081 w, 1055 m, 952 w, 850 s, 825 m, 801 m, 767 m, 735 s, 723 s, 713 s, 693 m, 672 s. m/z (ESI, 25 V) 466 (100% [(C,N)Pd]⁺), 500 (100% [(C,N)Pd(OH)₂]⁻). Anal. Calcd. for C₄₈H₆₂N₆O₂Pd₂: C, 59.56; H, 6.46; N, 8.68. Found C, 59.47; H, 6.30; N, 8.73 %.

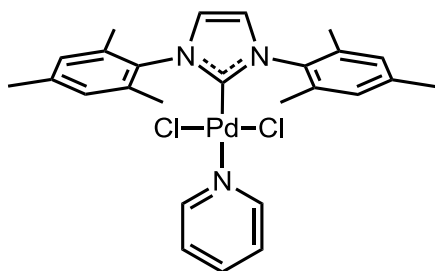
[C,NH₂]PdCl(allyl) (4.28)



Imidazolium salt **2.28b** (0.072 g, 0.22 mmol) and Ag₂O (0.026 g, 0.11 mmol) were stirred in 5 mL DCM at 35 °C for 15 h in the absence of light. NaCl (0.130 g, 2.20 mmol) and (PdCl(allyl))₂ (0.040 g, 0.11 mmol) were then added and the reaction mixture stirred for another 15 h. The crude mixture was filtered through Celite, concentrated to *ca.* 1 mL and pentane added to precipitate **4.28** as a white solid (0.071 g, 85%) m.p. 98 °C (dec.). **4.28** is unstable in solution for long periods of time. Crystals suitable for structure determination by X-ray diffraction were obtained by diffusion of pentane into a saturated DCM solution of **4.28**.

δ_{H} (400 MHz, CD₂Cl₂) 1.51 (6H, br, CH(CH₃)₂), 2.00 (1H, d, *J* = 11.8, *anti* CHH), 3.07 (1H, d, *J* = 13.6, *anti* CHH), 3.21 (1H, d, *J* = 4.9, *syn* CHH), 4.15 (1H, d, *J* = 7.6, *syn* CHH), 4.36 (2H, s, NH₂), 5.01 (1H, m, *meso* CH), 5.22 (1H, sept, *J* = 6.8, CH(CH₃)₂), 6.79 (1H, app t, *J* = 7.6, ArH), 6.86 (1H, d, *J* = 8.0, ArH), 7.11 (2H, m, NCHCHN + ArH), 7.20 (2H, m, NCHCHN + ArH); δ_{C} (125 MHz, CD₂Cl₂) 23.6 (CH(CH₃)₂), 49.5 (allyl CH₂), 53.3 (CH(CH₃)₂), 71.1 (allyl CH₂), 115.2 (allyl CH), 117.8, 117.9, 118.7, 123.4 (Ar CH), 127.7 (Ar C), 127.9, 130.1 (Ar CH), 143.4 (Ar C), 180.5 (NCN). *m/z* (ESI) 348 (100%, [M-Cl]⁺). Anal. Calcd. for: C₁₅H₂₂ClN₃Pd: C, 46.89; H, 5.25; N, 10.94; Found C, 44.72; H, 5.08; N, 10.18%.

IMesPdCl₂Py (4.30)

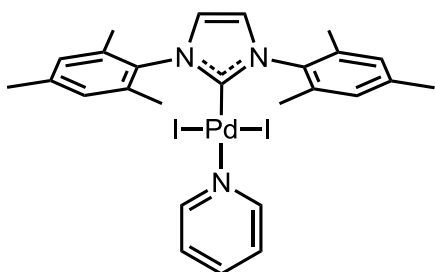


Imidazolium salt **IMes.HCl (4.29)** (1.057 g, 3.100 mmol), PdCl₂ (0.531 g, 3.00 mmol) and K₂CO₃ (2.070 g, 15.00 mmol) were suspended in pyridine (10 mL) and heated at 100 °C for 18 h.

After cooling to RT, the reaction mixture was diluted with DCM (30 mL), filtered through Celite and the volatiles removed *in vacuo*. 3 precipitations from DCM/Hexane gave **4.30** (1.312 g, 78%) as a yellow powder m.p. 240°C (dec.). Crystals suitable for structure determination by X-ray diffraction were obtained by diffusion of pentane into a saturated DCM solution of **4.30**.

δ_{H} (400 MHz, CDCl₃) 2.36 (12H, s, *o*-CH₃), 2.37 (6H, s, *p*-CH₃), 7.05 (4H, s, ArH), 7.06 (2H, s, NCHCHN), 7.09 (2H, m, pyH), 7.54 (2H, t, *J* = 7.6, pyH), 8.54 (2H, m, pyH); δ_{C} (125 MHz, CD₂Cl₂) 19.2 (*o*-CH₃), 21.3 (*p*-CH₃), 124.0 (NCHCHN), 124.3 (py CH), 129.4 (Ar CH), 135.3, 136.5 (Ar C), 137.5 (py CH), 139.3 (Ar C), 151.6 (py CH), 153.0 (NCN). *m/z* (ESI) 541 (100%, [M-Cl-py+MeCN+3H₂O]⁺), 505 (85%, [M-Cl-py+MeCN+H₂O]⁺), 566 (40%, [M-Cl+MeCN]⁺). Anal. Calcd. for: C₂₆H₂₉Cl₂N₃Pd: C, 55.68; H, 5.21; N, 7.49; Found C, 55.77; H, 5.14; N, 7.36%.

IMesPdI₂Py (4.31)



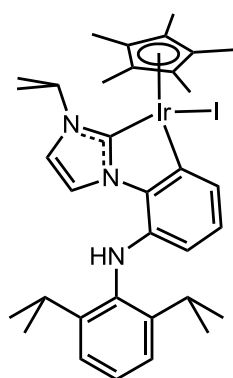
Imidazolium salt **IMes.HCl (4.39)** (1.057 g, 3.100 mmol), PdCl₂ (0.531 g, 3.00 mmol), K₂CO₃ (2.070 g, 15.00 mmol) and KI (2.490 g, 15.00 mmol)

Chapter 4 – Synthesis and Reactivity of Complexes of Bidentate Amino/Amido-NHC Ligands

were suspended in pyridine (10 mL) and heated at 100 °C for 18 h. After cooling to RT, the reaction mixture was diluted with DCM (30 mL), filtered through Celite and the volatiles removed *in vacuo*. 3 precipitations from DCM/Hexane gave **4.31** (2.150 g, 92%) as an orange powder m.p. 260°C (dec.). Crystals suitable for structure determination by X-ray diffraction were obtained by diffusion of pentane into a saturated DCM solution of **4.31**.

δ_{H} (400 MHz, CDCl_3) 2.38 (6H, s, *p*- CH_3), 2.46 (12H, s, *o*- CH_3), 7.03-7.05 (6H, br s, ArH + NCHCHN), 7.10 (2H, m, pyH), 7.51 (2H, t, $J = 7.7$, pyH), 8.47 (2H, m, pyH); δ_{C} (125 MHz, CD_2Cl_2) 20.4 (*p*- CH_3), 21.1 (*o*- CH_3), 123.1 (py CH), 123.9, 128.6 (Ar CH / NCHCHN), 135.0, 135.1 (Ar C), 136.1 (py CH), 138.2 (Ar C), 151.8 (NCN), 152.7 (py CH). m/z (ESI) 619 (100%, $[\text{M-I}]^+$), 595 (55%, $[\text{M-I-py+MeCN+H}_2\text{O}]^+$), 578 (30%, $[\text{M-I-py+MeCN}]^+$), 655 (10%, $[\text{M-I+MeCN}]^+$). Anal. Calcd. for: $\text{C}_{26}\text{H}_{29}\text{I}_2\text{N}_3\text{Pd}$ C, 41.99; H, 3.93; N, 5.65; Found C, 41.87; H, 3.97; N, 5.75%.

Cp*Ir(C,C)I (4.32)

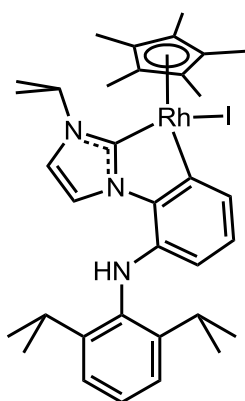


A suspension of $[\text{Cp}^*\text{IrCl}_2]_2$ (0.040 g, 0.050 mmol) and NaOAc (0.016 g, 0.20 mmol) in DCM (3 mL) were stirred at room temperature for 10 min. Imidazolium salt **2.28a** (0.048 g, 0.10 mmol) was then added and the mixture stirred for a further 15 h. After this time, a saturated solution of aq. KI (3 mL) was added, and the mixture stirred vigorously for 3 h. The organic layer was separated, dried (MgSO_4) and concentrated *in vacuo*. Purification by flash column

Chapter 4 – Synthesis and Reactivity of Complexes of Bidentate Amino/Amido-NHC Ligands

chromatography (DCM) gave **4.32** (0.050 g, 61%) as a yellow-orange solid m.p. 218-220 °C, $R_f = 0.67$ (DCM). Crystals suitable for structure determination by X-ray diffraction were obtained from an Et₂O/pentane solution of **4.32** at 3 °C. δ_H (400 MHz, CD₂Cl₂) δ 0.96 (3H, d, $J = 6.9$, CHCH₃), 1.13 (3H, d, $J = 6.9$, CHCH₃), 1.15 (3H, d, $J = 6.9$, CHCH₃), 1.17 (3H, d, $J = 6.9$, CHCH₃), 1.53 (3H, d, $J = 6.9$, NCHCH₃), 1.66 (3H, d, $J = 6.9$, NCHCH₃), 1.86 (15H, s, η^5 -C₅Me₅), 3.04 (1H, sept, $J = 6.9$, CHCH₃), 3.18 (1H, sept, $J = 6.9$, CHCH₃), 4.85 (2H, m, NCHCH₃ + NH), 6.00 (1H, d, $J = 7.9$, ArH), 6.68 (1H, app t, $J = 7.7$, ArH), 7.08 (1H, d, $J = 2.2$, NCHCHN), 7.23 – 7.15 (3H, m, 2,6-*i*PrC₆H₃), 7.27 (1H, d, $J = 7.5$, ArH), 8.39 (1H, d, $J = 2.2$, NCHCHN); δ_C (125 MHz, CD₂Cl₂) δ 10.3 (η^5 -C₅Me₅), 22.9, 23.3, 23.8, 24.5, 24.9, 25.1(CHCH₃), 28.3, 28.4 (2,6-C₆H₃-(CH(CH₃)₂)₂), 52.3 (NCH(CH₃)₂), 92.1 (η^5 -C₅Me₅), 115.0 (ArCH), 115.3 (NHC-CH), 119.4 (NHC-CH), 124.1, 124.2, 125.0, 125.3, 132.6, 134.3 (ArCH), 137.8, 138.9, 142.3, 143.5, 144.4 (ArC), 163.6 (N₂C-Ir); m/z (ESI) 727 (20%, [M-I+MeCN]⁺), 686 (15%, [M-I]⁺), 362 (100%, [(C,C)+2H]⁺); Anal. Calcd. for C₃₄H₄₅IrN₃: C, 50.11; H, 5.57; N, 5.16. Found C, 50.20; H, 5.48; N, 5.08%.

Cp*Rh(C,C)I (4.33)

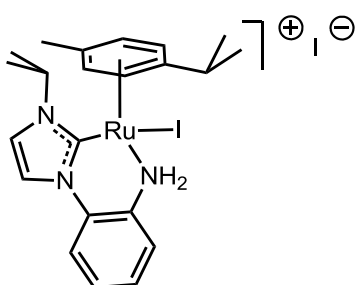


A suspension of [Cp*RhCl₂]₂ (0.100 g, 0.178 mmol) and NaOAc (0.052 g, 0.63 mmol) in DCM (5 mL) were stirred at room temperature for 10 min. Imidazolium salt **2.28a** (0.158 g, 0.324 mmol) was then added and the mixture stirred for 5 days. The mixture was then filtered through celite and evaporated to dryness. Purification by flash column chromatography (DCM) gave **4.33** (0.091 g, 40%) as a yellow-orange solid m.p. 230 °C (dec.), $R_f = 0.60$ (DCM).

Chapter 4 – Synthesis and Reactivity of Complexes of Bidentate Amino/Amido-NHC Ligands

Crystals suitable for structure determination by X-ray diffraction were obtained from DCM/hexane. δ_{H} (400 MHz, CDCl_3) δ 0.99 (3H, d, $J = 6.9$, CHCH_3), 1.10 (3H, d, $J = 6.8$, CHCH_3), 1.16 (3H, d, $J = 6.8$, CHCH_3), 1.17 (3H, d, $J = 6.9$, CHCH_3), 1.56 (3H, d, $J = 6.9$, NCHCH_3), 1.67 (3H, d, $J = 6.9$, NCHCH_3), 1.82 (15H, s, $\eta^5\text{-C}_5\text{Me}_5$), 3.04 (1H, sept, $J = 6.9$, CHCH_3), 3.13 (1H, sept, $J = 6.8$, CHCH_3), 4.78 (1H, s, NH), 4.88 (1H, sept, $J = 6.9$, NCHCH_3), 6.07 (1H, d, $J = 7.8$, ArH), 6.73 (1H, app t, $J = 7.7$, ArH), 7.04 (1H, d, $J = 2.1$, NCHCHN), 7.18 (3H, m, ArH), 7.35 (1H, d, $J = 7.4$, ArH), 8.40 (1H, d, $J = 2.2$, NCHCHN); δ_{C} (125 MHz, CDCl_3) δ 10.5 ($\eta^5\text{-C}_5\text{Me}_5$), 22.7, 23.3, 23.8, 24.3, 24.8, 24.9 (CHCH_3), 27.9, 28.1 ($2,6\text{-C}_6\text{H}_3\text{-(CH(CH}_3)_2)_2$), 52.1 ($\text{NCH(CH}_3)_2$), 98.0 (d, $J_{\text{Rh-C}} = 6$, $\eta^5\text{-C}_5\text{Me}_5$), 115.2 (ArCH), 115.6 (NHC-CH), 119.3 (NHC-CH), 123.8, 123.9, 124.5, 124.9, 133.1, 134.1, 136.5 (ArCH), 138.2, 142.7, 144.1, (ArC), 158.3 (d, $J_{\text{Rh-C}} = 40$, ArC–Rh), 163.6 (d, $J_{\text{Rh-C}} = 63$, $\text{N}_2\text{C-Rh}$); m/z (ESI) 726 (80%, $[\text{M}+\text{H}]^+$), 598 (100%, $[\text{M}-\text{I}]^+$); Anal. Calcd. for $\text{C}_{34}\text{H}_{45}\text{IN}_3\text{Rh}$: C, 56.28; H, 6.25; N, 5.79. Found C, 56.39; H, 6.19; N, 5.88.

$[(p\text{-cymene})\text{Ru}(\text{C},\text{NH}_2)\text{I}]\text{I}$ (4.34)

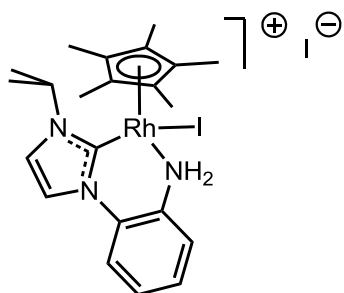


A suspension of $[(p\text{-cymene})\text{RuCl}_2]_2$ (0.090 g, 0.15 mmol), imidazolium salt **2.28b** (0.099 g, 0.30 mmol) and Ag_2O (0.036 g, 0.16 mmol) in DCM (20 ml) was stirred for 32 h at 33 °C in the dark. The solvent was removed *in vacuo*, and then the crude mixture was dissolved in acetone (20 mL). KI (0.498 g, 3.00 mmol) was added to the solution, which was then heated at reflux for 1 h. The solvent was removed *in vacuo* and the crude solid redissolved in DCM (20 mL) filtered through Celite, and then concentrated under vacuum. Purification by flash column

Chapter 4 – Synthesis and Reactivity of Complexes of Bidentate Amino/Amido-NHC Ligands

chromatography (gradient of DCM to 50% acetone/DCM) gave **4.34** (0.105 g, 51%) as a dark green/blue solid m.p. 200 °C (dec.). Crystals suitable for structure determination by X-ray diffraction were obtained by diffusion of Et₂O into a saturated CHCl₃ solution of **4.34**. δ_{H} (500 MHz, CD₂Cl₂) δ 0.90 (3H, d, $J = 6.9$, *p*-cymene CHCH₃), 0.92 (3H, d, $J = 6.9$, *p*-cymene CHCH₃), 1.56 (3H, d, $J = 6.7$, NCHCH₃), 1.58 (3H, d, $J = 6.7$, NCHCH₃), 2.06 (3H, s, *p*-cymene CH₃), 2.10 (1H, sept, $J = 6.9$, *p*-cymene CHCH₃), 4.17 (1H, d, $^2J_{\text{HH}} = 10.8$, NH), 4.99 (1H, sept, $J = 6.7$, NCHCH₃), 5.21 (2H, m, *p*-cymene ArH), 5.76 (1H, d, $J = 6.2$, *p*-cymene ArH), 6.22 (1H, d, $J = 6.2$, *p*-cymene ArH), 7.31-7.38 (3H, m, ArH), 7.39 (1H, d, $J = 2.3$, NCHCHN), 7.71 (1H, d, $J = 2.3$, NCHCHN), 8.52 (1H, d, $^2J_{\text{HH}} = 10.8$, NH), 8.63 (1H, d, $J = 7.7$ ArH); δ_{C} (125 MHz, CD₂Cl₂) δ 20.2 (*p*-cymene CH₃), 21.0, 23.9 (*p*-cymene CHCH₃), 24.0, 24.8 (NCHCH₃), 31.9 (*p*-cymene CHCH₃), 55.4 (NCHCH₃), 83.0, 83.2, 84.1, 89.5 (*p*-cymene ArCH), 103.0, 110.6 (*p*-cymene ArC), 121.08, 121.13, 121.9, 122.9, 127.7, 128.8 (ArCH), 133.0, 136.3 (ArC), 175.9 (N₂C-Ru); m/z (ESI) 564 (100 %, [M-I]⁺, 202 (100 % [(C,NH₂)+H]⁺); Anal. Calcd. for C₂₂H₂₉I₂N₃Ru: C, 38.27; H, 4.23; N, 6.09. Found C, 38.07; H, 4.02; N, 5.91%.

[Cp**Rh*(C,NH₂)I]I (**4.35**)



A suspension of [Cp**Rh*Cl₂]₂ (0.020 g, 0.032 mmol), NaO^{*t*}Bu (0.012 g, 0.13 mmol), imidazolium salt **2.28b** (0.021 g, 0.064 mmol) and KI (0.054 g, 0.32 mmol) in DCM (5 mL) was stirred at room temperature for 4 days.

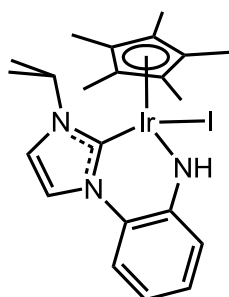
The mixture was then filtered through celite and evaporated to dryness. The crude residue was re-dissolved in acetone (3 mL) and stirred vigorously for 2 h with a

Chapter 4 – Synthesis and Reactivity of Complexes of Bidentate Amino/Amido-NHC Ligands

saturated solution of aq. KI (3 mL). Excess acetone was removed *in vacuo*, and DCM (5 mL) added. The organic layer was separated, dried (MgSO₄) and the volatiles removed *in vacuo*. Purification by flash column chromatography (10% acetone/CH₂Cl₂) gave **4.35** (0.020 g, 45%) as a dark red solid m.p. 95 °C, R_f = 0.6 (10% acetone/CH₂Cl₂).

Crystals suitable for structure determination by X-ray diffraction were obtained from CH₂Cl₂/hexane. δ_{H} (400 MHz, CDCl₃) δ 1.53 (3H, d, J = 6.7, CHCH₃), 1.59 (3H, d, J = 6.7, CHCH₃), 1.62 (15H, s, η^5 -C₅Me₅), 4.69 (1H, sept, J = 6.7, CHCH₃), 4.76 (1H, br, NH), 7.32 (3H, m, ArH, NH), 7.54 (2H, m, ArH, NCHCHN), 7.97 (1H, d, J = 2.2, NCHCHN), 8.31 (1H, dd, J = 7.0, 1.2, ArH); δ_{C} (125 MHz, CDCl₃) δ 10.3 (η^5 -C₅Me₅), 23.8, 25.8 (CHCH₃), 54.5 (CH(CH₃)₂), 98.1 (d, $J_{\text{Rh-C}}$ = 6, η^5 -C₅Me₅), 121.5 (NCHCHN), 122.2 (ArCH), 122.3 (NCHCHN), 123.0, 127.2, 128.0 (ArCH), 132.5, 134.7 (ArC), 169.5 (d, $J_{\text{Rh-C}}$ = 54, N₂C–Rh); m/z (FAB) 566 (100%, [M-I]⁺); Anal. Calcd. for C₂₂H₃₀N₃I₂Rh: C, 38.12; H, 4.36; N, 6.06. Found C, 38.05; H, 4.26; N, 5.87%.

Cp*Ir(C,NH)I (**4.36**)

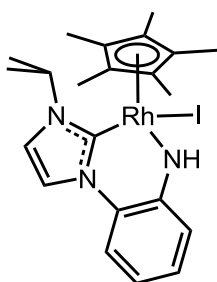


[Cp*IrCl₂]₂ (0.040 g, 0.050 mmol), imidazolium salt **2.28b** (0.033 g, 0.10 mmol) and NaO^tBu (0.019 g, 0.20 mmol) were suspended in THF (5 mL) and stirred for 15 h at room temperature. After this time, the solvent was removed *in vacuo* and the solid redissolved in DCM (10 mL) and filtered through Celite. The volatiles were then removed *in vacuo* to give a crude solid that was extracted with boiling Et₂O (5 x 15 mL). The Et₂O washings were combined, hot filtered through Celite and the filter pad washed with hot Et₂O (2 x 5 mL). Removal of the solvent *in vacuo* gave **4.36** (0.043 g, 65%) as a red-

Chapter 4 – Synthesis and Reactivity of Complexes of Bidentate Amino/Amido-NHC Ligands

orange solid m.p. 160 °C (dec.). Crystals suitable for structure determination by X-ray diffraction were obtained from an Et₂O/pentane solution of **4.36** at 3 °C. δ_{H} (500 MHz, CDCl₃) δ 1.59 (6H, d, $J = 6.8$, CHCH₃), 1.62 (15H, s, $\eta^5\text{-C}_5\text{Me}_5$), 2.39-2.59 (0.8H, br s, NH), 5.02 (1H, sept, $J = 6.8$, CHCH₃), 6.38 (1H, app t, $J = 7.6$, ArH), 6.67 (1H, d, $J = 7.6$, ArH), 6.85 (1H, app t, $J = 7.6$, ArH), 7.02-7.05 (2H, m, ArH + NCHCHN), 7.46 (1H, d, $J = 2.2$, NCHCHN); δ_{C} (125 MHz, CDCl₃) δ 9.6 ($\eta^5\text{-C}_5\text{Me}_5$), 23.2 – 26.4 (br, CHCH₃), 53.5 (CHCH₃), 88.8 ($\eta^5\text{-C}_5\text{Me}_5$), 114.4 (ArCH), 118.2, 118.3, 119.2, 119.7 (ArCH / NCHCHN), 126.4 (ArCH), 128.2, 151.4 (ArC), 154.6 (N₂C-Ir); m/z (ESI) 656 (100%, [M+H]⁺), 528 (10%, [M-I]⁺); Anal. Calcd. for C₂₂H₂₉IrN₃: C, 40.37; H, 4.47; N, 6.42. Found C, 40.48; H, 4.52; N, 6.31%.

Cp*Rh(C,NH)I (**4.37**)



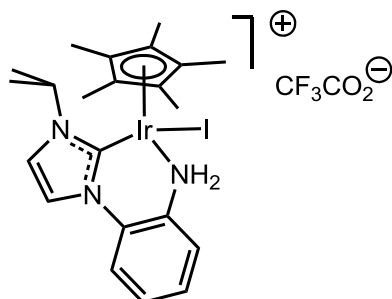
NaH (0.001 g, 0.04 mmol) was added to a stirred solution of **4.35** (0.020 g, 0.029 mmol) in THF (5 mL) under N₂. After 2.5 h, an aliquot was taken from the reaction mixture by syringe and added to a dry Young's tap NMR tube under nitrogen, the solvent was then removed *in vacuo*. In a glove box under an atmosphere of nitrogen, dry CDCl₃ was added to the NMR tube, which was then sealed and a ¹H NMR spectrum run immediately. The ¹H NMR spectrum showed > 90% conversion of **4.35** to major product **4.37**. Attempts to purify the crude **4.37** by precipitation/recrystallisation gave back **4.35**, presumably from adventitious water.

δ_{H} (400 MHz, CDCl₃) 1.59 (6H, d, $J = 6.7$, CH(CH₃)₂), 1.60 (15H, s, $\eta^5\text{-C}_5\text{Me}_5$), 5.10 (1H, sept, $J = 6.7$, CH(CH₃)₂), 5.29 (1H, s, NH), 6.39 (1H, app t, $J = 7.5$, ArH,), 6.74 (1H, d, $J = 7.5$, ArH,), 6.85 (1H, app t, $J = 8.0$, ArH,), 7.03 (1H, d, $J = 8.0$, ArH,), 7.16 (1H, d, $J = 2.1$,

Chapter 4 – Synthesis and Reactivity of Complexes of Bidentate Amino/Amido-NHC Ligands

NCHCHN), 7.51 (1H, d, $J = 2.1$, NCHCHN). m/z (ESI) 566 (100%, $[M+H]^+$), 438 (15%, $[M-I]^+$).

[Cp*Ir(C,NH₂)I][CF₃CO₂] (4.38)



Trifluoroacetic acid (6 μ L, 0.009 g, 0.08 mmol) was added to a stirred solution of **4.36** (0.050 g, 0.076 mmol) in CH₂Cl₂ (10 mL) at room temperature, resulting in an immediate colour change from dark orange to yellow. After stirring for 1 h, the solvent

was removed *in vacuo* to give **4.38** (0.058 g, 99%) as a yellow solid m.p. 100 °C (dec.).

Crystals suitable for structure determination by X-ray diffraction were obtained by

diffusion of pentane into a saturated CHCl₃ solution of **4.38**. δ_H (500 MHz, CDCl₃) δ 1.57

(15H, s, η^5 -C₅Me₅), 1.60 (6H, d, $J = 6.8$, CHCH₃), 4.78 (1H, sept, $J = 6.8$, CHCH₃), 5.87

(1H, d, $J = 11.9$, NH), 6.78 (1H, d, $J = 11.9$, NH), 7.30 (1H, d, $J = 2.2$, NCHCHN), 7.33 (1H,

app t, $J = 7.7$, ArH), 7.38 (1H, app t, $J = 7.7$, ArH), 7.45 (1H, d, $J = 7.7$, ArH), 7.48 (1H, d, J

= 7.7, ArH), 7.67 (1H, d, $J = 2.2$, NCHCHN); δ_C (125 MHz, CDCl₃) δ 9.4 (η^5 -C₅Me₅), 23.5,

26.0 (CHCH₃), 54.3 (CHCH₃), 91.1 (η^5 -C₅Me₅), 115.5 (q, $J = 287.4$, CF₃), 120.5, 120.6

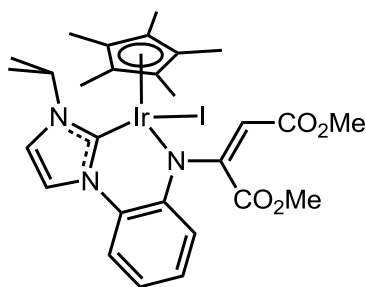
(NCHCHN), 121.6, 121.9, 128.0, 128.2 (ArCH), 132.9, 135.3 (ArC), 156.4 (N₂C-Ir), 160.1

(q, $J = 39.9$, CF₃CO₂); m/z (ESI) 656 (100%, $[M-CF_3CO_2]^+$), 528 (20%, $[M-HI-CF_3CO_2]^+$);

Anal. Calcd. for: C₂₄H₃₀F₃IrN₃O₂: C, 37.50; H, 3.93; N, 5.47. Found C, 37.58; H, 3.87; N,

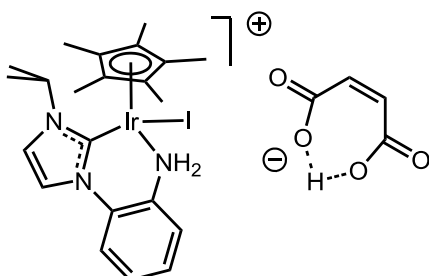
5.38%.

[Cp*Ir(C,NC(CO₂Me)CH(CO₂Me))] (4.39)



Complex **4.36** (0.050 g, 0.076 mmol) was dissolved in DCM (5 mL) and DMAD (0.011 g, 0.010 mL, 0.076 mmol) added. The mixture was stirred at RT for 1 h, and then hexane (70 mL) added to precipitate a red solid which was collected by filtration, washed with hexane (2 x 5 mL) and dried in vacuo. Product **4.39** was isolated as a red solid (0.040 g, 66%) m.p. 210 °C (dec.). Crystals suitable for structure determination by X-ray diffraction were obtained by diffusion of pentane into a saturated CHCl₃ solution of **4.39**. δ_{H} (400 MHz, CDCl₃) 1.47 (3H, d, $J = 6.9$, CHCH₃), 1.49 (3H, d, $J = 6.9$, CHCH₃), 1.60 (15H, s, $\eta^5\text{-C}_5\text{Me}_5$), 3.61 (3H, s, CO₂CH₃), 3.64 (3H, s, CO₂CH₃), 4.79 (1H, sept, $J = 6.9$, CHCH₃), 5.14 (1H, s, CHCO₂CH₃), 6.80 (1H, app t, $J = 7.5$, ArH), 7.03 (1H, app t, $J = 7.7$, ArH), 7.10 (1H, d, $J = 7.7$, ArH), 7.14 (1H, d, $J = 7.5$, ArH), 7.26 (1H, d, $J = 2.2$, NCHCHN), 7.40 (1H, d, $J = 2.2$, NCHCHN); δ_{C} (125 MHz, CDCl₃) 9.9 ($\eta^5\text{-C}_5\text{Me}_5$), 24.1, 26.4 (CHCH₃), 50.6, 52.0 (CO₂CH₃), 53.2 (CHCH₃), 90.0 ($\eta^5\text{-C}_5\text{Me}_5$), 91.4 (NCCO₂CH₃), 107.8 (CHCO₂CH₃), 118.8, 120.1 (NCHCHN), 121.2, 121.4, 125.7, 126.4 (Ar CH), 132.9, 145.7 (Ar C), 156.5 (N₂C-Ir), 168.1, 168.4 (CO₂CH₃). m/z (ESI) 798 (100 % [M+H]⁺), 670 (40 % [M-I]⁺). Anal. Calcd. for: C₂₈H₃₅IrN₃O₄, C, 42.21; H, 4.43; N, 5.27; Found C, 42.33; H, 4.45; N, 5.18%.

[Cp*Ir(C,NH₂)I (C₄H₃O₄)] (4.40)



Complex **4.36** (0.050 g, 0.076 mmol) was dissolved in DCM (5 mL) and maleic anhydride (0.007 g,

Chapter 4 – Synthesis and Reactivity of Complexes of Bidentate Amino/Amido-NHC Ligands

0.076 mmol) added. The mixture was stirred at RT for 1 h, and then hexane (40 mL) added to precipitate a yellow/green solid which was collected by filtration, washed with hexane (2 x 5 mL) and dried in vacuo. Product **4.40** was isolated as a yellow/green solid (0.042 g, 71%) m.p. 214–216 °C. Crystals suitable for structure determination by X-ray diffraction were obtained by diffusion of 50% benzene/pentane into a saturated DCM solution of **4.40**. δ_{H} (400 MHz, CDCl_3) 1.58 (21H, apparent br s, $\eta^5\text{-C}_5\text{Me}_5 + \text{CHCH}_3$), 4.75 (1H, sept, $J = 6.9$, CHCH_3), 5.51 (1H, br s, NH), 6.27 (2H, s, $\text{HC}(\text{CO}_2\text{H})$), 7.29 (2H, m, ArH), 7.37 (1H, d, $J = 2.2$, NCHCHN), 7.47 (1H, m, ArH), 7.82 (2H, m, $\text{ArH} + \text{NCHCHN}$), 8.70 (1H, br s, NH); δ_{C} (125 MHz, CDCl_3) 9.54 ($\eta^5\text{-C}_5\text{Me}_5$), 23.5, 26.1 (CHCH_3), 54.1(CHCH_3), 90.9 ($\eta^5\text{-C}_5\text{Me}_5$), 120.6, 120.7, 121.7, 122.1, 127.5, 127.8 (Ar CH), 132.9, 136.0 (Ar C), 136.2 ($\text{HC}(\text{CO}_2\text{H})$), 156.4 ($\text{N}_2\text{C-Ir}$), 169.2 (CO_2H). m/z (ESI) 656 (100 % $[\text{M-C}_4\text{H}_3\text{O}_4]^+$). Anal. Calcd. for: $\text{C}_{26}\text{H}_{33}\text{IrN}_3\text{O}_4$: C, 40.52; H, 4.32; N, 5.45; Found C, 41.29; H, 4.09; N, 5.55%.

X-ray Crystallographic Studies

All single crystal diffraction data were collected using graphite monochromated $\text{Mo-K}\alpha$ X-radiation ($\lambda = 0.71073 \text{ \AA}$) on a Bruker APEX 2000 CCD diffractometer at 150 K. The data were corrected for Lorentz and polarisation effects and empirical absorption corrections applied. Structures were solved by Patterson methods and structures refined by least-squares full-matrix refinement against F^2 employing SHELXTL version 6.10. Hydrogen atoms were included in calculated positions ($d(\text{C-H}) = 0.95$ to 0.99 \AA) riding on the bonded atom with isotropic displacement parameters set to $1.5 U_{\text{eq}}$ (C) or methyl H atoms and $1.2 U_{\text{eq}}$ for all other C atoms. All non-H atoms were refined

Chapter 4 – Synthesis and Reactivity of Complexes of Bidentate Amino/Amido-NHC Ligands

with anisotropic displacement parameters. Disordered solvent was removed using the SQUEEZE option of PLATON.²¹⁰

Crystal data for 4.22·(0.5CH₂Cl₂)(0.25C₆H₁₄). C₃₁H_{40.50}ClI₂N₄Pd, $M_w = 864.82 \text{ gmol}^{-1}$, $T = 150(2) \text{ K}$, triclinic space group P-1, $a = 13.616(9) \text{ \AA}$, $b = 15.293(10) \text{ \AA}$, $c = 18.724(13) \text{ \AA}$, $\alpha = 73.804(12)^\circ$, $\beta = 73.014(12)^\circ$, $\gamma = 64.088(12)^\circ$, $V = 3302(4) \text{ \AA}^3$, $Z = 4$, $\rho_{\text{calcd}} = 1.740 \text{ Mgm}^{-3}$, $\mu = 2.539 \text{ mm}^{-1}$, $F(000) = 1694$, crystal size $0.20 \times 0.20 \times 0.13 \text{ mm}^3$, 25832 reflections collected, 12785 unique [$R(\text{int}) = 0.0875$] (completeness to $\theta = 26.00^\circ$ 98.6 %). Empirical absorption correction made, T_{min} and $T_{\text{max}} = 0.831$ and 0.455 respectively. GOF = 0.952, final R indices [$I > 2\sigma$] $R_1 = 0.0589$, $wR_2 = 0.1341$, R indices (all data) $R_1 = 0.0825$, $wR_2 = 0.1428$. Largest diff. peak and hole 2.244 and $-0.858 \text{ e \AA}^{-3}$.

Crystal data for 4.23. C₂₉H₃₆I₂N₄Pt, $M_w = 889.51 \text{ gmol}^{-1}$, $T = 150(2) \text{ K}$, triclinic space group P-1, $a = 13.412(3) \text{ \AA}$, $b = 15.242(3) \text{ \AA}$, $c = 18.357(4) \text{ \AA}$, $\alpha = 95.858(4)^\circ$, $\beta = 104.069(4)^\circ$, $\gamma = 114.812(4)^\circ$, $V = 3214.0(12) \text{ \AA}^3$, $Z = 4$, $\rho_{\text{calcd}} = 1.838 \text{ Mgm}^{-3}$, $\mu = 6.309 \text{ mm}^{-1}$, $F(000) = 1688$, crystal size $0.23 \times 0.08 \times 0.04 \text{ mm}^3$, 25327 reflections collected, independent reflections 12490 [$R(\text{int}) = 0.0920$] (completeness to $\theta = 26.00^\circ$ 98.80%). Empirical absorption correction made, T_{min} and $T_{\text{max}} = 0.831$ and 0.518 respectively. GOF = 0.897, final R indices [$I > 2\sigma$] $R_1 = 0.0602$, $wR_2 = 0.1004$, R indices (all data) $R_1 = 0.1104$, $wR_2 = 0.1130$. Largest diff. peak and hole 3.255 and $-1.506 \text{ e \AA}^{-3}$.

Crystal data for 4.26. C₄₂H₄₅I₂N₃PPd, $M_w = 982.98$, Monoclinic, space group $P2_1/c$, $a = 17.655(13)$, $b = 14.789(11)$, $c = 15.851(12) \text{ \AA}$, $\alpha = 90.00$, $\beta = 93.26(2)$, $\gamma = 90.00^\circ$, $V = 4132(5) \text{ \AA}^3$, $Z = 4$, $\rho_{\text{calcd}} = 1.580 \text{ Mg/m}^3$, $\mu = 2.01 \text{ mm}^{-1}$, $F(000) = 1940$, crystal size $0.14 \times 0.12 \times 0.04 \text{ mm}^3$, 31797 reflections collected, 8116 unique [$R(\text{int}) = 0.199$] (completeness to $\theta = 26.00^\circ$ 99.9 %). Empirical absorption correction made, T_{max}

Chapter 4 – Synthesis and Reactivity of Complexes of Bidentate Amino/Amido-NHC Ligands

and T_{min} 0.831 and 0.564 respectively. GOF = 0.830, final R indices [$I > 2\sigma$] $R_1 = 0.0658$, $wR_2 = 0.0882$, R indices (all data) $R_1 = 0.1608$, $wR_2 = 0.1083$. Largest diff. peak and hole 1.085 and $-0.901 \text{ e.}\text{\AA}^{-3}$.

Crystal data for 4.27·(C₅H₁₂). C₅₃H₇₄N₆O₂Pd₂, $M_w = 1039.98 \text{ gmol}^{-1}$, $T = 150(2) \text{ K}$, tetragonal space group I4(1)/a, $a = 19.443(2) \text{ \AA}$, $b = 19.443(2) \text{ \AA}$, $c = 25.426(4) \text{ \AA}$, $\alpha = 90^\circ$, $\beta = 90^\circ$, $\gamma = 90^\circ$, $V = 9612(2) \text{ \AA}^3$, $Z = 8$, $\rho_{calcd} = 1.437 \text{ Mgm}^{-3}$, $\mu = 0.796 \text{ mm}^{-1}$, F(000) = 4336, crystal size $0.31 \times 0.24 \times 0.15 \text{ mm}^3$, 37121 reflections collected, independent reflections 4713 [R(int) = 0.0767] (completeness to theta = 26.00° 100.00%). Empirical absorption correction made, T_{min} and $T_{max} = 0.802$ and 0.634 respectively. GOF = 1.029, final R indices [$I > 2\sigma$] $R_1 = 0.0378$, $wR_2 = 0.0914$, R indices (all data) $R_1 = 0.0497$, $wR_2 = 0.0960$. Largest diff. peak and hole 0.690 and $-0.388 \text{ e.}\text{\AA}^{-3}$.

Crystal data for 4.30. C₂₆H₂₉Cl₂N₃Pd, $M_w = 560.82$, Monoclinic, space group $P2_1/c$, $a = 11.618(4)$, $b = 14.088(5)$, $c = 15.733(6) \text{ \AA}$, $\alpha = 90.00$, $\beta = 100.763(6)$, $\gamma = 90.00^\circ$, $V = 2529.7(16) \text{ \AA}^3$, $Z = 4$, $\rho_{calcd} = 1.473 \text{ Mg/m}^3$, $\mu = 0.963 \text{ mm}^{-1}$, F(000) = 1144, crystal size $0.44 \times 0.32 \times 0.23 \text{ mm}^3$, 20452 reflections collected, 5476 unique [R(int) = 0.0315] (completeness to theta = 27.00° 99.4 %). Empirical absorption correction made, T_{max} and T_{min} 0.831 and 0.664 respectively. GOF = 1.063, final R indices [$I > 2\sigma$] $R_1 = 0.0270$, $wR_2 = 0.0675$, R indices (all data) $R_1 = 0.0306$, $wR_2 = 0.0692$. Largest diff. peak and hole 0.407 and $-0.301 \text{ e.}\text{\AA}^{-3}$.

Crystal data for 4.31·CH₂Cl₂. C₂₆H₂₉I₂N₃Pd·CH₂Cl₂, $M_w = 828.65$, Triclinic, space group $P-1$, $a = 8.756(2)$, $b = 10.432(2)$, $c = 17.511(4) \text{ \AA}$, $\alpha = 100.304(4)$, $\beta = 102.695(4)$, $\gamma = 17.511(4)^\circ$, $V = 1500.1(6) \text{ \AA}^3$, $Z = 2$, $\rho_{calcd} = 1.834 \text{ Mg/m}^3$, $\mu = 2.875 \text{ mm}^{-1}$, F(000) = 800, crystal size $0.26 \times 0.20 \times 0.08 \text{ mm}^3$, 11689 reflections collected, 5828 unique [R(int) =

Chapter 4 – Synthesis and Reactivity of Complexes of Bidentate Amino/Amido-NHC Ligands

0.0297] (completeness to theta = 26.00° 99.0 %). Empirical absorption correction made, T_{max} and T_{min} 0.831 and 0.625 respectively. GOF = 1.056, final R indices [$I > 2\sigma$] $R_1 = 0.0316$, $wR_2 = 0.0762$, R indices (all data) $R_1 = 0.0368$, $wR_2 = 0.0786$. Largest diff. peak and hole 1.351 and -1.230 e.Å⁻³.

Crystal data for 4.32. C₃₄H₄₅IrN₃, $M_W = 814.83$, monoclinic, space group P2(1)/c, $a = 13.219(4)$, $b = 8.444(3)$, $c = 29.021(9)$ Å, $\alpha = 90$, $\beta = 95.654(5)$, $\gamma = 90^\circ$, $V = 3223.7(16)$ Å³, $Z = 4$, $\rho_{calcd} = 1.679$ Mgm⁻³, $\mu = 5.126$ mm⁻¹, F(000) = 1600, crystal size 0.23 x 0.19 x 0.13 mm³, 24406 reflections collected, 6341 unique [R(int) = 0.0652] (completeness to theta = 26.00° 99.9%). Empirical absorption correction made, T_{max} and T_{min} 0.831 and 0.587 respectively. GOF = 1.049, final R indices [$I > 2\sigma$] $R_1 = 0.0487$, $wR_2 = 0.1305$, R indices (all data) $R_1 = 0.0615$, $wR_2 = 0.1370$. Largest diff. peak and hole 2.542 and -2.850 eÅ⁻³.

Crystal data for 4.33. C₃₄H₄₅IN₃Rh, $M_W = 725.54$, monoclinic, space group P2(1)/c, $a = 13.277(5)$, $b = 8.466(3)$, $c = 28.869(11)$ Å, $\alpha = 90$, $\beta = 95.710(8)$, $\gamma = 90^\circ$, $V = 3229(2)$ Å³, $Z = 4$, $\rho_{calcd} = 1.493$ Mg/m³, $\mu = 1.511$ mm⁻¹, F(000) = 1472, crystal size 0.16 x 0.12 x 0.08 mm³, 24670 reflections collected, 6361 unique [R(int) = 0.1738] (completeness to theta = 26.00° = 99.9%). Empirical absorption correction made, T_{max} and T_{min} 0.831 and 0.521 respectively. GOF = 0.922, final R indices [$I > 2\sigma$] $R_1 = 0.0599$, $wR_2 = 0.1103$, R indices (all data) $R_1 = 0.0907$, $wR_2 = 0.1242$. Largest diff. peak and hole 2.034 and -1.294 eÅ⁻³.

Crystal data for 4.34.(0.5CHCl₃).(Et₂O). C_{26.50}H_{39.50}Cl_{1.50}I₂N₃ORu, $M_W = 824.16$, triclinic, space group P-1, $a = 11.772(6)$, $b = 14.552(7)$, $c = 16.056(8)$ Å, $\alpha = 77.716(9)$, $\beta = 88.809(9)$, $\gamma = 85.046(10)^\circ$, $V = 2678(2)$ Å³, $Z = 4$, $\rho_{calcd} = 2.044$ Mg/m³, $\mu = 3.068$ mm⁻¹,

Chapter 4 – Synthesis and Reactivity of Complexes of Bidentate Amino/Amido-NHC Ligands

F(000) = 1612, crystal size 0.15 x 0.10 x 0.04 mm³, 21113 reflections collected, 10398 unique [R(int) = 0.1013] (completeness to theta = 26.00° 98.7%). Empirical absorption correction made, T_{max} and T_{min} 0.831 and 0.574 respectively. GOF = 0.869, final R indices [$I > 2\sigma$] $R_1 = 0.0684$, $wR_2 = 0.1444$, R indices (all data) $R_1 = 0.1308$, $wR_2 = 0.1635$. Largest diff. peak and hole 1.183 and -1.139 eÅ⁻³.

Crystal data for 4.35.(5CH₂Cl₂). C_{27.50}H₄₁Cl₁₁I₂N₃Rh, $M_W = 1160.29$, triclinic, space group P-1, $a = 9.430(3)$, $b = 11.745(4)$, $c = 29.671(10)$ Å, $\alpha = 89.104(8)$, $\beta = 86.111(8)$, $\gamma = 75.463(7)^\circ$, $V = 3173.7(19)$ Å³, $Z = 4$, $\rho_{calcd} = 2.428$ Mg/m³, $\mu = 3.442$ mm⁻¹, F(000) = 2260, crystal size 0.23 x 0.13 x 0.08 mm³, 25014 reflections collected, 12332 unique [R(int) = 0.1037] (completeness to theta = 26.00° 98.7%). Empirical absorption correction made, T_{max} and T_{min} 0.831 and 0.535 respectively. GOF = 0.937, final R indices [$I > 2\sigma$] $R_1 = 0.0840$, $wR_2 = 0.2165$, R indices (all data) $R_1 = 0.1193$, $wR_2 = 0.2301$. Largest diff. peak and hole 2.920 and -1.356 e.Å⁻³.

Crystal data for 4.36. C₂₂H₂₉IrN₃, $M_W = 654.58$, triclinic, space group P-1, $a = 9.218(3)$, $b = 10.812(3)$, $c = 11.389(4)$ Å, $\alpha = 75.863(5)$, $\beta = 78.648(5)$, $\gamma = 86.600(5)^\circ$, $V = 1079.1(6)$ Å³, $Z = 2$, $\rho_{calcd} = 2.015$ Mg/m³, $\mu = 7.628$ mm⁻¹, F(000) = 624, crystal size 0.13 x 0.11 x 0.05 mm³, 8383 reflections collected, 4177 unique [R(int) = 0.0537] (completeness to theta = 26.00° 98.5%). Empirical absorption correction made, T_{max} and T_{min} 0.862 and 0.586 respectively. GOF = 1.012, final R indices [$I > 2\sigma$] $R_1 = 0.0471$, $wR_2 = 0.0963$, R indices (all data) $R_1 = 0.0612$, $wR_2 = 0.1008$. Largest diff. peak and hole 2.294 and -1.647 e.Å⁻³.

Crystal data for 4.38.(5C₅H₁₂). C₄₉H₉₀F₃IrN₃O₂, $M_W = 1129.34$, monoclinic, space group P2(1)/n, $a = 16.957(3)$, $b = 10.360(2)$, $c = 21.186(4)$ Å, $\alpha = 90$, $\beta = 110.741(4)$, $\gamma = 90^\circ$, V

Chapter 4 – Synthesis and Reactivity of Complexes of Bidentate Amino/Amido-NHC Ligands

= 3480.6(12) Å³, $Z = 4$, $\rho_{\text{calcd}} = 2.155 \text{ Mg/m}^3$, $\mu = 4.795 \text{ mm}^{-1}$, $F(000) = 2312$, crystal size 0.15 x 0.13 x 0.03 mm³, 26753 reflections collected, 6829 unique [R(int) = 0.1501] (completeness to theta = 26.00° 100.0 %). Empirical absorption correction made, T_{max} and T_{min} 0.862 and 0.539 respectively. GOF = 0.795, final R indices [$I > 2\sigma$] $R_1 = 0.0541$, $wR_2 = 0.1052$, R indices (all data) $R_1 = 0.0949$, $wR_2 = 0.1136$. Largest diff. peak and hole 0.991 and -1.925 e.Å⁻³.

Crystal data for 4.39. C₂₈H₃₅IrN₃O₄, $M_W = 796.69$, Orthorhombic, space group *Pccn*, $a = 21.063(6)$, $b = 16.326(4)$, $c = 16.530(5)$ Å, $\alpha = 90$, $\beta = 90$, $\gamma = 90^\circ$, $V = 5684(3)$ Å³, $Z = 8$, $\rho_{\text{calcd}} = 1.862 \text{ Mg/m}^3$, $\mu = 5.821 \text{ mm}^{-1}$, $F(000) = 3088$, crystal size 0.22 x 0.14 x 0.12 mm³, 45374 reflections collected, 6202 unique [R(int) = 0.0766] (completeness to theta = 27.00° 100.0 %). Empirical absorption correction made, T_{max} and T_{min} 0.831 and 0.614 respectively. GOF = 1.023, final R indices [$I > 2\sigma$] $R_1 = 0.0344$, $wR_2 = 0.0673$, R indices (all data) $R_1 = 0.0500$, $wR_2 = 0.0717$. Largest diff. peak and hole 1.151 and -0.708 e.Å⁻³.

Crystal data for 4.40. C₂₂H₃₀IrN₃·C₄H₃O₄, $M_W = 770.65$, Triclinic, space group *P-1*, $a = 8.5868(17)$, $b = 12.202(2)$, $c = 13.089(3)$ Å, $\alpha = 90.136(4)$, $\beta = 99.311(4)$, $\gamma = 95.941(4)^\circ$, $V = 1345.9(5)$ Å³, $Z = 2$, $\rho_{\text{calcd}} = 1.902 \text{ Mg/m}^3$, $\mu = 6.143 \text{ mm}^{-1}$, $F(000) = 744$, crystal size 0.20 x 0.10 x 0.03 mm³, 10618 reflections collected, 5222 unique [R(int) = 0.0710] (completeness to theta = 26.00° 98.8 %). Empirical absorption correction made, T_{max} and T_{min} 0.831 and 0.636 respectively. GOF = 0.894, final R indices [$I > 2\sigma$] $R_1 = 0.0478$, $wR_2 = 0.0826$, R indices (all data) $R_1 = 0.0673$, $wR_2 = 0.0886$. Largest diff. peak and hole 2.050 and -1.462 e.Å⁻³.

5: Chapter 5 – Bifunctional Catalysis by Amino/Amido-NHC Complexes

Chapter 5 will discuss the activity of the amino/amido-NHC metal complexes described in Chapters 3 and 4 in catalytic applications, in which the author investigated whether the metal-nitrogen bond can facilitate bifunctional catalysis.

The catalytic reactions discussed are the transfer hydrogenation of ketones, and the direct arylation of aromatic heterocycles; both reactions have the possibility to proceed by a bifunctional catalytic mechanism.

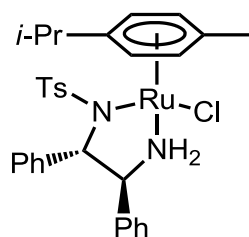
Transfer hydrogenation is a well-studied reaction, known to be catalysed by metal amido complexes (Ch. 5.1.1), which allowed us to test whether bifunctional catalysis occurs with amino/amido-NHC complexes **4.34-4.36**. Furthermore, as several other catalytic systems are known for transfer hydrogenation, the reactivity of complexes **4.34-4.36** could be compared with known catalysts.

In the case of direct arylation, the author wanted to explore if a metal-nitrogen bond could allow an AMLA(4) mechanism of C-H activation. AMLA(4) is a mechanism associated with very few catalytic reactions, and could allow control of the regioselectivity of C-H activation on substrates with several C-H sites available to react. The mechanism of the catalytic reactions will be discussed and commented on based on observations of reactivity.

5.1: Introduction

5.1.1: Transfer Hydrogenation

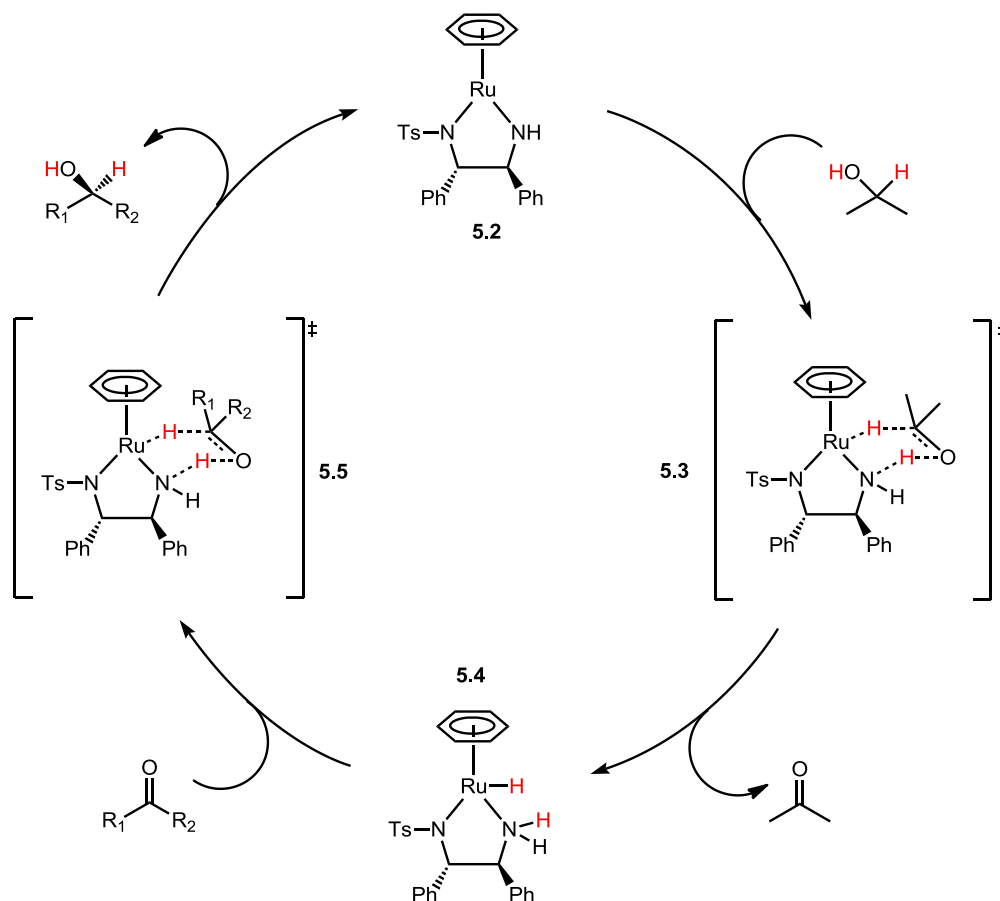
Transition metal catalysed transfer hydrogenation is an operationally simple and chemoselective method for the reduction of ketones to alcohols, with a wide substrate scope and functional group tolerance.²² Transfer hydrogenation is conceptually similar to the Meerwein-Ponndorf-Verley (MPV) reduction, in that a sacrificial hydrogen donor (alcohol) is used as the reductant in the presence of a catalyst.^{283,284} The MPV reduction, however, often requires the use of more than stoichiometric amounts of aluminium alkoxides, and the reaction is often slow or low-yielding, making it impractical.²⁸⁵ The advent of chiral half-sandwich diamine precatalysts [M(arene)(diamine)X], for example Ru(*p*-cymene)(TsDPEN)Cl (**5.1**, **Scheme 5.1**), introduced by Noyori and Ikariya, allowed access to catalytic asymmetric transfer hydrogenation reactions.²⁴



Scheme 5.1: Ru(*p*-cymene)(TsDPEN)Cl (**5.1**), a precatalyst for asymmetric transfer hydrogenation.

Catalytic transfer hydrogenation by the metal diamine catalysts is known to proceed by a bifunctional mechanism, and the two intermediates on the catalytic cycle, amide complex **5.2** and amine hydride complex **5.4** have been isolated and characterised,

Scheme 5.2.²⁴ The active amide catalyst **5.2**, generated by base from a [Ru(arene)(diamine)X] precatalyst, removes hydrogen from *isopropanol* via a 6-membered transition state **5.3**, in a bifunctional, concerted fashion between the metal and the amide ligand. The amine-hydride complex **5.4** then reduces the ketone via another 6-membered transition state, **5.5**.



Scheme 5.2: Bifunctional mechanism of transfer hydrogenation of ketones by Ru(arene)(diamine)X precatalysts.

Transfer hydrogenation is a reversible reaction that consequently gives the thermodynamic product. Therefore, transfer hydrogenation is most effective for electron deficient aryl ketones because addition of hydrogen is favoured across an electron deficient carbonyl C=O bond.¹

Conversely, electron-rich benzylic alcohols undergo the reverse reaction:

enantioselective dehydrogenative oxidation to aryl ketones.¹ Similarly, racemic

alcohols can undergo kinetic resolution with [Ru(arene)(diamine)X] precatalysts.¹ In

order to reduce problems with reversibility of the transfer hydrogenation reaction

formic acid can be used as a hydrogen donor, producing CO₂ as a gaseous byproduct

which, in principle, makes the transfer hydrogenation irreversible.²⁵

Ru(*p*-cymene)(TsDPEN)Cl **5.1** is a highly active transfer hydrogenation catalyst that gives high enantioselectivity, but further fine-tuning has led to improved catalyst

performance. For example, tethered arene diamine catalysts **5.6-5.8**, **Figure 5.1**,

synthesised by Wills *et al.*, show remarkably increased activity and enantioselectivity

in asymmetric transfer hydrogenation over untethered Ru diamine precatalysts.^{286–288}

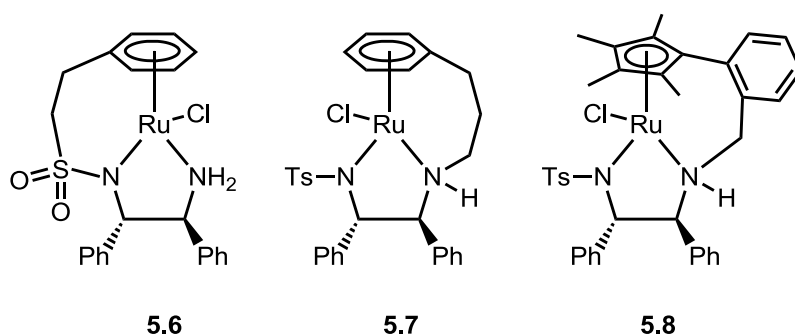


Figure 5.1: Tethered arene asymmetric transfer hydrogenation precatalysts^{286–288}

The replacement of the diamine ligand with a chiral β -amino alcohol ligand can lead to

increased activity in asymmetric transfer hydrogenation, although in some cases the

enantioselectivity is negatively affected.^{289–293}

Closely related to this project, Morris *et al.* have recently reported chelating bidentate

amino-NHC ruthenium complexes **4.19** and **4.20** (previously discussed in Chapter 4)

which are precatalysts for H₂ hydrogenation and transfer hydrogenation of ketones, **Figure 5.2.**^{18,17,19} Morris' precatalysts **4.19** and **4.20** are similar to complexes **4.34-4.40**, both having a bidentate primary amine-NHC ligand coordinated to a half-sandwich arene complex. The reactivity of these complexes in comparison to amino/amido-NHC complexes **4.34**, **4.35** and **4.36** will be discussed later in this chapter.

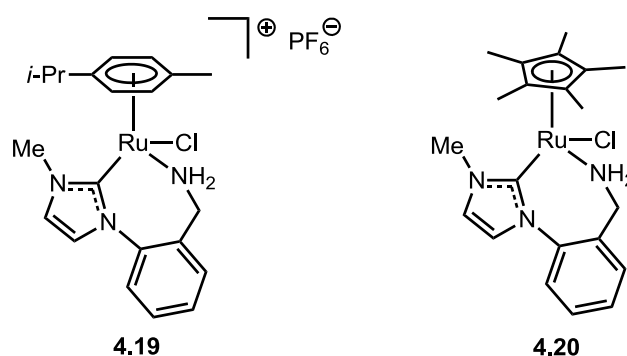
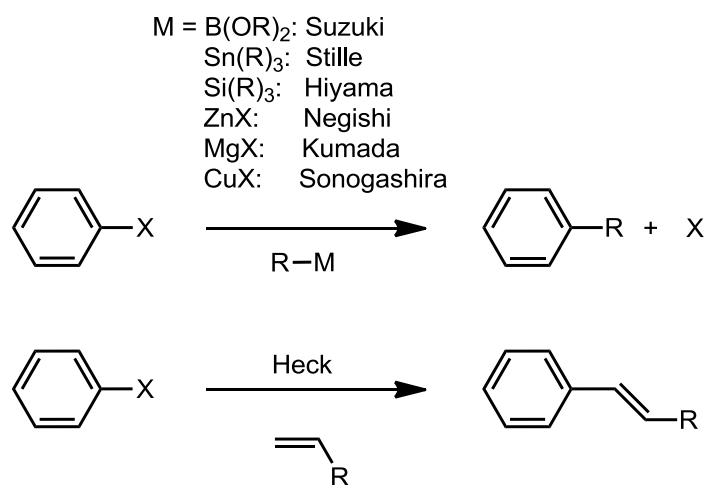


Figure 5.2: Chelating bidentate amino-NHC ruthenium complexes for hydrogenation.^{18,17,19}

5.1.2: Direct Arylation of Aromatic Heterocycles

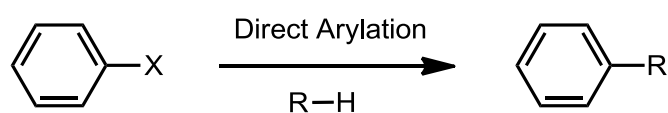
Palladium-catalysed cross-coupling reactions that form C-C bonds (**Scheme 5.3**) have been one of the most successful, synthetically useful transformations developed in organic chemistry, culminating in the award of the 2010 Nobel prize in chemistry to Heck, Suzuki and Negishi.²⁹⁴ Although incredibly effective, selective and generally applicable, cross-couplings require the activation of both coupling partners, one as an aryl halide, and the other as an organometallic reagent or unsaturated substrate. These preactivated substrates need to be prepared, often needing several steps, which impacts on the efficiency of the overall coupling reaction. In addition, some

organometallics are unstable to air/moisture. The activating group is also a byproduct in the reaction, generating potentially toxic, stoichiometric waste which must be disposed of.



Scheme 5.3: Palladium-catalysed C-C cross-coupling reactions.

A solution to these problems of preactivation and waste is to use only one activated coupling partner, an aryl halide, with the other coupling partner being an unactivated arene. Formally coupling a C-X and C-H bond to give the required aryl C-C bond is a process known as direct arylation, **Scheme 5.4**. In a direct arylation, the only byproducts are halogen acids which are environmentally benign and of low molecular weight, improving the atom economy of the reaction. However, direct arylation reactions introduce two challenges that are not present in conventional cross-coupling reactions: the low reactivity of the C-H bond, and the control needed to selectively functionalise one C-H in a molecule which could potentially have several.



Scheme 5.4: Direct arylation.

Aromatic heterocycles occur prominently in nature, such as the nucleobase adenine, alkaloid tryptamine and amino acid histidine; heteroarenes are also important components of pharmaceuticals, such as the best-selling drug atorvastatin, proton pump inhibitor esomeprazole and kinase inhibitor imatinib (**Figure 5.3**). Indeed, several modern drugs containing heterocyclic biaryl motifs are now synthesised using palladium-catalysed cross-couplings, an example being the kinase inhibitor crizotinib (**5.9**), which features a late stage Suzuki coupling of an pyrazole and pyridine in a synthetic route that has synthesised over 100 kg of product for Phase III trials, **Scheme 5.5**.²⁹⁵

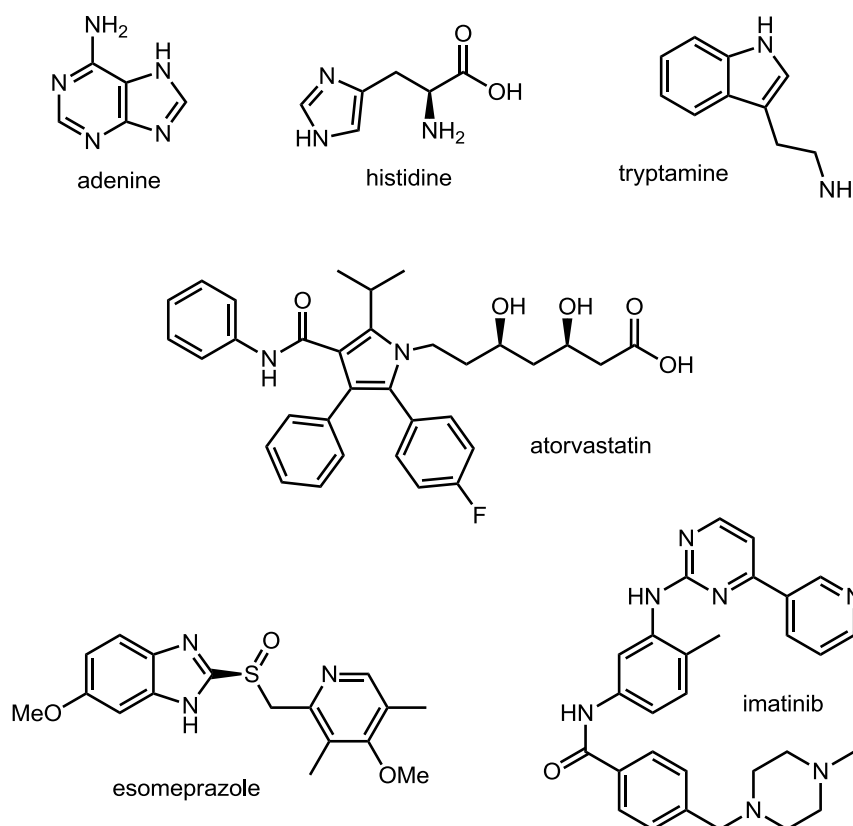
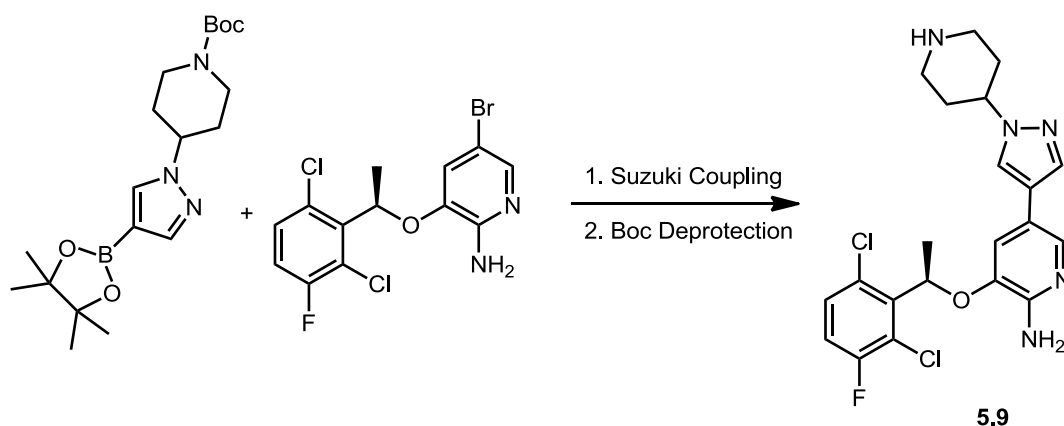


Figure 5.3: Representative natural and synthetic bioactive heteroarenes.



Scheme 5.5: Final synthetic steps of crizotinib (**5.9**), a kinase inhibitor.²⁹⁵

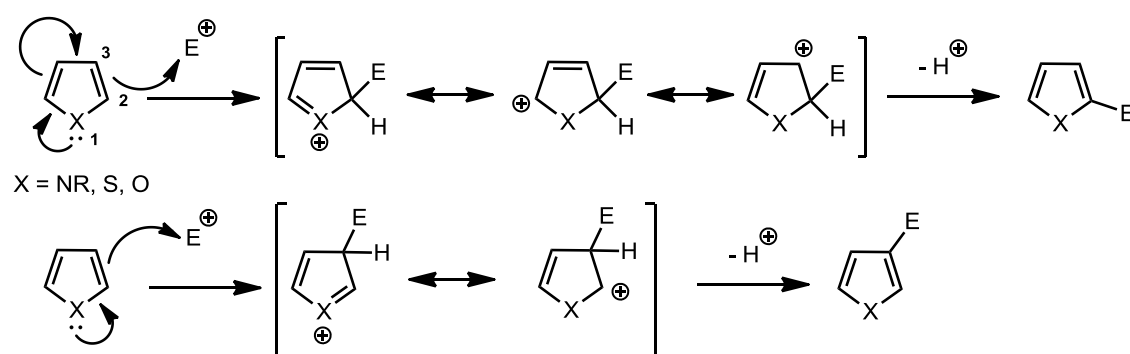
Direct arylation offers the ability to functionalise simple, inexpensive and readily available heterocycles in order to create biaryl molecules, and has been a topic of extensive research over the past 20 years, with several reviews published.^{105,296–299}

This introduction will focus only on direct arylation of the 5-membered heterocycles pyrrole, thiophene, furan, imidazole, thiazole and oxazole, as these substrates have several C-H bonds which can be functionalised, each with different electronic influences. The focus of this introduction is on the control of regioselectivity in direct arylations and it will attempt to give representative examples rather than an exhaustive review. For a review of strategies to control the regioselectivity of C-H activation, see Ch. 1.2.3.

Reactivity of 5-Membered Heteroarenes

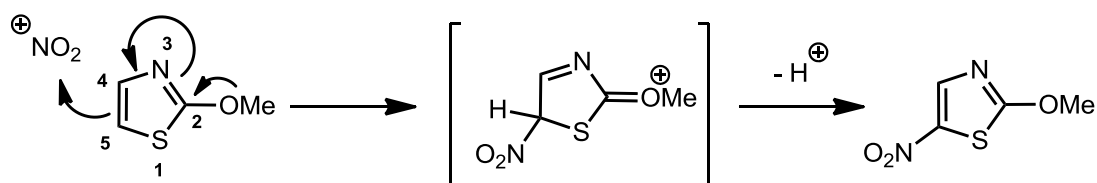
Aromatic heterocycles, due to the nature of their heteroatom, are generally more reactive to aromatic substitution reactions and deprotonation than their homocyclic equivalents. The related 5-membered ring heterocycles pyrrole, thiophene and furan are all electron rich and undergo electrophilic aromatic substitution, with possible

reactivity at C2 or C3, **Scheme 5.6**. In practice, the attack at C2 (top, **Scheme 5.6**) is favoured over C3 (bottom, **Scheme 5.6**), as the intermediate formed from C2 attack has greater delocalization of the resulting positive charge than the intermediate for C3 attack, lowering the energy of the C2 intermediate and therefore the activation energy for S_EAr at this position.³⁰⁰ The ease of S_EAr proceeds in the order pyrrole > furan > thiophene; electron-donating or –withdrawing substituents on the ring can increase or decrease reactivity respectively.



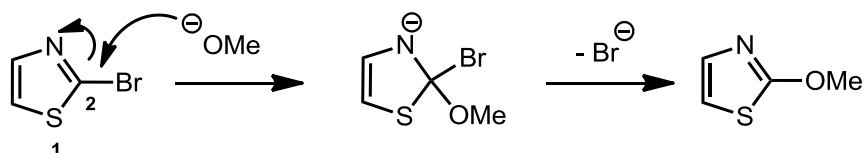
Scheme 5.6: Electrophilic aromatic substitution on pyrrole, thiophene and furan.

1,3-Azoles are considerably less reactive towards electrophilic attack than pyrrole, thiophene or furan, as the additional pyridine-like nitrogen in the ring has an electron-withdrawing and therefore deactivating effect. Under acidic conditions the nitrogen can protonate, producing an azolium cation which is even more inert. Electrophilic substitution of imidazole, thiazole and oxazole generally occurs only if activating groups are present, **Scheme 5.7**, although imidazole can be nitrated under forcing conditions; these substitutions occur at C5.³⁰⁰



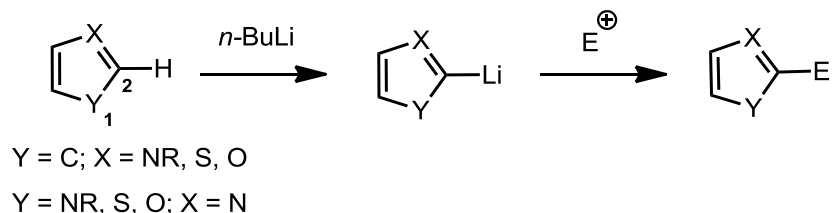
Scheme 5.7: Electrophilic aromatic substitution on an activated thiazole.

Nucleophilic aromatic substitution does not occur on pyrrole, thiophene or furan rings unless an extremely strong electron-withdrawing group and leaving group are present. 1,3-Azoles are reactive to S_NAr at the C2 position, due to the electron-withdrawing effect of the nitrogen atom, although this is slow unless an additional electron-withdrawing group is present, such as a halogen, **Scheme 5.8**.³⁰⁰



Scheme 5.8: Nucleophilic aromatic substitution on an activated thiazole.

The most acidic C-H on pyrrole, thiophene and furan is at C2 (C2 pK_a : pyrrole, 39.5; thiophene, 33; furan, 35.6), due to the electron-withdrawing effect of the adjacent heteroatom (pyrrole N-H is more acidic than C-H); this also applies to the 1,3-azoles which have two heteroatoms withdrawing electrons from the C2 position (C2 pK_a : imidazole, 33.7; thiazole, 29.4; oxazole, *ca.* 20).³⁰¹ C2 can be deprotonated with strong bases such as *n*-butyllithium and reacted with electrophiles, **Scheme 5.9**.



Scheme 5.9: Deprotonation of 1,3-azoles.

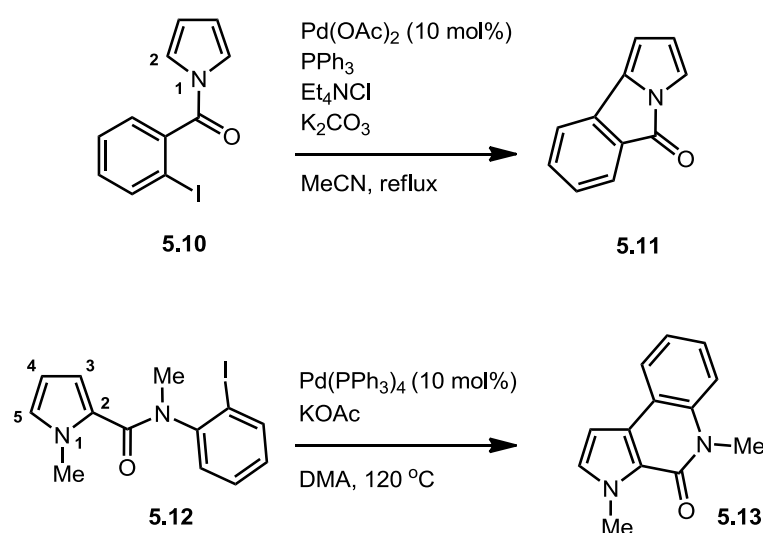
Due to the selectivity of these modes of reactivity, it can be seen that the C3 position on pyrrole, thiophene and furan, and the C4 position on 1,3-azoles are less reactive, and much more difficult to functionalise.

The regioselectivity of C-H activation in direct arylation reactions can be controlled by several methods, previously discussed in Ch. 1.2.3. The control of regioselectivity in direct arylations of pyrroles, thiophenes, furans, imidazoles, thiazoles and oxazoles will be discussed next.

Intramolecular Direct Arylation

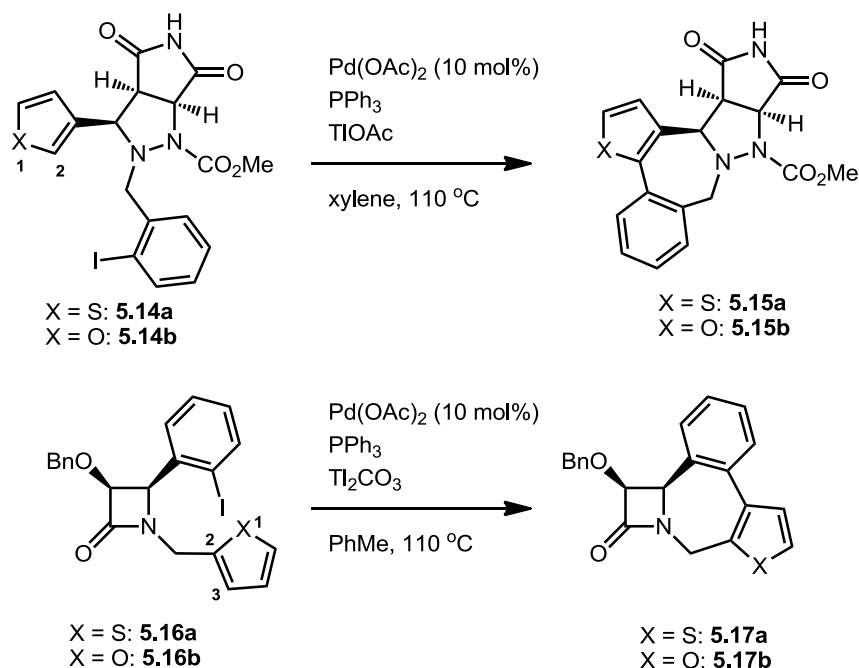
One method to control the regioselectivity and increase the rate of reaction of direct arylation is to perform the arylation in an intramolecular fashion. Tethering the heterocycle to an aryl halide in order to perform a direct arylation can also help to direct the arylation to a carbon on the heteroarene which would not be the most reactive in an intermolecular reaction. This control can be brought about kinetically, as the aryl halide tends to react with the most available C-H bond, and also thermodynamically, as the strain energy in the newly-formed ring has an effect. Nevertheless, the electronics of the C-H bond, as discussed for S_EAr / S_NAr / deprotonation, still play a significant role.

Intramolecular arylation of the *N*-acyl pyrrole **5.10** leads to a [6,5,5] ring system **5.11**, where arylation occurs at C2 on the pyrrole (**Scheme 5.10**).³⁰² This is the most reactive carbon on **5.10**, and would be the expected outcome, rather than arylation at the less reactive C3 position. However, the pyrrole **5.12**, with the aryl halide tethered by an amide group at C2 on the pyrrole, does not undergo reaction at the (now most reactive) C5 site, but instead at the kinetically accessible C3 position, giving product **5.13**.³⁰³



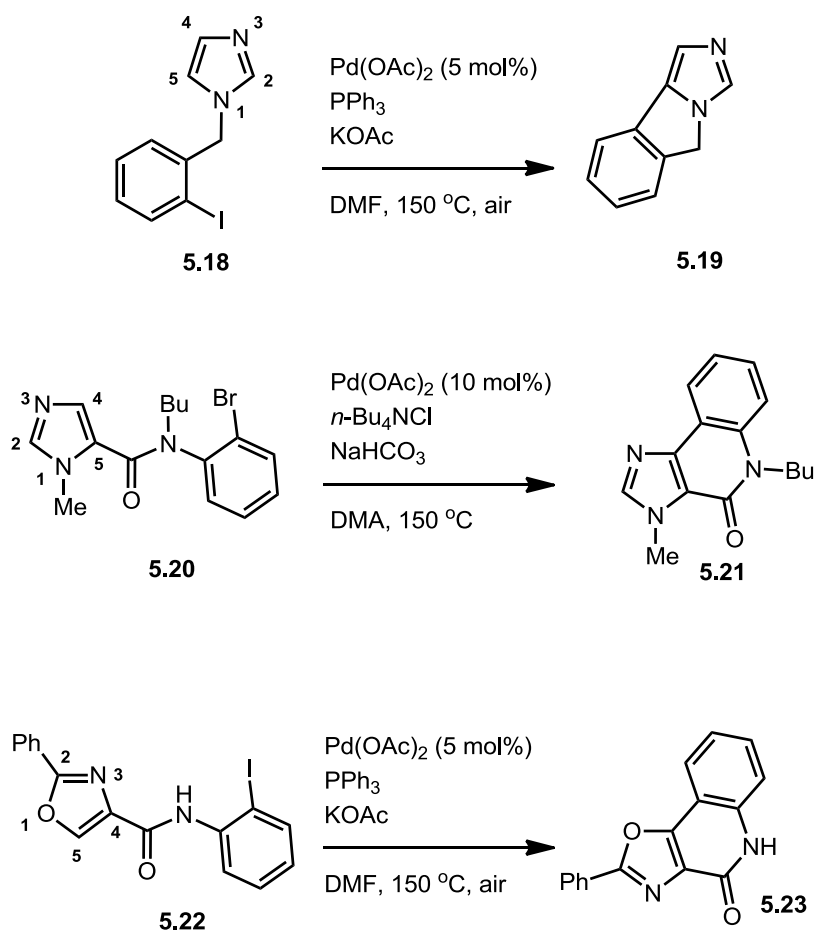
Scheme 5.10: Examples of intramolecular direct arylation of pyrroles.^{302,303}

Similar results are observed in the intramolecular arylation of thiophenes and furans. Thiophene **5.14a** and furan **5.14b** undergo direct arylation at the most reactive C2 site over C4, even though both are equally kinetically accessible, **Scheme 5.11**.³⁰⁴ When C2 is blocked or is the site of the intramolecular tether, as in **5.16a-b**, the arylation is now at C3 over C5, forming a 7-membered ring rather than a disfavoured 8-membered ring.³⁰⁵



Scheme 5.11: Examples of intramolecular direct arylation of thiophenes and furans.^{304,305}

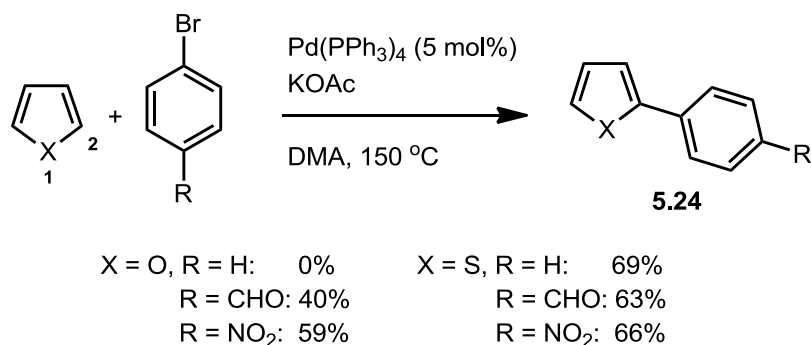
Intramolecular arylations of imidazoles and oxazoles are also known; C-H activation at the nucleophilic C5 position is usual, for example on *N*-substituted imidazole **5.18** (**Scheme 5.12**).³⁰⁶ If C5 is blocked, thermodynamic control generally directs arylation to the carbon that gives the lowest energy product, for example with C5-substituted imidazole **5.20**, which arylates at C4 forming a 6-membered ring product **5.21**, rather than reaction at C2 to give a 7-membered ring product.³⁰⁷ Sometimes regioselectivity of arylation is controlled simply by having only one C-H available to react, as with substituted oxazole **5.22**.³⁰⁸



Scheme 5.12: Examples of intramolecular direct arylation of imidazoles and oxazoles.^{306–308}

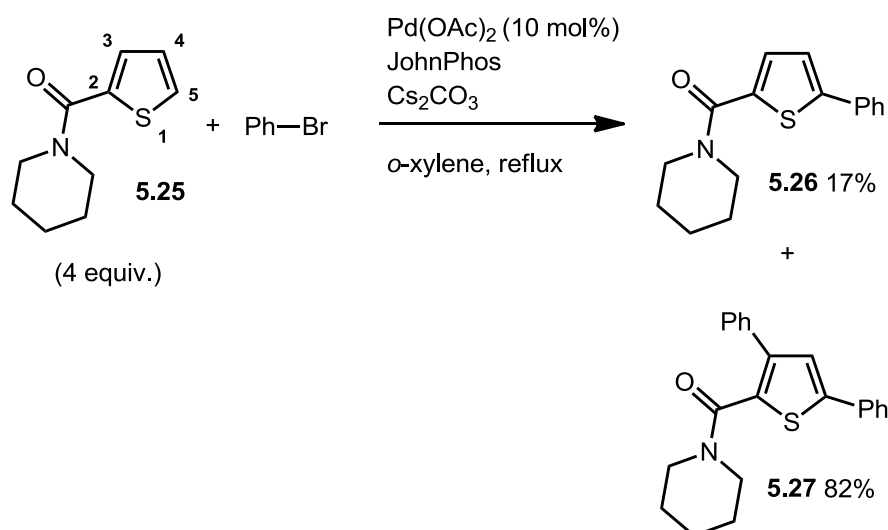
Intermolecular Direct Arylation

Intermolecular direct arylation often poses a more difficult challenge of regioselectivity than for a directed intramolecular arylation. In the case of simple thiophene and furan, arylation occurs at the C2 position preferentially. The first catalytic direct arylation conditions for thiophene and furan were reported by Ohta *et al.*, and were regioselective for C2, with no other arylation products reported, **Scheme 5.13**.³⁰⁹ Interestingly, only electron-deficient aryl bromides reacted with furan but thiophene reacted even with bromobenzene.



Scheme 5.13: Direct arylation of furan and thiophene with aryl bromides.³⁰⁹

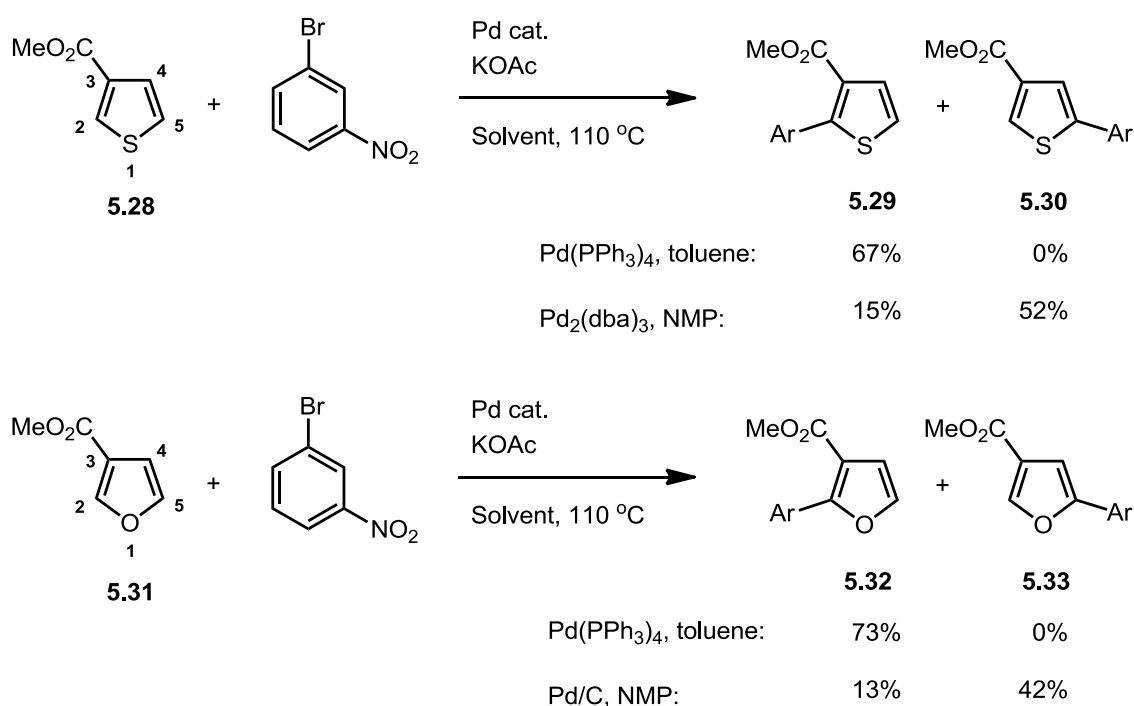
Substitution on the heteroaromatic ring can affect the regioselectivity of arylation. The 2-substituted thiophene **5.25** is observed to react at C5 to product **5.26**, but this product reacts again at the less reactive C3 position to give the 3,5-diphenyl product **5.27**, **Scheme 5.14**.³¹⁰ However, in this case, the starting thiophene **5.25** is in large excess compared to the aryl halide, suggesting the monoarylated product **5.26** is far more reactive to arylation than **5.25**.



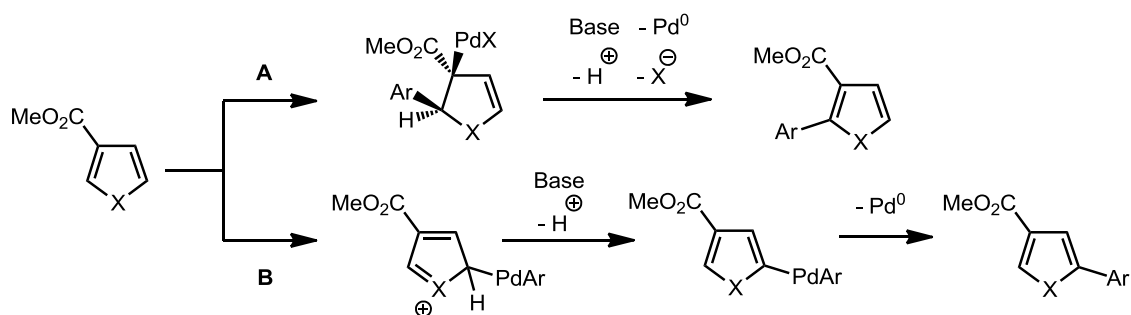
Scheme 5.14: Direct arylation of 2-substituted thiophene **5.25**.³¹⁰

A different regioselectivity issue arises with 3-substituted thiophenes (**5.28**) and furans (**5.31**), **Scheme 5.15**. In these cases, arylation can occur at C2 to form **5.29** and **5.32**, or

C5 to form **5.30** and **5.33**. Sharp *et al.* investigated these systems in support of a medicinal chemistry program to identify regioselective routes to 2-arylated products **5.29** and **5.32**. By screening of conditions, they found that the dielectric constant of the solvent correlated with the ratio of products (**5.29** and **5.32** vs. **5.30** and **5.33**), with non-polar solvents favouring arylation at C2 and polar solvents favouring arylation at C5. The catalyst/ligands used also had an effect, with phosphine ligands favouring arylation at C2. The authors suggest that two mechanisms are involved (**Scheme 5.16**): a Heck-type reaction at C2 with a non-polarised Pd-C bond in the intermediate, stabilised by the phosphine and non-polar solvent combination, and an electrophilic reaction at C5, where the polar solvent would stabilise an electrophilic Pd^{II} species which would then react at the most electron-rich C5 position.

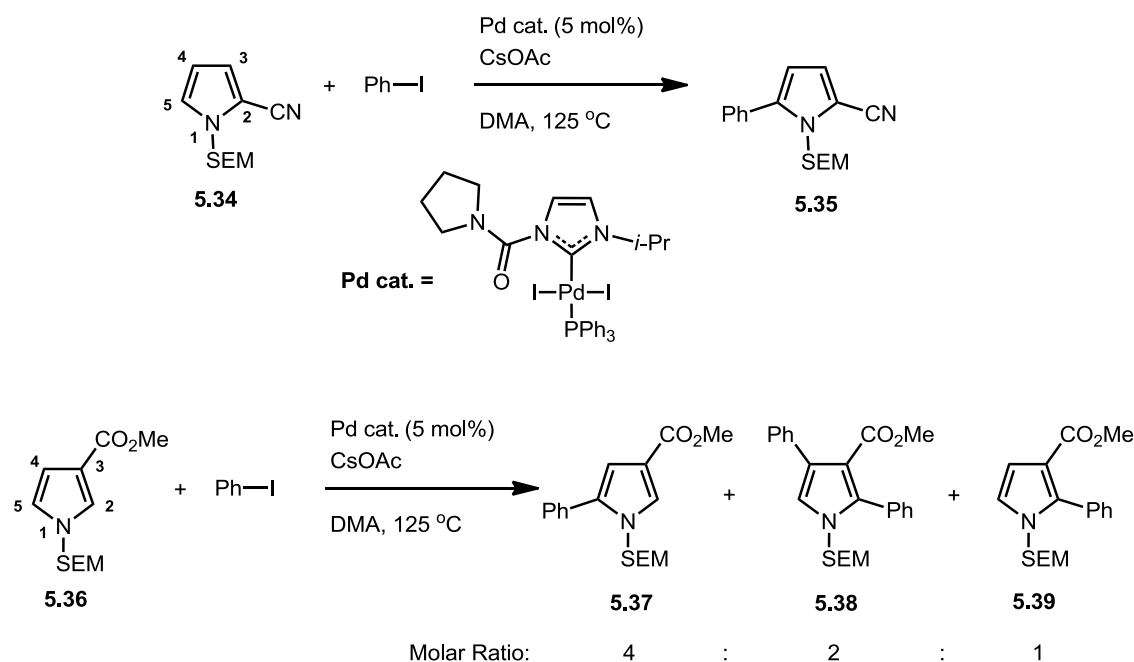


Scheme 5.15: Catalyst/solvent control of regioselectivity in the direct arylation of a 3-substituted thiophene or furan.³¹¹



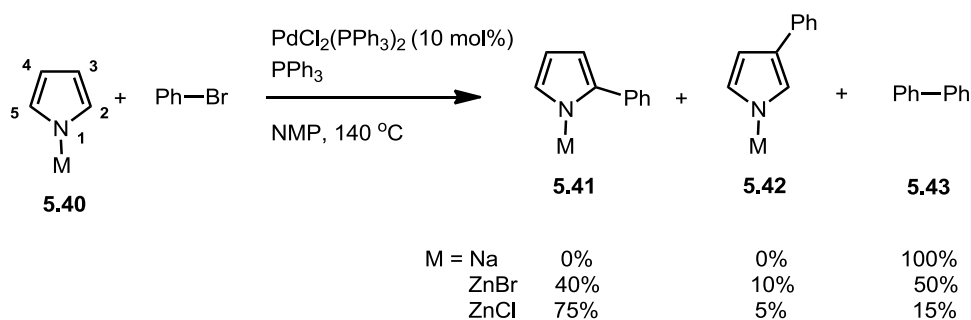
Scheme 5.16: Heck-like (A) and electrophilic (B) mechanisms for direct arylation of furan/thiophene, postulated by Sharp.³¹¹

Sames *et al.* have shown that similar regioselectivity is observed for the arylation of *N*-protected pyrroles, with electron-poor pyrrole **5.34** reacting at the available, reactive C5 site, **Scheme 5.17**.³¹² 3-Substituted pyrrole **5.36** reacts preferentially at C5 to form **5.37**, although some reaction occurs at C2 to form **5.39**;³¹² this is in line with the observations of Sharp *et al.* for the arylation of 3-substituted thiophenes and furan as discussed above.³¹¹ In contrast, however, the 2,4-diarylated product **5.38** is also a product of the reaction of the pyrrole **5.36** which is not observed for 3-substituted furan (**5.31**) or thiophene (**5.28**); this could be a reflection of the nucleophilicity of pyrroles compared with furans and thiophenes.³⁰⁰



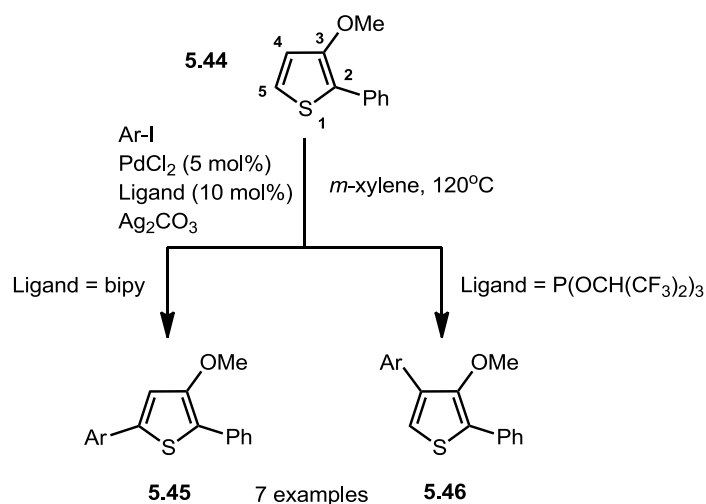
Scheme 5.17: Direct arylation of *N*-protected pyrroles **5.34** and **5.36**.³¹²

Other substituent effects on regioselectivity have also been observed; in the case of *N*-metallated pyrroles **5.40** the nature of the metal coordinated to the pyrrole anion affects the reactivity, **Scheme 5.18**. Pyrrol-1-ylsodium gives no arylation reaction, whereas pyrrol-1-ylzinc halides give a mixture of C2 (**5.41**) and C3 (**5.42**) arylation products, favouring C2 arylation. Furthermore, the nature of the halide (bromide or chloride) appears to impact on the ratio of C2/C3 arylation, although the reason for this is not clear.



Scheme 5.18: Direct arylation of *N*-metallated pyrroles **5.40**.³¹³

For the reactions discussed so far, the regioselectivity has been determined by the substituents on the heterocyclic ring. However, Irami has shown that for the direct arylation of thiophenes the regioselectivity can be controlled simply by changing the ligand used, **Scheme 5.19**.¹⁰⁶ In this work, selectivity for arylation at C5 or C4 is switched dependant on the ligand used: C5 arylation is preferred with the bipyridyl ligand, and C4 arylation is preferred with the $\text{P}(\text{OCH}(\text{CF}_3)_2)_3$ ligand. This selectivity is unaffected by the electronics of the aryl iodide used, giving more than 93:7 selectivity for all examples, including both highly electron-deficient and electron-rich arenes. The reasons for this selectivity were investigated computationally by Fu *et al.*,¹⁰⁷ who suggested that C5 arylation (bipy ligand) proceeded by an AMLA-type mechanism. The AMLA-type mechanism was also simulated with the $\text{P}(\text{OCH}(\text{CF}_3)_2)_3$ ligand, but this was also found to favour arylation at C5, contrary to the observed experimental results. However, the $\text{P}(\text{OCH}(\text{CF}_3)_2)_3$ ligand was calculated to stabilise an intermediate in a Heck-type arylation mechanism through hydrogen bonding, which in turn favoured arylation at C4, in agreement with experimental results. This catalyst/ligand-controlled selectivity is a very attractive strategy for selective C-H activation reactions.

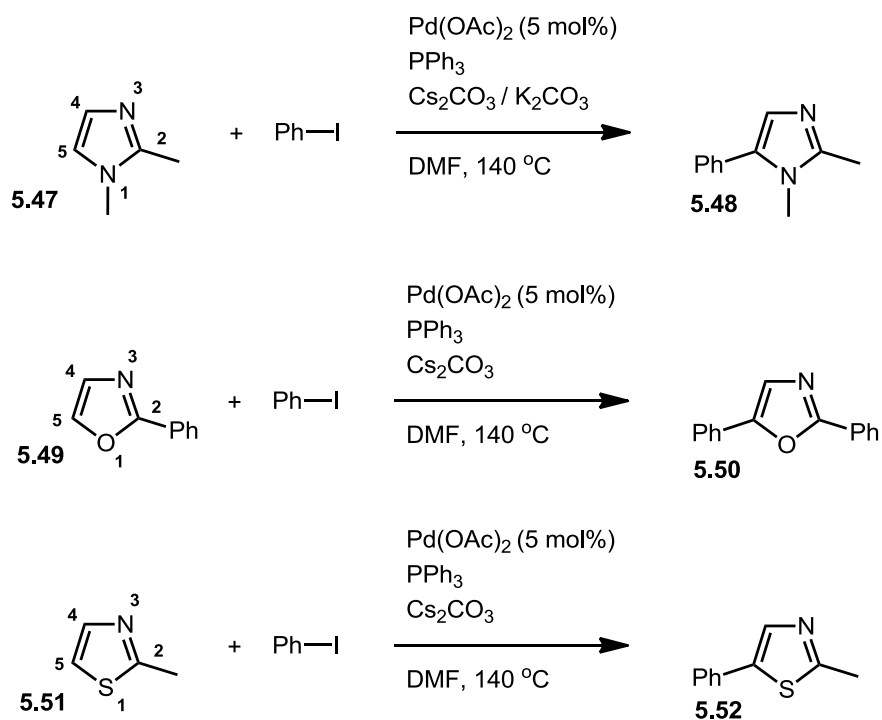


Scheme 5.19: Ligand-controlled change of direct arylation regioselectivity on substituted thiophene **5.44**.

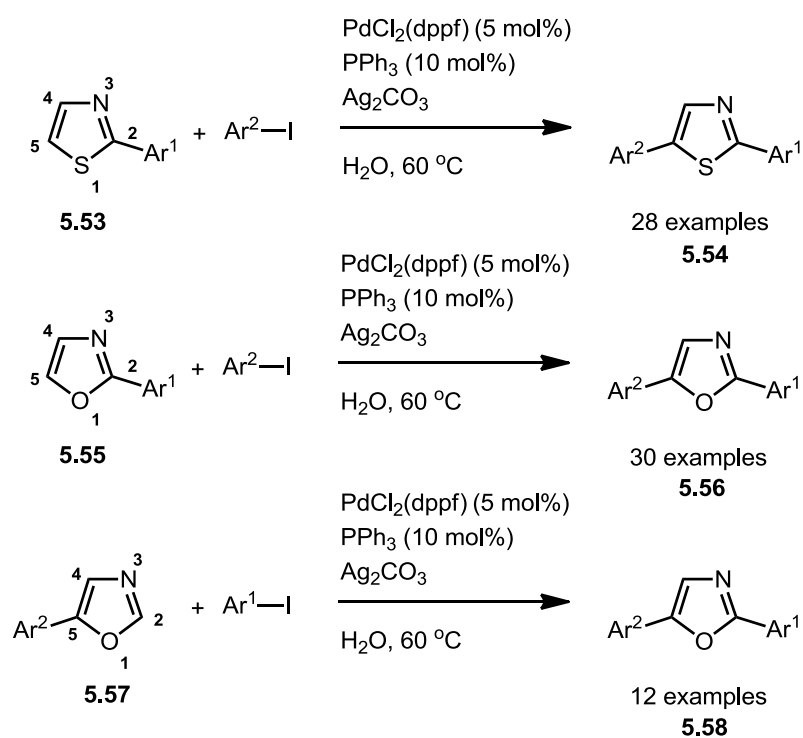
The regioselectivity of direct arylation of 1,3-azoles is apparently dependant on several factors. One strategy for obtaining regioselective arylations is to have a blocking group at positions where unwanted arylation would occur. C5-arylation is observed in the case of a C2-substituted 1,3-azole, **Scheme 5.20**.³¹⁴ In these cases, no C4 arylation is observed, and C5 is expected to be the most reactive in an electrophilic reaction.³⁰⁰

Greaney *et al.* have observed identical C5 arylation in the low temperature ‘on-water’ direct arylation reactions of C2-substituted oxazole and thiazole, **Scheme 5.21**.^{315,316}

Interestingly, when C5 substituted oxazoles **5.57** are subjected to the same direct arylation conditions, arylation occurs at C2, suggesting that both C5 and C2 positions are reactive, but not C4.³¹⁷

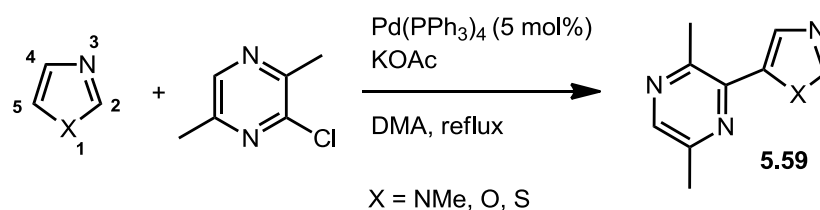


Scheme 5.20: Direct arylation of C2-substituted 1,3-azoles.³¹⁴



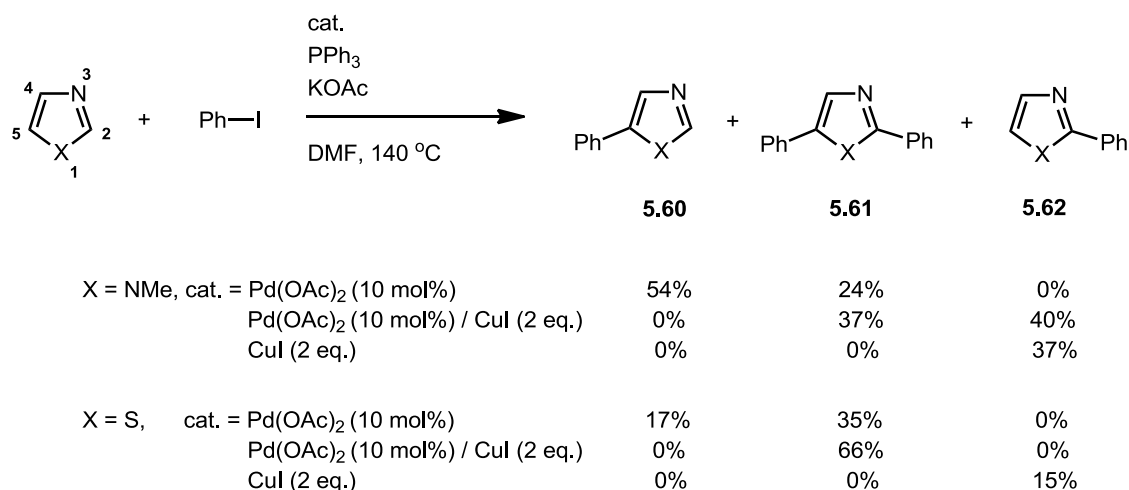
Scheme 5.21: 'On water' direct arylation of C2-substituted thiazoles,³¹⁵ and C2- and C5-substituted oxazoles.^{316,317}

In the case of unsubstituted 1,3-azoles, direct arylation appears to occur preferentially at C5, as exemplified by the reactions of *N*-methyl imidazole, thiazole and oxazole with 2-chloropyrazine, **Scheme 5.22**.³¹⁸ However, diarylation at C2 and C5 is observed with some catalyst systems.³¹⁴

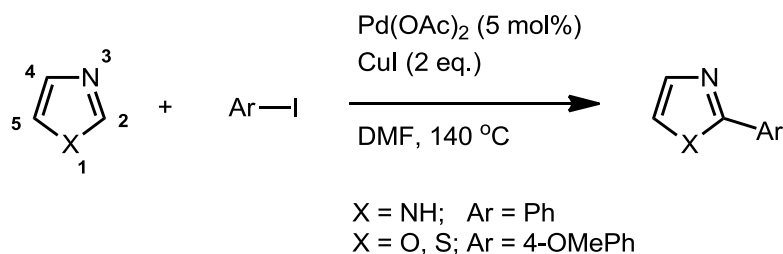


Scheme 5.22: Direct pyrazinylation of unsubstituted 1,3-azoles.³¹⁸

It has also been observed that the addition of copper salts can affect the regioselectivity of direct arylation. The use of Pd/Cu co-catalyst systems give C2 monoarylation and C2/C5 diarylation, with no C5 monoarylation observed, while using only CuI without palladium shows arylation only at C2, **Scheme 5.23**.³¹⁴ Similarly, a base-free arylation protocol using Pd(OAc)₂/CuI shows exclusive C2 arylation on imidazole, oxazole and thiazole, **Scheme 5.24**.³¹⁹ The drastic change in regioselectivity with copper salts suggest that reactions catalysed only by palladium prefer an electrophilic mechanism at the electron-rich C5 site, while the presence of copper changes the reaction mechanism to a deprotonation at the electron-poor C2 site.³¹⁴



Scheme 5.23: The effect of Pd/Cu catalyst systems on direct arylation of *N*-methylimidazole and thiazole.³¹⁴

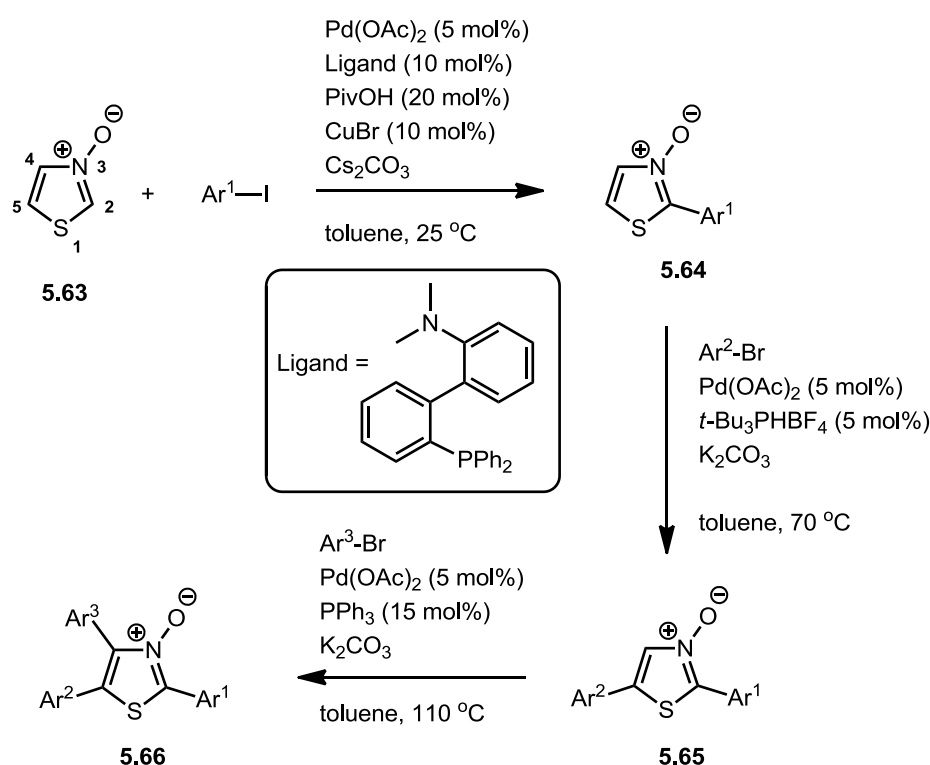


Scheme 5.24: Base-free C2 arylation of imidazole, oxazole and thiazole.³¹⁹

Complete C2 selectivity has also been observed to be favoured in direct arylation reactions on oxazole where strong bases such as KOH and *t*-BuOK are used in toluene; deprotonation is the most likely mechanism of C-H activation in this case.³²⁰

Fagnou *et al.* have shown that the regioselectivity of direct arylation on 1,3-azoles can also be manipulated by generating the azole-*N*-oxide, **Scheme 5.25**.^{75,8} Thiazole-*N*-oxide **5.63** is arylated selectively at C2, in extremely mild conditions. Subsequent selective C5 arylation and C4 arylation can be performed using harsher conditions. The authors suggest that the shift of reactivity and regioselectivity of thiazole-*N*-oxide

compared to thiazole is due to a change in π -nucleophilicity of the ring.³²¹ A DFT-calculated representation of the HOMO (**Figure 5.4**) of thiazole shows almost equal distribution of electron density around C2, C4 and C5, suggesting little differentiation between the three sites. The corresponding HOMO for thiazole-*N*-oxide (**Figure 5.4**) shows a much higher HOMO electron density on C2 than at C4/C5, making C2 more π -nucleophilic; similarly in C2-phenyl thiazole-*N*-oxide, C5 has a higher HOMO electron density than C4, making C5 the most π -nucleophilic carbon available for reaction. This reactivity pattern is also observed in imidazole-*N*-oxides.^{75,8}



Scheme 5.25: Sequential triarylation of thiazole-*N*-oxide.⁴⁵

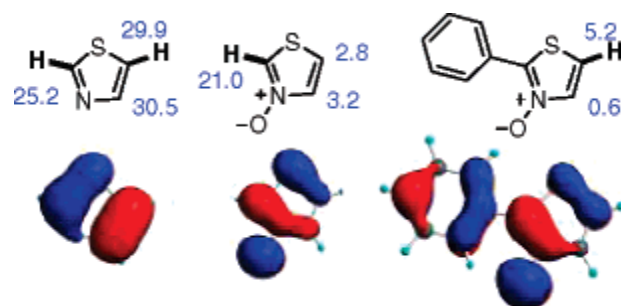


Figure 5.4: Representations of the HOMO for thiazole, thiazole-N-oxide, and C2-phenyl thiazole-N-oxide. The numbers represent % atomic contributions to the HOMO; image reproduced from Ref. 45.⁴⁵

5.1.3: Aims and Objectives

The aim of the work in this chapter was to investigate the activity of complexes synthesised in Chapters 3 and 4 as catalysts/precatalysts in two catalytic reactions: transfer hydrogenation of acetophenone and direct arylation of heteroarenes. These two reactions would allow investigation into whether a reactive late-transition metal amido-NHC complex could be used to facilitate bifunctional bond cleavage across the M-N bond, and offer ligand control of the regioselectivity in heteroarene C-H activation.

Transfer hydrogenation is a well researched example of bifunctional catalysis that enabled comparisons of the new amino/amido-NHC catalysts with a wide range of metal -ligand systems that have previously been reported. The author hoped to observe good catalytic activity and involvement of the amino/amido-NHC ligand in catalysis, in a bifunctional mechanism.

The direct arylation of heteroarenes allowed us to test whether the N-donor ligand of amino/amido-NHC complexes can have a positive effect on the rate of reaction or assist in the control of the regioselectivity of arylation. 5-Membered heteroarenes were chosen as substrates to test this hypothesis because they have several available C-H bonds at which to react allowing us to investigate regioselectivity of arylation. Attempts were made to determine if the nitrogen donor on the NHC ligand facilitated C-H activation by comparison to unfunctionalised-NHC complexes and traditional Pd(OAc)₂/PPh₃ catalytic mixtures.

5.2: Results and Discussion

5.2.1: Transfer Hydrogenation of Acetophenone

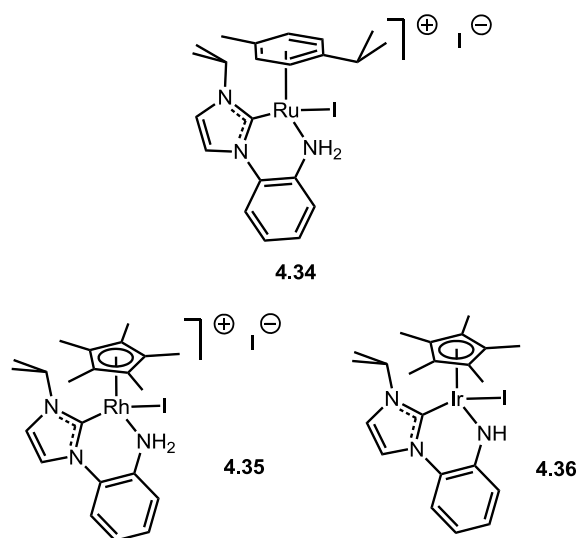


Figure 5.5: Complexes studied for activity in the transfer hydrogenation of acetophenone.

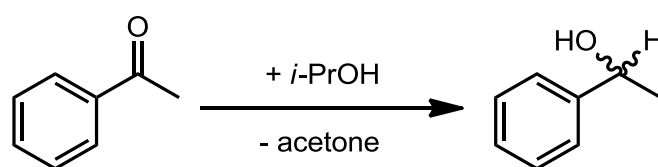
The transfer hydrogenation of acetophenone in *isopropanol* to 1-phenylethanol was investigated, as a well-studied reaction,²⁴ that enabled comparison of the reported amino/amido-NHC complexes to other catalytic metal-ligand systems. The Ru and Rh amino-NHC complexes **4.34** and **4.35** and Ir amido-NHC complex **4.36** (Figure 5.5, described in Chapter 4) were selected as potential precatalysts. Complexes **4.34-4.36** are similar to Noyori's diamine precatalysts for transfer hydrogenation: all are half-sandwich d^6 metal complexes containing an amine (or amide) ligand, with a halide ligand. However, **4.34-4.36** have a strongly donating, neutral NHC ligand, as with Morris's complexes **4.29**, **4.20** and **4.21**; the active catalytic amide for **4.34-4.36** is therefore expected to be a cationic amide complex, rather than a neutral amide

species as for Noyori's diamine complexes, for example Ru(*p*-cymene)(TsDPEN)Cl **5.1**.

As well as the presence of the amino-NHC ligand this different charge on the catalyst may have an influence on the reaction.

In the transfer hydrogenation reactions, *isopropanol* was present as both the solvent and the hydrogen donor for reduction of acetophenone. Sodium *tert*-butoxide (4 mol%) was used as a base in order to generate a catalytically active amide complex *in situ*, except for some runs using iridium precatalyst **4.36** which already contains an amido ligand. The catalyst loading was very low, at 0.5 mol%. All reaction conversions were determined by GC analysis and monitored over time, and all reactions were repeated to confirm the reproducibility of the reaction (conversions are the average of two runs). The results are displayed in **Table 5.1**.

Table 5.1: Results of catalytic transfer hydrogenation of acetophenone by complexes **4.34-4.36**.



Entry	Cat.	Base	Additive	Temp. (°C)	Conversion (%) (determined by GC)			
					0.5 h	1 h	24 h	72 h
1	4.34	<i>t</i> -BuONa	–	80	91	95	–	–
2	4.34	<i>t</i> -BuONa	AgPF ₆	80	93	93	–	–
3	4.34	<i>t</i> -BuONa	–	20	0	0	0	0
4	4.35	<i>t</i> -BuONa	–	80	–	7	86	99
5	4.35	<i>t</i> -BuONa	AgPF ₆	80	–	3	75	96
6	4.36	<i>t</i> -BuONa	–	80	–	7	78	96
7	4.36	<i>t</i> -BuONa	AgPF ₆	80	–	9	46	68
8	4.36	–	–	80	–	0	11	24
9	4.36	–	AgPF ₆	80	–	0	2	3

All reactions were performed in *i*-PrOH, with a cat./base/substrate ratio of 1:8:200

The ruthenium amine-NHC complex **4.34** was very active in the transfer hydrogenation reaction at 80 °C, giving a conversion of >90% after 30 min, with a maximum conversion of 95% after 1 h. The TON (190) for **4.34** was equal to that observed with Noyori's Ru(mesitylene)(TsDPEN)Cl (**5.66**) precatalyst; however, **5.66** operated at a lower temperature (28 °C) than **4.34**, albeit with longer reaction time of 15 h.²¹¹ The TOF for **4.34** over the first 0.5 h (364 h⁻¹) was comparable to that of Morris' analogous amine-NHC [Ru(*p*-cymene)(C,NH₂)Cl]PF₆ complex **4.19** over 3 h at 75 °C (326 h⁻¹).¹⁷

In comparison, the rhodium amine-NHC complex **4.35** was less active than ruthenium complex **4.34**, giving an excellent 99% conversion but over 72 h, with a TON of 198 but a TOF of only 2.75 h⁻¹. As far as the author is aware, no other amine-NHC Rh^{III} complexes have been tested for transfer hydrogenation. However, Fryzuk *et al.* have reported an amine-NHC Rh^I complex (**4.6**)¹⁶³ which was moderately active for transfer hydrogenation. The complex RhCp*(TsDPEN)Cl (**5.67**) showed lower activity than **4.35** (14% conversion over 12 h, TON = 28) but again at a lower temperature of 30 °C, while the related complex RhCp*(TscydN)Cl (**5.68**, **Figure 5.6**) was more active than both **5.67** and **4.35** at 30 °C (85% conversion over 12 h, TON = 170).²⁶

The iridium amido-NHC complex **4.36** showed comparable activity to the rhodium amino-NHC complex **4.35**, with 96% conversion over 72 h (TON: 198, TOF: 2.67 h⁻¹). This activity was again poor compared with the ruthenium complex **4.34**, and comparable to the activity displayed by IrCp*(TscydN)Cl (**5.69**, **Figure 5.6**) at 30 °C (36% conversion over 12 h, TOF: 6.00 h⁻¹).²⁶

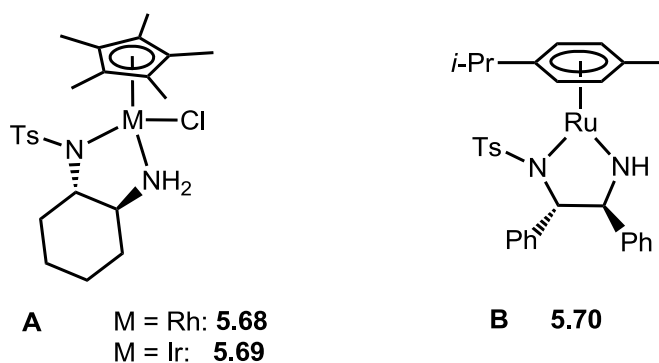


Figure 5.6: **A:** $M\text{Cp}^*(\text{Tscyd}n)\text{Cl}$ **5.68** and **5.69**, precatalysts for the asymmetric hydrogenation of imines; **B:** ruthenium amido complex **5.70** derived from $\text{Ru}(\text{p-cymene})(\text{TsDPEN})\text{Cl}$ (**5.1**)

1.2 equivalents of AgPF_6 were added into the catalytic reactions of complexes **4.34**-**4.36**, in order to remove the bound iodide ligand on the precatalyst and facilitate substrate binding. A control reaction was first performed containing AgPF_6 and no precatalyst; this showed no conversion of acetophenone to 1-phenylethanol over several hours, demonstrating that the silver salt alone has no catalytic activity.

Addition of AgPF_6 to the catalytic reactions containing **4.34** and **4.35** had no significant effect on the activity of the catalysts. In the case of **4.36**, the addition of AgPF_6 had an unexpected detrimental effect on the catalytic activity, reducing conversion after 72 h from 96% to 68%. The reason for this reduced activity is unclear; in contrast silver salts had a positive effect on the catalytic activity and enantioselectivity of $\text{IrCp}^*(\text{Tscyd}n)\text{Cl}$ (**5.69**) in the asymmetric hydrogenation of imines.³²² However, this promotion of imine hydrogenation has been ascribed to activation of the imine substrate by interaction between Ag and the imine N, which is not necessarily applicable to the transfer hydrogenation of ketones.

The active catalysts for transfer hydrogenation are metal amido species which are usually generated from a metal amino precatalyst through deprotonation by base *in situ*. However, a ruthenium amido complex **5.70** (Figure 5.6) derived from Ru(*p*-cymene)(TsDPEN)Cl (**5.1**) has been observed to catalyse the transfer hydrogenation of acetophenone in the absence of base.²⁴ It was decided to investigate if the iridium amido complex **4.36** would also catalyse this reaction without base present. In the absence of base, **4.36** gave a conversion of 24% over 72 h, with a TON of 48. Although this activity is much lower than that observed for **4.36** with base present, the fact that catalytic turnover was occurring suggests the amido ligand is promoting transfer hydrogenation.

Discussion of the Mechanism of Transfer Hydrogenation Catalysed by Amino/Amido-NHC Complexes

Morris *et al.* have performed detailed studies into the mechanism of catalytic transfer hydrogenation for the related ruthenium amino-NHC [Ru(*p*-cymene)(C,NH₂)Cl]PF₆ complexes **4.19** and **5.71**.¹⁷

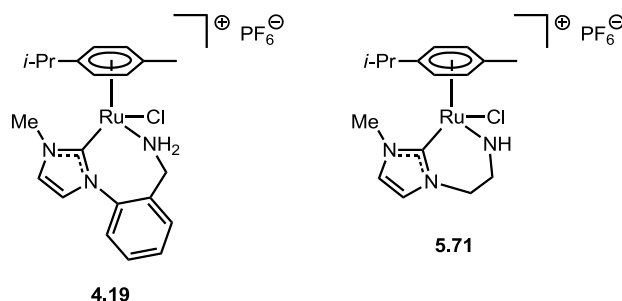
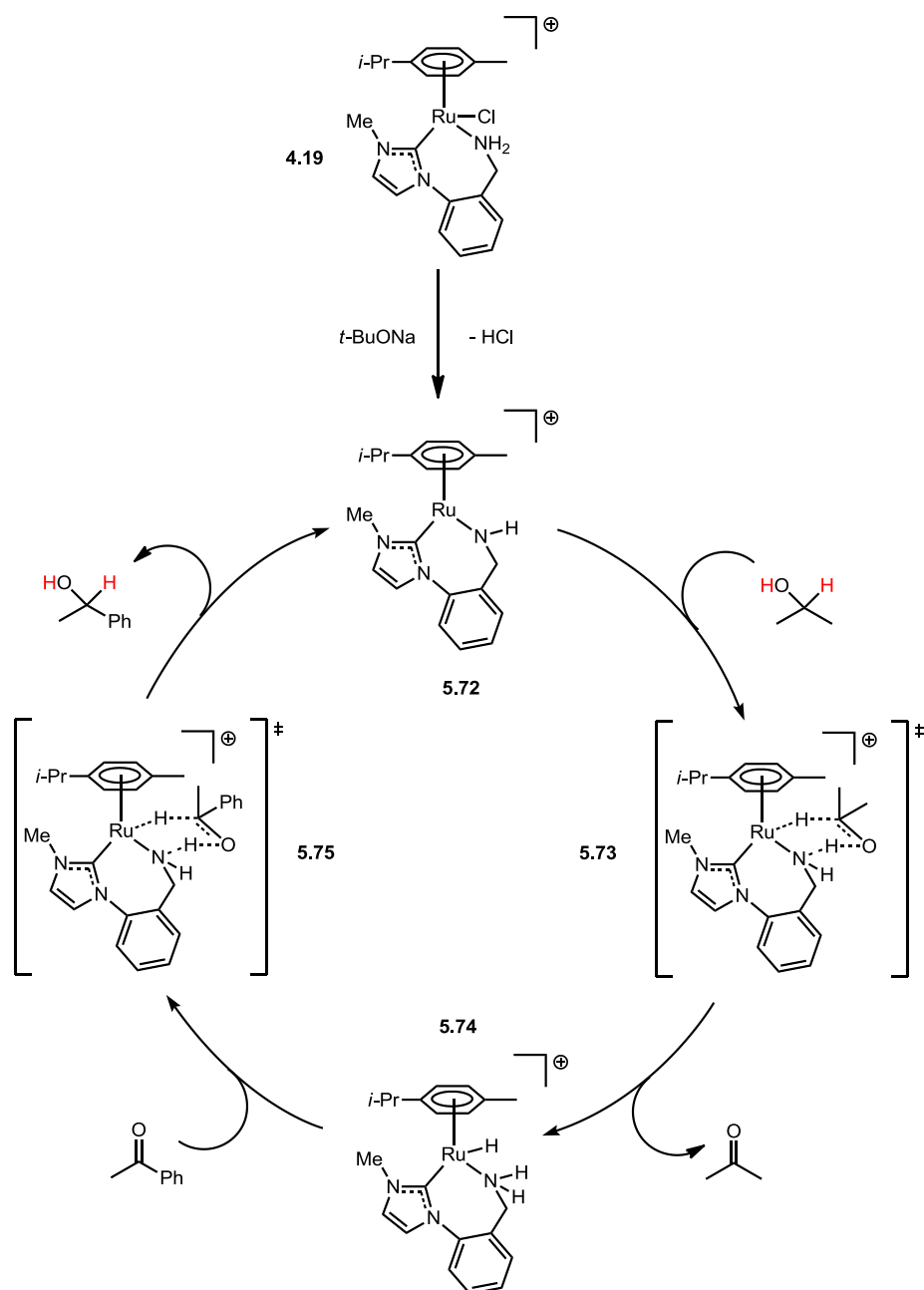
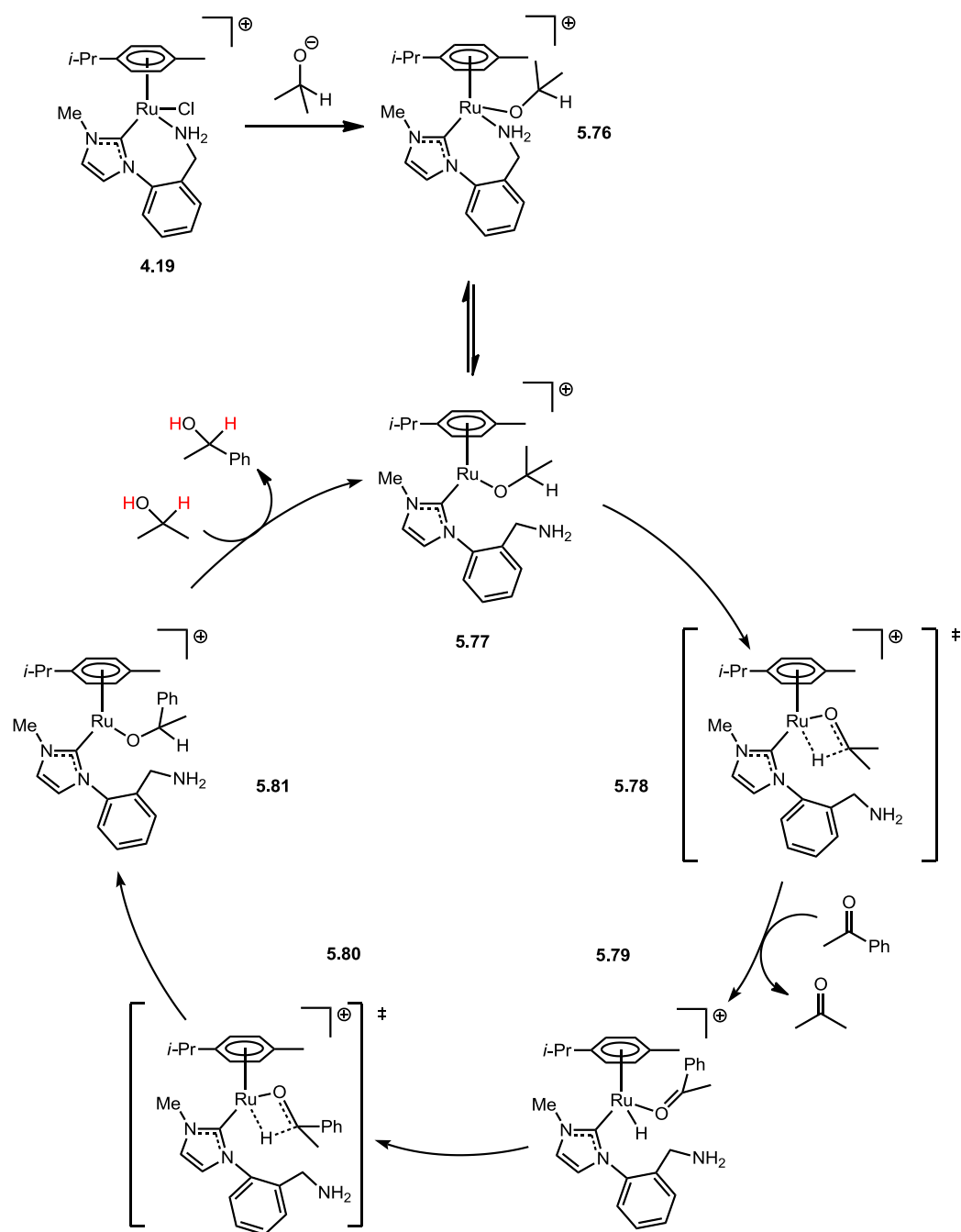


Figure 5.7: Ruthenium amino-NHC precatalysts studied computationally in the transfer hydrogenation of ketones.

Two potential mechanisms were investigated: an outer sphere mechanism (**Scheme 5.26**) and an inner sphere mechanism (**Scheme 5.27**). In the outer sphere mechanism, first postulated by Noyori (see also **Scheme 5.2**),²¹³ a reactive metal amide complex **5.72** removes hydrogen from an alcohol donor in a concerted, bifunctional fashion *via* a 6-membered transition state (**5.73**) to give an amine-hydride complex **5.74**. Complex **5.74** then reduces the substrate ketone in a concerted fashion *via* another 6-membered transition state (**5.75**) to regenerate the active metal amide **5.72**. In contrast, the inner sphere mechanism proceeds by coordination of an alkoxide to the metal centre (**5.76**) followed by dissociation of the amine arm of the bidentate (C,N) ligand to give the active metal alkoxy catalyst **5.77**. The metal centre then abstracts a hydride from the alkoxy ligand *via* β -hydrogen elimination (**5.78**) to generate a ketone that is exchanged for the substrate ketone giving a metal hydride complex (**5.79**) with a coordinated substrate molecule. The hydride ligand transfers to the substrate molecule *via* transition state **5.80** to give complex **5.81** which has an alkoxy ligand that exchanges with a solvent molecule to regenerate the reactive metal alkoxy complex **5.77** and release the product alcohol.



Scheme 5.26: Outer sphere mechanism for transfer hydrogenation of ketones by amino-NHC Ru complex **4.19**.^{17,213}



Scheme 5.27: Inner sphere mechanism for transfer hydrogenation of ketones by amino-NHC Ru complex **4.19**.¹⁷

Morris subsequently synthesised $[\text{Ru}(p\text{-cymene})(\text{C},\text{NH}_2)\text{H}]\text{PF}_6$ (**5.74**), an intermediate complex in the outer sphere mechanism, and found that it reacts only very slowly with acetophenone in the absence of an alkoxide base.¹⁷ This result suggests that complexes **4.19** and **5.71** do not catalyse the transfer hydrogenation of acetophenone by an outer sphere mechanism. Furthermore, DFT calculations on model complexes $[\text{Ru}(\text{benzene})(\text{C},\text{NH}_2)\text{Cl}]^+$ suggested that there is a large free energy barrier ($\Delta G^\ddagger = 32.3 \text{ kcal mol}^{-1}$) to the transfer of the H^+/H^- couple from the benzene-substituted analogue of amine/hydride complex **5.74** to acetophenone (transition state **5.75**), possibly due to decreased hydric character of the hydride ligand on the cationic metal centre.¹⁷ Calculated energetics for the inner sphere mechanism were more favourable than those for the outer sphere mechanism, suggesting the latter is in operation for complexes **4.19** and **5.71**, in line with the observation of lack of reactivity of **5.74**.

Morris also concluded from DFT calculations that dissociation of the amine arm of the NHC is slightly easier for the 6-membered ring of **5.71** ($\Delta H = 18.0 \text{ kcal mol}^{-1}$; $\Delta S = 14.4 \text{ cal mol K}^{-1}$) than the 7-membered ring of **4.19** ($\Delta H = 20.4 \text{ kcal mol}^{-1}$, $\Delta S = 16.6 \text{ cal mol K}^{-1}$). As the amino/amido-NHC complexes **4.34-4.36** all possess 6-membered chelate rings, these calculations would suggest that dissociation of the amine arm of the NHC to allow an inner sphere mechanism could be possible, but the increased rigidity of the aryl-linked amino-NHC ligand in **4.34-4.36** compared to the alkyl-linked amino-NHC ligand of **5.71** may also have an effect on the lability of the nitrogen donor.

The mechanism of transfer hydrogenation catalysed by **4.34-4.36** is currently unclear. It is possible that either (or both) inner and outer sphere mechanisms are operating

for precatalysts **4.34-4.36**; without a computational study it is difficult to distinguish the most likely pathway.

5.2.2: Direct Arylation of Heterocycles

One of the primary objectives of this work was to investigate complexes of amino/amido-NHC ligands as catalysts/precatalysts for direct arylation cross-coupling reactions. In particular the author aimed to investigate whether the amino/amido-NHC complexes allowed a bifunctional mechanism, and if choice of ligand on the complex could affect the regioselectivity of these reactions.

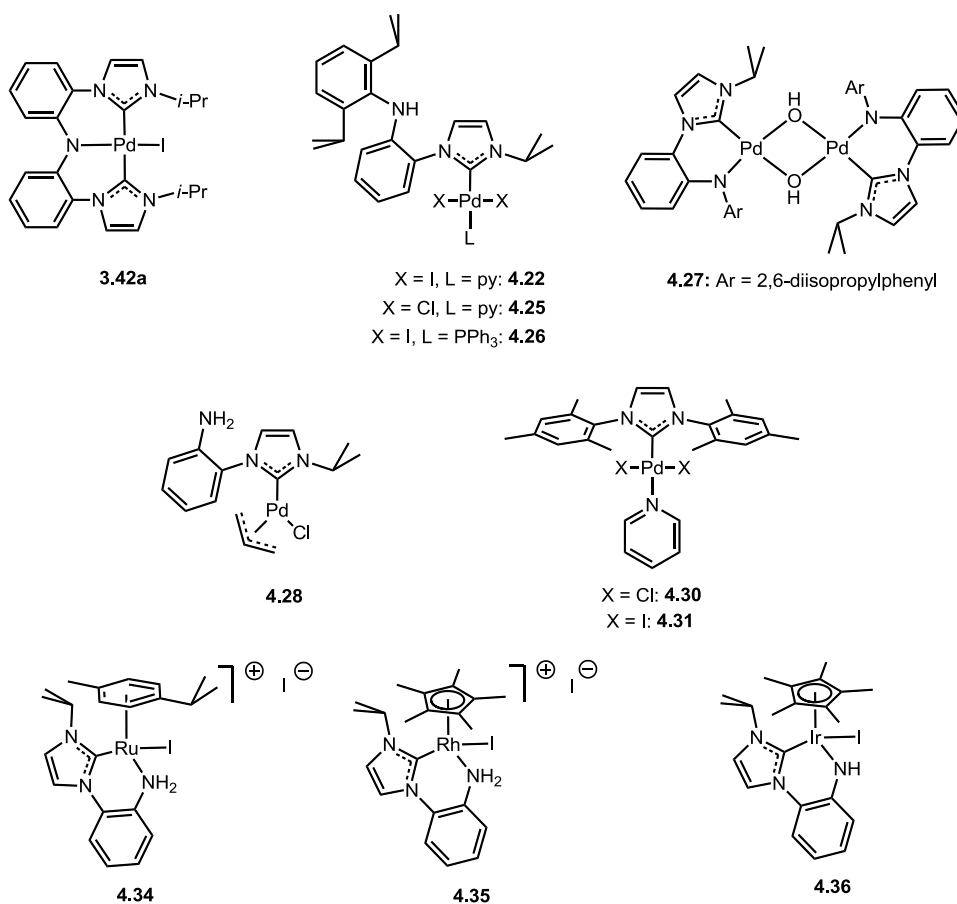
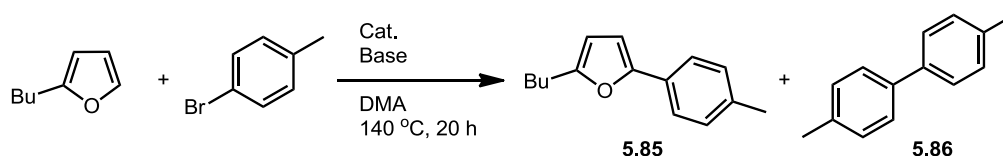


Figure 5.8: Complexes studied for activity in the direct arylation of heteroarenes.

The complexes chosen to study in this reaction (**Figure 5.8**) were the palladium complexes **3.42a**, **4.22**, **4.25**, **4.26**, **4.27**, **4.28**, **4.30** and **4.31**, as most cross-coupling reactions, including direct arylation, are catalysed by palladium with neutral ligands such as phosphines or NHCs. **4.34**, **4.35** and **4.36** were also chosen, as half-sandwich complexes are well-studied in C-H activation chemistry^{266,77} and ruthenium catalysed direct arylations are also known.³²³

The first reaction to be investigated was the direct arylation of 2-*n*-butylfuran with an aryl bromide, **Scheme 5.28**. This relatively simple reaction was chosen to identify conditions that would allow direct arylation using the amino/amido-NHC complexes. 2-*n*-butylfuran has the advantage that reactivity is primarily expected at C5, as this site is the most active for electrophilic aromatic substitution and also the proton joined to C5 is the most acidic (See Ch. 5.1.2); this allowed the identification of reaction conditions easily.³⁰⁰ The aryl bromide 4-bromotoluene was chosen as it has a simple ¹H NMR spectrum, which makes identification of starting material and product facile. The molar ratio of starting furan and aryl bromide was fixed at 1:1.

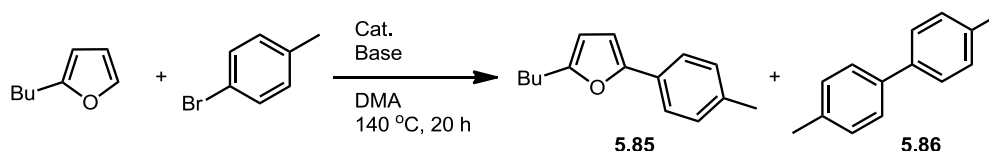


Scheme 5.28: Direct arylation of 2-*n*-butylfuran with 4-bromotoluene.

4.22 was chosen as the initial precatalyst as the PEPPSI-type architecture has been shown to be highly effective for precatalysts in traditional cross-coupling reactions.^{233,324,231} It was also decided to begin with a relatively low 1 mol% catalyst loading as a lower loading of catalyst is desirable from an economic and

environmental perspective. An initial screening of conditions was conducted and it was found that in the highly polar solvent DMA direct arylation would occur in the presence of K_2CO_3 as base. The reaction product was the expected 5-*p*-tolyl-2-*n*-butylfuran **5.85** (36% yield) which was identified by comparison to literature NMR data.³²⁵ A major byproduct, 4,4'-dimethyl-1,1'-biphenyl **5.86** (16% yield), formed from the homocoupling of 4-bromotoluene, was also identified by comparison to literature data.³²⁶ Other bases were trialed: NEt_3 gave no conversion, KOAc and Cs_2CO_3 gave only trace conversion while KOH and *t*-BuONa were incompatible with the solvent under the reaction conditions. The concentration of the reaction was also determined to have an effect on yield (**Table 5.2**), with a 0.33 M concentration with respect to 2-*n*-butylfuran optimal.

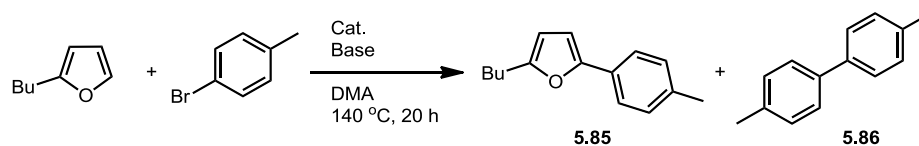
Table 5.2: Effect of concentration on direct arylation of 2-*n*-butylfuran.



Entry	Concentration(M)	Yield (%) (Determined by NMR)	
		5.85	5.86
1	1.00	25	23
2	0.33	36	16
3	0.20	11	7

Conditions: 2-*n*-butylfuran (1.0 mmol) with 4-bromotoluene (1.0 mmol), **4.22** (1 mol%), K_2CO_3 (1.5 mmol), DMA, 140 °C, 20 h. Yields quoted are with respect to 2-*n*-butylfuran.

With these conditions in hand, the author undertook screening of the aforementioned complexes in this reaction, **Table 5.3**, in order to compare the activity of amino/amido-NHC complexes as precatalysts.

Table 5.3: Catalyst screening for direct arylation of 2-*n*-butylfuran.

Entry	Cat.	Cat. Loading (mol %)	Yield (%) (Determined by NMR)	
			5.85	5.86
1	4.22	1	36	16
2	4.25	1	5	9
3	4.31	1	26	18
4	4.30	1	35	21
5	4.27	1	14	5
6	4.26	1	18	11
7	3.42a	1	0	0
8	4.34	1	0	0
9	4.35	1	0	0
10	4.36	1	0	0
11	4.22	3	6	11
12	4.31	3	7	10
13	4.30	3	32	27

Conditions: 2-*n*-butylfuran (1.0 mmol) with 4-bromotoluene (1.0 mmol), K₂CO₃ (1.5 mmol), DMA (3 mL), 140 °C, 20 h. Yields quoted are with respect to 2-*n*-butylfuran.

The chloride complex **4.25** (entry 2) showed much lower reactivity (**5.85**: 5%; **5.86**: 9%) than **4.22**; this is in contrast to the complexes of non-functionalised NHC IMes **4.31** (iodide complex, entry 3) and **4.30** (chloride complex, entry 4), in which the chloride complex was more reactive. **4.31** gave a slightly lower yield of **5.85** (26%) than **4.22**, with a similar degree of homocoupling. **4.30** gave a similar yield of desired product (35%) to that observed with **4.22**, but with more homocoupling of aryl bromide. The palladium amido/hydroxide dimer **4.27** (entry 5) had poor reactivity compared to **4.22** (entry 1), giving *ca.* half the yield of **5.85**. The PPh₃ substituted complex **4.26** (entry 6)

was also less active than **4.22**; PPh₃ is more strongly bound as a ligand than pyridine and so the initiation step to form the active Pd⁰ catalyst may be slowed, also PPh₃ may bind to the active catalyst and temporarily prevent catalysis.

In contrast to the PEPPSI-type complex **4.22**, the CNC pincer complex **3.42a** (entry 7) did not catalyse the direct arylation of 2-*n*-butylfuran. This may be attributable to the limited number of coordination sites available for catalysis due to the strongly-bound pincer ligand. Likewise, the half-sandwich complexes **4.34-4.36** showed no catalytic activity in this reaction (entries 8-10).

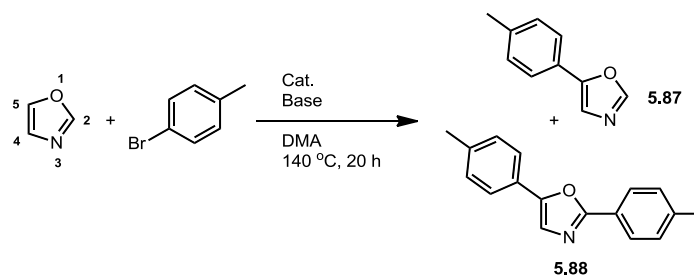
Increasing the catalyst loading to 3 mol% had a detrimental effect on the yield of the arylated product (**5.85**) for the iodide precatalysts **4.22** (from 36% to 6% yield, entry 11) and **4.31** (26% to 7% yield, entry 12). However, an increased catalyst loading had virtually no effect on the yield of the product for the chloride precatalyst **4.30** (entry 13). Fagnou has reported that a build-up of iodide from aryl iodide substrates in direct arylation reactions can have a detrimental effect on the reaction;³²⁷ perhaps iodide released during generation of the active catalytic species from the precatalysts **4.22** and **4.31** has a similar influence on the reaction.

The addition of silver salts into the arylation reaction was investigated as a way to remove the halide ligands and free active sites on the catalyst for coordination of the substrate and/or amino ligand, in order to increase the yield of the reaction. However, when AgPF₆ or AgOTf was added to an arylation catalysed by **4.22** (entries 2 and 3) the reaction was suppressed. An AgPF₆ additive did not enable catalytic activity with **4.34**, **4.35** or **4.36** (entries 4-6).

The addition of carboxylates can help C-H activation proceed by an AMLA(6) mechanism:^{4,5} the positive effect of pivalic acid as an additive alongside a carbonate base in direct arylation reactions was first noted by Fagnou,⁵ and is believed to arise from coordinated pivalate acting as an internal base in an AMLA(6) mechanism.⁷⁶ It was decided to see if sub-stoichiometric quantities of carboxylates could improve the yields of arylation. Addition of 0.3 eq. NaOAc (entry 7) to a reaction catalysed by **4.22** had little effect on the yield of arylated product **5.85**; however, the addition of 0.3 eq. pivalic acid (entry 8) increased the yield of arylated product **5.85** to 59%, while reducing the yield of homocoupled product **5.86** to 10%. The addition of pivalic acid to an arylation reaction catalysed by **3.42a** (entry 9) resulted in little change in product yield, probably due to the limited number of available coordination sites on the metal. The addition of pivalic acid improved the yield of arylated product **5.85** in reactions catalysed by **4.31** (68%, entry 10) and **4.30** (99%, entry 11), while also completely suppressing homocoupling of aryl bromide to **5.86**; indeed, the combination of **4.30** and pivalic acid gave the best result of all those reported in **Table 5.4**. The **4.22** / pivalic acid cocatalyst combination gave an identical yield to that of Pd(OAc)₂ / PPh₃ / pivalic acid (molar ratio 1:2:0.3 respectively, entry 12).

Having determined the optimum conditions for the direct arylation of 2-*n*-butylfuran, the same conditions were applied to the direct arylation of a more challenging substrate, oxazole. As previously mentioned, 1,3-azoles are poorly nucleophilic compared to pyrrole, thiazole or furan; even powerfully electrophilic reactions such as nitration and sulfonation fail to functionalise oxazole. If activating groups are present on the oxazole ring, electrophilic aromatic substitutions can occur at C5.³⁰¹ The most acidic proton on oxazole resides on C2 but deprotonation here can lead to ring-opening of the anion to form a 2-*isocyanoenolate*.³⁰¹ In terms of the regioselectivity of direct arylation, oxazole presents an excellent challenge, as potentially seven products can be formed: 2-, 4- or 5-monoarylated, 2,4-, 2,5- or 4,5-diarylated or 2,4,5-triarylated oxazoles.

Table 5.5: Catalyst screening for direct arylation of oxazole.



Entry	Cat.	Additive	Yield (%) (Determined by NMR)	
			5.87	5.88
1	4.22	-	0	0
2	4.22	PivOH (0.3 eq.)	49	17
3	4.25	PivOH (0.3 eq.)	50	20
4	4.31	PivOH (0.3 eq.)	55	19
5	4.30	PivOH (0.3 eq.)	56	17
6	Pd(OAc) ₂ / 2 PPh ₃	PivOH (0.3 eq.)	53	18
7	4.28	-	2	0
8	4.28	PivOH (0.3 eq.)	52	16

Conditions: oxazole (1.0 mmol) with 4-bromotoluene (1.0 mmol), K₂CO₃ (1.5 mmol), DMA (3 mL), 140 °C, 20 h. Yields quoted are with respect to oxazole.

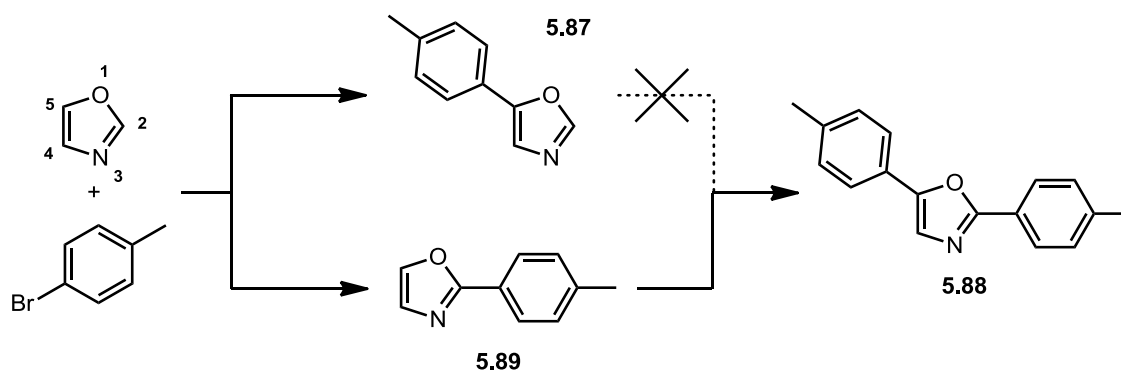
Direct arylation of oxazole with 4-bromotoluene, catalysed by **4.22** with K_2CO_3 base, initially failed to give any conversion, **Table 5.5** (entry 1). The addition of 30 mol% pivalic acid (entry 2) to this reaction resulted in two products being formed; 5-*p*-tolylloxazole **5.87** (49% yield) and 2,5-di-*p*-tolylloxazole **5.88** (17% yield). No other identifiable product could be observed in the 1H NMR spectrum of the reaction mixture; although there was some unreacted oxazole and *p*-bromotoluene along with trace aromatic impurities. **5.87**³²⁸ and **5.88**³¹⁶ were isolated by column chromatography and identified by comparison of their 1H NMR spectra with the literature; the 2-monoarylated,³¹⁶ 4-monoarylated³²⁹ and 4,5-diarylated³³⁰ oxazoles are known compounds but were not observed. Very similar yields and product ratios of **5.87** and **5.88** were given by the direct arylation reactions catalysed by **4.25**, **4.31**, **4.30**, and $Pd(OAc)_2 / PPh_3$ (entries 3-6) in the presence of pivalic acid as were given by **4.22** (entry 2), with total conversions in the range of 83-93%.

The author hypothesised that the bulky aryl substituent on the amine nitrogen of **4.22** and **4.25** could be preventing coordination of the nitrogen during the catalytic cycle. The primary aryl-amino NHC complex **4.28** was tested in the direct arylation of oxazole (entry 7); however, it gave only a trace (2%) yield of 5-*p*-tolylloxazole **5.87**. The addition of pivalic acid to the reaction catalysed by **4.28** (entry 8) gave increased yields. Nevertheless, the obtained yields (**5.87**: 52%; **5.88**: 16%) were not significantly different than those for reactions catalysed by **4.22** and **4.25**.

As it was hypothesised that an M-N bond would facilitate an AMLA(4) mechanism of C-H activation, the author anticipated that amido complexes would be generated *in situ* by deprotonation and coordination of the amino-NHC nitrogen. The potassium

carbonate base used in these direct arylation reactions may be insufficient to deprotonate the amine nitrogen, and so a number of bases were screened in the direct arylation reaction of oxazole catalysed by **4.22**, **4.25** and **4.28** in the absence of pivalic acid. Reactions with the bases KOAc, Cs₂CO₃, *t*-BuONa, KOH, NEt₃, DBU, and proton sponge resulted in < 5% conversion to product.

To gain more insight into the regioselectivity of the first direct arylation reaction of oxazole, it was of interest whether **5.88** was obtained from 5-*p*-tolylloxazole **5.87** (the major product in the reaction) or from 2-*p*-tolylloxazole **5.89**, which was not observed in the product mixture, **Scheme 5.29**. By monitoring the reaction conversion over time, it could be observed whether any 2-*p*-tolylloxazole was formed and subsequently reacted to form **5.88**. The direct arylation of oxazole catalysed by **4.22** was monitored over 9 hours, **Chart 5.1**. It is apparent that the rate of formation of **5.87** is faster than for **5.88**, with a tailing off of the reaction after *ca.* 6 h. In order to ascertain whether **5.87** is the origin of **5.88**, **5.87** was isolated from the crude product by chromatography and placed back under arylation conditions: no further arylation of **5.87** was observed whatsoever, implying that it is not an intermediate in the synthesis of **5.88**. This observation in turn suggests that **5.88** must be formed *via* 2-*p*-tolylloxazole **5.89**. In order to confirm this hypothesis, **5.89** was synthesised by a Negishi reaction (conditions adapted from Greaney *et al.*³¹⁶) and subjected to the arylation reaction conditions. Complete conversion of **5.89** to **5.88** was observed over 15 h, confirming that **5.88** is formed from **5.89**, not **5.87**.



Scheme 5.29: Origin of 2,5-di-p-tolyloxazole **5.88**.

The fact that no traces of **5.89** were observed in the monitored reaction (**Chart 5.1**) suggests that **5.89** is consumed very quickly on formation to give **5.88**, and so **5.89** is more reactive at C5 than unsubstituted oxazole. The increased reactivity of **5.89** over oxazole could be rationalised as the weakly electron donating tolyl substituent at C2 activating **5.89** to electrophilic attack at C5. If the C-H activation step proceeds by an AMLA(6) mechanism, the electrophilic component of the mechanism (metal-carbon interaction) would be also enhanced by the tolyl substituent at C2.

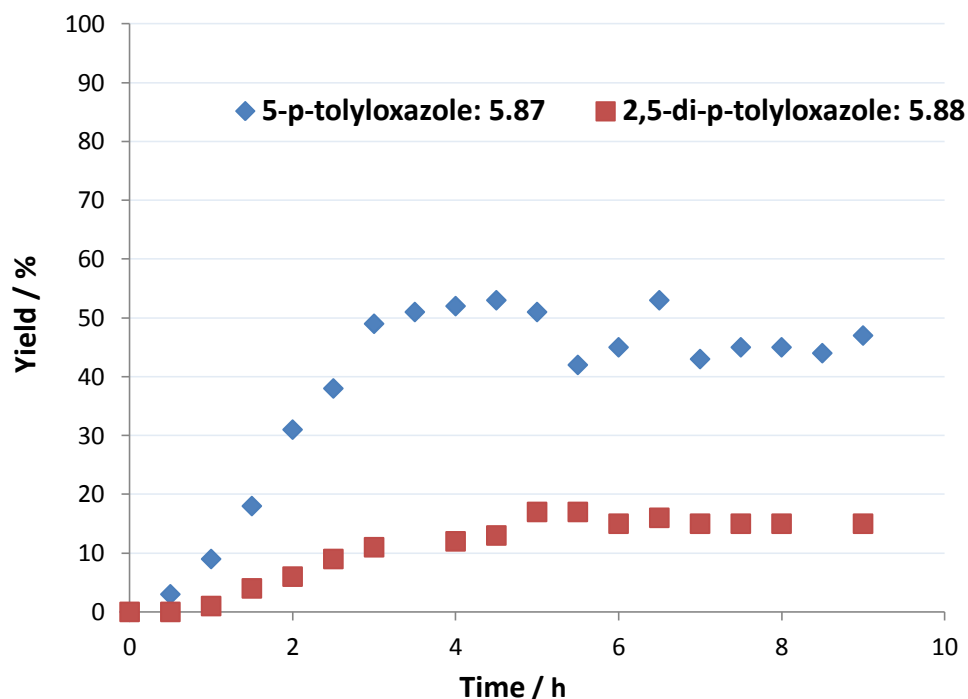


Chart 5.1: Monitored direct arylation of oxazole (1.0 mmol) with 4-bromotoluene (1.0 mmol) (conditions: **4.22** (1 mol%), PivOH (0.3 mmol), K_2CO_3 (1.5 mmol), DMA, 140 °C; yields determined by 1H NMR spectroscopy).

As the direct arylation of oxazole by all 6 catalyst systems with pivalic acid (**Table 5.5**, entries 2-7) gave similar yields of product, it was decided to compare the rate of reaction catalysed by amine-NHC complex **4.22** with one catalysed by an unfunctionalised NHC complex, **4.31**, **Chart 5.2**. The reactions to form both **5.87** and **5.88** (not shown) were faster with **4.31** than **4.22**, with the reaction reaching completion after *ca.* 1 h for **4.31**, compared with *ca.* 4-5 h for **4.22**.

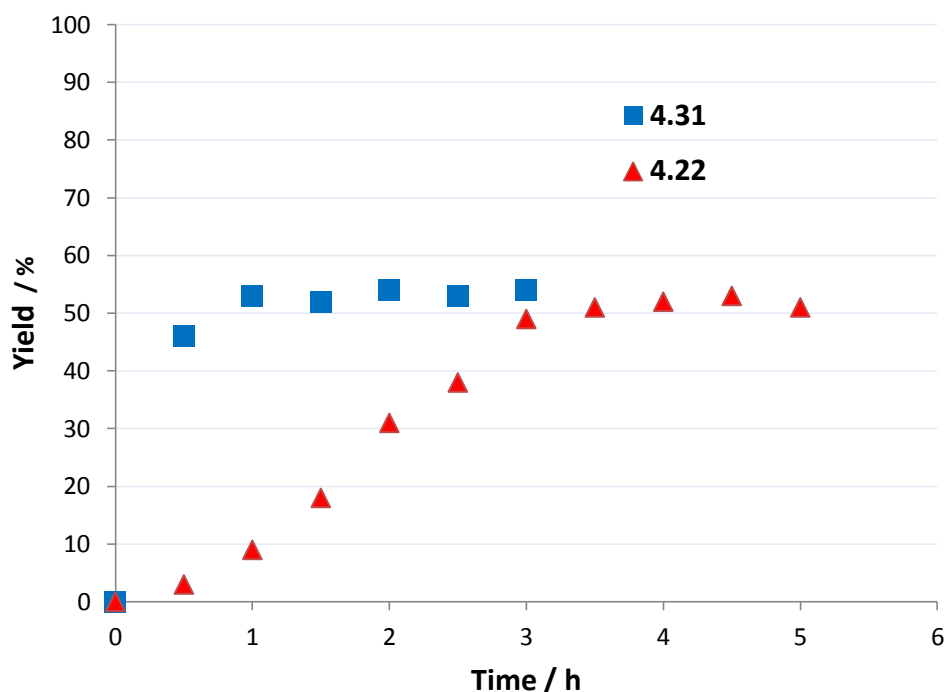
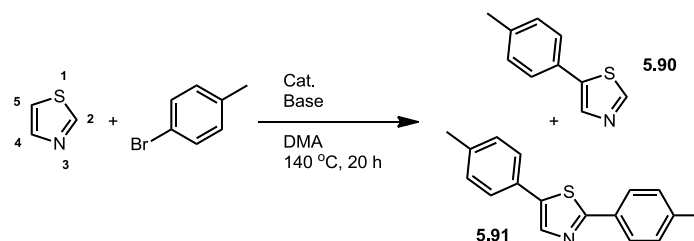


Chart 5.2: Reaction progress of direct arylation of oxazole (1.0 mmol) with 4-bromotoluene (1.0 mmol) catalysed by **4.31** (blue) and **4.22** (red) (conditions: cat. (1 mol%), PivOH (0.3 mmol), K₂CO₃ (1.5 mmol), DMA, 140 °C; yields shown are for the major product **5.87** and are determined by ¹H NMR spectroscopy).

The faster rate of direct arylation catalysed by **4.31** compared with **4.22**, along with the similar regioselectivity and yields obtained in the reactions of all the catalysts, suggests that the amine functionality of the amine-NHC ligands of **4.22** and **4.28** is not increasing the rate of reaction, or changing the regioselectivity of direct arylation of oxazole.

The reactions conditions used for the direct arylation of oxazole were also applied to the direct arylation of thiazole, **Table 5.6**.

Table 5.6: Catalyst screening for direct arylation of thiazole.

Entry	Cat.	Additive	Yield (%) (Determined by NMR)	
			5.90	5.91
1	4.22	-	0	0
2	4.22	PivOH (0.3 eq.)	60	20
3	4.25	PivOH (0.3 eq.)	28	6
4	4.31	PivOH (0.3 eq.)	59	20
5	4.30	PivOH (0.3 eq.)	41	13
6	Pd(OAc) ₂ / 2 PPh ₃	PivOH (0.3 eq.)	67	10

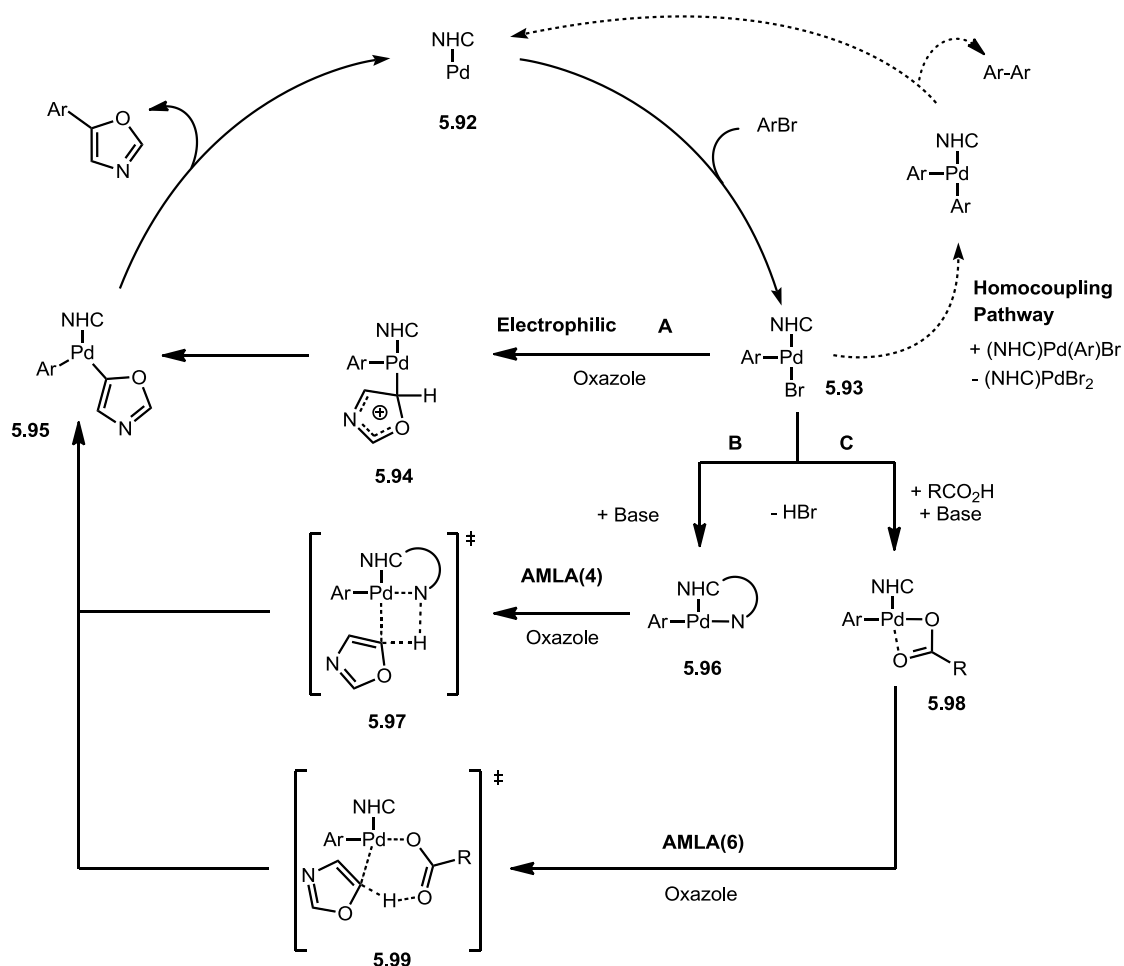
Conditions: thiazole (1.0 mmol) with 4-bromotoluene (1.0 mmol), cat. (1 mol%), K₂CO₃ (1.5 mmol), DMA (3 mL), 140 °C, 20 h. Yields quoted are with respect to thiazole.

The arylation catalysed by **4.22** in the absence of pivalic acid (entry 1) produced no conversion of the starting materials. However, upon the inclusion of 0.3 eq. pivalic acid (entries 2-6) two products were observed in the reaction mixture: 5-*p*-tolylthiazole **5.90**³³¹ and 2,5-di-*p*-tolylthiazole **5.91**,³¹⁵ which were identified by comparison with literature NMR data. No 2-*p*-tolylthiazole was observed in the reaction, this is consistent both with the arylation of oxazole reported above, and with literature precedent for the direct arylation of thiazole (**Scheme 5.23**).³¹⁴ Arylation of thiazole was, in general, more sensitive to oxygen and water than that of oxazole, requiring absolutely dry and oxygen free conditions to ensure reproducibility; a detrimental effect of small amounts of water in organic solvent has been observed before for direct arylation of thiazoles.³¹⁵ Interestingly, the iodide precatalysts **4.22** and **4.31** performed better (*ca.* 100% conversion of starting materials), than the

chloride precatalysts **4.25** and **4.30** (40% and 67% conversion, respectively). The yields of **5.90** and **5.91** are similar for the precatalysts **4.22** (60%, 20% respectively) and **4.31** (59%, 20% respectively); however, the Pd(OAc)₂ / PPh₃ catalyst system gives a higher yield of **5.90** (67%) and a lower yield of **5.91** (10%). The observed yields are in contrast to the similar conversions and yields observed between all these catalysts in the direct arylation of oxazole (**Table 5.5**). The reason for the disparity between the reactivity of the chloride and iodide precatalysts in thiazole arylation is unclear. As no significant differences in the yield of either arylated thiazole product are observed between the reactions catalysed by **4.22** or **4.31**, it can be concluded that the amine-NHC ligand of **4.22** is having no significant effect on the reaction yields or regioselectivity beyond that of a normal, unfunctionalised NHC.

Discussion of the Mechanism of Direct Arylations Catalysed by Amino-NHC Complexes

It is possible to discuss some aspects of this chemistry in order to hypothesise a mechanism. It has been proposed that the direct arylation reaction, as with other palladium-catalysed cross-coupling reactions, proceeds *via* a Pd⁰/Pd^{II} manifold.³³² The Pd^{II} precatalyst would be reduced to a NHC-Pd⁰ active catalytic species, and then oxidative addition of the aryl bromide to this Pd⁰ intermediate presumably gives a Pd^{II} intermediate (NHC)PdArBr **5.92**, **Scheme 5.30**. The key mechanistic step in the reaction that is of interest is the C-H activation of the heteroarene substrate.



Scheme 5.30: Possible mechanisms of direct arylation of oxazole: electrophilic activation **A**; AMLA(4) **B**; AMLA(6) **C**.

Reactions in the absence of pivalic acid using **4.22** catalyst gave lower yields of 5-*p*-tolyl-2-*n*-butylfuran **5.85**, and no reaction with oxazole or thiazole; this suggests that an AMLA(4) C-H activation mechanism involving a Pd-N bond (**Scheme 5.30B**) is not occurring in these cases.

The beneficial effect of adding substoichiometric pivalic acid to these reactions strongly suggests an AMLA(6) mechanism (**Scheme 5.30C**), where coordinated pivalate acts as the internal base in a concerted metallation and deprotonation step.^{5,6} Further evidence for the involvement of an AMLA(6) mechanism comes from the fact that

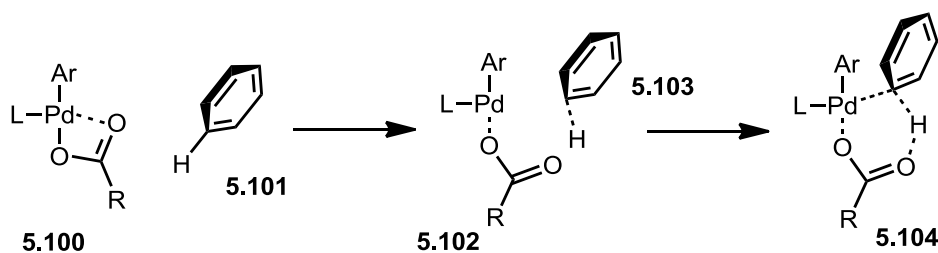
oxazole and thiazole were observed to arylate at both C2 and C5, which are sites associated with deprotonation (C2) and electrophilic attack (C5). If the reaction went by a purely $S_{E}Ar$ mechanism (**Scheme 5.30A**), *i.e.* no assistance from the coordinated base, reaction only at C5 would be expected. On the other hand, a deprotonation mechanism would give only reaction at C2.¹ However, the observation that the first arylation reaction occurs both at C5 and C2 suggests that the C-H activation step proceeds by an AMLA mechanism in which the electrophilic metal and basic ligand work together.

The faster rate of production of 5-*p*-tolylloxazole (**5.87**) compared with 2,5-di-*p*-tolylloxazole (**5.88**) indicates that the rate of arylation is faster at C5 than C2 on oxazole; and as no intermediate **5.89** is observed in the reaction it can be inferred that reaction at C5 is even faster when the ring is activated by an electron donating substituent at C2.

DFT analysis of the AMLA mechanism in palladium-catalysed direct arylation reactions by Gorelsky *et al.* suggests that the major contributions to regioselectivity of C-H activation (**Scheme 5.31**) are (i) the combination of the energetic cost of distortion of the catalyst and arene from ground states **5.100** and **5.101** to the transition state geometries **5.102** and **5.103** (distortion energy, E_{dist}) and (ii) the energetic gain that arises from bringing **5.102** and **5.103** together to form transition state **5.104** (electronic interaction energy, E_{int}).^{6,74} In π -electron rich heteroarenes such as furan and thiazole, E_{int} is calculated to be the determining factor for the most reactive C-H

¹ Complete C2 selectivity has been observed to be favoured in direct arylation reactions on oxazole where strong bases such as KOH and *t*-BuOK are used, and in this case deprotonation is the most likely mechanism of C-H activation.³²⁰

bond in arylation reactions.⁷⁴ For C2-substituted thiophenes E_{int} and E_{dist} are linked to the nucleophilicity of the thiophenes but little data exists on the nucleophilicity of carbon sites on most heteroarenes, making the prediction and explanation of regioselectivity for other heteroarenes such as oxazole difficult.⁷⁴ E_{dist} was shown to be correlated with the C-H bond deprotonation energy, suggesting that the acidity of the C-H bond, as well as the electronics around the carbon, has an effect on regioselectivity.⁷⁴ In order to determine the relative influence of the E_{dist} and E_{int} factors on the direct arylation of 2-*n*-butylfuran and oxazole reported in this chapter, DFT calculations would be required. However, the direct arylation of thiazole reported in this chapter showed regioselectivity (reactivity order C5 > C2 > C4) which agrees with the order of calculated values of ΔG for C-H bond activation *via* AMLA(6) with the model catalyst $[\text{Pd}(\text{C}_6\text{H}_5)(\text{PMe}_3)(\text{OAc})]$ ($\Delta G = \text{C5: } 23.7; \text{C2: } 26.3; \text{C4: } 29.7 \text{ kcal mol}^{-1}$).⁷⁴



Scheme 5.31: Transition states in the AMLA-type mechanism for direct arylation of an example arene **5.101** (benzene).

5.3: Conclusions

In conclusion, the amino-NHC complexes **4.34**, **4.35** and the amido-NHC complex **4.36** were found to be competent precatalysts for the transfer hydrogenation of acetophenone at 80 °C in *isopropanol*. Ruthenium amino-NHC complex **4.34** was highly active, with a TON observed over 1 h that was comparable with that of the well-studied Ru(*p*-cymene)(TsDPEN)Cl (**5.1**) precatalyst over 10 h; however, higher temperatures were necessary for the reaction to proceed with **4.34**.²⁴ Rhodium amino-NHC complex **4.35** and iridium amido-NHC complex **4.36** were capable of high TONs but over a much longer time of 72 h. The activities of the rhodium complex **4.35** and the iridium complex **4.36** were similar to that observed for known rhodium and iridium transfer hydrogenation catalysts.²⁶ The amido-NHC complex **4.36** catalysed transfer hydrogenation even in the absence of base; this suggested that the amido ligand was involved in the catalytic cycle. DFT calculations and experimental observations by Morris *et al.* suggest an inner sphere mechanism is operative for similar amine-NHC ruthenium complexes **4.19** and **5.71**;¹⁷ without further investigation, such as DFT calculations, it is unclear if this mechanism is also operative for **4.34-4.36**.

Palladium-catalysed direct arylation of heteroarenes were also investigated, in order to determine if the amino/amido-NHC ligands can assist in C-H activation and have an effect on reaction rate and regioselectivity. Precatalysts **4.22**, **4.25**, **4.26**, **4.27**, **4.28**, **4.30** and **4.31** catalysed the direct arylation of 2-*n*-butylfuran. The addition of pivalic acid led to higher yields for all the catalysts investigated. Complexes **4.22**, **4.25**, **4.30** and **4.31** catalysed the direct arylation of oxazole and thiazole, but for these

substrates the presence of pivalic acid was essential for any conversion. Similarly, the primary amino-NHC complex **4.28** was only an effective precatalyst for the direct arylation of oxazole in the presence of pivalic acid.

In general, the amine-NHC precatalysts **4.22** and **4.25** were no more active than complexes of the unfunctionalised NHC **4.30** and **4.31** or Pd(OAc)₂ / 2 PPh₃ in the direct arylation reactions. Furthermore, no difference in regioselectivity was observed between **4.22**, **4.25**, **4.30** and **4.31** in the direct arylation of oxazole and thiazole. These results suggest that the amine-NHC ligands investigated do not have a positive influence on the activity or regioselectivity of the catalytic species. Based upon the positive effect of pivalic acid on the reaction yields, and the observed regioselectivity patterns on the heteroarenes, an AMLA(6) mechanism of C-H activation is proposed.

5.4: Experimental

All manipulations were performed under dry, oxygen free nitrogen using standard Schlenk techniques unless otherwise stated. *i*-PrOH was distilled from Mg turnings and toluene was distilled from sodium prior to use; anhydrous DMA was purchased from Sigma-Aldrich. All other reagents were obtained from Sigma-Aldrich, Johnson Matthey or Alfa Aesar and used as supplied. NMR spectra were recorded on a Bruker DPX300, DRX400 or AV500 spectrometer; chemical shifts have been referenced to the residual protonated solvent peak and *J* values are given in Hz.

Catalytic Transfer Hydrogenation – General Procedure

In a Schlenk flask under an atmosphere of nitrogen, a solution of acetophenone (0.200 g, 1.70 mmol) in *iso*-propanol (6 mL) was preheated to 80 °C with stirring. The appropriate pre-catalyst (**4.34-4.36**) (0.0085 mmol), sodium *tert*-butoxide (6 mg, 0.062 mmol) and AgPF₆ (0.003 g, 0.01 mmol) were then added as appropriate. Periodically, aliquots were removed from the reaction mixture by syringe. The aliquots were immediately quenched by dilution with EtOAc and then analysed by gas chromatography using a Perkin-Elmer Clarus 500 chromatograph equipped with a Perkin-Elmer Elite 5 column (PE5 30 m x 0.25 mm). Helium was used as a mobile phase with a flow rate of 1 mL/min and a split rate of 50 mL/min. The injector temperature was 250 °C, the oven temperature was 130 °C and the FID temperature was 280 °C. Retention times (*t_R*/min) were: acetophenone, 3.54; (*R/S*)-1-phenylethanol, 3.45. All reported conversions are an average of two reactions.

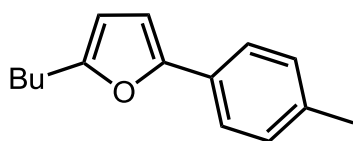
Catalytic Direct Arylation – General Procedure

In a screw-capped vial equipped with a gastight Teflon valve under an atmosphere of nitrogen, DMA (3 mL) was added to a mixture of K_2CO_3 (0.207 g, 1.50 mmol), 4-bromotoluene (0.171 g, 1.00 mmol), the appropriate catalyst (0.010 mmol) and the internal standard 1,3,5-trimethoxybenzene (0.084 g, 0.50 mmol). Where indicated, pivalic acid (0.031 g, 0.30 mmol) or a silver salt (0.030 mmol) were added also. The heterocyclic substrate (1.00 mmol) was added *via* syringe through the Teflon valve and the reaction heated at 140 °C with stirring for 20 h. After cooling to room temperature, the sample was opened to air, homogenised by stirring and a sample (*ca.* 0.1 mL) removed. The sample was diluted with $CDCl_3$ and transferred through a pipette filter into a NMR tube and the 1H NMR spectrum recorded immediately. The reported yields are based upon the relative integration of peaks for the product and internal standard (1,3,5-trimethoxybenzene: *CH* resonances) in the 1H NMR spectrum. Reactions were repeated to ensure reproducibility, with reported yields an average of two runs. In some cases, as reported in Ch. 5.2.2, an increased amount of catalyst was used or the solvent, base or concentration of the reaction varied.

All products from direct arylation catalysis were isolated by column chromatography (10% EtOAc/ pet. ether (40-60)) after loading the crude reaction mixture directly onto silica. The products were characterised by comparison of 1H NMR spectra to reported compounds in literature; product spectral data is reported below.

Products from the Direct Arylation of 2-*n*-Butylfuran

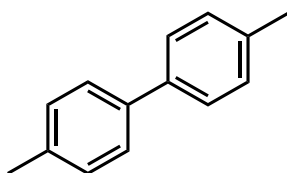
2-Butyl-5-(*p*-tolyl)furan (5.85)



Previously reported by Doucet *et al.*³²⁵

δ_{H} (400 MHz, CDCl_3) 0.94 (3 H, t, $J = 7.4$, CH_2CH_3), 1.41 (2H, sext., $J = 7.4$, $\text{CH}_2\text{CH}_2\text{CH}_3$), 1.67 (2H, quint., $J = 7.4$, CCH_2CH_2), 2.34 (3H, s, CCH_3), 2.67 (2H, t, $J = 7.4$, CCH_2), 6.02 (1H, d, $J = 3.2$, furan CH), 6.46 (1H, d, $J = 3.2$, furan CH), 7.14 (2H, d, $J = 8.0$, aryl CH), 7.51 (2H, d, $J = 8.3$, aryl CH).

4,4'-Dimethylbiphenyl (5.86)

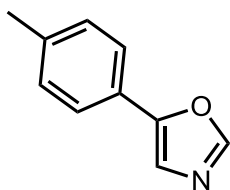


Previously reported by Li *et al.*³²⁶

δ_{H} (400 MHz, CDCl_3) 2.38 (6H, s, CH_3), 7.23 (4H, d, $J = 8.1$, CH), 7.47 (4H, d, $J = 8.1$, CH).

Products from the Direct Arylation of Oxazole

5-(*p*-tolyl)oxazole (5.87)

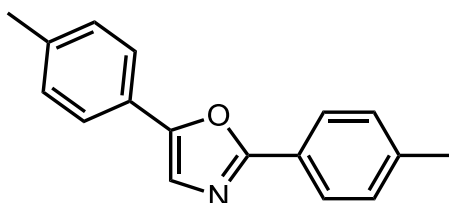


Previously reported by Vedejs *et al.*³²⁸

δ_{H} (400 MHz, CDCl_3) 2.38 (3H, s, CH_3), 7.23 (2H, d, $J = 8.1$, aryl CH), 7.29 (1H, s, oxazole CH), 7.54 (2H, d, $J = 8.1$, aryl CH), 7.88 (1H, s, oxazole CH).

2,5-di(*p*-tolyl)oxazole (5.88)

Previously reported by Greaney *et al.*³¹⁶



δ_{H} (400 MHz, CDCl_3) 2.39 (3H, s, CH_3), 2.41 (3H, s, CH_3), 7.22-7.30 (4H, m, aryl CH), 7.37 (1H, s, oxazole CH), 7.61 (2H, d, $J = 8.1$, aryl CH), 7.99 (2H, d, $J = 8.1$, aryl CH).

Products from the Direct Arylation of Thiazole

5-(*p*-tolyl)thiazole (5.90)

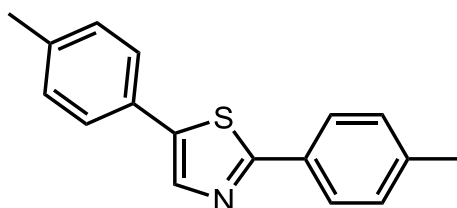
Previously reported by Jensen *et al.*³³¹



δ_{H} (400 MHz, CDCl_3) 2.39 (3H, s, CH_3), 7.21 (2H, d, $J = 8.0$, aryl CH), 7.47 (2H, d, $J = 8.0$, aryl CH), 8.04 (1H, s, thiazole CH), 8.71 (1H, s, thiazole CH).

2,5-di(*p*-tolyl)thiazole (5.91)

Previously reported by Greaney *et al.*³¹⁵



δ_{H} (400 MHz, CDCl_3) 2.39 (3H, s, CH_3), 2.40 (3H, s, CH_3), 7.21-7.26 (4H, m, aryl CH), 7.49 (2H, d, $J = 8.1$, aryl CH), 7.85 (2H, d, $J = 8.1$, aryl CH), 7.95 (1H, s, thiazole CH).

6: Chapter 6 – Conclusions and Future Work

6.1: Conclusions

In this project, the author aimed to determine whether complexes containing amido-NHC ligands could act as bifunctional catalysts. Bifunctional catalysis can facilitate several efficient, practical organic transformations, including C-C bond formation;^{1-4,333} cross-coupling reactions are a useful tool for the synthesis of high value chemical products.^{10,11}

Direct arylation offers a low-waste alternative to traditional cross-coupling by requiring no prefunctionalisation of the substrate;^{12,13} however, the challenge of regioselectivity in the C-H activation step is yet to be fully solved.⁶ With this in mind, it was investigated whether amido-NHC complexes could perform direct arylation reactions, and whether the ligand-metal combination could allow any control over the regioselectivity of the C-H activation step.

A late transition metal amido-NHC complex was identified as a promising target for the investigation of bifunctional reactivity. Late transition metals are electrophilic, yet have mostly filled d-orbitals that would act to repulse the nitrogen-based lone pair of an amido ligand, keeping the amido ligand nucleophilic. This combination of electrophilic metal and nucleophilic ligand are required for bifunctional reactivity. NHC ligands have had a huge impact on homogeneous catalysis,¹⁴⁻¹⁶ but have not been investigated in many bifunctional reactions.¹⁷⁻²⁰ The strong NHC-metal bond should

allow the amido functionality to remain tethered to the metal during catalysis, supporting the metal-amido bifunction.

Few examples of late transition metal amido-NHC complexes were known at the start of this project (several more examples have since been published).^{18,19,169,170,163,228–230}

Hence, the author set about preparing several novel amido-NHC complexes based upon amine functionalised imidazolium salts.

The first objective was to synthesise suitable amine-functionalised imidazolium salts (**Figure 6.1**) as precursors to amido-NHC complexes, this work is described in Chapter 2. Imidazolium salts **2.25a-c** and **2.28a-b** were synthesised by metal-catalysed C-N coupling reactions and a final alkylation step; this was an efficient route to high-purity products. The synthetic methodology gave imidazolium salts that allowed access to two different ligand scaffolds: (i) amido-*bis*NHC (CNC) pincer ligands; and (ii) bidentate amino/amido-NHC ligands.

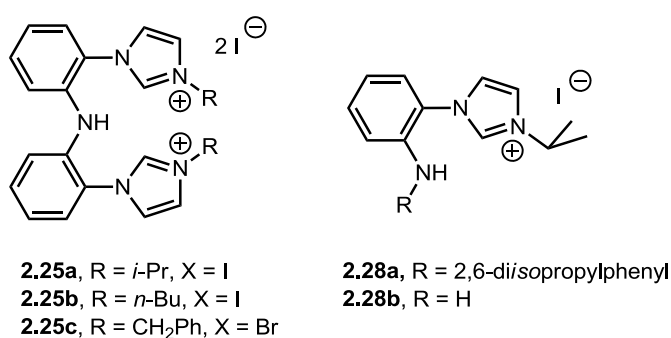


Figure 6.1: Amine-functionalised imidazolium salts prepared in this project.

The amine-*bis*imidazolium salts **2.25** were used as precursors to amido-*bis*NHC (CNC) pincer complexes (**Figure 6.2**), described in Chapter 3. Complexes containing pincer

ligands are often highly stable,¹⁷⁷ with numerous applications in catalytic reactions.

The stability of the CNC ligand could support the reactive metal amido functionality.

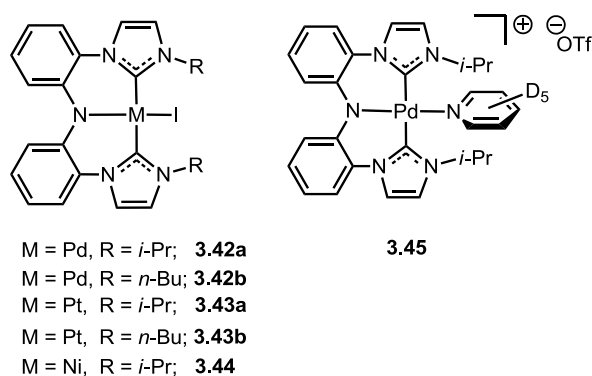


Figure 6.2: (CNC) pincer complexes prepared in this project.

Several strategies for preparing the CNC complexes were attempted. Formation of a silver carbene and subsequent transmetallation has been used to prepare amido-*bis*NHC complexes previously.¹⁷⁰ However, no silver carbene complex of the investigated CNC ligand could be isolated, and *in situ* formation and subsequent transmetallation of a silver carbene to a metal salt was also unsuccessful. It was found that treatment of the imidazolium salt **2.25a** with a strong base did not allow isolation of a free carbene; however, reaction of the imidazolium salts **2.25a-b** with KHMDS in the presence of an appropriate metal salt gave the palladium and platinum complexes **3.42-3.43** in low to moderate yield. The same methodology applied to nickel gave an unstable complex **3.44** which could not be isolated / fully characterised.

3.42a was found to decompose under an atmosphere of H₂ above 60 °C, a temperature at which the iodide ligand was found to be labile. A bifunctional mechanism of H-H bond breaking by the Pd-N bond could be involved; this initial

result was a promising first insight into the bifunctional reactivity of amido-*bis*NHC complexes.

The amine imidazolium salts **2.28a-b** were used to prepare amino/amido-NHC complexes of two different architectures (**Figure 6.3**): (i) square-planar Pd and Pt (d^8) complexes; and (ii) half-sandwich Ru, Rh and Ir (d^6) complexes. The complexes in **Figure 6.3** were described in Chapter 4.

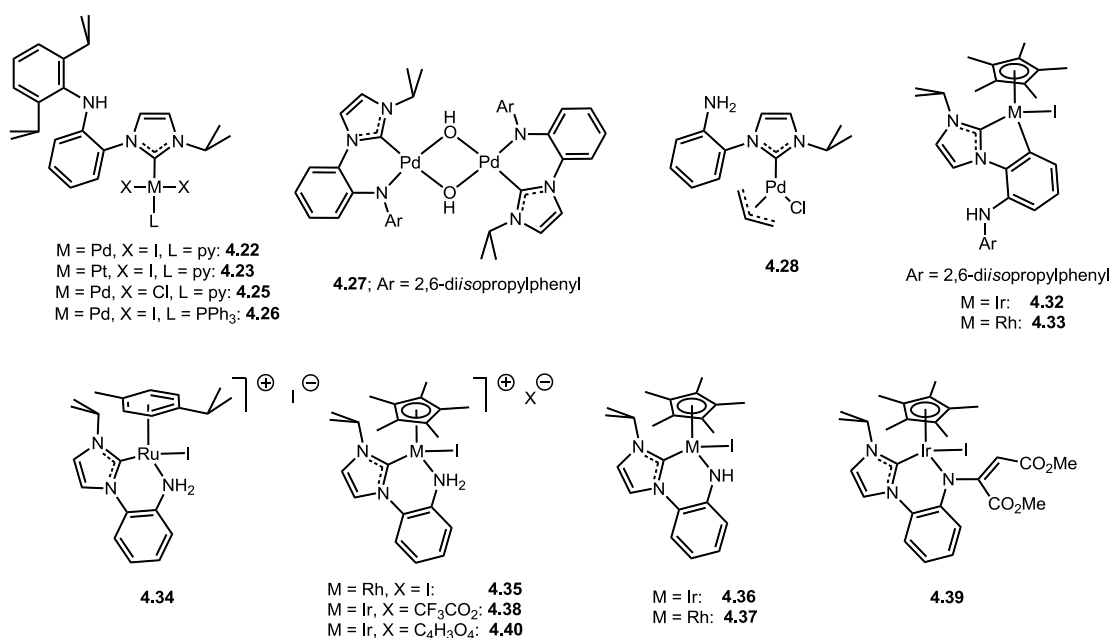


Figure 6.3: (C,NR) complexes prepared in this project.

Complexes **4.22** and **4.23** were prepared by reaction of imidazolium salt **2.28a** and K₂CO₃ with PdCl₂ or K₂PtCl₄ in pyridine. These complexes are structurally similar to highly active PEPPSI precatalysts for cross-coupling reactions.²³² Attempts to repeat this reaction with imidazolium salt **2.28b** led to intractable mixtures; however, reaction of **2.28b** and [Pd(allyl)Cl]₂ with Ag₂O afforded complex **4.28**. Halide extraction from **4.22** with AgNO₃, followed by stirring with brine gave the chloride complex **4.25**, which later allowed the effect of halide ligands on catalysis to be investigated.

Reaction of **4.22** with PPh_3 resulted in displacement of the pyridine ligand to form **4.26**, proving the lability of the pyridine ‘throw-away’ ligand. Deprotonation of the amine group on the NHC ligand of **4.27** with aqueous KOH gave the amido-NHC hydroxide dimer **4.27**, proving that an amido complex could be formed from an amino-NHC precatalyst and an appropriate base during a catalytic reaction.

Reaction of **2.28a** and $[\text{IrCp}^*\text{Cl}_2]_2$ or $[\text{RhCp}^*\text{Cl}_2]_2$ with NaOAc did not give expected amino/amido-NHC complexes but instead gave cyclometallated complexes **4.32** and **4.33**, resulting from the C-H activation of the NHC aryl ring. No sign of the coordination of the amine group of the NHC ligand derived from **2.28a** was observed; cyclometallated complexes **4.32** and **4.33** lacked a M-N bond and were therefore unsuitable for studies of metal-amido bifunctional catalysis.

Reaction of **2.28b** and $[\text{Ru}(p\text{-cymene})\text{Cl}_2]_2$ with Ag_2O gave complex **4.34**, with the intended bidentate amino-NHC (C,NH_2) ligand. Reaction of **2.28b** and $[\text{RhCp}^*\text{Cl}_2]_2$ with *t*-BuONa gave the rhodium amino-NHC complex **4.35**; attempts to isolate a rhodium amido-NHC complex **4.37** were unsuccessful due to the sensitivity of the rhodium amide to protonation. In contrast, reaction of **2.28b** and $[\text{IrCp}^*\text{Cl}_2]_2$ with *t*-BuONa gave a stable iridium amido-NHC complex **4.36**.

In order to probe the basicity of the amido donor in the iridium amide **4.36**, the complex was treated with trifluoroacetic acid, which gave amino-NHC complex **4.38** by protonation of the amido donor. The nucleophilicity of the amido donor was investigated by reacting iridium amide **4.36** with electrophiles. Maleic anhydride was hydrolysed in the presence of **4.36**, giving amine-NHC complex **4.40** by protonation of the amide ligand. The electron-deficient alkyne dimethylacetylenedicarboxylate

(DMAD) inserted into the N-H bond of **4.36** giving **4.39**: this interesting insertion of a Michael-acceptor into an iridium amide N-H has been observed before, but is rare.^{129,282}

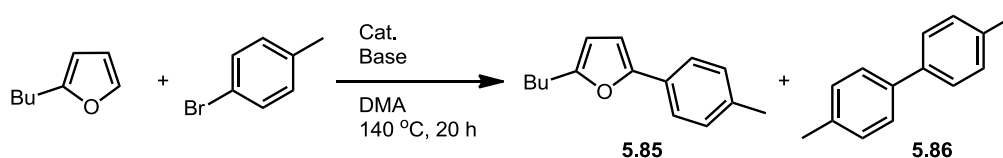
With a synthetic route to several different amino/amido-NHC complexes established, the reactivity of several of the complexes in transfer hydrogenation reactions was examined, in order to determine whether the metal-nitrogen bond could be involved in bifunctional catalysis.

Complexes **4.34-4.36** proved to be competent precatalysts in the transfer hydrogenation of acetophenone in isopropanol with *t*-BuONa base. **4.35** and **4.36** were moderately active at 80 °C, both giving > 95% conversion over 72 h, and displayed a similar activity to previously reported Cp*Ir and Rh diamine complexes.²⁶ However, **4.34** was much more active, reaching 85% conversion over 1 h at 80 °C, and displayed a comparable TON (190) to known Ru diamine^{211,24,2} and amine-NHC complexes.¹⁹ **4.36** was shown to catalyse transfer hydrogenation in the absence of base, suggesting that the Ir-N bond is participating in a bifunctional bond-cleavage event.

Having proved that complexes of amino- and amido-NHC ligands were competent precatalysts for transfer hydrogenation, the subsequent investigations examined the competency of the ligands in catalytic CH activation reactions.

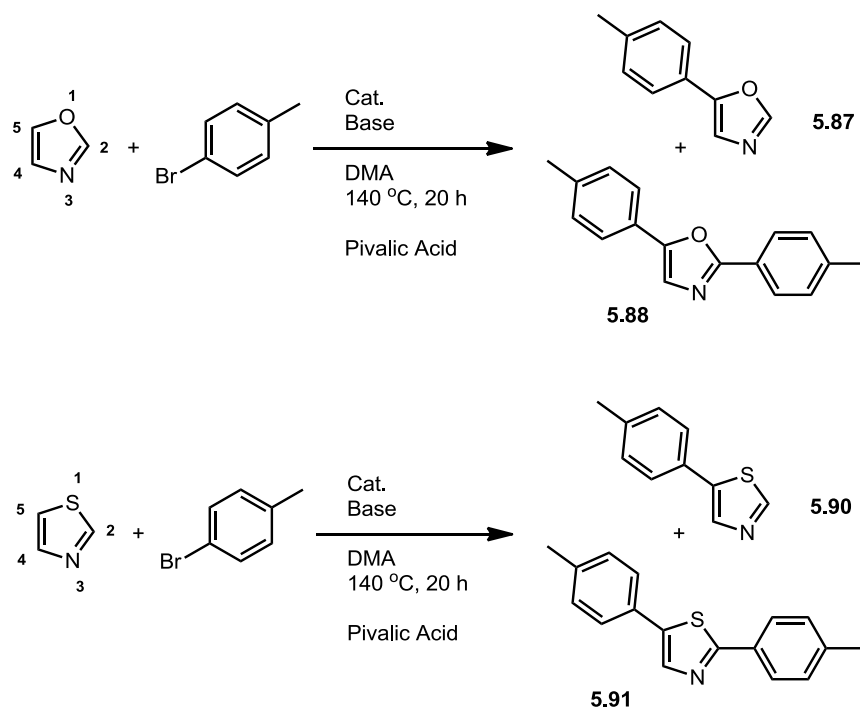
Complexes **4.22, 4.25, 4.26, 4.27, 4.28, 4.30** and **4.31** were active precatalysts for the direct arylation of 2-*n*-butylfuran, giving arylation exclusively at the C5 position, **Scheme 6.1**. However, unfunctionalised NHC complexes **4.30** and **4.31** performed

comparably to complexes having an amine-functionalised NHC ligand, suggesting that there was no positive effect on the reaction yield by the amino/amido-NHC ligand; it is doubtful that a bifunctional mechanism was involved in these direct arylation reactions.



Scheme 6.1: Direct arylation of 2-*n*-butylfuran with 4-bromotoluene.

Addition of pivalic acid to the direct arylation reaction with all active precatalysts increased the yields of product **5.85**; this suggested that direct arylation proceeded more easily when C-H activation was performed by a metal carboxylate species in an AMLA(6) mechanism.⁵ Indeed, complexes **4.22**, **4.28**, **4.30**, and **4.31** were found to be effective precatalysts for direct arylation of oxazole only in the presence of catalytic pivalic acid, **Scheme 6.2**. Similarly, direct arylation of thiazole required the addition of pivalic acid with precatalysts **4.22**, **4.30**, and **4.31**. Arylation of oxazole and thiazole was observed at both the C2 and C5 position, leading to 5-*p*-tolyl(1,3-azole) and 2,5-di-*p*-tolyl(1,3-azole) products; diarylation was discovered to occur through a reactive 2-*p*-tolylloxazole intermediate rather than *via* arylation of 5-*p*-tolylloxazole.



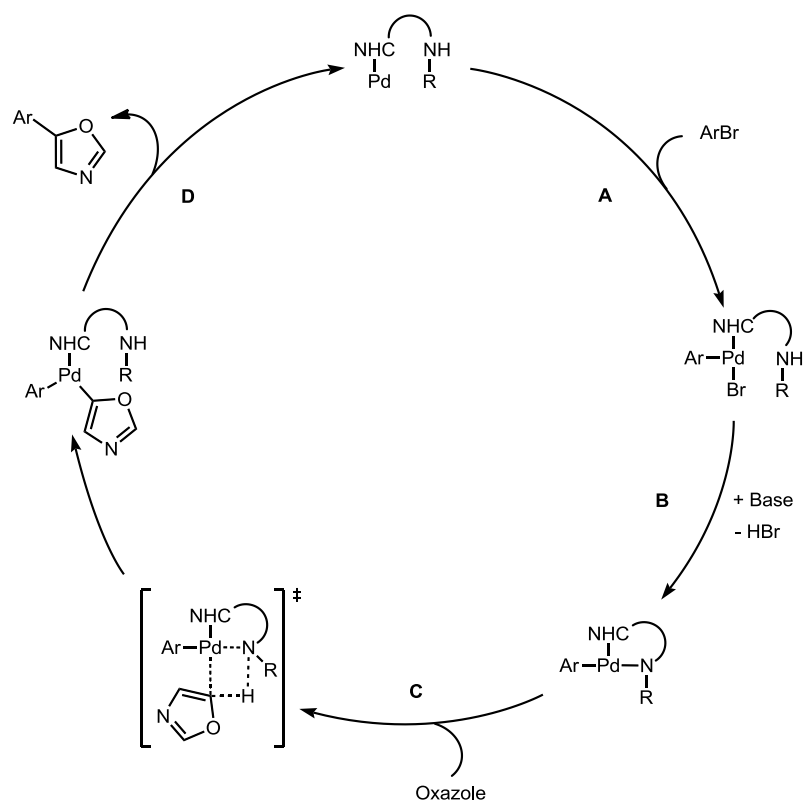
Scheme 6.2: Direct arylations of oxazole and thiazole.

No significant change in regioselectivity or yield was observed between the direct arylations of oxazole and thiazole catalysed by unfunctionalised NHC complexes **4.30** and **4.31** and amino/amido-NHC complexes **4.22** and **4.28**. The requirement for pivalic acid for successful direct arylation of oxazole and thiazole, along with the lack of difference in reactivity between unfunctionalised NHC and amino/amido-NHC complexes, suggests a bifunctional mechanism involving the amine-functionalised NHC ligand is not occurring in these cases. It is again likely that an AMLA(6) mechanism, involving C-H activation by a metal-carboxylate, is occurring here.

6.2: Future Work

Although the author has demonstrated that direct arylation of oxazole can proceed with precatalysts containing an amino-NHC ligand, pivalic acid was required for efficient conversion to product. This suggested that an AMLA(6) mechanism of C-H activation was occurring, with a metal carboxylate being the active species involved in the C-H activation step. Therefore, the next priority of this work is to try to involve an amido-NHC complex in the bifunctional C-H activation step, by an AMLA(4) mechanism.

A proposed mechanism for direct arylation by an AMLA(4) pathway involving bifunctional C-H activation by an amido-NHC complex is shown in **Scheme 6.3**. It was demonstrated that the direct arylation of oxazole proceeded in the presence of pivalic acid, which suggested that steps A (oxidative addition) and D (reductive elimination) of **Scheme 6.3** are functioning in the presence of an amino-functionalised NHC complex. Therefore, steps A and D were unlikely to be a problem if direct arylation proceeded by AMLA(4). The problematic part of the catalytic cycle is expected to be the formation of an amido-NHC complex, step B, or the C-H activation step, C.



Scheme 6.3: Proposed catalytic cycle for the direct arylation of oxazole involving AMLA(4).

If step B is not operating, a palladium amido species is not accessible, preventing the C-H activation step. This is likely because the base in the reaction, K_2CO_3 , is insufficiently basic enough to deprotonate the primary arylamine and secondary arylamine donors of the amine-functionalised NHC ligands of precatalysts **4.22** and **4.28** (for comparison: pK_a of $PhNH_2 = 30.6$; ³³⁴ $Ph_2NH = 25.0$ ³³⁵). However, as demonstrated by the different basicities of the iridium and rhodium amido complexes **4.36** and **4.37**, the acidity of a coordinated amine is also dependent on the nature of the metal centre.

Two strategies could be used to try to make step B operative. First, stronger bases could be used in the reaction. Indeed, in Chapter 5 a number of bases were screened

(KOAc, Cs₂CO₃, *t*-BuONa, KOH, NEt₃, DBU, and proton sponge) in the direct arylation of oxazole catalysed by **4.22** and **4.28**. Although this list of bases was not exhaustive, it covered a large range of basicity; yet none of these bases gave more than 5% conversion. However, it was noted that strong bases such as KOH and *t*-BuONa appeared to be incompatible with the DMA solvent, and this could be having an effect.

The second strategy could involve using an amino-NHC ligand with a more acidic amine functionality. The acidity of the amine could be increased by preparing imidazolium salts containing electron-withdrawing groups either on the amine itself (**6.1**, **Figure 6.4**, for example tosyl group), or on the aniline ring, *para*- to the amine (**6.2**, **Figure 6.4**, for example nitro group). These imidazolium salts could be accessed by coupling imidazole to a functionalised *o*-bromoaniline and subsequent alkylation; this is a similar strategy to the one used to prepare amine-functionalised imidazolium salts **2.28**. Once amino-NHC complexes derived from imidazolium salts **6.1** and **6.2** were made, the acidity of the amine could be investigated by stoichiometric reaction of these amino-NHC complexes with various bases, in order to find out whether an amido-NHC complex is easily accessible. The amino/amido-NHC complexes could then be used as precatalysts in the direct arylation reaction, allowing investigations into whether step B can be made operative.

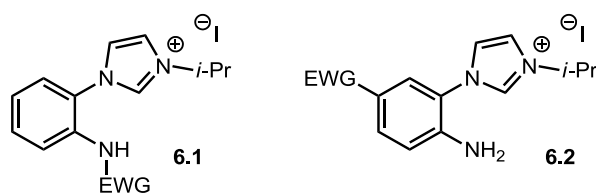


Figure 6.4: Imidazolium salts with acidic amine donors; EWG = electron-withdrawing group.

If step B could be made to function, investigations into whether the C-H activation step, C, can proceed *via* an AMLA(4) mechanism could be performed. If catalytic direct arylation of oxazole can proceed efficiently without pivalic acid, computational methods would be needed in order to determine whether an AMLA(4) mechanism is operating, rather than an electrophilic mechanism of C-H activation or simple deprotonation. The scope and regioselectivity of these direct arylation reactions could then be determined.

It is clear that bifunctional catalysis is an important and growing field, which can allow new methodology and improved efficiency in organic synthesis. In the future, functionalised NHC ligands may allow increased activity and control in catalytic reactions.

7: Appendix

List of Publications

1. W.B. Cross, C.G. Daly, R.L. Ackerman, I.R. George and K. Singh, *Dalton Trans.*, **2011**, 40, 495-505
2. C.G. Daly, K. Singh and W.B. Cross, *Acta Cryst.* **2011**, E67, m668
3. W.B. Cross, C.G. Daly, Y. Boutadla and K. Singh, *Dalton Trans.*, **2011**, 40, 9722-9730

Postgraduate Modules

Advanced Structure Determination – 1st Class

Symposia and Conferences Attended

RSC East Midlands Organic Section Meetings

2009, 2010, 2011, 2012

Exploiting the Chemistry of Metals for Catalysis, Synthesis and Spectroscopy: Award Symposium

May 2009, University of York, UK

Dalton Discussion 12 – Catalytic C-X and C-H Activation

Sept 2010, Durham University, UK

Poster presented: 'Exploring a New Mechanism for C-H Activation'

19th EuCheMS Conference on Organometallic Chemistry (EuCOMC XIX)

July 2011, Toulouse, France

Poster presented: 'Half-Sandwich Amine-NHC Complexes of Ru, Rh and Ir: C-H and N-H Activation'

8: References

1. T. Ikariya, K. Murata and R. Noyori, *Org. Biomol. Chem.*, 2006, **4**, 393–406.
2. R. Noyori, M. Yamakawa and S. Hashiguchi, *J. Org. Chem.*, 2001, **66**, 7931–7944.
3. T. Ikariya and I. D. Gridnev, *Chem. Rec.*, 2009, **9**, 106–23.
4. Y. Boutadla, D. L. Davies, S. A. Macgregor and A. I. Poblador-Bahamonde, *Dalton Trans.*, 2009, 5820–31.
5. M. Lafrance and K. Fagnou, *J. Am. Chem. Soc.*, 2006, **128**, 16496–7.
6. S. I. Gorelsky, D. Lapointe and K. Fagnou, *J. Am. Chem. Soc.*, 2008, **130**, 10848–9.
7. T. R. Cundari, T. V. Grimes and T. B. Gunnoe, *J. Am. Chem. Soc.*, 2007, **129**, 13172–82.
8. L.-C. Campeau, D. R. Stuart, J.-P. Leclerc, M. Bertrand-Laperle, E. Villemure, H.-Y. Sun, S. Lasserre, N. Guimond, M. Lecavallier and K. Fagnou, *J. Am. Chem. Soc.*, 2009, **131**, 3291–306.
9. M. Catellani, M. Costa, E. Motti, G. Maestri, M. Catellani, E. Motti and G. Maestri, *Coord. Chem. Rev.*, 2009.
10. N. Yasuda, *J. Organomet. Chem.*, 2002, **653**, 279–287.
11. C. Torborg and M. Beller, *Adv. Synth. Catal.*, 2009, **351**, 3027–3043.
12. R. H. Crabtree, *J. Organomet. Chem.*, 2004, **689**, 4083–4091.
13. J. A. Labinger and J. E. Bercaw, *Nature*, 2002, **417**, 507–14.
14. S. Díez-González, N. Marion and S. P. Nolan, *Chem. Rev.*, 2009, **109**, 3612–76.
15. N. Marion and S. P. Nolan, *Chem. Soc. Rev.*, 2008, **37**, 1776–82.
16. G. C. Fortman and S. P. Nolan, *Chem. Soc. Rev.*, 2011.
17. H. Ohara, W. W. N. O, A. J. Lough and R. H. Morris, *Dalton Trans.*, 2012, **41**, 8797–808.
18. W. W. N. O, A. J. Lough and R. H. Morris, *Chem. Commun.*, 2010, **46**, 8240–2.

References

19. W. W. N. O, A. J. Lough and R. H. Morris, *Organometallics*, 2009, **28**, 6755–6761.
20. D. Patel, S. T. Liddle, S. A. Mungur, M. Rodden, A. J. Blake and P. L. Arnold, *Chem. Commun.*, 2006, 1124–6.
21. H. Grützmacher, *Angew. Chem. Int. Ed.*, 2008, **47**, 1814–8.
22. T. Ikariya and A. J. Blacker, *Acc. Chem. Res.*, 2007, **40**, 1300–8.
23. M. Fryzuk, *Coord. Chem. Rev.*, 1989, **95**, 1–40.
24. K.-J. Haack, S. Hashiguchi, A. Fujii, T. Ikariya and R. Noyori, *Angew. Chem. Int. Ed. Engl.*, 1997, **36**, 285–288.
25. A. Fujii, S. Hashiguchi, N. Uematsu, T. Ikariya and R. Noyori, *J. Am. Chem. Soc.*, 1996, **118**, 2521–2522.
26. K. Murata, T. Ikariya and R. Noyori, *J. Org. Chem.*, 1999, **64**, 2186–2187.
27. K. Murata, H. Konishi, M. Ito and T. Ikariya, *Organometallics*, 2002, **21**, 253–255.
28. M. Watanabe, A. Ikagawa, H. Wang, K. Murata and T. Ikariya, *J. Am. Chem. Soc.*, 2004, **126**, 11148–9.
29. M. Watanabe, K. Murata and T. Ikariya, *J. Am. Chem. Soc.*, 2003, **125**, 7508–9.
30. H. Wang, M. Watanabe and T. Ikariya, *Tetrahedron Lett.*, 2005, **46**, 963–966.
31. L. C. Gregor, C.-H. Chen, C. M. Fafard, L. Fan, C. Guo, B. M. Foxman, D. G. Gusev and O. V. Ozerov, *Dalton Trans.*, 2010, **39**, 3195–202.
32. Y. Shvo, D. Czarkie, Y. Rahamim and D. F. Chodosh, *J. Am. Chem. Soc.*, 1986, **108**, 7400–7402.
33. B. L. Conley, M. K. Pennington-Boggio, E. Boz and T. J. Williams, *Chem. Rev.*, 2010, **110**, 2294–312.
34. C. Gunanathan and D. Milstein, *Acc. Chem. Res.*, 2011, **44**, 588–602.
35. J. Zhang, G. Leitus, Y. Ben-David and D. Milstein, *J. Am. Chem. Soc.*, 2005, **127**, 10840–1.
36. C. Gunanathan, Y. Ben-David and D. Milstein, *Science*, 2007, **317**, 790–2.
37. B. Gnanaprakasam, J. Zhang and D. Milstein, *Angew. Chem. Int. Ed. Engl.*, 2010, **49**, 1468–71.

References

38. C. Gunanathan, L. J. W. Shimon and D. Milstein, *J. Am. Chem. Soc.*, 2009, **131**, 3146–7.
39. S. W. Kohl, L. Weiner, L. Schwartsburd, L. Konstantinovski, L. J. W. Shimon, Y. Ben-David, M. A. Iron and D. Milstein, *Science*, 2009, **324**, 74–7.
40. J. Zhang, G. Leitus, Y. Ben-David and D. Milstein, *Angew. Chem. Int. Ed. Engl.*, 2006, **45**, 1113–5.
41. E. Balaraman, B. Gnanaprakasam, L. J. W. Shimon and D. Milstein, *J. Am. Chem. Soc.*, 2010, **132**, 16756–8.
42. E. Balaraman, C. Gunanathan, J. Zhang, L. J. W. Shimon and D. Milstein, *Nature Chem.*, 2011, **3**, 609–14.
43. H. Zeng and Z. Guan, *J. Am. Chem. Soc.*, 2011, **133**, 1159–61.
44. J. G. Stark and H. G. Wallace, *Chemistry Data Book*, Hodder Murray, London, 3rd edn., 2006.
45. D. J. C. Constable, P. J. Dunn, J. D. Hayler, G. R. Humphrey, J. L. Leazer, R. J. Linderman, K. Lorenz, J. Manley, B. A. Pearlman and A. Wells, *Green Chem.*, 2007, **9**, 411.
46. L. V. Desai, K. J. Stowers and M. S. Sanford, *J. Am. Chem. Soc.*, 2008, **130**, 13285–93.
47. J. Chatt and J. Davidson, *J. Chem. Soc.*, 1965.
48. D. L. Milner and M. A. Bennett, *Chem. Commun.*, 1967, 581–582.
49. P. Foley and G. M. Whitesides, *J. Am. Chem. Soc.*, 1979, **101**, 2732–2733.
50. R. G. Bergman and A. H. Janowicz, *J. Am. Chem. Soc.*, 1982, **104**, 352–354.
51. W. A. G. Graham and J. K. Hoyano, *J. Am. Chem. Soc.*, 1982, **104**, 3723–3725.
52. P. L. Watson, *J. Am. Chem. Soc.*, 1983, **105**, 6491–6493.
53. M. E. Thompson, S. M. Baxter, A. R. Bulls, B. J. Burger, M. C. Nolan, B. D. Santarsiero, W. P. Schaefer and J. E. Bercaw, *J. Am. Chem. Soc.*, 1987, **109**, 203–219.
54. P. Burger and R. G. Bergman, *J. Am. Chem. Soc.*, 1993, **115**, 10462–10463.
55. D. M. Tellers, C. M. Yung, B. A. Arndtsen, D. R. Adamson and R. G. Bergman, *J. Am. Chem. Soc.*, 2002, **124**, 1400–1410.

References

56. D. L. Strout, S. Zarić, S. Niu and M. B. Hall, *J. Am. Chem. Soc.*, 1996, **118**, 6068–6069.
57. S. Niu and M. B. Hall, *J. Am. Chem. Soc.*, 1998, **120**, 6169–6170.
58. J. F. Hartwig, K. S. Cook, M. Hapke, C. D. Incarvito, Y. Fan, C. E. Webster and M. B. Hall, *J. Am. Chem. Soc.*, 2005, **127**, 2538–52.
59. R. N. Perutz and S. Sabo-Etienne, *Angew. Chem. Int. Ed. Engl.*, 2007, **46**, 2578–92.
60. J. Oxgaard, R. A. Periana and W. A. Goddard, *J. Am. Chem. Soc.*, 2004, **126**, 11658–65.
61. Z. Lin, *Coord. Chem. Rev.*, 2007, **251**, 2280–2291.
62. B. A. Vastine and M. B. Hall, *J. Am. Chem. Soc.*, 2007, **129**, 12068–9.
63. K. M. Waltz and J. F. Hartwig, *Science*, 1997, **277**, 211–213.
64. C. E. Webster, Y. Fan, M. B. Hall, D. Kunz and J. F. Hartwig, *J. Am. Chem. Soc.*, 2003, **125**, 858–9.
65. N. F. Gol'dshleger, M. B. Tyabin, A. E. Shilov and A. A. Shteinman, *Zh. Fiz. Khim.*, 1969, 2174.
66. N. F. Gol'dshleger, V. V. Es'cova, A. E. Shilov and A. A. Shteinman, *Zh. Fiz. Khim.*, 1972, 1353.
67. W.-H. Cheng and H. H. Kung, *Methanol Production and Use*, Marcel Dekker, New York, 1994.
68. R. A. Periana, D. J. Taube, S. Gamble, H. Taube, T. Satoh and H. Fujii, *Science*, 1998, **280**, 560–564.
69. M. Muehlhofer, T. Strassner and W. A. Herrmann, *Angew. Chem. Int. Ed.*, 2002, **41**, 1745–1747.
70. A. N. Vedernikov, *Chem. Commun.*, 2009, 4781–90.
71. A. N. Vedernikov, *Acc. Chem. Res.*, 2012, **45**, 803–13.
72. D. H. Ess, W. A. Goddard III, R. J. Nielsen and R. A. Periana, *J. Am. Chem. Soc.*, 2009, **131**, 11686–11688.
73. D. H. Ess, T. B. Gunnoe, T. R. Cundari, W. A. Goddard and R. A. Periana, *Organometallics*, 2010, **29**, 6801–6815.

References

74. S. I. Gorelsky, D. Lapointe and K. Fagnou, *J. Org. Chem.*, 2011, **77**, 658–668.
75. L.-C. Campeau, M. Bertrand-Laperle, J.-P. Leclerc, E. Villemure, S. Gorelsky and K. Fagnou, *J. Am. Chem. Soc.*, 2008, **130**, 3276–7.
76. M. Lafrance, D. Lapointe and K. Fagnou, *Tetrahedron*, 2008, **64**, 6015–6020.
77. Y. Boutadla, O. Al-Duaij, D. L. Davies, G. A. Griffith and K. Singh, *Organometallics*, 2009, **28**, 433–440.
78. Y. Boutadla, D. L. Davies, S. A. Macgregor and A. I. Poblador-Bahamonde, *Dalton Trans.*, 2009, 5887–93.
79. P. J. Walsh, F. J. Hollander and R. G. Bergman, *J. Am. Chem. Soc.*, 1988, **110**, 8729–8731.
80. C. C. Cummins, S. M. Baxter and P. T. Wolczanski, *J. Am. Chem. Soc.*, 1988, **110**, 8731–8733.
81. N. Ochi, Y. Nakao, H. Sato and S. Sakaki, *J. Am. Chem. Soc.*, 2007, **129**, 8615–8624.
82. B. C. Bailey, J. C. Huffman and D. J. Mindiola, *J. Am. Chem. Soc.*, 2007, **129**, 5302–3.
83. W. J. Tenn, K. J. H. Young, G. Bhalla, J. Oxgaard, W. A. Goddard and R. A. Periana, *J. Am. Chem. Soc.*, 2005, **127**, 14172–3.
84. J. Oxgaard, W. J. Tenn, R. J. Nielsen, W. A. Goddard and R. A. Periana, *Organometallics*, 2007, **26**, 1565–1567.
85. S. M. Bischof, D. H. Ess, S. K. Meier, J. Oxgaard, R. J. Nielsen, G. Bhalla, W. A. Goddard and R. A. Periana, *Organometallics*, 2010, **29**, 742–756.
86. Y. Feng, M. Lail, N. A. Foley, T. B. Gunnoe, K. A. Barakat, T. R. Cundari and J. L. Petersen, *J. Am. Chem. Soc.*, 2006, **128**, 7982–94.
87. Y. Feng, M. Lail, K. A. Barakat, T. R. Cundari, T. B. Gunnoe and J. L. Petersen, *J. Am. Chem. Soc.*, 2005, **127**, 14174–5.
88. R. F. Jordan and D. F. Taylor, *J. Am. Chem. Soc.*, 1989, **111**, 778–779.
89. E. J. Moore, W. R. Pretzer, T. J. O’Connell, J. Harris, L. LaBounty, L. Chou and S. S. Grimmer, *J. Am. Chem. Soc.*, 1992, **114**, 5888–5890.
90. S. Oi, S. Fukita, N. Hirata, N. Watanuki, S. Miyano and Y. Inoue, *Org. Lett.*, 2001, **3**, 2579–2581.

References

91. D. Kalyani, N. R. Deprez, L. V. Desai and M. S. Sanford, *J. Am. Chem. Soc.*, 2005, **127**, 7330–1.
92. F. Kakiuchi, T. Sato, M. Yamauchi, N. Chatani and S. Murai, *Chem. Lett.*, 1999, 19–20.
93. B. Sezen and D. Sames, *J. Am. Chem. Soc.*, 2004, **126**, 13244–6.
94. S. Murai, F. Kakiuchi, S. Sekine, Y. Tanaka, A. Kamatani, M. Sonoda and N. Chatani, *Nature*, 1993, **366**, 529–531.
95. F. Kakiuchi, M. Yamauchi, N. Chatani and S. Murai, *Chem. Lett.*, 1996, 111–112.
96. L. V. Desai, K. L. Hull and M. S. Sanford, *J. Am. Chem. Soc.*, 2004, **126**, 9542–3.
97. H. A. Chiong, Q.-N. Pham and O. Daugulis, *J. Am. Chem. Soc.*, 2007, **129**, 9879–84.
98. O. Daugulis and V. G. Zaitsev, *Angew. Chem. Int. Ed. Engl.*, 2005, **44**, 4046–8.
99. S. Yanagisawa, T. Sudo, R. Noyori and K. Itami, *J. Am. Chem. Soc.*, 2006, **128**, 11748–9.
100. L. Caron, L.-C. Campeau and K. Fagnou, *Org. Lett.*, 2008, **10**, 4533–6.
101. L.-C. Campeau, M. Parisien, M. Leblanc and K. Fagnou, *J. Am. Chem. Soc.*, 2004, **126**, 9186–7.
102. L.-C. Campeau, M. Parisien, A. Jean and K. Fagnou, *J. Am. Chem. Soc.*, 2006, **128**, 581–90.
103. J. Peng, T. Chen, C. Chen and B. Li, *J. Org. Chem.*, 2011, **76**, 9507–13.
104. G. P. McGlacken and L. M. Bateman, *Chem. Soc. Rev.*, 2009, **38**, 2447–64.
105. F. Bellina and R. Rossi, *Tetrahedron*, 2009, **65**, 10269–10310.
106. S. Yanagisawa, K. Ueda, H. Sekizawa and K. Itami, *J. Am. Chem. Soc.*, 2009, **131**, 14622–3.
107. S.-Y. Tang, Q.-X. Guo and Y. Fu, *Chem. Eur. J.*, 2011, 1–12.
108. K. Öfele, W. A. Herrmann, D. Mihalios, M. Elison, E. Herdtweck, W. Scherer and J. Mink, *J. Organomet. Chem.*, 1993, **459**, 177–184.
109. W. A. Herrmann, K. Öfele, M. Elison, F. E. Kühn and P. W. Roesky, *J. Organomet. Chem.*, 1994, **480**, c7–c9.

References

110. H.-W. Wanzlick and H.-J. Schönherr, *Angew. Chem. Int. Ed. Engl.*, 1968, **7**, 141–142.
111. K. Öfele, *J. Organomet. Chem.*, 1968, **12**, P42–P43.
112. A. J. Arduengo, R. L. Harlow and M. Kline, *J. Am. Chem. Soc.*, 1991, **113**, 361–363.
113. A. J. Arduengo, H. V. R. Dias, R. L. Harlow and M. Kline, *J. Am. Chem. Soc.*, 1992, **114**, 5530–5534.
114. S. Díez-González and S. P. Nolan, *Coord. Chem. Rev.*, 2007, **251**, 874–883.
115. W. A. Herrmann, M. Elison, J. Fischer, C. Köcher and G. R. J. Artus, *Angew. Chem. Int. Ed. Engl.*, 1995, **34**, 2371–2374.
116. R. W. Alder, P. R. Allen and S. J. Williams, *J. Chem. Soc. Chem. Commun.*, 1995, 1267.
117. A. Azua, S. Sanz and E. Peris, *Chem. Eur. J.*, 2011, **17**, 3963–7.
118. H. M. J. Wang and I. J. B. Lin, *Organometallics*, 1998, **17**, 972–975.
119. M. R. L. Furst and C. S. J. Cazin, *Chem. Commun.*, 2010, **46**, 6924–5.
120. D. S. McGuinness, K. J. Cavell, B. F. Yates, B. W. Skelton and A. H. White, *J. Am. Chem. Soc.*, 2001, **123**, 8317–8328.
121. A. Fürstner, G. Seidel, D. Kremzow and C. W. Lehmann, *Organometallics*, 2003, **22**, 907–909.
122. D. Kremzow, G. Seidel, C. W. Lehmann and A. Fürstner, *Chem. Eur. J.*, 2005, **11**, 1833–53.
123. A. M. Voutchkova, M. Feliz, E. Clot, O. Eisenstein and R. H. Crabtree, *J. Am. Chem. Soc.*, 2007, **129**, 12834–46.
124. A. M. Voutchkova, L. N. Appelhans, A. R. Chianese and R. H. Crabtree, *J. Am. Chem. Soc.*, 2005, **127**, 17624–5.
125. M. Lappert, P. Power, A. Protchenko and A. L. Seeber, *Metal Amide Chemistry*, Wiley, Hoboken, 2009.
126. H. E. Bryndza and W. Tam, *Chem. Rev.*, 1988, **88**, 1163–1188.
127. J. R. Fulton, A. W. Holland, D. J. Fox and R. G. Bergman, *Acc. Chem. Res.*, 2002, **35**, 44–56.

References

128. H. E. Bryndza, W. C. Fultz and W. Tam, *Organometallics*, 1985, **4**, 939–940.
129. D. S. Glueck, L. J. N. Winslow and R. G. Bergman, *Organometallics*, 1991, **10**, 1462–1479.
130. S. Park, *Bull. Korean Chem. Soc.*, 2001, **22**, 15–16.
131. L. A. Villanueva, K. A. Abboud and J. M. Boncella, *Organometallics*, 1992, **11**, 2963–2965.
132. P. S. Hanley, D. Marković and J. F. Hartwig, *J. Am. Chem. Soc.*, 2010, **132**, 6302–3.
133. L. Benhamou, E. Chardon, G. Lavigne, S. Bellemin-Laponnaz and V. César, *Chem. Rev.*, 2011, **111**, 2705–33.
134. I. C. Calder, T. M. Spotswood and W. H. P. Sasse, *Tetrahedron Lett.*, 1963, **4**, 95–100.
135. S. Würtz and F. Glorius, *Acc. Chem. Res.*, 2008, **41**, 1523–33.
136. L. Jafarpour, E. D. Stevens and S. P. Nolan, *J. Organomet. Chem.*, 2000, **606**, 49–54.
137. A. Arduengo, *Tetrahedron*, 1999, **55**, 14523–14534.
138. J. Clayden, N. Greeves, S. Warren and P. Wothers, *Organic Chemistry*, Oxford University Press, Oxford, 2001.
139. A. J. Arduengo, *U.S. Pat.*, 1991, 5077414.
140. F. A. Cotton, P. Lei, C. A. Murillo and L.-S. Wang, *Inorg. Chim. Acta*, 2003, **349**, 165–172.
141. A. Bertogg, F. Camponovo and A. Togni, *Eur. J. Inorg. Chem.*, 2005, **2005**, 347–356.
142. K. Hirano, S. Urban, C. Wang and F. Glorius, *Org. Lett.*, 2009, **11**, 1019–22.
143. A. Fürstner, M. Alcarazo, V. César and C. W. Lehmann, *Chem. Commun.*, 2006, 2176–8.
144. S. Carda-Broch, A. Berthod and D. W. Armstrong, *Anal. Bioanal. Chem.*, 2003, **375**, 191–9.
145. V. C. Vargas, R. J. Rubio, T. K. Hollis and M. E. Salcido, *Org. Lett.*, 2003, **5**, 4847–9.

References

146. R. J. Rubio, G. T. S. Andavan, E. B. Bauer, T. K. Hollis, J. Cho, F. S. Tham and B. Donnadieu, *J. Organomet. Chem.*, 2005, **690**, 5353–5364.
147. J. Cho, T. K. Hollis, T. R. Helgert and E. J. Valente, *Chem. Commun.*, 2008, 5001–3.
148. J. Cho, T. K. Hollis, E. J. Valente and J. M. Trate, *J. Organomet. Chem.*, 2011, **696**, 373–377.
149. T. R. Helgert, T. K. Hollis and E. J. Valente, *Organometallics*, 2012, **31**, 3002–3009.
150. A. T. Normand and K. J. Cavell, *Eur. J. Inorg. Chem.*, 2008, **2008**, 2781–2800.
151. A. M. Magill, D. S. McGuinness, K. J. Cavell, G. J. . Britovsek, V. C. Gibson, A. J. . White, D. J. Williams, A. H. White and B. W. Skelton, *J. Organomet. Chem.*, 2001, **617-618**, 546–560.
152. J. A. Loch, M. Albrecht, E. Peris, J. Mata, J. W. Faller and R. H. Crabtree, *Organometallics*, 2002, **21**, 700–706.
153. S. Gründemann, M. Albrecht, J. A. Loch, J. W. Faller and R. H. Crabtree, *Organometallics*, 2001, **20**, 5485–5488.
154. E. Peris, J. Mata, J. A. Loch and R. H. Crabtree, *Chem. Commun.*, 2001, 201–202.
155. A. A. D. Tulloch, A. A. Danopoulos, G. J. Tizzard, S. J. Coles, M. B. Hursthouse, R. S. Hay-Motherwell and W. B. Motherwell, *Chem. Commun.*, 2001, 1270–1271.
156. P. L. Chiu, C.-L. Lai, C.-F. Chang, C.-H. Hu and H. M. Lee, *Organometallics*, 2005, **24**, 6169–6178.
157. R. Wang, B. Twamley and J. M. Shreeve, *J. Org. Chem.*, 2006, **71**, 426–9.
158. V. César, S. Bellemin-Laponnaz and L. H. Gade, *Organometallics*, 2002, **21**, 5204–5208.
159. L. H. Gade, V. César and S. Bellemin-Laponnaz, *Angew. Chem. Int. Ed. Engl.*, 2004, **43**, 1014–7.
160. V. César, S. Bellemin-Laponnaz, H. Wadepohl and L. H. Gade, *Chem. Eur. J.*, 2005, **11**, 2862–73.
161. L. P. Spencer, S. Winston and M. D. Fryzuk, *Organometallics*, 2004, **23**, 3372–3374.
162. L. P. Spencer and M. D. Fryzuk, *J. Organomet. Chem.*, 2005, **690**, 5788–5803.

References

163. H. Jong, B. O. Patrick and M. D. Fryzuk, *Can. J. Chem.*, 2008, **86**, 803–810.
164. H. Jong, B. O. Patrick and M. D. Fryzuk, *Organometallics*, 2011, **30**, 2333–2341.
165. P. L. Arnold, S. A. Mungur, A. J. Blake and C. Wilson, *Angew. Chem. Int. Ed. Engl.*, 2003, **42**, 5981–4.
166. P. L. Arnold, J. McMaster and S. T. Liddle, *Chem. Commun.*, 2009, 818–20.
167. I. S. Edworthy, A. J. Blake, C. Wilson and P. L. Arnold, *Organometallics*, 2007, **26**, 3684–3689.
168. P. L. Arnold, I. S. Edworthy, C. D. Carmichael, A. J. Blake and C. Wilson, *Dalton Trans.*, 2008, 3739–46.
169. R. E. Douthwaite, J. Houghton and B. M. Kariuki, *Chem. Commun.*, 2004, 698–9.
170. W. Wei, Y. Qin, M. Luo, P. Xia and M. S. Wong, *Organometallics*, 2008, **27**, 2268–2272.
171. M. Uchiyama, Y. Matsumoto, S. Nakamura, T. Ohwada, N. Kobayashi, N. Yamashita, A. Matsumiya and T. Sakamoto, *J. Am. Chem. Soc.*, 2004, **126**, 8755–9.
172. A. R. Chianese, P. T. Bremer, C. Wong and R. J. Reynes, *Organometallics*, 2009, **28**, 5244–5252.
173. R. A. Altman and S. L. Buchwald, *Org. Lett.*, 2006, **8**, 2779–82.
174. R. A. Altman, E. D. Koval and S. L. Buchwald, *J. Org. Chem.*, 2007, **72**, 6190–9.
175. A. J. Blake, B. A. J. Clark, H. McNab and C. C. Sommerville, *J. Chem. Soc. Perkin Trans. 1*, 1997, 1605–1608.
176. J. T. Singleton, *Tetrahedron*, 2003, **59**, 1837–1857.
177. C. J. Moulton and B. L. Shaw, *J. Chem. Soc. Dalton Trans.*, 1976, 1020.
178. R. A. Gossage, L. A. van de Kuil and G. van Koten, *Acc. Chem. Res.*, 1998, **31**, 423–431.
179. M. Ohff, A. Ohff, M. E. van der Boom and D. Milstein, *J. Am. Chem. Soc.*, 1997, **119**, 11687–11688.
180. D. Morales-Morales, R. Redón, C. Yung and C. M. Jensen, *Chem. Commun.*, 2000, 1619–1620.

References

181. D. E. Bergbreiter, P. L. Osburn and Y.-S. Liu, *J. Am. Chem. Soc.*, 1999, **121**, 9531–9538.
182. S. Sjövall, O. F. Wendt and C. Andersson, *J. Chem. Soc. Dalton Trans.*, 2002, 1396–1400.
183. D. Zim, A. S. Gruber, G. Ebeling, J. Dupont and A. L. Monteiro, *Org. Lett.*, 2000, **2**, 2881–2884.
184. R. B. Bedford, S. M. Draper, P. Noelle Scully and S. L. Welch, *New J. Chem.*, 2000, **24**, 745–747.
185. M. A. Stark and C. J. Richards, *Tetrahedron Lett.*, 1997, **38**, 5881–5884.
186. H. M. Lee, J. Y. Zeng, C.-H. Hu and M.-T. Lee, *Inorg. Chem.*, 2004, **43**, 6822–9.
187. S. Gischig and A. Togni, *Eur. J. Inorg. Chem.*, 2005, **2005**, 4745–4754.
188. S. Gischig and A. Togni, *Organometallics*, 2004, **23**, 2479–2487.
189. D. J. Nielsen, A. M. Magill, B. F. Yates, K. J. Cavell, B. W. Skelton and A. H. White, *Chem. Commun.*, 2002, 2500–2501.
190. A. A. Danopoulos, N. Tsoureas, J. C. Green and M. B. Hursthouse, *Chem. Commun.*, 2003, 756–757.
191. D. J. Nielsen, K. J. Cavell, B. W. Skelton and A. H. White, *Inorg. Chim. Acta*, 2002, **327**, 116–125.
192. A. A. Danopoulos, A. A. D. Tulloch, S. Winston, G. Eastham and M. B. Hursthouse, *Dalton Trans.*, 2003, 1009–1015.
193. J. R. Miecznikowski, S. Gründemann, M. Albrecht, C. Mégret, E. Clot, J. W. Faller, O. Eisenstein and R. H. Crabtree, *Dalton Trans.*, 2003, 831–838.
194. P. Ren, O. Vechorkin, Z. Csok, I. Salihu, R. Scopelliti and X. Hu, *Dalton Trans.*, 2011, **40**, 8906–11.
195. Z. Csok, O. Vechorkin, S. B. Harkins, R. Scopelliti and X. Hu, *J. Am. Chem. Soc.*, 2008, **130**, 8156–7.
196. J. C. Peters, S. B. Harkins, S. D. Brown and M. W. Day, *Inorg. Chem.*, 2001, **40**, 5083–5091.
197. S. B. Harkins and J. C. Peters, *Organometallics*, 2002, **21**, 1753–1755.
198. Z.-X. Wang and L. Wang, *Chem. Commun.*, 2007, 2423.

References

199. L.-C. Liang, P.-S. Chien, J.-M. Lin, M.-H. Huang, Y.-L. Huang and J.-H. Liao, *Organometallics*, 2006, **25**, 1399–1411.
200. M.-H. Huang and L.-C. Liang, *Organometallics*, 2004, **23**, 2813–2816.
201. L.-C. Liang, J.-M. Lin and W.-Y. Lee, *Chem. Commun.*, 2005, 2462–4.
202. L.-C. Liang, P.-S. Chien and Y.-L. Huang, *J. Am. Chem. Soc.*, 2006, **128**, 15562–3.
203. L. Fan, B. M. Foxman and O. V. Ozerov, *Organometallics*, 2004, **23**, 326–328.
204. O. V. Ozerov, C. Guo, L. Fan and B. M. Foxman, *Organometallics*, 2004, **23**, 5573–5580.
205. L. Fan, L. Yang, C. Guo, B. M. Foxman and O. V. Ozerov, *Organometallics*, 2004, **23**, 4778–4787.
206. Y. Zhu, C.-H. Chen, C. M. Fafard, B. M. Foxman and O. V. Ozerov, *Inorg. Chem.*, 2011, **50**, 7980–7.
207. J. Kuroda, K. Inamoto, K. Hiroya and T. Doi, *Eur. J. Org. Chem.*, 2009, **2009**, 2251–2261.
208. F. H. Allen, *Acta Crystallogr., Sect. B: Struct. Sci.*, 2002, **58**, 380–388.
209. A. S. Goldman and K. I. Goldberg, in *Activation and Functionalization of C-H Bonds*, eds. A. S. Goldman and K. I. Goldberg, ACS Symposium Series 885; American Chemical Society, Washington, DC, 2004.
210. P. van der Sluis and A. L. Spek, *Acta Crystallogr. Sect. A: Found. Crystallogr.*, 1990, **46**, 194–201.
211. S. Hashiguchi, A. Fujii, J. Takehara, T. Ikariya and R. Noyori, *J. Am. Chem. Soc.*, 1995, **117**, 7562–7563.
212. C. A. Sandoval, T. Ohkuma, N. Utsumi, K. Tsutsumi, K. Murata and R. Noyori, *Chem. Asian J.*, 2006, **1**, 102–10.
213. R. Noyori, M. Yamakawa and S. Hashiguchi, *J. Org. Chem.*, 2001, **66**, 7931–7944.
214. M. Ito, S. Kitahara and T. Ikariya, *J. Am. Chem. Soc.*, 2005, **127**, 6172–3.
215. S. Kuwata and T. Ikariya, *Dalton Trans.*, 2010, **39**, 2984–92.
216. S. Arita, T. Koike, Y. Kayaki and T. Ikariya, *Organometallics*, 2008, **27**, 2795–2802.

References

217. M. Ito, A. Sakaguchi, C. Kobayashi and T. Ikariya, *J. Am. Chem. Soc.*, 2007, **129**, 290–1.
218. M. Ito, M. Hirakawa, A. Osaku and T. Ikariya, *Organometallics*, 2003, **22**, 4190–4192.
219. M. Ito, *Pure Appl. Chem.*, 2008, **80**, 1047–1053.
220. M. Ito, Y. Shibata, A. Watanabe and T. Ikariya, *Synlett*, 2009, **2009**, 1621–1626.
221. W. A. Herrmann, C. Köcher, L. J. Gooßen and G. R. J. Artus, *Chem. Eur. J.*, 1996, **2**, 1627–1636.
222. H. Jong, B. O. Patrick and M. D. Fryzuk, *Organometallics*, 2011, **30**, 2333–2341.
223. G. C. Vougioukalakis and R. H. Grubbs, *Chem. Rev.*, 2010, **110**, 1746–87.
224. S. Warsink, S. Y. de Boer, L. M. Jongens, C.-F. Fu, S.-T. Liu, J.-T. Chen, M. Lutz, A. L. Spek and C. J. Elsevier, *Dalton Trans.*, 2009, 7080–6.
225. S. Warsink, P. Hauwert, M. A. Siegler, A. L. Spek and C. J. Elsevier, *Appl. Organomet. Chem.*, 2009, **23**, 225–228.
226. P. Hauwert, R. Boerleider, S. Warsink, J. J. Weigand and C. J. Elsevier, *J. Am. Chem. Soc.*, 2010, **132**, 16900–10.
227. L. G. Bonnet, R. E. Douthwaite, R. Hodgson, J. Houghton, B. M. Kariuki and S. Simonovic, *Dalton Trans.*, 2004, 3528–35.
228. W. W. N. O, A. J. Lough and R. H. Morris, *Organometallics*, 2012, **31**, 2137–2151.
229. W. W. N. O, A. J. Lough and R. H. Morris, *Organometallics*, 2011, **30**, 1236–1252.
230. W. W. N. O, A. J. Lough and R. H. Morris, *Organometallics*, 2012, **31**, 2152–2165.
231. C. J. O'Brien, E. A. B. Kantchev, C. Valente, N. Hadei, G. A. Chass, A. Lough, A. C. Hopkinson and M. G. Organ, *Chem. Eur. J.*, 2006, **12**, 4743–8.
232. J. Nasielski, N. Hadei, G. Achonduh, E. A. B. Kantchev, C. J. O'Brien, A. Lough and M. G. Organ, *Chem. Eur. J.*, 2010, **16**, 10844–53.
233. L. Ray, M. M. Shaikh and P. Ghosh, *Dalton Trans.*, 2007, 4546–55.
234. L. Ray, S. Barman, M. M. Shaikh and P. Ghosh, *Chem. Eur. J.*, 2008, **14**, 6646–55.
235. C. Pubill-Ulldemolins, C. Bo, J. A. Mata and E. Fernández, *Chem. Asian J.*, 2010, **5**, 261–4.

References

236. M. Konkol, C. Wagner, S. Schwieger, R. Lindner and D. Steinborn, *Z. Anorg. Allg. Chem.*, 2005, **631**, 1456–1462.
237. P. A. Lord, B. C. Noll, M. M. Olmstead and A. L. Balch, *J. Am. Chem. Soc.*, 2001, **123**, 10554–10559.
238. L. Ray, M. M. Shaikh and P. Ghosh, *Organometallics*, 2007, **26**, 958–964.
239. C.-F. Fu, C.-C. Lee, Y.-H. Liu, S.-M. Peng, S. Warsink, C. J. Elsevier, J.-T. Chen and S.-T. Liu, *Inorg. Chem.*, 2010, **49**, 3011–8.
240. J. D. Blakemore, M. J. Chalkley, J. H. Farnaby, L. M. Guard, N. Hazari, C. D. Incarvito, E. D. Luzik and H. W. Suh, *Organometallics*, 2011, **30**, 1818–1829.
241. W. A. Herrmann, V. P. . Böhm, C. W. . Gstöttmayr, M. Grosche, C.-P. Reisinger and T. Weskamp, *J. Organomet. Chem.*, 2001, **617-618**, 616–628.
242. A. Flahaut, K. Toutah, P. Mangeney and S. Roland, *Eur. J. Inorg. Chem.*, 2009, **2009**, 5422–5432.
243. O. Esposito, P. M. P. Gois, A. K. de K. Lewis, S. Caddick, F. G. N. Cloke and P. B. Hitchcock, *Organometallics*, 2008, **27**, 6411–6418.
244. A. D. Getty and K. I. Goldberg, *Organometallics*, 2001, **20**, 2545–2551.
245. A. Fujii, E. Hagiwara and M. Sodeoka, *J. Am. Chem. Soc.*, 1999, **121**, 5450–5458.
246. L. Díez, P. Espinet and J. A. Miguel, *J. Chem. Soc. Dalton Trans.*, 2001, 1189–1195.
247. D. Nama, D. Schott, P. S. Pregosin, L. F. Veiros and M. J. Calhorda, *Organometallics*, 2006, **25**, 4596–4604.
248. A. Hadzovic and D. Song, *Inorg. Chem.*, 2008, **47**, 12010–7.
249. G. Pieri, M. Pasquali, P. Leoni and U. Englert, *J. Organomet. Chem.*, 1995, **491**, 27–30.
250. *CCDC 239623*, .
251. A. Peloso, *Coord. Chem. Rev.*, 1973, **10**, 123–181.
252. J. J. Pesek and W. R. Mason, *Inorg. Chem.*, 1983, **22**, 2958–2959.
253. F. Basolo, J. Chatt, H. B. Gray, R. G. Pearson and B. L. Shaw, *J. Chem. Soc.*, 1961, 2207.

References

254. O. Navarro, H. Kaur, P. Mahjoor and S. P. Nolan, *J. Org. Chem.*, 2004, **69**, 3173–80.
255. M. S. Viciu, O. Navarro, R. F. Germaneau, R. A. Kelly, W. Sommer, N. Marion, E. D. Stevens, L. Cavallo and S. P. Nolan, *Organometallics*, 2004, **23**, 1629–1635.
256. N. Marion, O. Navarro, J. Mei, E. D. Stevens, N. M. Scott and S. P. Nolan, *J. Am. Chem. Soc.*, 2006, **128**, 4101–11.
257. Y. Kashiwame, S. Kuwata and T. Ikariya, *Chem. Eur. J.*, 2010, **16**, 766–70.
258. X.-Q. Xiao and G.-X. Jin, *J. Organomet. Chem.*, 2008, **693**, 316–320.
259. X.-Q. Xiao and G.-X. Jin, *J. Organomet. Chem.*, 2008, **693**, 3363–3368.
260. X. Wang, S. Liu, L.-H. Weng and G.-X. Jin, *Chem. Eur. J.*, 2007, **13**, 188–95.
261. R. Corberán, M. Sanaú and E. Peris, *Organometallics*, 2006, **25**, 4002–4008.
262. R. Corberán, M. Sanaú and E. Peris, *J. Am. Chem. Soc.*, 2006, **128**, 3974–9.
263. R. Corberán, V. Lillo, J. A. Mata, E. Fernandez and E. Peris, *Organometallics*, 2007, **26**, 4350–4353.
264. M. Poyatos, W. McNamara, C. Incarvito, E. Clot, E. Peris and R. H. Crabtree, *Organometallics*, 2008, **27**, 2128–2136.
265. L. Li, W. W. Brennessel and W. D. Jones, *Organometallics*, 2009, **28**, 3492–3500.
266. Y. Boutadla, D. L. Davies, R. C. Jones and K. Singh, *Chem. Eur. J.*, 2011, **17**, 3438–48.
267. R. D. Shannon, *Acta Crystallogr. Sect. A: Found. Crystallogr.*, 1976, **32**, 751–767.
268. Y. Tanabe, F. Hanasaka, K. Fujita and R. Yamaguchi, *Organometallics*, 2007, **26**, 4618–4626.
269. T. P. Brewster, J. D. Blakemore, N. D. Schley, C. D. Incarvito, N. Hazari, G. W. Brudvig and R. H. Crabtree, *Organometallics*, 2011, **30**, 965–973.
270. F. Hanasaka, Y. Tanabe, K. Fujita and R. Yamaguchi, *Organometallics*, 2006, **25**, 826–831.
271. R. Lalrempuia, N. D. McDaniel, H. Müller-Bunz, S. Bernhard and M. Albrecht, *Angew. Chem. Int. Ed.*, 2010, **49**, 9765–8.
272. T. Arthur and T. A. Stephenson, *J. Organomet. Chem.*, 1981, **208**, 369–387.

References

273. R. G. Wilkins, in *Kinetics and Mechanisms of Reactions of Transition Metal Complexes*, Wiley-VCH, Weinheim, 2002.
274. J. R. Fulton, M. W. Bouwkamp and R. G. Bergman, *J. Am. Chem. Soc.*, 2000, **122**, 8799–800.
275. D. S. Glueck, J. Wu, F. J. Hollander and R. G. Bergman, *J. Am. Chem. Soc.*, 1991, **113**, 2041–2054.
276. D. D. VanderLende, K. A. Abboud and J. M. Boncella, *Inorg. Chem.*, 1995, **34**, 5319–5326.
277. L. A. Villanueva, K. A. Abboud and J. M. Boncella, *Organometallics*, 1992, **11**, 2963–2965.
278. R. D. W. Kemmitt, S. Mason, M. R. Moore, J. Fawcett and D. R. Russell, *J. Chem. Soc. Chem. Commun.*, 1990, 1535.
279. L. Dahlenburg and K. Herbst, *J. Chem. Soc. Dalton Trans.*, 1999, 3935–3939.
280. J. M. Boncella, T. M. Eve, B. Rickman and K. A. Abboud, *Polyhedron*, 1998, **17**, 725–736.
281. R. Severin and S. Doye, *Chem. Soc. Rev.*, 2007, **36**, 1407–20.
282. D. P. Klein, J. C. Hayes and R. G. Bergman, *J. Am. Chem. Soc.*, 1988, **110**, 3704–3706.
283. W. Ponndorf, *Angew. Chem.*, 1926, **39**, 138–143.
284. H. Meerwein and R. Schmidt, *Justus Liebigs Ann. Chem.*, 1925, **444**, 221–238.
285. E. J. Campbell, H. Zhou and S. T. Nguyen, *Org. Lett.*, 2001, **3**, 2391–2393.
286. J. Hannedouche, G. J. Clarkson and M. Wills, *J. Am. Chem. Soc.*, 2004, **126**, 986–7.
287. A. M. Hayes, D. J. Morris, G. J. Clarkson and M. Wills, *J. Am. Chem. Soc.*, 2005, **127**, 7318–9.
288. D. J. Morris, A. M. Hayes and M. Wills, *J. Org. Chem.*, 2006, **71**, 7035–44.
289. J. Takehara, S. Hashiguchi, A. Fujii, S. Inoue, T. Ikariya and R. Noyori, *Chem. Commun.*, 1996, 233.
290. D. A. Alonso, S. J. M. Nordin, P. Roth, T. Tarnai, P. G. Andersson, M. Thommen and U. Pittelkow, *J. Org. Chem.*, 2000, **65**, 3116–3122.

References

291. D. G. I. Petra, P. C. J. Kamer, P. W. N. M. van Leeuwen, K. Goubitz, A. M. Van Loon, J. G. de Vries and H. E. Schoemaker, *Eur. J. Inorg. Chem.*, 1999, **1999**, 2335–2341.
292. M. J. Palmer, J. A. Kenny, T. Walsgrove, A. M. Kawamoto and M. Wills, *J. Chem. Soc. Perkin Trans. 1*, 2002, 416–427.
293. K. Everaere, A. Mortreux, M. Bulliard, J. Brussee, A. van der Gen, G. Nowogrocki and J.-F. Carpentier, *Eur. J. Org. Chem.*, 2001, **2001**, 275–291.
294. C. C. C. Johansson Seechurn, M. O. Kitching, T. J. Colacot and V. Snieckus, *Angew. Chem. Int. Ed. Engl.*, 2012, **51**, 5062–85.
295. P. D. de Koning, D. McAndrew, R. Moore, I. B. Moses, D. C. Boyles, K. Kissick, C. L. Stanchina, T. Cuthbertson, A. Kamatani, L. Rahman, R. Rodriguez, A. Urbina, A. Sandoval (née Accacia) and P. R. Rose, *Org. Process Res. Dev.*, 2011, **15**, 1018–1026.
296. D. Alberico, M. E. Scott and M. Lautens, *Chem. Rev.*, 2007, **107**, 174–238.
297. I. V. Seregin and V. Gevorgyan, *Chem. Soc. Rev.*, 2007, **36**, 1173–93.
298. T. Satoh and M. Miura, *Chem. Lett.*, 2007, **36**, 200–205.
299. K. Hirano and M. Miura, *Synlett*, 2011, **2011**, 294–307.
300. D. T. Davies, *Aromatic Heterocyclic Chemistry*, Oxford University Press, Oxford, 1992.
301. J. A. Joule and K. Mills, *Heterocyclic Chemistry*, Blackwell Publishing, Oxford, 4th edn., 2000.
302. R. Grigg, V. Sridharan, P. Stevenson, S. Sukirthalingam and T. Worakun, *Tetrahedron*, 1990, **46**, 4003–4018.
303. E. M. Beccalli, G. Broggin, M. Martinelli, G. Paladino and C. Zoni, *Eur. J. Org. Chem.*, 2005, 2091–2096.
304. M. Burwood, B. Davies, I. Diaz, R. Grigg, P. Molina, V. Sridharan and M. Hughes, *Tetrahedron Lett.*, 1995, **36**, 9053–9056.
305. C. W. G. Fishwick, R. Grigg, V. Sridharan and J. Virica, *Tetrahedron*, 2003, **59**, 4451–4468.
306. J. Huang and M.-M. Gu, *Youji Huaxue*, 1994, **14**, 604.
307. T. Kuroda and F. Suzuki, *Tetrahedron Lett.*, 1991, **32**, 6915–6918.

References

308. K. J. Hodgetts and M. T. Kershaw, *Org. Lett.*, 2003, **5**, 2911–4.
309. A. Ohta, Y. Akita, T. Ohkuwa, M. Chiba, R. Fukunaga, A. Miyafuji, T. Nakata, N. Tani and Y. Aoyagi, *Heterocycles*, 1990, **31**, 1951.
310. T. Okazawa, T. Satoh, M. Miura and M. Nomura, *J. Am. Chem. Soc.*, 2002, **124**, 5286–5287.
311. B. Glover, K. A. Harvey, B. Liu, M. J. Sharp and M. F. Tymoschenko, *Org. Lett.*, 2003, **5**, 301–4.
312. B. B. Touré, B. S. Lane and D. Sames, *Org. Lett.*, 2006, **8**, 1979–82.
313. L. Filippini, M. Gusmeroli and R. Riva, *Tetrahedron Lett.*, 1992, **33**, 1755–1758.
314. S. Pivsa-Art, T. Satoh, Y. Kawamura, M. Miura and M. Nomura, *Bull. Chem. Soc. Jpn.*, 1998, **71**, 467–473.
315. G. L. Turner, J. A. Morris and M. F. Greaney, *Angew. Chem. Int. Ed. Engl.*, 2007, **46**, 7996–8000.
316. S. A. Ohnmacht, P. Mamone, A. J. Culshaw and M. F. Greaney, *Chem. Commun.*, 2008, 1241–3.
317. E. F. Flegeau, M. E. Popkin and M. F. Greaney, *Org. Lett.*, 2008, **10**, 2717–20.
318. A. Ohta, Y. Aoyagi, A. Inoue, I. Koizumi, R. Hashimoto, K. Tokunaga, K. Gohma, J. Komatsu, K. Sekine, A. Miyafuji, J. Kunoh, R. Honma and Y. Akita, *Heterocycles*, 1992, **33**, 257.
319. F. Bellina, S. Cauteruccio and R. Rossi, *Eur. J. Org. Chem.*, 2006, **2006**, 1379–1382.
320. N. A. Strotman, H. R. Chobanian, Y. Guo, J. He and J. E. Wilson, *Org. Lett.*, 2010, **12**, 3578–81.
321. L.-C. Campeau, M. Bertrand-Laperle, J.-P. Leclerc, E. Villemure, S. Gorelsky and K. Fagnou, *J. Am. Chem. Soc.*, 2008, **130**, 3276–7.
322. S. Shirai, H. Nara, Y. Kayaki and T. Ikariya, *Organometallics*, 2009, **28**, 802–809.
323. L. Ackermann and A. V. Lygin, *Org. Lett.*, 2011, **13**, 3332–5.
324. C. Valente, M. E. Belowich, N. Hadei and M. G. Organ, *Eur. J. Org. Chem.*, 2010, 4343–4354.
325. A. Battace, M. Lemhadri, T. Zair, H. Doucet and M. Santelli, *Organometallics*, 2007, **26**, 472–474.

References

326. M. Yu, R.-Y. Tang and J.-H. Li, *Tetrahedron*, 2009, **65**, 3409–3416.
327. L.-C. Campeau, M. Parisien, A. Jean and K. Fagnou, *J. Am. Chem. Soc.*, 2006, **128**, 581–90.
328. E. Vedejs and L. M. Luchetta, *J. Org. Chem.*, 1999, **64**, 1011–1014.
329. S. Brahma and J. K. Ray, *J. Heterocycl. Chem.*, 2008, **45**, 311–317.
330. K. Taniguchi, M. Nagano, K. Hattori, K. Tsubaki, O. Okitsu and S. Tabuchi, *U.S. Pat.*, 1998.
331. J. Jensen, N. Skjaerbaek and P. Vedsø, *Synthesis*, 2001, **2001**, 0128–0134.
332. M. Lafrance, C. N. Rowley, T. K. Woo and K. Fagnou, *J. Am. Chem. Soc.*, 2006, **128**, 8754–6.
333. M. Lafrance and K. Fagnou, *J. Am. Chem. Soc.*, 2006, **128**, 16496–7.
334. F. G. Bordwell, D. Algrim and N. R. Vanier, *J. Org. Chem.*, 1977, **42**, 1817–1819.
335. F. G. Bordwell, J. C. Branca, D. L. Hughes and W. N. Olmstead, *J. Org. Chem.*, 1980, **45**, 3305–3313.